NOTE TO USERS

I Kappa B Kinases Control Virus Activation of Interferon Regulatory Factor Signaling

by

Sonia Sharma

A thesis submitted to the Faculty of Graduate Studies and Research in partial fulfillment of the requirements for the degree of Doctor of Philosophy

Department of Microbiology and Immunology
McGill University, Montreal
March 2004

Your file Votre référence
ISBN: 0-494-12944-1
Our file Notre référence
ISBN: 0-494-12944-1

Abstract

Virus infection of a mammalian host initiates a set of rapid and coordinated cellular events designed to limit and ultimately eradicate pathogen replication and spread. Development of an efficient anti-viral response is dependent upon communication between pathogen-susceptible cells at the site of infection and the immune effectors. In response to cellular detection of a viral threat, communication is achieved through production and secretion of secondary protein messengers called cytokines. Interferons (IFN) are cytokines that are crucial to the establishment of anti-viral immunity; type I IFNs secreted by virus-infected cells activate the innate immune machinery, modulate adaptive immune responses, promote apoptosis of infected cells and induce an anti-viral genetic program in uninfected cells. Extensive study of type I IFN gene regulation has yielded information on the nature of cellular responses elicited by viral pathogens: signaling events initiated by the cell to eliminate the virus as well as counter-measures initiated by the virus to appropriate anti-viral signaling or inhibit it altogether. Transcription of the type I IFN genes requires activation of multiple transcription factors, including Nuclear Factor kappa B (NF-κB), Activating Protein-1 (AP-1) and the Interferon Regulatory Factors (IRFs). While signaling pathways leading to NF-κB and AP-1 activation are relatively well characterized, regulation of IRF activity represents a critical missing link in the understanding of immune signaling. This study provides a mechanistic analysis of two IRF-related signaling pathways that are triggered in response to virus infection. First, chronic activation of the *irf4* gene in T-cells infected with Human T-cell Leukemia Virus-I (HTLV-I), an event that is associated with leukemic development, is induced by viral appropriation of NF-κB signaling through the classical regulatory IκB kinases (IKK). Second, virus-inducible activation of IRF-3 and IRF-7 signaling, which precipitates the type I IFN anti-viral state, is triggered through direct phosphorylation events mediated by the IKK-related kinases IKKε and TBK-1. These experiments demonstrate an essential role for regulatory components of NF-κB signaling, specifically the IKK kinases, for IRF activation within the context of virus infection.

Résumé

L'infection virale d'un hôte mammifère initie une série rapide et coordonnée d'événements ayant pour objectif de limiter et, à terme, d'éradiquer la réplication et la dissémination du pathogène. Le développement de cette réponse anti-virale depend d'une communication efficace entre les cellules susceptibles d'être infectées et les cellules effectrices du système immunitaire. En réponse à la détection d'une menace virale, cette communication est réalisée par la production et la sécrétion de messagers secondaires protéiques appelés cytokines. Les interférons (IFN) sont des cytokines cruciales pour l'établissement d'une réponse immunitaire anti-virale: Les intérferons IFNα et IFNβ sécretés par les cellules infectées activent la machinerie immuitaire innée, modulent la réponse immunitaire acquise, favorisent l'apoptose des cellules infectées et induisent l'expression de genes anti-viraux dans les cellules non-infectées. Les études détaillées de la regulation des gènes l'interféron a apporté des informations sur la nature de la réponse intracellulaire stimulée par des pathogens viraux: la cellule initie une cascade d'événements pour éliminer le virus, alors que ce dernier tend de les contrecarrer en s'appropriant et/ou en inhibant la signalisation intracellulaire anti-virale. La transcription du gene interféron nécessite l'activation de multiples facteurs transcriptionels, don't le facteur NF-κB (nuclear factor kappa B), la proteine AP-1 (activating protein 1), et les facteurs IRF (interferon regulatory factor) récemment identifies. Bien quels les voies de signalisation conduisant à l'activation de NF-κB et AP-1 soient bien caractérisées, les mécanismes d'activation des facteurs IRF manquent à la comprehension de la réponse immunitaire. Cette étude se propose d'étudier deux voies de regulation liées aux facteurs IRF activé au cours de l'infection virale. La première voie conduit à l'activation chronique du gene lymphoide *irf4* dans les cellules T transformées par le virus HTLV-I (Human T-cell Leukemia/Lymphotropic Virus I). Cette activation est initiée par l'appropriation virale de la signalisation NF-κB ce qui contribue à la leukomogenèse induite par ce virus. La seconde voie de regulation entraine la phosphorylation de IRF-3 et IRF-7, puis l'activation des voies de regulation sous leur contrôle. Cette êtape du phosphorylation, qui est un événement immediate precoce suivant l'infection par de nombreux types de virus, est catalysée par les kinases régulatrices de NF-κB, IKKε et TBK-1. Il en résulte l'induction de l'expression des interférons de type I et des gènes

anti-viraux. Ces expériences montrent que les composantes régulatrices de la cascade de signalisation de NF-κB, en particulier les kinases reliées à NF-κB ont un rôle essentiel dans l'activation des facteurs IRF dans le contexte de l'infection virale et de l'établissement d'un état anti-virale.

Acknowledgements

First and foremost, I would like to thank my supervisors: Dr. John Hiscott, who I appreciate for his guidance and support from the first day I started in his lab as a virtual neophyte. Dr. Rongtuan Lin, whose work ethic and expertise I am still trying to emulate. I would also like to thank my friend and compatriot Benjamin tenOever, who has represented an ideal scientific collaborator for the bulk of this Ph.D (and has provided some healthy competition along the way). Dr. Nathalie Grandvaux, who taught me how assertion is key to success and Dr. Yäel Mamane, who was responsible for much of my training during the early years in the lab (we'll always have Dublin). I am very grateful to friends and colleagues, past and present, in the Lady Davis Institute: Dr. Hakju Kwon, John Cho, David Hamilton, Maria Ricci, Tudor Baetu as well as the 531 group, Meztli Arguello, Benjamin Péant and Catherine Courriveau-Bourke. You will all be greatly missed. A big thanks to Ben P. and Raphaelle Romieu for translating my abstract, and Ben T. and Catherine for editing this document. In particular, I would like to thank my best friend Yazz, because I really believe that had she not been there to ground me during these past five years, my sense of humor (and maybe even a little bit of my sanity) would not have survived. And after all, only a true friend would give up blood for the sake of experiments. Thank you to my family, including my parents Dharam and Pramod, for much love and support, as well as my brother Sanjay, because he never lets me take myself too seriously. I would also like to acknowledge Les Fonds de la recherche en santé du Québec (FRSQ) and the Canadian Institutes of Health Research (CIHR) for having provided me with M.SC and Ph.D fellowships. I must say that life in the Hiscott lab has been quite an eclectic experience: in the end, the moments of despair have been surpassed by the sum of all successes; I've been lucky to have worked with such a good team.

Preface

In accordance with "Guidelines for Thesis Preparation," the candidate has chosen the option of presenting her results in the classical format. A general introduction is presented in chapter I and appears, in part, in the following review articles:

1. Mamane Y, Sharma S, Grandvaux N, Hernandez E, Hiscott J. 2002. IRF-4 activities in HTLV-I-induced T-cell leukemogenesis. *J. Interferon Cytokine Res.* 22: 135-43.

2. Hiscott J, Grandvaux N, Sharma S, tenOever, BR, Servant MJ, Lin R. 2003. Convergence of the NF-κB and interferon signaling pathways in the regulation of antiviral defense and apoptosis. *Ann. N.Y. Acad. Sciences.* 1010: 237-249.

3. Sharma S, Grandvaux N, tenOever BR, Lin R, Hiscott J. 2004. Triggering innate immunity through TBK1/IKKε activation of the IRF-3/IRF-7 signaling program. In press.

Materials and methods for research presented in this document are detailed in chapter II; the results described in chapters III, IV and V have been published, in part, in the following journal articles following subjection to the peer review process; an asterix (*) denotes publications for which the indicated authors contributed equally:

4. Mamane Y, Sharma S, Petropoulos L, Lin R, Hiscott J. 2000. Posttranslational regulation of IRF-4 activity by the immunophilin FKBP52. *Immunity* 12: 129-40.

5. Sharma S, Mamane Y, Grandvaux N, Bartlett J, Petropoulos L, Lin R, Hiscott J. 2000. Activation and regulation of IRF-4 in HTLV-I-infected T-lymphocytes. *AIDS Res. Hum. Retroviruses* 16: 1613-22.

6. Sharma S, Grandvaux N, Mamane Y, Genin P, Azimi N, Waldmann T, Hiscott J. 2002. Regulation of IRF-4 expression in HTLV-I. *J. Immunol.* 169: 3120-30. *Copyright 2002. The American Association of Immunologists, Inc.*

7. Sharma S*, tenOever BR*, Grandvaux N*, Zhou GP, Lin R, Hiscott J. 2003. Triggering the interferon antiviral response through an IKK-related pathway. *Science* 300: 1148-51.

8. tenOever BR*, Sharma S*, Zhou W, Sun, Q, Hernandez E, Yeh WC, Lin R, Hiscott J. 2004. Virus-activation of the IKK-related complex involves intra- and extracellular detection mechanisms. (manuscript in preparation).

All research presented in Chapter III was performed by the candidate, with the exception of these specific contributions:

Dr. Yael Mamane participated in co-immunoprecipiation experiments in Figures 10 and 11.

Dr. Nathalie Grandvaux performed *in vivo* genomic footprinting studies in Figures 17A, 18A and 19A.

Research presented in chapters III and IV was part of an active collaboration between the candidate and several members of the lab. Specific contributions are:

Dr. Nathalie Grandvaux is responsible for Figure 23C

Dr. Rongtuan Lin is responsible for Figures 24, 26, 27B, 33 and 35C. He is responsible for cloning all IRF-3 and IRF-7 expression plasmids and GST fusion vectors used in this study, with the exception of GST-IRF-3(S398/402A), which was cloned by Benjamin R. tenOever. He generated recombinant baculoviruses expressing IKKε and TBK-1 fused to a His epitope tag.

Benjamin R. tenOever is responsible for Figures 27A, 28 and 30.

Dr. Qiang Sun was responsible for the purification of the recombinant IKKε and TBK-1 proteins used in Figures 32 and 34.

The candidate was also involved in several collaborations with respect to research that is beyond the scope of this document. This research has been in the following journal articles following subjection to the peer review process:

9. Baetu TM, Kwon H, Sharma S, Grandvaux N, Hiscott J. 2001. Disruption of NF-κB signaling reveals a novel role for NF-κB in the regulation of TNF-related apoptosis-inducing ligand (TRAIL) expression. *J. Immunol.* 167: 3164-73.

10. Mamane Y, Grandvaux N, Hernandez E, Sharma S, Innocente SA, Lee JM, Azimi N, Lin R, Hiscott J. 2002. Repression of IRF-4 target genes in human T-cell leukemia virus-I infection. *Oncogene* 21: 6751-65.

11. Arguello M, Sgarbanti M, Hernandez E, Mamane Y, Sharma S, Servant M, Lin R, Hiscott J. 2003. Disruption of the B-cell specific transcriptional program in HHV-8 associated primary effusion lymphoma cell lines. *Oncogene* 22: 964-73.

Table of Contents

List of Figures and Tables

Figures

Chapter I

General Introduction

Chapter I

General Introduction

1. The NF-κB signaling network: developing innate to adaptive immunity

1.1 Introduction to NF-κB/Rel proteins

The evolutionarily conserved nuclear factor kappa B (NF-κB)/Rel transcription factors regulate immune responses through modulation of genes that encode cytokines and chemokines, antigen presentation receptors, immune recognition receptors, adhesion molecules and proteins involved in apoptosis (1,2). As a central regulator of both innate and adaptive immunity, proper NF-κB activation is essential to develop an appropriate yet effective immune response: disruption or deregulation of NF-κB signaling is associated with abnormalities ranging from immunodeficiency at one end of the scale to acute inflammation and cancer on the other (1,2).

Activation of the NF-κB transcriptional program is a fundamental immediate early step of immune activation; as a result, NF-κB signaling represents a prime candidate for viral appropriation: Human Immunodeficiency Virus type I (HIV-I), Human T-cell Leukemia Virus type I (HTLV-I), Human Herpesvirus 8 (HHV8) and Epstein-Barr Virus (EBV) have incorporated NF-κB signaling into their life cycle and pathogenesis (3). NF-κB proteins are differentially activated through numerous external and internal stimuli, including immune/antigen receptor engagement, pro-inflammatory cytokine signaling as well as unique properties of the specific pathogen.

1.1.1 The NF-κB/Rel family

Organization of the mammalian NF-κB/Rel family of transcription factors is schematically represented in Figure 1, which details the structural and functional domains of NF-κB subunits. Dimers of NF-κB are formed between the five mammalian NF-κB subunits: RelA (p65), NF-κB1 (p50/p105), NF-κB2 (p52/p100), c-Rel and RelB (1,4). All NF-κB proteins share a conserved, amino-terminal region of 300 amino acids (aa) termed the Rel-homology domain (RHD), which encompasses an NF-κB homo/hetero-dimerization domain (DD), a nuclear localization sequence (NLS) and a DNA

Figure 1. The NF-κB/Rel proteins Schematic representation of the NF-κB/Rel family. The NF-κB/Rel superfamily can be subdivided into the DNA binding (p65, c-Rel, p50, p52, RelB) and non-DNA binding (p105/NFκB1, p100/NFκB2) subunits. All NF-κB proteins are identified by a 300-aa amino-terminal region termed the rel homology domain (RHD), which encompasses a DNA Binding Domain (DBD), a dimerization domain (DD) and a nuclear localization signal (NLS). The p65, c-Rel and RelB proteins contain variable carboxy-terminal transactivation domains (TD) that promote transcriptional activation of NF-κB-driven target genes and can be subject to post-translational modifications such as phosphorylation and acetylation, which influence transcriptional capacity. p65, c-Rel and p50 contain multiple serine or threonine phosphoacceptor sites within the RHD and TD that are targets for regulatory kinases; phosphorylation at these sites is required for transactivation potential in the nucleus. p105/NF-κB1 and p100/NF-κB2 contain a large carboxy-terminal domain encompassing seven ankyrin repeats which interact with the RHD of NF-κB subunits such as RelB. Ubiquitin-dependent proteolic processing of p105/NF-κB1 and p100/NF-κB2 involves cleavage near a flexible glycine rich hinge region (GRR) to generate the DNA binding p50 and p52 proteins, respectively.

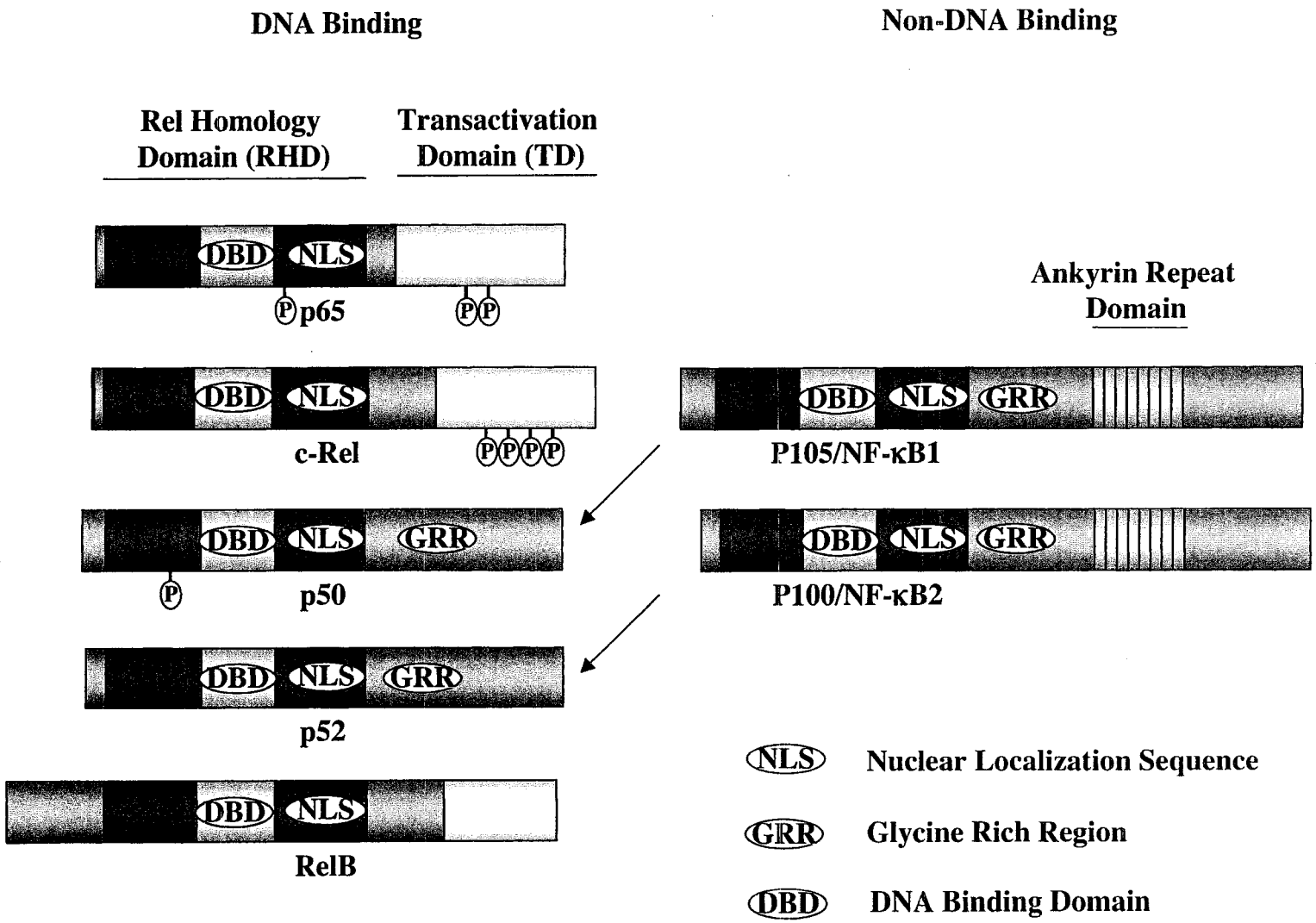
DNA Binding
Non-DNA Binding
Rel Homology Domain (RHD)
Transactivation Domain (TD)
Ankyrin Repeat Domain
DBD
NLS
GRR
P
p65
c-Rel
P105/NF-κB1
p50
P100/NF-κB2
p52
RelB
Nuclear Localization Sequence
Glycine Rich Region
DNA Binding Domain

binding domain (DBD). The DBD mediates recognition and binding of NF-κB dimers to the palindromic 5'-GGGRNNYYCC-3' DNA consensus sequence (1,4-6), albeit each dimer with selective affinity (7-9). The nuclear factor of activated T-cells (NF-AT) transcription factors (10) are sometimes considered part of the Rel/NF-κB superfamily, because they share limited homology to NF-κB proteins within the RHD (11). However, the cellular signaling pathways leading to NF-κB and NF-AT activation are distinct and differentially regulated, so they will be described separately for the purposes of this document.

Three mammalian NF-κB subunits, p65, c-Rel and RelB (as well as the Drosophila morphogen *dorsal* (12)), possess a variable carboxy-terminal transactivation domain (TD) that promotes gene transcription from target promoters (1,13). Variability within the TD confers differential regulation to the transactivator proteins, mainly through subunit-specific phosphorylation by regulatory kinases, which is described in section 1.2.4. The Rel proteins p50 (14,15) and p52 (16) are generated by ubiquitin-dependent, proteolic processing of precursors p100 and p105, respectively (17). Lacking a carboxy-terminal transactivation domain, p50 or p52 homodimers repress NF-κB-driven gene transcription (18) unless complexed to a transcriptionally active NF-κB subunit.

1.1.2 Expression and distribution of NF-κB/Rel proteins

The canonical activating heterodimer of p65/p50 that has been most expansively studied is ubiquitously expressed. In comparison, c-Rel expression is prevalent in hematopoietic cells, particularly those of lymphoid lineage, while expression of RelB is confined to particular regions of the thymus, lymph nodes and Peyer's Patches (2). Expression of c-Rel, RelB and p105 is inducible at the transcriptional level, through a positive feedback loop driven by NF-κB (19-21).

1.1.3 Targeted disruption of NF-κB/Rel genes

All five Rel genes have been disrupted in mice through homologous recombination (2). These knockout (KO) studies have demonstrated the essential and often distinct roles for

NF-κB subunits for the regulation of innate and adaptive immune responses, particularly for the function of mature immune cells in the periphery. Subunit p65 plays an essential role in embryonic development, as a gene deletion of p65 is lethal at day 16 of gestation due to massive liver degeneration (22,23). This phenotype is precipitated by increased hepatocyte sensitivity to tumor necrosis factor α (TNFα)-induced cell death, a receptor-driven pro-apoptotic pathway that is favored in the absence of p65 signaling (22,23). When mice lacking p65 are brought to term by breeding onto a TNF receptor 1 (TNFRI) or TNF-deficient background, embryogenesis proceeds normally (24,25). However, the animals lack lymph nodes, Peyer's patches, and an organized splenic micro-architecture; moreover, they display profound defects in T-cell-dependent antigen responses (26). Analyses of *tnfr1/p65*-deficient embryonic tissues suggest that the dependence on p65 is not manifested in the hematopoietic cells, but rather in the stromal cells essential for development of the secondary lymphoid organs (26).

Mice deficient for expression of c-Rel develop equivalent levels of hemopoietic cells compared to control littermates, and the relative quantity of nuclear NF-κB complexes is normal in *crel*-deficient lymphocytes due to compensation by p65 dimers (27). However, p65 cannot functionally replace c-Rel during lymphocyte activation, and KO animals display gross defects with respect to antigen-stimulated B- and T-cell proliferation and subsequent generation of adaptive immune responses (27-29). Inactivation of the *relb* gene results in post-natal death at day 10 (30,31). The pathology involves thymic atrophy, splenomegaly, bone marrow hyperplasia and a severely dysfunctional immune response. Burkly et al. have suggested that RelB is important in the commitment of immune precursor cells to a particular lineage, as the development of dendritic cells (DC) in the bone marrow and medullary epithelial cells in the thymus is impaired in the absence of RelB expression (30). Disruption of the *nfkb2* gene results in architectural abnormities of the spleen and lymph nodes, as well as impaired germinal center formation due to defects in B-cell development and antigen-specific activation (2). Recent characterization of the "non-canonical" pathway to NF-κB activation, which is described in section 1.3.5, has shed light on this essential role of NF-κB2 in the regulation of B-cell development and effector function.

1.2 Regulation of NF-κB activation

Signal-responsive induction of NF-κB signaling is primarily regulated at the level of cytoplasmic to nuclear translocation. In unstimulated cells, latent NF-κB dimers are sequestered in the cytosol by interaction with inhibitory κB (IκB) proteins. Cellular stimulation with NF-κB inducers initiates a rapid sequence of events that results in the phosphorylation and degradation of IκB; subsequently, freed NF-κB dimers translocate to the nucleus to bind κB sites within the promoters of NF-κB target genes.

1.2.1 The inhibitory κB (IκB) proteins

Schematic representations of the IκB repressors are detailed in Figure 2. The IκB proteins are characterized by central 33 aa repeat motifs called ankyrin repeats, which bind and sequester NF-κB dimers through interaction with the RHD in latent cells (32). Canonical IκB subunits are IκBα, IκBβ and IκBε, although most analysis has focused on IκBα. Subunits p100 and p105 are IκB-like pro-proteins (33,34), both possessing functional ankyrin repeats that interact with the RHD of NF-κB subunits prior to the ubiquitin-dependent proteolic processing (17) which removes the ankyrin repeats to generate mature p50 and p52, respectively (14-16). In addition to sequestration of latent NF-κB dimers, p105 has recently been demonstrated to inhibit upstream regulatory components of the NF-κB signaling pathway (35). In unstimulated cells p105 forms a stable and inactive complex with Cot/Tpl2, a regulatory kinase involved in NF-κB activation in hematopoietic cells (36). Activation of Tpl2 requires dissociation from inhibitory p105, which activates NF-κB signaling by promoting degradation of IκB, illustrating how p105, an effector of the NF-κB cascade, regulates upstream signaling components of its own pathway (35). The IκBγ protein represents the carboxy-terminal portion of p105, which is produced from an alternative transcriptional start site in the intron of the NF-κB1 gene (37,38). In contrast to p105 and p50, which are ubiquitously expressed, IκBγ expression is restricted to the lymphoid tissue. The only IκB molecule that promotes NF-κB gene transcription is BCL-3, through its selective binding affinity for

Figure 2. The IκB proteins Schematic representation of IκB repressors. All IκB proteins contain an ankyrin repeat domain (ARD) involved in binding and sequestration of NF-κB/Rel proteins through the RHD. IκBα, IκBβand IκBε contain an amino-terminal signal-responsive domain (SRD) containing two critical serine (S) phosphoacceptor sites for the IκB kinases; phosphorylation at these sites is the signal for ubiquitination and degradation of the proteins. IκBα, IκBβ, IκBε, Bcl-3, p105 and p100 contain a nuclear localization signal (NLS). IκBα and IκBε also contain an amino- and carboxy-terminal (IκBα) and amino-terminal (IκBε) nuclear export signal (NES) that promotes cytoplasmic-nuclear shuttling of IκB-NF-κB complexes. IκBα and IκBβ contain a carboxy terminal PEST (Proline, Glutamic acid, Serine, Threonine) region involved in basal turnover and half-life. p105 p105/NF-κB1 and p100/NF-κB2 contain functional ankyrin repeats prior to proteolic cleavage of the carboxy-terminal ARD near the glycine rich region (GRR). IκBγ represents the carboxy-terminal domain of p105, and is generated by an alternative start site within the p105 intron.

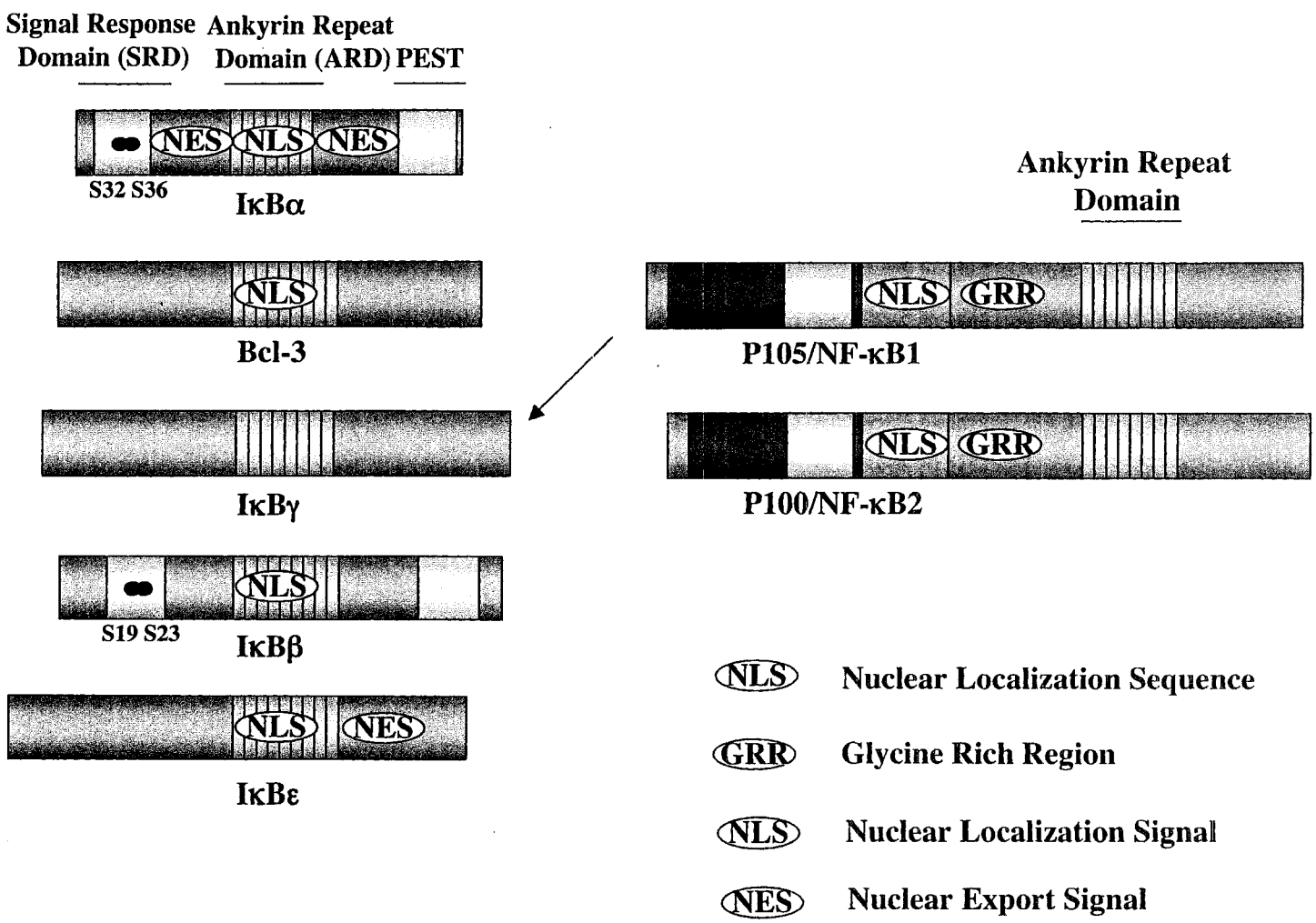
Signal Response Domain (SRD)
Ankyrin Repeat Domain (ARD)
PEST
NES
NLS
NES
S32 S36
IκBα
NLS
Bcl-3
IκBγ
NLS
S19 S23
IκBβ
NLS
NES
IκBε
Ankyrin Repeat Domain
NLS
GRR
P105/NF-κB1
NLS
GRR
P100/NF-κB2
NLS Nuclear Localization Sequence
GRR Glycine Rich Region
NLS Nuclear Localization Signal
NES Nuclear Export Signal

repressive p50 or p52 homodimers (39,40), as well as its transcriptional coactivator function in complex with DNA-bound p52 in the nucleus (41).

Repressor IκBα is characterized by an amino-terminal signal-response domain (SRD), a central ankyrin repeat domain (ARD) that interacts with NF-κB, and a carboxy-terminal PEST (proline, glutamine, serine, threonine) domain that regulates basal turnover of the protein (42). The ARD of IκBα interacts with NF-κB dimers through the RHD, which masks the NF-κB NLS (32,43). However, a combination of structural and biochemical analyses of IκBα in complex with p50/p65 reveal that the interaction with IκBα covers one NLS per NF-κB dimer, such that partial shielding permits the inactive trimer to enter the nucleus via the one exposed NLS (44-46). A nuclear export sequence (NES) within IκBα efficiently exports the complex back to the cytoplasm, ensuring that unstimulated cells contain low levels of nuclear NF-κB complexes (45,46). Experiments using the pharmacological inhibitor Leptomycin B, which blocks the nuclear export process, demonstrate that IκBα-bound NF-κB dimers will accumulate in the nucleus, yet they are unable to bind DNA or promote transcription (45,46). Although the shuttling phenomenon has been well documented, the functional relevance of this energy-driven process is not fully understood. Like IκBα, IκBε contains a functional NES that allows for nuclear to cytoplasmic shuttling of IκBε-bound complexes. In contrast, IκBβ covers both NLS per NF-κB dimer and lacks a functional NES; as a result, IκBβ does not promote dynamic shuttling but instead remains stably associated with NF-κB dimers in the cytoplasm (47).

The IκBα protein regulates immediate early, inducible NF-κB activation through selective sequestration of p65 and c-Rel-containing NF-κB dimers (9,48). In response to NF-κB-stimulating signals, IκBα is rapidly phosphorylated in the amino-terminal SRD; two amino-terminal phosphoacceptor sites are critical to initiation of signal-responsive IκBαdegradation (49-51). Phosphorylation on serines (S) 32 and S36 of IκBα represents the key signal for dissociation from NF-κB dimers; subsequently, the phosphorylated protein is recognized by the E3 ubiquitin ligase Slimb/β-transducin

repeat-containing protein (β-TRCP), in the presence of ubiquitin-activating (E1) and ubiquitin-conjugating (E2) enzymes (52-54). Following ubiquitination at lysines (K) 21 and K22 (55), IκBα dissociates from NF-κB dimers and is degraded via the 26S proteosome pathway (49,56,57). A S32/36 to alanine (A) substitution within the SRD of IκBα abolishes its signal-responsive phosphorylation, ubiquitination and degradation (49,58-60). Furthermore, coupling the S32/36A mutation with a carboxy-terminal that deletes two casein kinase II (CKII) phosphoacceptor sites regulating basal turnover of IκBα(61-63) generates a powerful inhibitor of signal-induced NF-κB activation. The 2NΔ4 IκBα super-repessor remains stably associated with NF-κB dimers due to two factors: increased half-life and insensitivity to degradation.

Following signal-responsive degradation, IκBα proteins are resynthesized in an NF-κB-dependent manner, due to functional κB sites in the IκBα promoter (64-66). Via an intrinsic NLS, newly synthesized IκBα re-enters the nucleus to bind and displace NF-κB dimers bound to DNA (67), and the sequestered NF-κB dimers are then shuttled out of the nucleus to complete an NF-κB-dependent negative feedback loop (68). In contrast, IκBβ is not transcriptionally upregulated by NF-κB and lacks a functional NES; thus, IκBβ does not actively displace NF-κB dimers from enhancer DNA (69,70). During signal-induced NF-κB activation an interaction between a small guanosine triphosphatase of the mammalian Ras protein family, κB-Ras, with the PEST domain of IκBβ maintains protein integrity when compared to IκBα (71). Being less sensitive to signal-induced degradation, IκBβ is thought to regulate a persistent NF-κB response (69,70).

Genetic KO studies indicate that there is redundancy with respect to the IκB proteins (72,73). With respect to the hematopoietic tissues, IκBα–deficient cells displayed elevated NF-κB activity that was manifested by severe runting, skin defects, and extensive granulopoiesis in the KO mice (72). However, mouse embryonic fibroblasts (MEFs) derived from these mice did not exhibit increased NF-κB activity, suggesting a redundancy of function for the IκB subunits in non-hematopoietic cells (72). Further analyses of MEFs derived from IκBα KO mice demonstrated a specific defect in

downregulation of NF-κB activation following signal-responsive stimulation, a result which underscores the essential role of IκBα for post-induction repression of NF-κB signaling in non-hematopoietic cells (72,74).

1.2.2 The classical IκB kinases (IKK)

As a key regulator of the immune response, NF-κB signaling is rapidly triggered in response to a wide array of stimuli: host cell detection of a foreign pathogen, secretion of pro-inflammatory cytokines such as TNFα and interleukin-1 (IL-1) by the patrolling immune surveillance machinery, or T-cell receptor (TCR) and B-cell receptor (BCR) engagement (1). Although various NF-κB-activating stimuli initiate from different focal points at the cell surface or within the cytoplasm, the majority of these signaling pathways will ultimately converge upon the ubiquitous, highly conserved machinery immediately upstream of NF-κB activation, the classical IκB kinase (IKK) complex that controls signal-responsive NF-κB activation.

With the exception of ultraviolet radiation and hydrogen peroxide, inducible activation of classical NF-κB signaling is absolutely dependent upon the key event of IκB phosphorylation by the 700-900 kDa multi-protein IKK complex, which was isolated by several groups by biochemical purification or interaction cloning experiments (75). The classical IKK complex contains two catalytic kinase components, IKKα/IKK1 and IKKβ/IKK2 (76-80), as well as a non-enzymatic regulatory subunit IKKγ/NF-κB essential modulator (NEMO) (81,82). In addition, the chaperone molecule heat shock protein 90 (Hsp90) and cell division cycle 37 (Cdc37), are accessory molecules that directly interact with the classical IKK complex through the kinase domain of IKKα and IKKβ (83). With respect to TNFα signaling, pre-treatment with the Hsp90 binding agent Geldanamycin impairs NF-κB activation through disruption of proper Hsp90/cdc37-dependent trafficking of thecytoplasmic IKK complex to the TNFR1 at the membrane (83).

The classical kinases IKKα and IKKβ exhibit an overall sequence identity of 52%, each containing an amino-terminal catalytic kinase domain as well as central helix loop helix

(HLH) and carboxy-terminal leucine zipper (LZ) domains responsible for protein-protein interactions (77,80). Both kinases directly phosphorylate IκBα, -β and -ε on their respective signal-responsive residues (76-79,84). Dimerization of the classical IKKs is essential for catalytic activation; both kinases efficiently homo- and heterodimerize *in vitro*, although a heterodimeric complex is always detected *in vivo* (79). The classical IKK kinases contain an activation loop that is located between kinase subdomains VII and VIII. The activation loop contains two key serine residues placed within a mitogen activated protein/extracellular signal-regulated kinase (MAP/MEK) target consensus motif of S172XXXS176, where X represents any aa residue. Phosphorylation at S172/176 of IKKβ is induced in response to TNFα and IL-1 stimulation (77,85), or by overexpression of regulatory kinases such as MEKK1 or NF-κB-inducing kinase (NIK) (78,86,87). A S172/176A substitution within the activation-loop of IKKα or IKKβ generates a dominant-negative kinase that blocks signal-induced NF-κB activation, while a phosphomimetic substitution with glutamic acid (E) creates a constitutively activated protein (77,85). Similarly, treatment with protein phosphatase 2A (PP2A) inhibits the enzymatic activity of purified IKK complexes (76), which complements earlier studies using the PP2A inhibitor okadaic acid to enhance IKK catalytic activity (88). Recent experiments show that protein phosphatase PP2Cβ associates with the IKK complex *in vivo*, an interaction that is required to shut-off IKK activation through dephosphorylation of IKKβ (89).

IKKα/β double knock out (DKO) embryos die at day E.12 from a combination of severe liver and neural apoptosis, and MEFs derived from these mice are unresponsive to pro-inflammatory cytokines, virus infection/dsRNA or bacterial lipopolysaccharide (LPS) stimulation with respect to NF-κB activation (90). But single gene targeting has truly underscored the distinct role of each kinase; although they are highly homologous, IKKα and IKKβ are not fully interchangeable *in vivo*. Gene inactivation of IKKβ generates a phenotype that is reminiscent of the p65 KO mouse: deficiency of IKKβ is embryonic lethal between days E12.5-E14.5 due to massive liver degeneration from TNFα-induced apoptosis (91-93). Significantly, even in the presence of IKKα homodimers, MEFs

derived from IKKβ-/- KO mice display a minimum of inducible NF-κB activation in response to TNF or IL-1 treatment (91-93).

Single deletion of the IKKα gene precipitates a vastly different phenotype from that of IKKβ: IKKα KO mice exhibit severe developmental defects relating to skeletal abnormalities and an absence of limb, tail and ear development, which precipitate death soon after birth (94-96). Epidermal differentiation is almost completely absent in IKKα–deficient mice, and the epidermal layer is five to ten-fold thicker compared to control littermates due to excessive proliferation of the epidermal basal cells, which may account for the improper extension of limb structures in IKKα-deficient mice. It has been proposed that IKKα controls the production of a soluble factor important for keratinocyte differentiation (97), because inducible NF-κB activation does not appear to play a role in the epidermal defect (94-96). In this regard, NF-κB activation by TNF, IL-1 or dsRNA is only partially diminished in cells derived from IKKα-deficient mice, with IKKβ homodimers functionally compensating for the lack of IKKα (94-96).

Like IKKβ, the non-enzymatic component of the classical IKK complex, IKKγ/NEMO, is required for signal-responsive activation of classical NF-κB signaling (81,82). Homozygous disruption of the X-linked *nemo* gene is embryonic lethal at day E.12 from apoptotis in the liver, which can be rescued by subsequent breeding onto a *tnfr1* -/- genetic background (98,99). Cells deficient for IKKγ/NEMO expression (81) or functional IKKγ/NEMO activity (82), as well as MEFs derived from IKKγ/NEMO-deficient embryos (98,99) are unresponsive to stimulation by TNF, IL-1, LPS, dsRNA and expression of the viral HTLV-I Tax oncoprotein, which is an efficient activator of NF-κB signaling that is discussed in detail in section 1.5.1. Purified IKK complexes from NEMO-deficient cells are heterodimers of IKKα and IKKβ, but measure at approximately half the expected molecular mass; furthermore, these complexes are catalytically inert (81). While IKKγ/NEMO has a higher affinity for IKKβ than for IKKα, in the absence of IKKβ it is still found in association with IKKα homodimers *in vivo* (82).

Interestingly, the pathology of NEMO deficiency in mice is sex-linked: in males, the disruption is lethal, while heterozygote females exhibit severe dermatopathic symptoms that are reminiscent of the human X-linked genodermatosis incontinetia pigmenti (IP) disorder, a relatively rare syndrome associated with numerous skin abnormalities and congenital defects (99). In humans, IP has been shown to be associated with mutations at the NEMO locus, and NF-κB activation is defective in IP cells due to decreased NEMO expression (100,101).

1.2.3 The non-classical IKK complex

The family of IKK kinases has expanded to include two novel members, based on a limited sequence homology and a potential to stimulate NF-κB signaling (102). Inducible IKK (IKKi/IKKε) was isolated using a subtractive hybridization technique from LPS-stimulated RAW264.7 murine macrophages (103), as well as from an EST database search for IKK homologues (104). The TBK-1/NAK/T2K kinase was characterized in several contexts as an IKK homologue involved in TNFα-mediated NF-κB activation (105,106) upstream of IKKβ (107). While TBK-1 expression is ubiquitous and constitutive (105-107), IKKε expression is primarily relegated to the immune compartment (102,103), but is inducible in non-hematopoietic cells by stimulation with TNF, PMA and LPS (103,108,109) through an NF-κB-dependent mechanism (109).

A schematic representation of the IKK kinase family is detailed in Figure 3. Like the classical IKK kinases IKKα and IKKβ, the novel IKK kinases IKKε and TBK-1 contain a catalytic kinase domain, an LZ domain and a HLH domain involved in protein-protein interactions (102,103,105,107). The novel IKK kinases are 64% homologous to each other, but exhibit limited homology to the classical IKK kinases, about 33% within the kinase domain (103-105,107). IKKε and TBK-1 also posses a kinase activation loop located between kinase subdomains VII and VIII; serine phosphorylation within the

Figure 3. The family of IκB kinases (IKK): classical vs. non-classical Organization of the IKK kinases. Catalytic kinase domain, leucine zipper and helix-loop-helix domain are represented. The four IKK kinases are classified into two subgroups, based on sequence homology and substrate specificity. Classical IKK kinases IKKα and IKKβ share 52% overall homology to each other; each phosphorylate both serine residues within the S32XXXS36 motif of IκBα. The non-canonical IKK-related kinases IKKε and TBK-1 share 61% overall homology to each other; each phosphorylate the second serine residue within the S32XXXS36 motif of IκBα. Homology between the subgroups is limited at 27% overall homology and 33% homology within the catalytic kinase domain. Positions of critical residues involved in catalytic activity are represented. Critical mutation K44A (IKKα and IKKβ) or K38A (IKKε and TBK-1) within the ATP-binding pocket of the kinase domain generates a dominant negative kinase; phosphomimetic mutation S176/180E (IKKα) or S177/181E (IKKβ) within the activation loop of the kinase domain generates a constitutively active kinase.

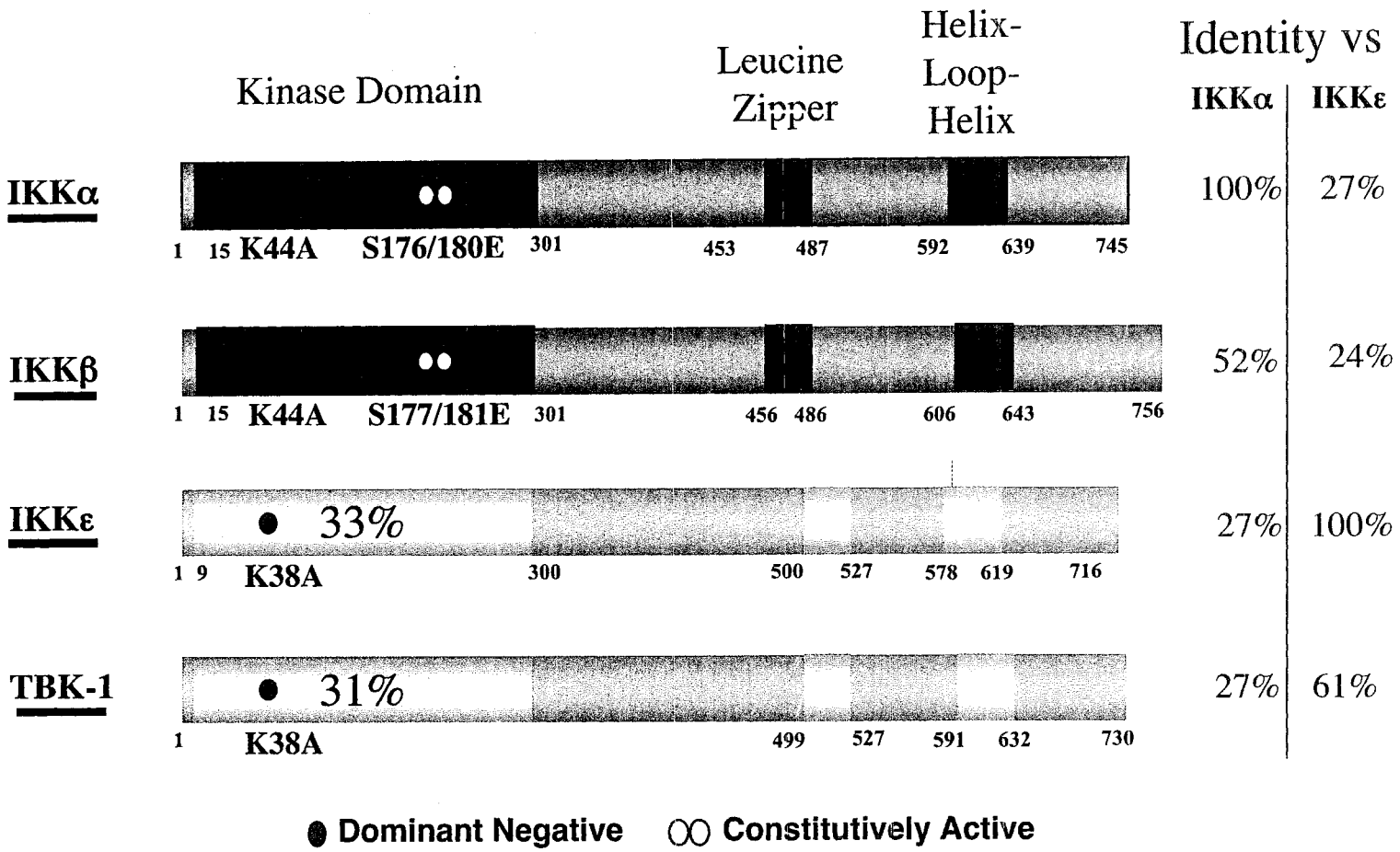
Kinase Domain
Leucine Zipper
Helix-Loop-Helix
Identity vs
IKKα
IKKε
IKKα
100%
27%
1 15 K44A S176/180E 301 453 487 592 639 745
IKKβ
52%
24%
1 15 K44A S177/181E 301 456 486 606 643 756
IKKε
33%
27%
100%
1 9 K38A 300 500 527 578 619 716
TBK-1
31%
27%
61%
1 K38A 499 527 591 632 730
Dominant Negative
Constitutively Active

activation loop is required for kinase autophosphorylation and induction of enzymatic activity (103,104,110). However, in contrast to IKKα and IKKβ, the aa sequence of the IKKε and TBK-1 activation loop does not fit a canonical MEK consensus motif (103,104,110). In the non-classical IKK activation loop the S176 residue is replaced with glutamate, for a SXXXG sequence, where a critical mutation of S172A abolishes IKKε and TBK-1 catalytic activation. Differences within the activation loop sequence are consistent with the failure of MEKK1 or NIK expression to augment IKK-related kinase activity as for classical IKK kinase activity (103). Interestingly, in contrast to IKKα and IKKβ, a S172E phosphomimetic mutation does not generate a constitutively active IKKε and TBK-1 kinase, but instead decreases the catalytic activity (103,104).

Differential homology emphasizes a distinct function for the IKK-related kinases. Both IKKε and TBK-1 directly phosphorylate only one of the two signal responsive serine residues within the SRD of IκBα, which is S36 (103,104,106). These results suggest that IκBα does not represent the physiological substrate for the novel IKKs, a notion that is consistent with defective IκB degradation in MEFs derived from IKKα/β DKO mice (90). Interestingly, TBK-1 KO mice exhibit embryonic lethality from massive apoptosis in the liver, which suggests that TBK-1 plays an essential role in cytokine-induced NF-κB activation (106). Both TBK-1 and IKKε interact with the TNF-receptor-associated factor (TRAF)-interacting protein/TRAF family member-associated NF-κB activator (I-TRAF/TANK) protein, a modulator of TNFα-induced NF-κB activation (111,112). Overexpression of IKKε or TBK-1 induces phosphorylation of I-TRAF/TANK, which results in its dissociation from TRAF2 and subsequent activation of NF-κB transcription through the classical IKK pathway (105,113). However, analyses of MEFs derived from TBK KO mice show that TBK-1 expression is dispensable for signal-responsive IκBα degradation and NF-κB DNA binding events, but required for NF-κB-dependent gene transcription in the nucleus (105,106). Although the physiological role of the IKK-related kinases remains to be fully elucidated, it has been proposed that IKKε and TBK-1 may regulate NF-κB subunits at the level of carboxy-terminal phosphorylation, which regulates transactivation capability downstream of IκB degradation (102).

1.2.4 Enhancement of NF-κB transcriptional potential

Although the primary events governing inducible NF-κB activation occur at the level of cytoplasmic to nuclear localization, NF-κB signaling is subject to additional regulation post IκB degradation. In response to cellular stimulation with TNFα, IL-1, PMA or LPS, p65 is phosphorylated at multiple serine residues within the RHD and the carboxy-terminal TD, which modulates its transactivation capacity in the nucleus (114). For example, p65 phosphorylation in response to TNFα stimulation at residues S529 (115) or S536 (116,117) is dispensable for nuclear translocation and DNA binding, but essential for the transactivation of p65-driven promoters (115). Similarly, phosphorylation of p65 at S276, which can be mediated by the catalytic subunit of protein kinase A (PKAc) in the cytoplasm (118) or mitogen- and stress-activated protein kinase 1 (Msk-1) in the nucleus (114), is necessary to recruit transcriptional co-activators in the form of histone acetyltransferase proteins like cAMP-responsive element binding factor (CREB) binding protein (CBP) or its paralogue p300 (118,119).

Another target of inducible carboxy-terminal phosphorylation, c-Rel requires serine/threonine phosphorylation to activate transcription in response to TNF and PMA treatment or CD28 cross-linking (120-122). Although the specific phosphoacceptor sites as well as the kinase(s) involved in c-Rel carboxy-terminal phosphorylation have yet to be fully characterized, protein kinase C ζ (PKCζ) and Akt/protein kinase B (Akt/PKB) target a critical S471 residue of c-Rel in response to TNFα, but not PMA treatment (121,123). The phosphorylation status of NF-κB subunits is ultimately determined via the interplay between kinase and phosphatase activity. For example, in resting melanocytes an association between PP2A and p65 precipitates shut-off for NF-κB activation following IL-1 stimulation, through dephosphorylation of p65 (124).

Reversible acetylation of p65 represents another level of NF-κB regulation post IκB degradation (125). Acetylation at K122 and K123 by the intrinsic acetyl transferase activity of p300/CBP or the p300/CBP-associated factor (PCAF) prolongs p65 DNA binding and transactivation potential in the nucleus, by inhibiting IκB-mediated export

while sustaining the CBP/p300 interaction (126-128). Treatment with the deacetylase inhibitor trichostatin A (TSA) prolonged both basal and inducible p65-dependent gene transcription through enzymatic inhibition of the histone deacetylase (HDAC)-1, which directly associates with p65 (129). Phosphorylation state directly modulates the acetylation state of p65, such that phosphorylation at S276 promotes association with CBP/p300, while in the unphosphorylated state p65 preferentially interacts with HDAC activity (130).

1.3 Inducible NF-κB signaling pathways

1.3.1 Innate immune signaling

Innate immunity represents an ancient and evolutionarily conserved mechanism for detection and clearance of foreign material and pathogens (131,132). In the plant and animal kingdoms, innate immune responses are triggered by a set of germline-encoded pathogen receptors called Toll-like receptors (TLRs) (132,133). In mammalian cells, TLRs display limited expression on the surface of pathogen-susceptible cells of the epithelia and endothelium, and higher representation on effector cells of the innate immune machinery such as macrophages, polymorphonucleur leukocytes, mast cells and DC (134). TLRs recognize biochemically conserved molecules that are exclusive to foreign pathogens. Collectively termed pathogen-associated molecular patterns (PAMPs), gram-negative bacterial LPS, bacterial flagellin or viral dsRNA represent ligands that initiate innate immune responses through TLR signaling (133).

Activation of NF-κB is crucial to establishment of innate immunity, and engagement of all 10 mammalian TLR induces NF-kB signaling (133). Signaling events from TLR ligation to NF-κB activation have been particularly well characterized with respect to mammalian TLR4, which recognizes the lipotechoic acid moiety within gram negative bacterial LPS (135,136). In association with LPS binding protein (LBP), LPS is recognized by a receptor heterocomplex of TLR4, the membrane receptor CD14 (137), and the TLR4-associated protein MD-2 (138). Engagement of TLR4 by LPS precipitates a sequential recruitment of signaling molecules to the conserved, intracellular region of the receptor called the Toll/IL-1 receptor (TIR) domain (139). Common to all

mammalian TLRs, the TIR domain adaptor molecule myeloid differentiation factor 88 (MyD88) (140-142) in association with the TIR adaptor protein/MyD88 adaptor (TIRAP/Mal) (143,144) mediates NF-κB activation downstream of TLR4. Once bound to the receptor as a dimer via carboxy-terminal TIR-TIR interactions, the amino-terminal region of MyD88 recruits the serine/threonine IL-1 receptor-associated kinases IRAK4 and IRAK1, through protein-protein interactions mediated via intrinsic death domains (141,145-147). Activated upon recruitment to MyD88, IRAK4 hyperphosphorylates IRAK1, which interacts with the adaptor molecule TNF receptor associated factor 6 (TRAF6), an E3 ubiquitin ligase (148). A complex of IRAK1-IRAK4-TRAF6 then disengages from the receptor, to associate with a membrane-bound complex of the serine/threonine kinase transforming growth factor-β-activated kinase 1 (TAK1) (149), TAK1 binding protein 1 (TAB1) and TAK1 binding protein 2 (TAB2) (150). Formation of the IRAK1-IRAK4-TRAF6-TAB2-TAB1-TAK1 complex (151,152) mediates direct activation of the IKK complex downstream of TRAF6 (151,153). This event is regulated via essential proteolysis-uncoupled ubiquitination signals: the E3 ubiquitin ligaseTRAF6 functions with the ubiquitin conjugating enzyme Ubc13 and the Ubc-like protein Uev1A to catalyze the synthesis of unique K63-linked polyubiquitin chains (154) attached to TAK1 (155), the IKK complex and TRAF6 itself (154).

Because they mediate the downstream events of TLR signaling through specific protein-protein interactions, the differential use of TIR adaptor molecules such as MyD88, TIRAP/Mal, TIR-containing adaptor molecule-1/Toll/IL-1 receptor domain-containing adaptor inducing IFN-β (TICAM-1/TRIF) (156-158), TIR-containing adaptor molecule-2/TRIF-related adaptor molecule (TICAM-2/TRAM) (159,160) and sterile alpha and HEAT/armadillo motif (SARM) (161) confers some of the specificity to TLR signaling. For example, MyD88 and TIRAP/Mal are absolutely required for NF-κB activation downstream of TLR2, TLR5, TLR7 and TLR9 (162,163). However, in response to TLR4 ligation, activation of NF-κB signaling is partially intact in MyD88-deficient DC at a delayed kinetics (164). Similarly, TLR3 recognition of viral dsRNA stimulates IκBα degradation at a slightly slower rate in MyD88-/- macrophages than in WT cells (165). The compensation occurs through the MyD88-independent pathway mediated by the TIR

adaptor molecules TICAM-1/TRIF (156,158,160) for TLR3, and TICAM-1/TRIF (156,158,160) and TICAM-2/TRAM (159,160) for TLR4. Macrophages and DC isolated from MyD88 and TRIF DKO mice are completely refractory for NF-κB activation induced by TLR3 and TLR4 ligation (158,166). However, the MyD88 and TRIF-specific pathways to NF-κB activation are not redundant. Proper induction of the innate immune response through TLR3 or TLR4 ligation requires both MyD88-dependent and TRIF-dependent signaling, because there are distinct genetic profiles elicited by each one (156,158-160,166,167). MyD88- and TRIF-dependent signaling is discussed in detail in section 3.0, with respect to the interferon regulatory factor 3 (IRF-3) and IRF-7 signaling pathway. Downstream of TLR3 and TLR4 engagement, activation of IRF-3 and IRF-7 lies parallel to NF-κB signaling and confers specificity to the TRIF-dependent genetic profile (156,157,159,160,166,168).

1.3.2 Pro-inflammatory cytokine signaling

Once activated through pathogen-recognition receptors, effector cells of the innate immune machinery produce proinflammatory cytokines such as IL-1 and TNFα, which activate circulating lymphocytes and leukocytes. Signaling events initiated by IL-1 are highly analogous to LPS (141,146,151,169), due to homology between the cytoplasmic domains of the IL-1 receptor and TLR4 (170). In contrast, TNF signaling is initiated from a heterologous superfamily of TNF receptors that are expressed by a wide variety of cells (171). Binding of TNF to the extracellular domain of TNFR1 results in receptor homotrimerization and dissociation of an intrinsic receptor-associated inhibitor, silencer of death domains (SODD), from the cytoplasmic portion of TNFR1 (172,173). The exposed TNFR1 death domain (DD) is subsequently recognized by the TNF receptor-associated death domain (TRADD) adaptor molecule (174), which recruits DD-containing proteins such as TNF receptor-associated factor 2 (TRAF2) (175). Signaling from TRAF2 to classical IKK activation involves a number of intermediate kinases, including mitogen activated protein (MAP)/extracellular signal-regulated kinase (ERK) kinase kinase 3 (MEKK3) and receptor-interacting serine/threonine kinase (RIP) (176-178). The mechanism involves direct IKK recruitment to TNFR1 at the membrane, via an association between TRAF2-associated RIP and IKKγ/NEMO (176). Activation of NF-

κB signaling downstream of TNFR1 requires signaling that involves proteolysis-uncoupled ubiquitination events specific for TRAF2 and NEMO. Brooke-Spiegler syndrome (BSS, familial cylindromatosis or turban tumor syndrome) is an inheritable disease that is characterized by neoplasms of the skin appendages (179,180). Recently, the protein encoded at the familial cylindromatosis (CYLD) gene locus (179,180) was shown to encode for a deubiquitinase activity specific for K63-linked ubiquitin chains, which are not coupled to protein degradation (181,182). The CYLD tumor suppressor directly interacts with both TRAF2 and NEMO, to negatively regulate TRAF-mediated NF-κB activation through deubiquitination of K63-specific ubiquitin linkages (181,182). It has been proposed that heritable mutations in *cyld* that reduce its enzymatic activity are associated with a loss of negative regulation of cytokine-induced NF-κB activation, which is required for appropriate cellular homeostasis of the skin appendages (181,182). While these observations demonstrate the essential role of K63-specific ubiquitin signaling for activation of NF-κB signaling by TRAFs, they also emphasize how disruption of proper NF-κB homeostatic control is associated with tumor formation and cancer.

1.3.3 T-cell receptor engagement

In T-lymphocytes, activation of NF-κB signaling by antigenic stimulation requires signals delivered through an antigen-specific TCR and a co-stimulatory CD28 receptor. High affinity TCR engagement induces antigen receptor clustering by reorganization of the plasma membrane by TCR-associated lipid raft domains, which promotes the recruitment of a multi-protein signaling complex to the "immunological synapse" formed between an antigen-specific T-lymphocyte and a proffesional antigen presenting cell (APC) (183,184). In response to antigen or antigen-mimetic stimuli, members of the PKC family of serine/threonine kinases translocate to the site of TCR clustering to initiate signaling events that are essential for mature T-lymphocyte activation (185,186). Preferentially expressed in T-lymphocytes (187), PKCθ co-localizes with the TCR at the immunological synapse. Antigen-mediated T-cell responses activate PKCθ signaling, which regulates transcription of early immune-response genes through activation of the activating protein 1 (AP-1) and NF-κB pathways (188,189). While thymocyte

development and differentiation occurs normally in PKCθ-deficient mice, the mature T-cells display reduced proliferative responses to antigen-mimetic stimulation which are associated with decreased expression of the T-cell growth factor Interleukin 2 (IL-2) as well as the high affinity IL-2 Receptor α chain (IL-2Rα) (190). In PKCθ-/- T-cells, degradation of IκBα and DNA binding of NF-κB were specifically abolished in response to antigen mimetic CD3/CD28 cross-linking and PMA treatment, but not TNF or IL-1 stimulation. Treatment with PMA in combination with ionophore, which increases intracellular calcium concentration, partially restored NF-κB activation and the proliferative response of PKCθ-/- deficient mice, presumably through functional compensation by heterologous PKC isoforms activated by calcium signaling (190). Although numerous signaling intermediates have been implicated the process, signaling from PKC to the classical IKK complex is not well understood, and may include regulatory kinases such as Cot/TPL2, MEKK1, NIK and mixed lineage kinase (MLK) (36,191,192). The major signaling pathways that lead to inducible NF-κB activation in mammalian cells are summarized schematically by Figure 4.

1.3.4 The non-canonical pathway

An IκB-independent, alternate NF-κB signaling pathway involving post-translational processing of pro-protein p100 to mature p52 has recently been characterized. In contrast to cleavage of precursor p105 to liberate mature p50, a constitutive event *in vivo* (193,194), generation of p52 from p100 is signal-responsive, ensuring that the majority of cells have a low p52 to p100 ratio (194). Analysis of cells derived from KO animals demonstrated that the regulatory kinases NIK and IKKα were required, in a non-redundant manner, for p100 processing to p52 (195,196). This observation is underscored by a marked phenotypic similarity shared by NIK, IKKα and NF-κB2/p100-deficient mice, which show specific abnormalities in B-cell development and associated humoral responses (195,197). In fact, these defects are reminiscent to those observed in mice deficient for the B-cell activating factor (BAFF), a TNF superfamily ligand expressed on monocytes, macrophages and DC (198). Examination of the secondary lymphoid organs of BAFF-deficient mice revealed a near complete loss of follicular and

Figure 4. Signaling pathways to inducible NF-κB activation Cellular signaling pathways to inducible NF-κB activation converge upon catalytic induction of the classical IKK complex, catalytic kinase subunits IKKα and IKKβ and structural adaptor subunit NEMO/IKKγ. Signaling components and intermediates for the pro-inflammatory cytokine TNFα are shown at the far left. Binding of a homotrimer of TNF to its receptor can trigger opposing pathways to apoptosis/cell death or NF-κB activation. TNF-mediated binding of TRADD and TRAF2 to the intracellular portion of the receptor recruits the IKK complex to the receptor via interactions mediated by NIK. These events require proteolysis-uncoupled ubiquitination events specific to TRAF2 and NEMO, mediated in part by the ubiquitin ligase complex Ubc13-Uev1. LPS/TLR4 signaling to NF-κB by the MyD88-depedent pathway is shown in the middle. MyD88 recruits IRAK1, IRAK4 and TRAF6. The complex dissociates from the receptor to interact with TAK1-TAB1-TAK2 at the membrane. The TRAF6-TAK complex dissociates from the membrane to activate the IKK complex, an event that is also dependent on proteolysis-uncoupled ubiquitination events specific to TRAF6, TAK1 and NEMO, mediated in part by the ubiquitin ligase complex Ubc13-Uev1. Signaling from the TCR to classical IKK activation can be mediated by the PKC or Akt/PKB kinases. Activation of the classical IKK complex results in phosphorylation of IκBα on serines 32 and 36, which induces proteolysis-coupled ubiquitination via the β-TRCP ubiquitin ligase complex. Release of NF-κB dimers results in their nuclear import, DNA binding and transactivation capacity; NF-κB-driven upregulation of IκBα completes a negative feedback loop.

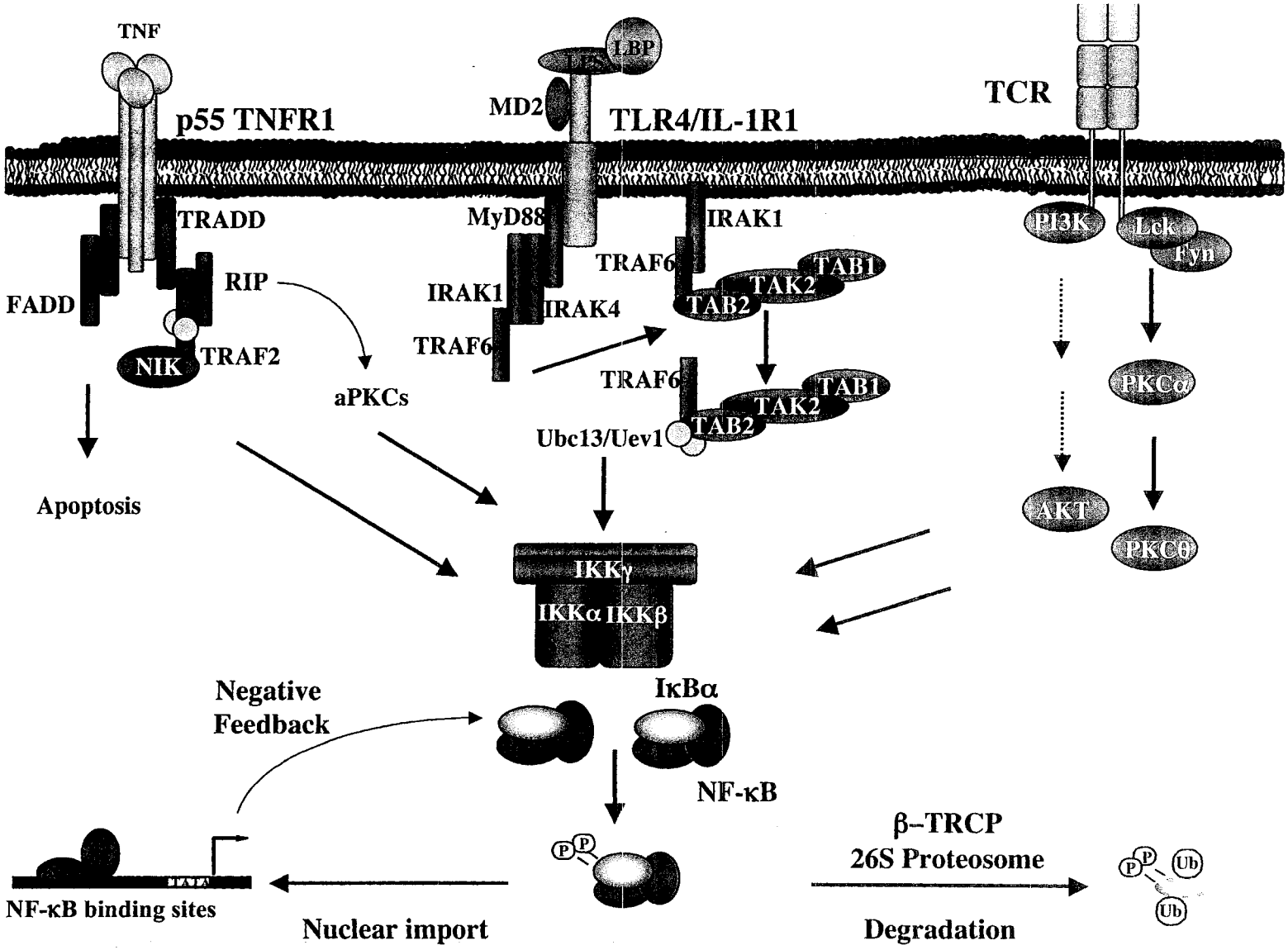
TNF
p55 TNFR1
TRADD
FADD
RIP
NIK
TRAF2
Apoptosis
aPKCs
LBP
MD2
TLR4/IL-1R1
MyD88
IRAK1
IRAK4
TRAF6
TRAF6
IRAK1
TAB1
TAK2
TAB2
TRAF6
TAB1
TAK2
TAB2
Ubc13/Uev1
TCR
PI3K
Lck
Fyn
PKCα
AKT
PKCθ
IKKγ
IKKα IKKβ
IκBα
NF-κB
Negative
Feedback
NF-κB binding sites
Nuclear import
β-TRCP
26S Proteosome
Ub
Ub
Degradation

marginal zone B- lymphocytes, due to increased sensitivity of the developing B-lymphocytes to apoptosis (198). Applying an *in vivo* culture system to monitor B-cell differentiation from bone marrow precursors, Claudio et al. demonstrated that BAFF signaling through the BAFF Receptor (BAFF-R) on the surface of B-cells and immature splenocytes stimulates p100 processing, which is required to promote B-cell survival and subsequent progression through the maturation process (199). While absolutely dependent upon expression of NIK and IKKα, this non-canonical pathway to NF-κB activation is independent of IKKβ, IKKγ/NEMO and IκBα (199).

The non-canonical pathway to NF-κB activation also lies downstream of CD40 receptor ligation (200), which promotes B-cell survival at the immunological synapse (201), and lymphotoxin β(LTβ) signaling, which regulates organization of the lymphoid tissue (202). Alternate NF-κB signaling is subunit specific, liberating a dimer of p52 bound to RelB that is pre-associated with p100 in latent splenic B-cells (200). The specificity of non-canonical NF-κB signaling, as highlighted by gene profiling of the LTβ response by DNA microarrays (202), is defined by the two distinct subsets of NF-κB-driven genes activated downstream of LTβ ligation: the classical NF-κB pathway regulates a set that includes proinflammatory molecules such as VCAM-1, MIP-1β, and MIP-2, while non-canonical NF-κB signaling controls induction of specific chemokines and cytokines that modulate lymphoid organogenesis, notably BAFF itself (202). Characterization of classical and non-canonical NF-κB activation emphasizes the complex organization of the cellular NF-κB response *in vivo*, and illustrates how specificity is achieved for NF-κB-driven gene expression within the global response.

1.4 NF-κB signaling during virus infection

1.4.1 Activation of cytokine gene transcription

During virus infection, activation of NF-κB signaling represents an immediate early event that is essential to establishment of an anti-viral immune response. Virus-inducible NF-κB activation can be mediated by multiple and distinct mechanisms. For example, engagement of TLR3 by viral dsRNA (165) activates the classical IKK complex through MyD88-dependent and MyD88-independent mechanisms (163). However, it is not

entirely clear whether dsRNA/TLR3 signaling represents a mechanism for direct, intracellular detection of viral replication in an infected cell, or if TLR3/dsRNA signaling is initiated as a secondary signal by neighboring cells responding to extracellular dsRNA released by virus-infected cells. Intracellular activation of NF-κB signaling by virus infection is mediated in part by the viral dsRNA-activated protein kinase (PKR), an upstream activator of the classical IKK complex (203-206). However, it is still controversial if the serine/threonine kinase activity of PKR is required during NF-κB activation, or if PKR functions as a structural/scaffolding molecule upstream of IKK activation by dsRNA (206,207). Nevertheless, activation of the IKK complex drives the production of a multitude of immunomodulatory genes, encoding chemokines (RANTES, IL-8), adhesion molecules (endothelial leukocyte adhesion molecule, vascular cell adhesion molecule and intercellular adhesion molecule), cytokines (Interferons, IL-1, IL-2, IL-6, TNFα and IL-12), transcription factors (c-Rel, c-Myc) and co-stimulatory molecules (B7.1, B7.2) in innate immune cells (1).

The importance of inducible NF-κB activation in development of innate anti-viral immunity is underscored by studies undertaken in MEFs derived from IKKβ–deficient mice. Loss of IKKβ expression severely impaired inducible NF-κB activation in response to dsRNA treatment or Vesicular Stomatitis Virus (VSV) infection (208). The lack of NF-κB activation in IKKβ–deficient cells was associated with significant decreases in virus-induction of immune response cytokines such as type I interferon β (IFNβ), IL-6 and IL-12 (208). Inducible NF-κB activation therefore plays an essential role in promotion of the cellular anti-viral response, however this is discussed in detail with respect to transcriptional regulation of type I IFNβ in section 2.1.3.

1.4.2 Development of adaptive immunity

As detailed in section 1.1.3, KO mice for individual NF-κB subunits exhibit immunodeficiency with respect to the mature lymphocyte adaptive responses, including reduced T- and B-cell proliferation, reduced immunoglobulin secretion and an overall impaired immune function in response to antigen-specific stimulation (2). Although gene disruptions of individual NF-κB subunits have not been correlated with abnormalities in

early lymphocyte development, this phenomenon was long thought to reflect a functional redundancy of NF-κB in lymphocyte development. For example, p50/p52 DKO mice completely lack mature T-cells, while p65/p50 DKO mice exhibit aberrant lymphoid architecture and an absence of mature T-cells in the periphery (2). Irradiated mice reconstituted with *ikk2-/-* fetal liver stem cells do not undergo lymphopoiesis; however, deletion of the TNFR1 in *ikk2-/-* chimaeras restores T-cell development, indicating that IKK2-dependent NF-κB activation does not serve a developmental role *per se*, but is required to protect from TNF-induced apoptosis (209). Transgenic mice engineered to express the 2NΔ4 IκBα super-repressor under the control of a T-cell-specific promoter showed an impaired T-cell proliferative responses from inhibition of classical NF-κB signaling in the T-cell compartment (210). Development of Th1 responses was impaired in these mice, due to diminished induction of pro-inflammatory cytokines such as IL-2, IL-18 and IFNγ in the mutant T-cells (2,210).

1.5 Viral appropriation of NF-κB signaling by HTLV-I

One of the most well characterized examples of viral interference with NF-κB signaling is appropriation of the pathway by the Human T-cell Leukemia/Lymphotropic Virus Type I (HTLV-I) (211,212). At present, between 20 and 30 million people worldwide are infected with HTLV-I, a deltaretrovirus that is endemic to parts of South America and the Middle East, the Caribbean basin, sub-Saharan and central Africa, southern Japan and southeast Asia (213,214). Infection with HTLV-I is etiologically associated with Adult T-cell Leukemia (ATL), an aggressive and often fatal malignancy of CD4+ T-cells (215-217) as well as HTLV-I-associated Myelopathy/Tropical Spastic Paraperesis (HAM/TSP), a demyelinating syndrome of the central nervous system (CNS) (218). While the cumulative lifetime risk of developing these incurable diseases represents approximately 5% of infected individuals, HTLV-I infection and its associated diseases are presenting an increasing challenge in areas where the virus is endemic (213). Furthermore, co-infection with HTLV-I and HIV has been shown to accelerate the progression of acquired immune deficiency syndrome (AIDS), which represents an increasing phenomenon encountered by clinicians in North America and Europe (213,219,220).

1.5.1 The Tax oncoprotein

The HTLV-I core particle contains two copies of genomic RNA associated with the viral reverse transcriptase, protease, RNase H and integrase (221). Upon virus entry into activated T-cells via the glucose transporter GLUT-1 component of the cellular HTLV-I receptor (222), viral RNA is reverse transcribed and integrated into the host genome as a provirus. Although proviral insertion is not site-specific, HTLV-I appears to have a slight preference for GC rich regions of the host genome (223). The integrated HTLV-I provirus encodes for proteins involved in virus infetivity, replication and transformation; the 9 032 base pair sequence is organized into 5' and 3' long terminal repeats (LTR), a *gag* gene that encodes structural proteins, an *env* gene that encodes the envelope proteins, *pro* and *pol* genes that respectively encode for the viral protease and reverse transcriptase genes, and a 3' regulatory region termed pX, which encodes regulatory proteins involved in reprogramming host cell function (224).

While HTLV-I has the capacity to infect several cell types *in vitro*, including lymphocytes, macrophages, DC, immature bone cells and neural cells, the majority of provirus is detected in CD4+CD45RO+ T-cells *in vivo* (225). HTLV-I infection of these cells alone is associated with oncogenesis, which may reflect the capacity of the virus to replicate to higher levels in these cells when compared to CD8+ T-cells, for example (226). HTLV-I infection transforms CD4+ T-cells *in vitro* (227) and *in vivo* (216), a process that has been associated with deregulation of cellular genes involved in T-cell activation and proliferation during the course of virus infection (228). Virus-induced deregulation of the lymphocyte gene expression pattern, a key event in HTLV-I-induced transformation, is attributed to the activity of the HTLV-I encoded 40-kDa Tax oncoprotein. A regulator of cellular and viral gene expression, Tax is transcribed early in virus infection from the distal pX coding region of the HTLV-I genome, which lies adjacent to the 3' LTR (229,230). Several independent lines of evidence indicate that Tax represents the oncogenic potential of HTLV-I (231). Ectopic expression of the *tax* gene is necessary and sufficient to immortalize primary human T-lymphocytes (232,233). Also, Tax synergizes with the cellular Ras oncogene to transform primary Rat-1

fibroblasts *in vitro*, which form tumors when subsequently injected into nude mice (234,235). Depending on the nature of the targeting vector used for delivery, mice stably expressing the *tax* transgene have been shown to develop soft tissue tumors (236,237) or large granular lymphocytic leukemia (238).

The mechanism by which Tax induces cellular transformation has been the focus of intensive research. To modulate both viral and cellular gene expression, phosphoprotein Tax (239) shuttles between the cytoplasmic and nuclear compartments of the infected T-cell (240,241); lacking a classical DBD, Tax alters gene expression through functional protein-protein interactions with the cellular transcription and cell cycle machinery (211,212,228). Figure 5 describes several discrete domains of Tax involved in specific interactions with host cell proteins. For example, proviral gene transcription from the 5' HTLV-I LTR is driven by an interaction between the amino-terminal domain of Tax with the basic leucine zipper (bZip) domain of the cellular cyclic AMP response element binding factor/activating transcription factor (CREB/ATF) proteins (211,242,243). Through selective affinity for the G/C-rich regions flanking the 21 base pair cAMP responsive element (CRE) binding sites within the 5' LTR, Tax guides CREB/ATF dimers to the proviral promoter (244,245). Acting as a molecular bridge, the carboxy-terminal of Tax recruits the transcriptional coactivator CBP to the CREB/ATF dimer, which drives proviral transcription (246,247). The limiting CBP concentrations within a host cell ensure that high Tax expression during the early stages of HTLV-I infection alters the cellular gene expression profile, by favoring transcription driven by proteins which bind to Tax, such as CREB/ATF, serum response factor (SRF) and NF-κB (211,212,228,248). Alterations in gene expression occur at the expense of cellular genes regulated by proteins that do not bind the viral oncoprotein, a passive repression through competition for limiting cellular CBP (249-251).

1.5.2 Tax activation of NF-κB signaling

HTLV-I infected, Tax-expressing cells are characterized by constitutively nuclear, chronically activated NF-κB dimers which drive the expression of numerous genes

Figure 5. The HTLV-I Tax oncoprotein The oncogenic potential of HTLV-I is largely attributed to the 353 amino acid, 40-kDa viral Tax protein. Tax contains an amino-terminal nuclear localization signal (NLS) that permits cytoplasmic-nuclear shuttling. Tax modulates host T-cell homeostasis by specific protein-protein interactions with cellular proteins, which is mediated through its zinc domain (ZN) as well as two activation domains (AD-I and AD-II). AD-I contain specific regions involved in CBP/p300 binding (aa81-95), NF-κB activation and dimerization (aa123-204). AD-II contains specific regions involved in HTLV-I LTR transactivation (aa284-325). Specific residues necessary for CREB activation (aa113, aa130, aa160, aa258) and NF-κB activation (aa315, aa317, aa319, aa325) are interspersed throughout the protein.

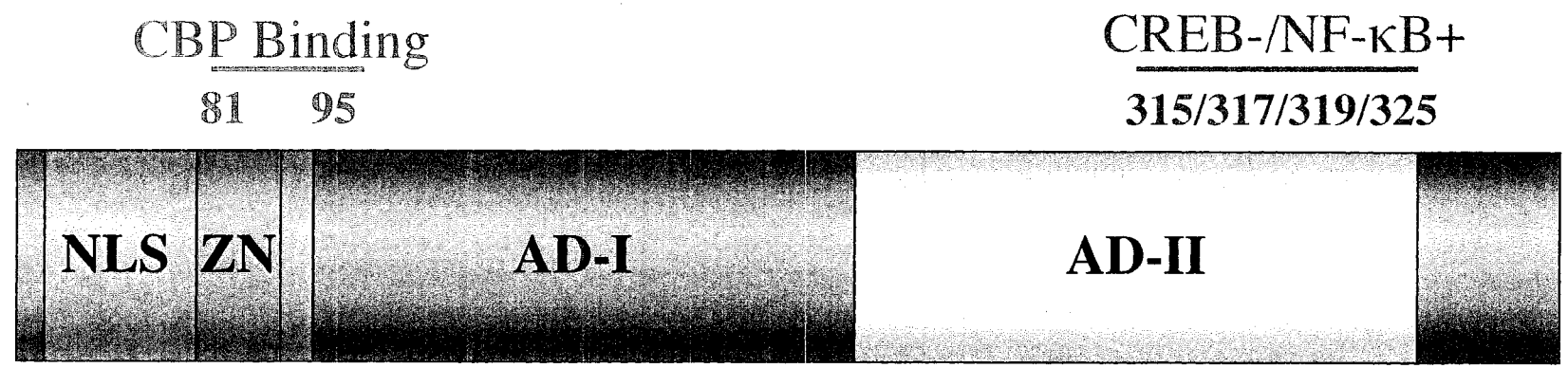
CBP Binding
81 95
CREB-/NF-κB+
315/317/319/325
NLS
ZN
AD-I
AD-II
2 59
113 130 160 258
353
CREB Binding
CREB+/NF-κB-
Dimerization Domain
NF-κB Activation
aa123-204
HTLV-I
Transactivation
aa284-325

(211,212,228), including IL-6 (252), granulocyte macrophage colony stimulating factor (GM-SCF) (253) and c-Myc (254). Activation of NF-κB signaling in HTLV-I infected cells is proposed to mediate virus-induced T-cell leukemogenesis. For example, growth of the chronically HTLV-I infected cell line MT2 or fibroblastic tumors isolated from Tax-transgenic mice are inhibited by anti-sense oligonucleotides to p65 or p50 (255). Several observations might explain the mechanism of Tax-mediated NF-κB activation. For example, Tax physically interacts with the PKC isoforms PKCα, PKCδ and PKCη, and pre-treatment with a pharmacological inhibitor of PKC, Calphostin C, blocks NF-κB DNA binding in Tax-expressing T-cells (256). Transfection of Tax mutant M22, which is specifically defective in activation of NF-κB signaling (257), fails to induce PKC membrane translocation (256). The link between Tax-PKC interaction and activation of NF-κB signaling is strengthened by recent experiments demonstrating that TCR-derived signals to NF-κB activation require the catalytic activity of PKCα, which is upstream of PKCθ activation (258).

Expression of Tax directly transactivates the c-Rel and p100 promoters, through an NF-κB-driven positive feedback loop (259). In addition, direct interactions between Tax and several IκB and NF-κB proteins has also been reported. Tax physically associates with the ankyrin repeats of IκBγ (260) and with the RHD of p50 (261), p65 (262,263), c-Rel (259,263), p100 (259,264) and p105 (265). In a manner similar to CREB/ATF, interaction with the DNA binding subunits of NF-κB favors gene expression by bridging to p300 (266,267). Furthermore, recent characterization of non-canonical NF-κB activation in HTLV-I infected cells indicates that Tax interaction with p100 (259,264) is associated with constitutive processing of p100 to p52 in a NIK and IKKα-dependent manner (195,268).

The primary mechanism for Tax-mediated NF-κB activation involves direct activation of the classical IKK complex, which mediates constitutive IκB processing. Kinase dead, dominant negative mutants of IKKα and IKKβ inhibit Tax-mediated activation of NF-κB-driven promoters, while Tax mutants incapable of interacting with the IKK complex

do not activate NF-κB-driven gene transcription (269). In T-cell lines, Tax expression is associated with an elevated enzymatic activity of endogenous IKK complexes, which correlated with the phosphorylation and increased turnover of IκBα (269,270). Results obtained from genetic complementation in fibroblasts deficient for expression of IKKγ/NEMO indicate that expression of the adaptor protein is essential for the formation of an active complex between Tax and the classical IKK complex (81), and T-cell clones defective for Tax-mediated NF-κB-activation were rescued by forced expression of wild type IKKγ/NEMO (271). Similarly, interference with NEMO/IKKγ expression in T-cell lines using anti-sense oligonucleotides specifically abolished Tax-mediated NF-κB activation, although activation CREB/ATF remained intact. A direct interaction between Tax and IKKγ/NEMO is required to activate classical IKK signaling (272-274). Specifically, Tax contacts two carboxy-terminal LZ domains within IKKγ/NEMO, which is linked to IKKα and IKKβ through the amino-terminal. The interaction is believed to recruit heterologous upstream regulatory kinases such as NIK or MEKK1, which phosphorylate IKKα and IKKβ within the activation loop. Alternatively, Tax interaction with IKKγ/NEMO may be sufficient to confer constitutive kinase activity in HTLV-I infected cells through enhanced autophosphorylation of IKKα and IKKβ (272-274).

1.5.3 Tax activation of NF-AT signaling

The nuclear factor of activated T-cells (NF-AT) family of transcription factors play a pivotal role in inducible gene expression during the immune response (10). Five structurally related subsets of NF-AT proteins are differentially expressed in various classes of immune and non-immune cells (10), and have been implicated in the direct regulation of cytokines, cell surface receptors and transcription factors (275). The NF-AT proteins are activated through stimuli that elicit calcium mobilization, such as engagement of the antigen receptor on B- and T-cells or the Fcγ receptor on Natural Killer (NK) cells and macrophages (10). In unstimulated cells, hyperphosphorylation confines NF-AT proteins to the cytoplasm in a closed conformation that masks the NLS (276-278). Signals that elicit intracellular calcium concentrations to rise rapidly activate a number of cytoplasmic enzymes, including the serine/threonine phosphatase calcineurin (279), a direct upstream regulator of NF-AT signaling (278,280,281). Active calcineurin

dephosphorylates NF-AT proteins, which induces a conformational change that unmasks the NLS and allows for nuclear translocation (278,282) and DNA binding, which is favored in the unphosphorylated state (277,278,280). Activation of NF-ATs is sensitive to immunosuppressive drugs cyclosporin A (CsA) and FK506, which bind and inhibit calcineurin (279).

The NF-AT signaling cascade is also a target for viral appropriation by the HTLV-I Tax oncoprotein. Consistent with the essential role of NF-AT transcription in regulation of mature T-cell activation events and cytokine signaling (283,284), NF-AT signaling during HTLV-I infection upregulates a number of T-cell specific immunomodulatory genes. Stable expression of the *tax* gene in a T-cell line is sufficient to induce nuclear accumulation and DNA binding of NF-ATs, specifically subunits NF-ATp/NF-AT1 and NF-ATx/NF-AT4 (285). A Tax-responsive DNA enhancer region termed the CD28-response element (CD28RE), which binds NF-AT subunits in conjunction with NF-κB proteins (286), drives production of the T-cell growth factor IL-2 in HTLV-I infected T-cells (285,287). In fact, T-cell lines transformed by HTLV-I or expressing Tax are characterized by nuclear NF-AT complexes (285,287), which directly transactivate the IL-2 promoter through the CD28RE enhancer (285,287). Although the precise mechanism of NF-AT activation by Tax remains to be fully understood, a correlation may be made with the HBx transactivator protein of Hepatitis B Virus (HBV) (288). Similar to Tax, expression of HBx is likewise associated with alterations in cytosolic calcium concentrations, which is a fundamental requirement for HBV replication (288). It was recently demonstrated that HBx specifically targets mitochondrial calcium stores within the cell, which is associated with activation of cytosolic calcium-dependent signaling molecules such as calcineurin and the proline-rich tyrosine kinase-2 (Pyk2). This property of HBx is essential for its transactivator function, and inhibition of mitochondrial calcium signaling abolished HBx-induced replication of the HBV genome (288).

2. Interferon regulatory factors (IRF) and virus infection

Initially identified for their capacity to regulate the virus-inducible type IFN promoters in synergy with NF-κB proteins, the interferon regulatory factor (IRF) transcription factors incorporate nine mammalian proteins (289). IRFs regulate numerous aspects of the immune response, from cytokine signaling and cell growth regulation to hematopoietic development and effector function in the periphery (289-291). IRFs are identified by a canonical amino-terminal DBD containing a characteristic helix-turn-helix motif and five tryptophan repeat sequence that mediates differential recognition of the DNA consensus sequence G(A)AAAG/CT/CGAAAG/CT/C. These IRF elements (IRF-E), or Interferon Stimulated Response Elements (ISRE) regulate the expression of genes that include cytokines, chemokines, cell surface receptors and proteins involved in anti-viral defense (289-291).

2.1 Type I Interferon: an archetype of virus-activated signal transduction

Virus infection of a mammalian host triggers the innate immune program, a set of rapid and coordinated cellular events designed to elicit genetic responses that will limit and ultimately eradicate pathogen replication and spread (292). During virus infection, development of an efficient anti-viral response depends on proper communication between cells at the site of infection and immune effector cells. Once the viral threat is recognized, communication is achieved through production and secretion of cytokines that recruit immune machinery while restricting virus multiplication in infected or susceptible cells (293-295). IFN are cytokines that are crucial to establishment of the innate anti-viral immune response: virus-inducible type I IFN (IFNα and IFNβ) act in a n autocrine and paracrine fashion through cognate IFN receptors to induce a multitude of inteferon stimulated genes (ISG) that modulate innate and adaptive immunity, promote apoptosis of virally infected cells and provoke a well-characterized genetic anti-viral program in uninfected cells (294,296,297).

2.1.1 Biological activity of type I interferon

As one of the first lines of defense against virus infection, rapid induction of type I IFN represents the first wave of the cytokine response, occurring hours to days before development of adaptive immunity (294,296,297). Genes of the type I IFN superfamily are divided into four structurally related groups found clustered together on the short arm of chromosome 9: a single IFNβ, at least 12 functional IFNα, an IFNω and an IFNτ display differential expression patterns (298). IFNβ production and secretion is mediated by fibroblasts, expression of IFNα subsets and IFNω is predominantly associated with hematopoietic cells, while IFNτ is expressed by trophoblasts in early pregnancy (294). Sharing between 25 and 30% homology within the coding sequence, IFNα and β are often co-expressed due to additional homology within the upstream regulatory regions (298). The virus-inducible type I IFNα and -β genes are further subdivided into two groups, based on their temporal pattern of expression during the course of a virus infection (294): in humans, the immediate-early IFNβ and IFNα1 genes are rapidly induced without the need for *de novo* protein synthesis to be joined by a second set of IFNα genes, including IFNα4, which are synthesized and expressed later as a result of ongoing cellular protein synthesis (294,299).

The type I IFNs were isolated based on their fundamental ability to inhibit virus replication (300-302). As a result, recombinant type I IFNs are clinically applied to the treatment of chronic hepatitis associated with HCV and HBV infection as well as genital warts caused by infection by papilloma virus (297). In tissue culture conditions pre-treatment with type I IFN decreases viral output, while virus challenge to type I IFN-sensitized mice reduces viral load and pathogenesis *in vivo* (294). The importance of type I IFNs for anti-viral immunity is truly underscored by the defective immunological response of mice that lack genes encoding essential components of type I IFN signaling. Disruption of the type I IFN Receptor (IFNAR1) gene precipitates unresponsiveness to the effects of type I IFN (303,304). While control littermates mounted an efficient anti-viral response and effectively cleared viral challenge, *ifnar1*-/- mice could not control the virus infection, and exhibited increased morbidity and high viral load in the organs (303,304). Analysis of cell lines derived from *ifnar1*-/- mice revealed an absence of

virus-induced expression of Interferon Stimulated Genes (ISGs), the effector molecules of type I IFN signaling that directly precipitate the cellular anti-viral state (294,296,297,303,304). Transcriptional profiling of the IFN-response using DNA microarrays indicates that ISGs account for 100 to 300 distinct loci, depending on the particular cell type or IFN subtype analyzed (305-307). The ISG superfamily incorporates signaling intermediates, transcription factors, cytokines and chemokines, antigen presentation proteins and apoptotic regulators that mediate the pleiotropic effects of IFN with respect to anti-viral immunity, immunomodulation and cell growth inhibition (296,297,308). In susceptible cells, induction of ISGs directly targets the virus life cycle at every step, from virus fusion/entry and genome uncoating to viral gene transcription and translation initiation to assembly/maturation and release (296). Although the anti-viral properties of the majority of ISGs remain to be characterized, several molecular systems are well understood as fundamental components of the type I IFN anti-viral genetic program (296,297,308).

The multiprotein family of type I IFN-induced 2'-5' oligoadenylate (2'-5'oligo(A)) synthetase enzymes catalyze polymerization of ATP into short, 2'-5'-linked oligoadenylate signaling molecules (309). In addition to regulation at the transcriptional level, each enzyme within the family is regulated at the level of catalytic activation: for maximal activity, they require activation by a 15-25 bp stretch of viral dsRNA (310). The relatively small proteins must oligomerize to function, and once activated initiate a cellular response by 2'-5' oligo(A)-mediated activation of the latent ribonuclease RNase L. Dimerization of RNase L upon binding to 2'-5' oligo(A) (311) initiates non-specific cleavage of mRNA species within virus infected cells, ensuring that both cellular and viral protein synthesis is impaired by activation of this system.

One of the most well characterized components of the ISG system, the constitutively expressed dsRNA activated serine/threonine kinase PKR (312) is upregulated by type I IFN signaling (313). Latent PKR is activated through recognition of viral dsRNA within a virus-infected cell (312). Once activated by direct binding to dsRNA, PKR targets cellular translation through phosphorylation of the eukaryotic initiation factor 2α (eIF2α)

component of the translation initiation machinery, which inhibits nucleotide exchange within the translation initiation complex and results in a global inhibition of protein translation in virus-infected cells (312). In addition to its role in inhibition of protein synthesis, PKR mediates some of the apoptotic and anti-proliferative effects of type I IFN (314,315). The importance of PKR in type I IFN signaling is underscored by the wide array of viral agents that have evolved to block PKR function. For example, Vaccinia Virus, HCV, HIV, Adenovirus, EBV and Influenza A have all evolved specific molecular mechanisms to counteract the anti-viral effects of PKR in virus-infected cells (312).

Another ISG that targets host cellular translation in virus-infected cells is ISG p56 (ISG56), which represents the most highly induced ISG (305). The ISG56 gene is rapidly upregulated as an early response gene in the absence of ongoing protein synthesis (316), and its expression further amplified through the effects of type I IFN signaling (305,316). DNA microarray profiling of immediate early, type I IFN-independent signaling indicates that ISRE within the promoter of ISG56 are responsive to induction by the IRF-3 transcription factor, an immediate early mediator of virus-inducible gene transcription that is detailed in detail in section 2.2 (317). The ISG56 protein is structurally similar to the ISG54, ISG60 and ISG58 proteins (318), particularly within the multiple tetratricopeptide repeat (TPR) domains that mediate protein-protein interactions. The TPR domains of ISG56 interact with the cellular translational initiation machinery, specifically the p48 subunit of eukaryotic initiation factor 3 (eIF3) (319). The interaction with ISG56 interferes with the function of p48 in translational initiation (320), which complements the function of activated PKR in ISG56-expressing cells.

In addition to directly inhibiting the virus life cycle, type I IFN performs important immunomodulatory functions during development of the anti-viral immune response. For example, IFNα/β signaling positively regulates the type I IFN immune response through amplification and diversification of IFN subtype expression via a positive feedback loop involving the IRF-3 and IRF-7 transcription factors (299,321). This signaling cascade, which is essential for type I IFN production, is discussed in section 2.2. Type I IFNs promote the production of type II IFNγ, which favors development of

the inflammatory Th1-type response that is required to clear an intracellular pathogen (322). In addition, IFNα/β signaling modulates innate immune responses that control the development of adaptive immunity. Natural IFN α/β producing cells (IPCs) are a subset of DC that play two major roles during the anti-viral immune response: direct inhibition of viral replication through large-scale production of IFNα/β, and stimulation of adaptive immune responses through differentiation into mature DC effectors. Type I IFNs skew immature DC differentiation towards a DC1 subset that promotes a Th1-type inflammatory response, as opposed to a DC2 subset that favors a Th2-type humoral response. Activated DC1 produce vast quantities of type I IFN (323-325), which act in an autocrine fashion to stimulate DC1 survival in the periphery. Furthermore, exposure to IFNα/βmay favour the formation of a DC:T-lymphocyte immunological synapse, through upregulation of costimulatory molecules such as CD80, CD83, CD86 or CD40 (326). IFNα/β signaling also induces IL-15 transcription, which promotes T-lymphocyte growth and proliferation (327).

2.1.2 Interferon signaling: the JAK/STAT pathway

Upon type I IFN secretion into the extracellular environment, ISGs are rapidly and transiently induced by signals initiated from the heterodimeric type I IFN receptor present on the surface of most cell types. The primary events that comprise the type I IFN signaling cascade are categorized into five major steps following ligation of the receptor by a homo- or heterodimer of type I IFN (296). These steps are summarized in Figure 6. They involve (1) ligand-induced receptor dimerization; (2) receptor-associated tyrosine phosphorylation events by Janus kinases (JAK); (3) activation and dimerization of STAT transcription factors, the effectors of type I IFN signaling; (4) nuclear translocation of STATs; (5) STAT DNA binding and subsequent transcription of ISGs.

All type I IFN subtypes signal through the same receptor to elicit anti-viral, antiproliferative and immunomodulatory effects. The two heterologous type I IFN

Figure 6. The type I IFN JAK-STAT signaling cascade Binding of a homo- or heterodimer of type I IFN induces the type I IFN signaling cascade through the JAK-STAT signaling. Ligand binding to IFNAR1 and IFNAR2c induces receptor dimerization, followed by cross-tyrosine phosphorylation of the receptor-associated kinases, JAK1 and Tyk2. Activated kinases phosphorylate the IFNAR1 to create phosphotyrosine docking sites for STAT transcription factors, which are constitutively associated with inactive IFNAR2c. Bound STATs are tyrosine phosphorylated by JAK kinases, which induces STAT dimerization, nuclear translocation and association with IRF-9/p48 to form the trimeric type I IFN effector complex ISGF3. ISGF3 bind to Interferon stimulated Response Elements (ISRE) in the nucleus to transactivate promoters of genes involved in establishment of the anti-viral response.

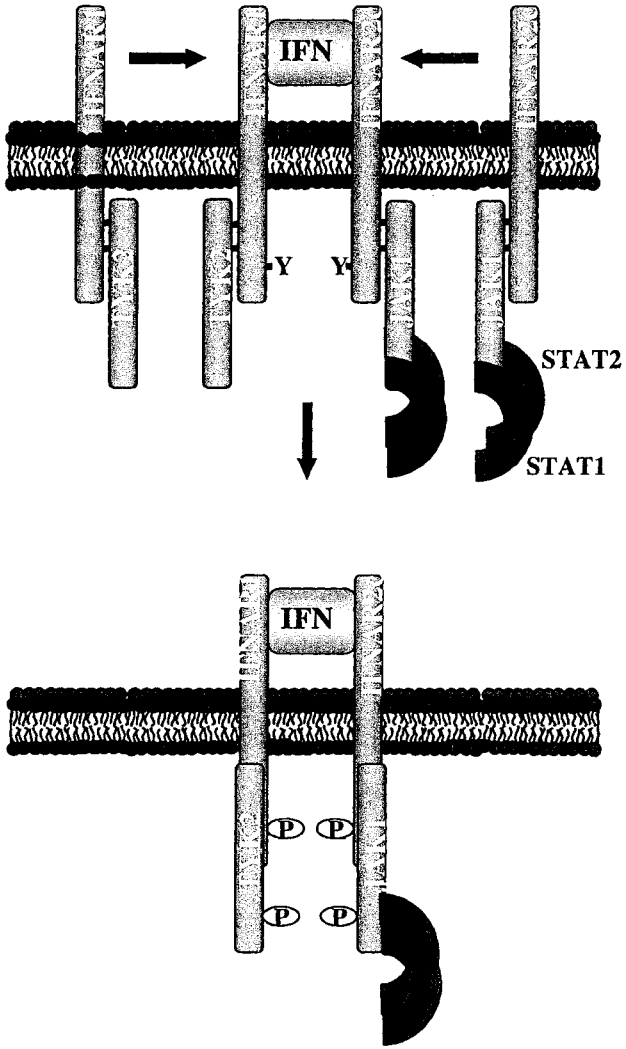

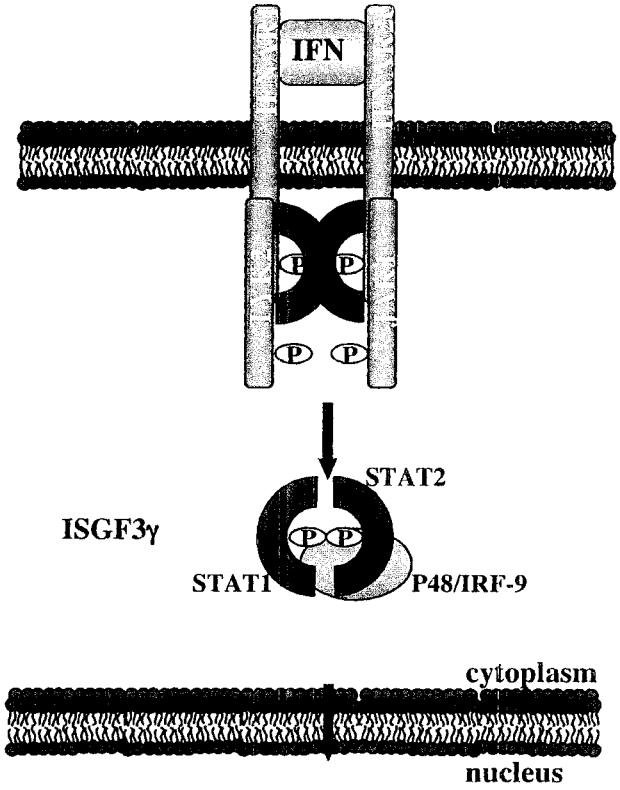

Cytokine Signaling (IFNα/β, RANTES, MIP1α)
Immunomodulation (IRF-7,IRF-1, IFNα/β)
Inhibiton of Protein Synthesis (PKR, Rnase L, ISG56,)
Inhibiton of viral replication (Viperin, ADAR, Mx, 2'5'OAS)

ESTABLISHMENT OF THE ANTI-VIRAL STATE

receptor subunits, IFNAR1 and IFNAR2c, each possess a single transmembrane domain and a cytoplasmic tail that lacks intrinsic enzymatic activity (328,329). Binding to a homo- or heterodimer of type I IFN in the extracellular environment induces the receptor subunits to heterodimerize (330), bringing into close proximity the two IFNAR-associated tyrosine kinases Tyk2 and JAK1, which catalyze receptor-associated signal transduction through phosphorylation events (331-334). IFNAR1-associated Tyk2 is tyrosine phosphorylated by IFNAR2c-bound JAK1, whereupon activated Tyk2 cross-phosphorylates JAK1 to augment its kinase activity (333). Activation of the receptor-associated tyrosine kinases results in phosphorylation of the IFNAR1 at tyrosine (Y)466, a key event that creates a docking site on IFNAR1 (335) for STAT transcription factors pre-associated with IFNAR2c (336). Latent STAT2 specifically binds to the phosphorylated Y466 docking site on IFNAR1 via intrinsic Src homology 2 (SH2) domain protein-protein interactions (335). Subsequently, STAT1 and STAT2 and are phosphorylated on Y690 and Y701, respectively, by JAK1 and Tyk2. The phosphorylated STATs homo- or heterodimerize, translocate to the nucleus and bind Interferon Stimulated Response Elements (ISRE) in complex with the IRF-9/p48/interferon stimulated gene factor γ (ISGF3γ) transcription factor. The transcriptionally active trimer, termed interferon stimulated gene factor 3 (ISGF3), represents the primary effector complex that elicits the pleiotropic effects of type I IFN through ISG transcription (337-340).

The JAK-STAT signaling cascade is subject to further downstream regulation, which explains why distinct biological effects are elicited by different type I IFN subtypes utilizing the same surface receptor. For example, STAT transcription factors can serve as substrates for serine/threonine kinases of the MAPK/ERK family, which directly associate with the IFNAR1 *in vivo* (341). MAPK/ERK activation through type I IFN signaling has been suggested to modulate the intensity and duration of the type I IFN signaling cascade by STAT serine phosphorylation, which has been shown to increase the transactivation capacity of STAT1 (342-344). The transient nature of type I IFN signaling is negatively regulated by internalization of type I IFN receptors, or more specifically through the activity of tyrosine phosphatases such as Src homology phosphatase-2 (SHP-

2), which inhibit the JAK/STAT signaling cascade (345). The sensitivity of the IFN response is further modulated by subunits of the suppressors of cytokine signaling (SOCs) superfamily, which negatively regulate IFN signaling through JAK binding and inactivation, blockade of SH2 docking sites on IFNAR1, or ubiquitination and degradation of STAT proteins (346-348). Similarly, protein inhibitors of activated STATs (PIAS) proteins bind STAT dimers and inactivate them, at least in part through covalent modification via an intrinsic E3-type small ubiquitin-like modifier (SUMO) ligase activity that inactivates STAT transcriptional capacity (349-351).

2.1.3 Assembly of the interferon β enhanceosome

Type I IFN gene transcription is scrupulously regulated. High levels of expression are induced as a consequence of signal transduction events triggered by pathogen detection (296,297). Initiated via intra and extracellular mechanisms, anti-viral signaling rapidly converges upon the cellular transcription factors ATF-2/c-Jun, NF-κB and IRF, which are rapidly activated following virus-infection via post-translational modifications that do not require ongoing protein synthesis. Once activated through the virus-inducible signaling network, these transcriptional modulators are specifically recruited to the promoters of type I IFN and other immediate early virus-inducible genes in a precise and coordinated manner, to trigger a genetic program that will establish the global cellular anti-viral state (352-354).

The type I IFNβ promoter has been extensively studied, and represents a paradigm within the study of virus-activated signaling. Transcription of IFNβ requires the formation of a large, high-order multi-protein complex called the enhanceosome, which consists of multiple promoter-specific transcription factors, associated structural components and basal transcription machinery bound to enhancer DNA (355-358). The enhanceosome is believed to assemble as a single cooperative unit that is stabilized by numerous protein-protein and DNA-protein interactions, and the absence of any one component will destabilize the entire nucleoprotein complex. The requirement for such cooperation ensures that the activation threshold for an enhanceosome-driven gene

remains precise and fastidious, through the obligatory integration of multiple signals (359).

Schematic representation of protein-DNA interactions regulating the virus-responsive element (VRE) of the type I IFNβ promoter is illustrated in Figure 7. The regulatory region located between the –115 to –45 nucleotides relative to the transcriptional start site of the IFNβ gene contains both positive and negative regulatory domains that function as a VRE when inserted upstream of a heterologous reporter gene (360-363). A combination of deletion and saturation mutagenesis studies involving reporter gene assay identified four overlapping but distinct positive regulatory domains (PRDI-PRDIV) within the –115 to -45 region of the human IFNβ promoter as *cis*-regulatory elements selective for the transcription factors responsible for driving IFNβ transcription. Although no one PRD can function alone as a virus-inducible element, two or more copies can confer this response (364), and deletion or mutation of any one PRD reduces the efficiency of IFNβ transcriptional. Insertion of a half but not a full helical turn of DNA between PRD sequences reduces promoter transcription, which suggests that each transcription factor contributes in a synergistic manner that necessitates the specific protein alignment on the same face of the DNA helix to allow for cooperative protein-protein interactions. Synergism within IFNβ transcription requires cooperative binding events, but also depends on recruitment of histone acetyl transferase (HAT) enzymes such as CBP/p300 or PCAF by more than one transcription factor (365).

Much study has focused on identification of the cellular transcription factors recruited to the IFNβ VRE in response to virus infection. Because gene transcription of IFNβ is rapidly triggered in response to virus infection independently of *de novo* protein synthesis, two defining characteristics of an IFNβ transactivator are a ubiquitous and constitutive pattern of expression coupled with a virus-inducible kinetics of activation. Rapidly activated in response to virus infection and dsRNA treatment, NF-κB is an immediate early signaling molecule that plays an essential role in IFNβ promoter activation through specific recognition of PRDII (208,366-369). Mutation of the specific

Figure 7. Structure of the virus-responsive type I IFNβ enhanceosome The virus-inducible enhancer of the IFNβ promoter contains four distinct but overlapping positive regulatory domains (PRD) PRDIV, PRDIII, PRDI and PRDII. In response to virus infection, IFNβ transcription is driven by the recruitment of transcription factors belonging to the AP-1, IRF and NF-κB families, which bind in a synergistic and coordinated manner with the structural protein HMGI(Y) to promote IFNβ production in virus infected cells.

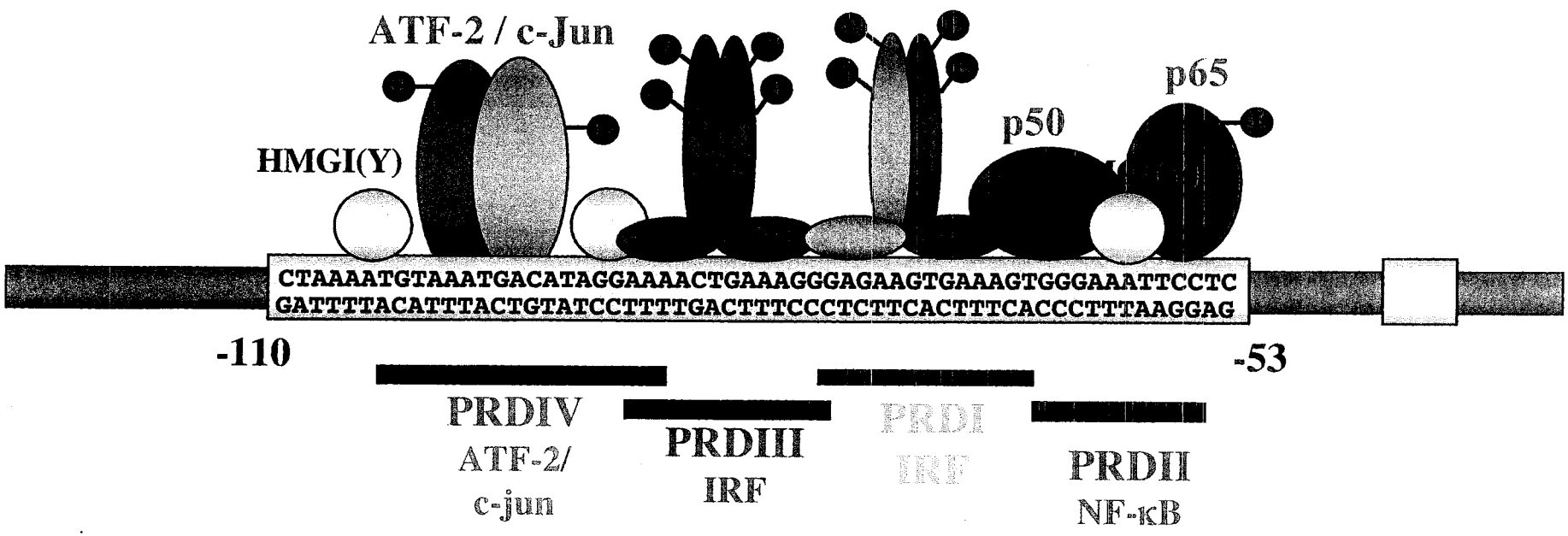
IRF-1/IRF-3
ATF-2 / c-Jun
HMGI(Y)
p50
p65
CTAAAATGTAAATGACATAGGAAAACTGAAAGGGAGAAGTGAAAGTGGGAAATTCCTC
GATTTTACATTTACTGTATCCTTTTGACTTTCCCTCTTCACTTTCACCCTTTAAGGAG
-110
-53
PRDIV
ATF-2/
c-jun
PRDIII
IRF
PRDI
IRF
PRDII
NF-κB

residues that reduce or abolish binding of NF-κB to the IFNβ promoter respectively decrease or abolish induction of IFNβ gene transcription *in vivo*, while anti-sense RNA directed against p65 diminish endogenous IFNβ production in response to virus infection and dsRNA treatment. The PRDII site of the IFNβ promoter represents a consensus NF-κB site that is sensitive to a wide array of stimuli such as TNFα, PMA and LPS in isolation (369). Mutation of the inner AT-rich region of PRDII reduces IFNβ transcription without disrupting NF-κB binding *in vitro*, indicating that a heterologous protein may recognize PRDII in conjunction with NF-κB *in vivo* (360,369,370). The protein was identified as HMG I(Y), a basic low molecular weight protein that was initially identified by virtue of its association with chromatin (370). Structural analysis reveals that HMG I(Y) contacts the inner AT-rich portion of PRDII in the minor groove, while NF-κB binds the outer GC-rich region from the major groove. Binding of HMG I(Y) is required for IFNβ transcription, but in contrast to NF-κB, does not perform a role in transcriptional activation *per se*. *In vitro* binding experiments indicate that HMG I(Y) functions as an architectural scaffolding molecule, altering the curvature of DNA to enhance transcription factor binding to PRD with the IFNβ promoter (371).

In vitro binding and saturation mutagenesis assays identified PRDIV as a binding site for ATF-2/c-jun proteins (372). Like PRDII, sequences adjacent to PRDIV are required to confer inducibility by virus infection, but not by ATF-2 activators such as cAMP. *In vitro* footprinting analysis indicates that HMG I(Y) interacts with the flanking sequences of PRDIV, performing the necessary structural role required for virus induction of PRDIV by ATF-2 homodimers or ATF-2/c-jun heterodimers (363). Detailed analysis using an *in vivo* formaldehyde cross-linking and chromatin immunoprecipitation approach (chIP) indicated that induction of endogenous IFNβ transcription was dependent upon acetylation of HMG I(Y) at specific lysine residues; whereas acetylation of HMGI(Y) at K65 by CBP destabilized the enhanceosome, acetylation of HMGI(Y) by PCAF/GCN5 at K71 potentiated gene IFNβ transcription by stabilizing the enhanceosome and preventing acetylation by CBP (363).

2.1.4 Discovery and characterization of the cellular IRFs

The first member of the IRF family of transcription factors, IRF-1, was identified and cloned as a factor binding to the VRE of the IFNβ promoter; subsequently, the 62% homologous IRF-2 was isolated from cross-hybridization experiments using IRF-1 cDNA (373-377). Co-transfection experiments demonstrate that IRF-1 is an efficient transactivator of the IFNβ promoter *in vitro* and a modest inducer of IFNβ secretion *in vivo*; in contrast, IRF-2 fails to activate IFNβ transcription and represses IRF-1-mediated activation of the IFNβ promoter (373,375-377). Within the amino-terminal DBD, IRF-1 and IRF-2 share 62% homology, while homology within the carboxy-terminal is limited at 25%. In the carboxy-terminal region, IRF-1 is abundant in acidic aa and serine/threonine residues while the corresponding portion of IRF-2 is rich in basic aa (376). The acidic carboxy-terminal of IRF-1 contains a potent transactivation domain (TD) that is subject to post-translational phosphorylation by numerous regulatory kinases, including PKA, PKC and CKII (289,378). Mutation of carboxy-terminal phosphoacceptor sites within the IRF-1 TD abolishes its capacity to transactivate the IFNβ promoter(378,379). The basic carboxy-terminal of IRF-2 contains a transrepression domain, which upon deletion renders IRF-2 a transcriptional activator (380). The crystal structure of IRF-1 bound to PRDI reveals a novel helix-turn-helix DNA binding motif that secures itself to a core GAAA DNA consensus sequence with three of the five amino-terminal tryptophan repeats (381). Binding of IRF-1 causes bending of the DNA axis towards the transcription factor, which is believed to force cooperative associations with proteins such as NF-κB and AP-1 bound to PRDII and PRDIV, respectively, on the IFNβ promoter.

Although initial observations implicated IRF-1 and IRF-2 as respective activator and repressor of the IFNβ VRE, the low expression of IRF-1 in unstimulated cells alluded to the existence of at least one IRF-1-independent pathway to IFNβ production (382). Phenotypic analysis of mice deficient for IRF-1 expression emphasized its fundamental role during delayed type I IFN signaling events: *irf1* -/- mice displayed impaired thymic CD8+ cell development, absent NK cell development and reduced transcription of ISG such as TAP-1 and MHC class I in response to virus infection (383-385). However, in

stark contrast to *irf9/p48/isgf3g*, *stat1* or *ifnar* deficient mice, which demonstrated a moderate reduction of IFNβ expression and a drastic reduction of IFNα expression in response to virus infection (386-388), *irf1*-/- mice retained the capacity to induce type I IFN in response to Newcastle Disease Virus (NDV) infection to wild type levels (383,389,390).

2.2 The IRF-3 and IRF-7 anti-viral program

Rapid induction of type I IFN expression, a central event in establishing the innate anti-viral response, requires activation of a cooperative of transcription factors that function in a synergistic fashion. Activation of the transcription factors IRF-3 and closely related IRF-7 are required for expression of type I IFN and numerous immunomodulatory genes in response to foreign pathogen (321). IRF-3 acts in synergy with AP-1 and NF-κB as an immediate early activator of innate immune transcription (353). Subsequently, IFN-dependent upregulation of IRF-7 further develops the type I IFN response by amplification of IFNβ expression and diversification of IFNα subtype expression (321). Although the signaling pathways leading to NF-κB and ATF-2/c-Jun activation have been relatively well characterized, the molecular mechanisms that modulate IRF-3 and IRF-7 activity represent a critical missing link in the understanding of immune signaling. As a result, intensive study has focused on identification of the regulatory components that trigger IRF-3 and IRF-7 activation in response to pathogen infection, as these intermediates represent a key target for stimulating an efficient host immune response to pathogen infection.

2.2.1 Characterization of IRF-3 and IRF-7

The search for immediate early transcriptional activator(s) of the type I IFN response led to isolation of the IRF-3 sequence from an EST database search for IRF homologues (391). IRF-3 and the transcriptional co-activator CBP were soon identified as components of a high molecular weight dsRNA-activated factor (DRAF) complex binding to the ISRE of ISG15 *in vitro* (392,393). Significantly, recognition of a selective subset of ISRE by the IRF-3/CBP complex in response to dsRNA treatment (392-394) or virus infection (395-400) occurred independently of *do novo* protein synthesis and type I IFN signaling.

The ubiquitous IRF-3 message is constitutively expressed from a TATA-less promoter that does not respond to virus infection or type I IFN treatment (391,398,401). Overexpression of IRF-3 augments virus-inducible transactivation of the IFNβ promoter (396,399,400,402) while, co-transfection of IRF-3ΔN, a dominant negative mutant of IRF-3 that lacks the amino-terminal DBD, inhibits virus induction of IFNβ and subsequent ISG induction (399,402).

While overexpression studies have implicated the IRF proteins -1, -2, -3, -5 and -7 in transcriptional regulation of type I IFN promoters (289,291), gene targeting studies in mice have truly emphasized the essential role of IRF-3 and the closely related IRF-7 for type I IFN transcription in response to virus infection (321). In contrast to IRF-3, basal expression of IRF-7 is confined to hematopoietic cells, although it is transcriptionally induced in most cell types through type I IFN signaling (289). In the context of virus infection, immediate early activation of latent IRF-3 in conjunction with ATF-2/c-jun and NF-κB promotes rapid transcription of the IFNβ and IFNα1 genes, as well as a subset of ISG that includes chemokines RANTES (403) and IP-10 (404), the ubiquitin analogue ISG15 (392,393) and the translational inhibitor ISG56 (317). Virus-inducible IRF-3-driven gene transcription represents an essential component of the type I IFN response. Deletion of the *irf3* gene was associated with 100% mortality in response to Encephalomyocarditis Virus (EMCV) challenge, as opposed to the 50% mortality in control littermates (321). Increased susceptibility to virus infection was attributed to a substantial reduction of type I IFN production in *irf3* deficient mice. However, pre-treatment with type I IFN rescued the phenotype (321) through type I IFN signaling, which induced the full spectrum of ISG expression through the activity of ISGF3 (386-388,405,406). In particular, upregulation of the ISG IRF-7 in type I IFN-sensitized cells (299,407,408) promotes amplification of the type I IFN response through enhancement of IFNβ gene transcription in conjunction with NF-κB and AP-1 (299,407). Furthermore, the response is diversified of by the capacity of IRF-7 to transactivate specific IFNα subtypes that are not efficiently recognized by IRF-3(299,402,407,409). Significantly, in cells lacking the p48/IRF-9 component of ISGF3, ectopic expression of IRF-7 but not IRF-3 rescued virus-inducible transcription of the IFNα genes (407).

Therefore, differential expression and DNA binding capacities of IRF-3 and IRF-7 regulate temporal expression of type I IFN in response to virus infection, which is summarized by Figure 8 (353). The early response genes are rapidly induced by virus infection by latent, pre-existing IRF-3 in conjunction with ATF-2/c-jun and NF-κB without the need for *de novo* protein synthesis; in non-hematopoietic cells, type I IFN signaling in a paracrine fashion results in the upregulation of IRF-7, which acts to amplify and diversify the type I IFN response (299,402,407,409).

Selective DNA binding and transactivation analyses reveal that differences in DNA binding affinity account for the differential recognition of type I IFN promoters by IRF-3 and IRF-7 (402,410). With respect to the human IRF-3 and IRF-7 proteins, the IRF-3 DBD preferentially recognizes IRF-1 and -2 consensus sites that can be found within the human IFNβ, IFNα1, IFNα2 and RANTES promoters. In comparison, the IRF-7 DBD binds these elements, as well as to ISRE-like sequences found in the human IFNα4, IFNα7 and IFNα14 promoters with a greater flexibility than IRF-3 (402). Analysis of the DNA binding capacity of recombinant IRFs revealed distinct subunit preferences for the VRE of the IFNβ promoter: IRF-3 exclusively bound PRDIII, while IRF-7 preferentially recognized PRDI (402). Amino-terminal sequence alignment identified three short aa sequences specific to the IRF-7 DBD, when compared with IRF-1, -2 and –3 (402). Although these unique sequences have been postulated to confer promiscuous binding activity to the IRF-7 DBD, analysis of three-dimensional structure may ultimately confirm how and which of these residues confer to IRF-7 its unique DNA binding properties.

2.2.2 Virus-inducible modification of IRF-3 and IRF-7

Adjacent to the amino-terminal DBD, the region between aa 134 and 394 contains the IRF-3 transactivation domain, which encompasses an NES, a proline rich domain and an IRF association domain (IAD) involved in protein homo- and heterodimerization (411). Interaction of two autoinhibitory domains at the amino- and carboxy-termini, encompassing residues 98 to 240 and 380 to 427, respectively, creates a closed conformation that masks the IAD of IRF-3 in unstimulated cells (411). Latent IRF-3

Figure 8. Virus activation of IRF-3 and IRF-7 signaling and establishment of the anti-viral state Upon virus infection of a susceptible host cell, recognition of pathogen initiates a number of cellular signal transduction cascades; molecular signals ultimately converge upon rapid activation of transcription factors by post-translational modifications, primarily phosphorylation events. Virus-inducible activation of transcription factors of the Ap-1, NF-κB and IRF (IRF-3) families initiates immediate early innate immune response genes, such as those encoding the type I IFN (IFNα1 and IFNβ). Once secreted, type I IFN initiate type I IFN JAK-STAT signaling in an autocrine and paracrine manner, which results in delayed upregulation of a wider array of interferon stimulated genes (ISG), such as the transcription factor IRF-7. Transcriptional and virus-inducible activation of IRF-7 contributes to amplification and diversification of the type I IFN response, through induction of delayed type I IFNα genes and genes involved in establishment of the anti-viral state (PKR, Mx, 2'5'OAS).

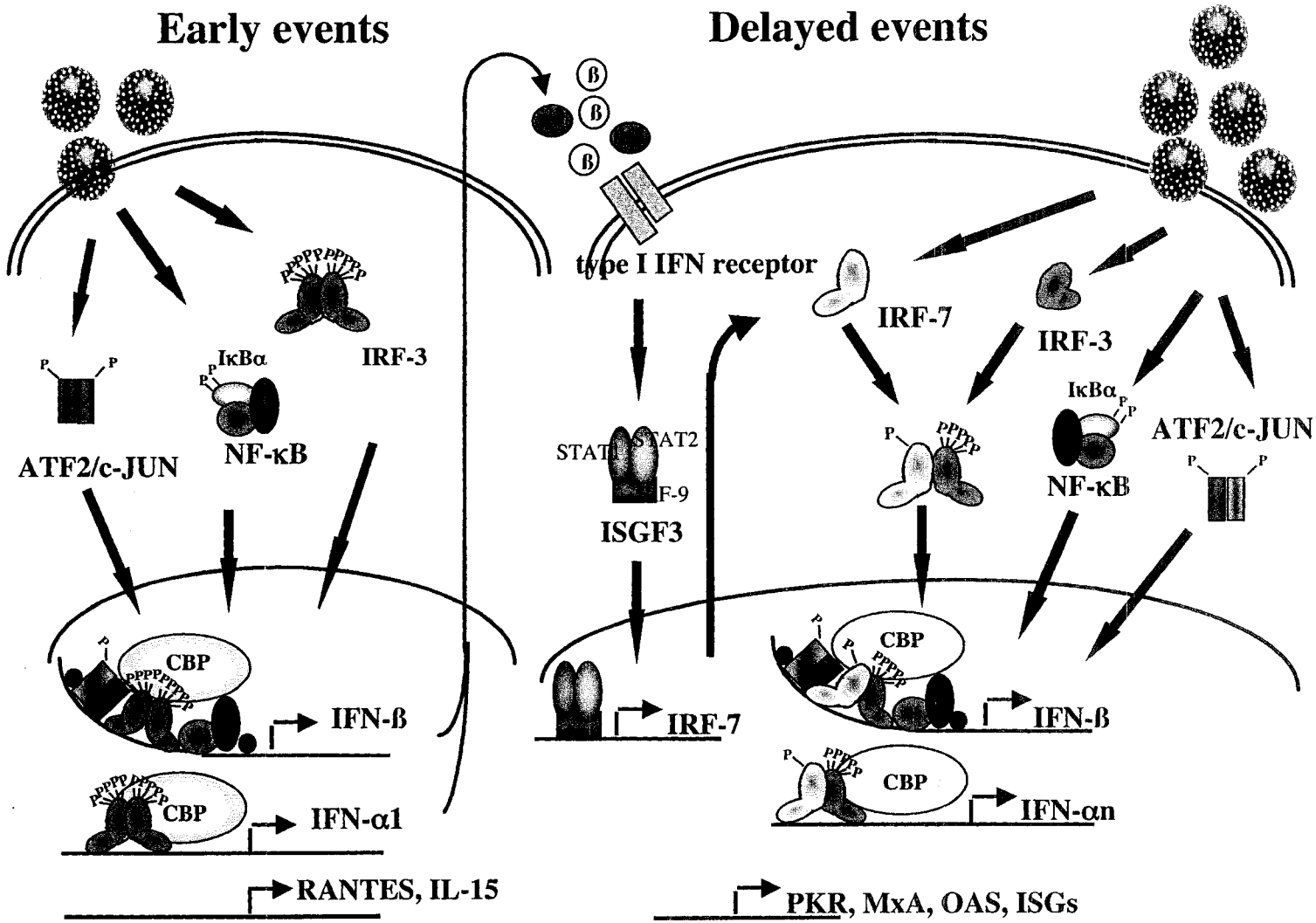
Early events
Delayed events
ß
ß
ß
type I IFN receptor
IRF-3
IκBα
ATF2/c-JUN
NF-κB
IRF-7
IRF-3
IκBα
ATF2/c-JUN
NF-κB
STAT1
STAT2
F-9
ISGF3
CBP
IFN-ß
CBP
IFN-α1
IRF-7
CBP
IFN-ß
CBP
IFN-αn
RANTES, IL-15
PKR, MxA, OAS, ISGs

exists at equilibrium in this closed conformation as a monomer of two distinct phosphoforms (412) that shuttle constitutively between the cytoplasmic and nuclear compartments (399). Upon infection with a broad array of viral agents including Sendai Virus (SV), Measles Virus (MeV), VSV or NDV, activation of virus-inducible signal transduction triggers the virus activated kinase(s) (VAK) that hyperphosphorylates IRF-3 within the carboxy-terminal on specific serine/threonine residues (392,394,396-400). Carboxy-terminal hyperphosphorylation relieves IRF-3 autoinhibition (411), which precipitates IAD-mediated dimerization, nuclear accumulation, DNA binding and transactivation of IRF-3-target genes in conjunction with CBP/p300 (392,394,396-400). Seven specific carboxy-terminal residues have been implicated in the phosphorylation and activation of IRF-3 in response to virus infection. These are S385 and S386 (399,413,414) (cluster I) and S396, S398, S402, T404 and S405 (398,411,415) (cluster II). Mutation of these serine/threonine residues to inactive alanine (S-T/A) or to phosphomimetic aspartic acid (S-T/D) followed by functional analysis by reporter gene assay (398,403,411,415) or dimerization assay (413,414,416,417) have been applied to analyze the role of cluster I and II residues for IRF-3 activation. Alanine substitution of cluster I (399,411), or cluster II (398,411) generates an inactive form of IRF-3 that is unresponsive to virus infection. Phosphomimetic substitution of S385/386D within cluster I renders the protein transcriptionally inert (411); however, phosphomimetic substitution of cluster II residues generates a constitutively activated IRF-3 protein, IRF-3(5D) (398,411). Expression of IRF-3(5D) induces endoegenous RANTES mRNA (403), and is sufficient to induce cellular apoptosis in the absence of virus infection (418,419). Detailed analysis of S/T residues within cluster II have shown that a minimal phosphomimetic substitution of S396D is sufficient to confer full IRF-3 activation, as evidenced by nuclear accumulation, DNA binding, CBP association and transactivation of the RANTES and IFNβ promoters (415). Furthermore, IRF-3 S396 phosphorylation is detectable *in vivo* in response to virus infection and dsRNA treatment, using S396-specific phosphospecific IRF-3 antisera (415).

In response to virus infection, IRF-7 is also subject to activation by carboxy-terminal hyperphosphorylation (299,407,410,420), such that IRF-3 and IRF-7 undergo virus-

induced phosphorylation with a similar kinetics when co-expressed (421). With respect to human IRF-7, a constitutive activation domain (CAD) is located between aa 150 and 246, which is adjacent to the amino-terminal DBD (420). In contrast to IRF-3, IRF-7 stimulates gene expression if expressed to high enough levels in the absence of virus infection (420), which is consistent with the fact that IRF-7 efficiently homodimerizes and binds DNA in the absence of stimulation. However, phosphorylation within the carboxy-terminal domain spanning residues 468 to 503 is required to promote cytoplasmic to nuclear translocation, and is believed to relieve a negative regulatory effect with respect to the IRF-7 CAD by an internal transcriptional inhibitory domain present between residues 416 to 467 (420). The regulatory element spanning aa 468 to 503 contains several serine residues targeted by the virus-activated signaling machinery; serine to alanine substitution of specific residues with this stretch suggest that at least three distinct serine clusters in the carboxy-terminal domain are involved in virus-inducible IRF-7 activation (420). The complex organization of the IRF-7 carboxy-terminal underscores a distinct rather than redundant function compared to IRF-3; furthermore, activation of IRF-7 signaling is regulated by at least two mechanisms: type I IFN-dependent transcriptional regulation, and virus-induced carboxy-terminal phosphorylation.

2.2.3 Multiple signaling pathways to IRF-3 and IRF-7 activation

The cellular and viral signaling components that modulate activation of the IRF-3 and IRF-7 anti-viral program have been the focus of considerable investigation. The broad range of viral agents that provoke IRF-3/IRF-7 signaling range from simple RNA viruses that replicate in the cytoplasm, such as VSV (395) and MeV (412,422), to larger, more complex DNA viruses whose life cycle takes place predominantly in the nucleus, including Cytomegalovirus (CMV) (423). Phosphorylation of IRF-3 and IRF-7 by RNA viruses such as NDV and SV is sensitive to viral replication and viral protein synthesis (412,421), and yet the nature of the virus-specific signal(s) responsible for triggering VAK activation appear to be multiple and distinct.

Several lines of evidence indicate that viral dsRNA is not the only viral component capable of inducing type I IFN via activation of IRF-3 (421,422). Cells derived from mice deficient in PKR, a protein that represents a primary intracellular sensor for viral dsRNA (312), are deficient for type I IFN production in response to dsRNA treatment but not to *de novo* virus infection (203,424,425). Similarly, MEFs derived from mice deficient in the TLR3 TIR adaptor protein TRIF are unable to induce type I IFN in response to dsRNA treatment, because IRF-3 activation via TLR3 does not occur in the absence of the MyD88-indepedent pathway (166). However, it remains to be established whether *trif-/-* cells are able to produce type I IFN in response to *de novo* virus infection, as opposed to dsRNA treatment alone.

Both CMV and HSV have been reported to induce type I IFN synthesis via membrane disruption at the cell surface independently of viral entry and replication, suggesting at least one dsRNA-independent mechanism for IRF-3/IRF-7 activation involves membrane or cytoskeletal perturbation (421). The mechanism has recently been shown to involve recognition of HSV-2 DNA sequences by TLR9 at the cell surface of natural IFN-producing (IPC) DC, which demonstrates a mechanism whereby viral genomic DNA can induce IFNα secretion through engagement of TLR (426). Furthermore, expression of the nucleocapsid (N) protein of MeV has been shown to be sufficient to trigger activation of IRF-3 signaling in fibroblasts, thereby representing an intracellular viral trigger for type I IFN production that is distinct from viral dsRNA, because it requires a protein component (422).

In addition to virus infection, as DNA damaging agents, stress inducers and LPS have also been reported to stimulate IRF-3 signaling (419,427,428). However, the specificity the IRF-3 response is highlighted by microarray profiling of the TLR-specific genetic responses of primary murine bone marrow-derived macrophages or immortalized RAW 264.7 murine macrophages (429). These studies define a particular subset of primary immune response genes common and specific to TLR3 and TLR4 signaling via dsRNA and LPS, respectively. Using dominant negative constructs to specifically disrupt NF-κB or IRF-3 signaling, Doyle et al. demonstrated that NF-κB activation was required to

express a majority of primary immune response genes activated by all TLRs, while IRF-3 signaling conferred specificity through activation of the TLR3/4-specific subset of immune response genes, which include the cytokines IFNβ and IP-10 and the chemokine RANTES (429). These studies underscore the importance of the IRF-3 and IRF-7-specific genetic program for establishment of anti-viral immunity, because expression of these genes was required to inhibit the replication of murine γherpesvirus 68 (MHV68) *in vivo* (429). Similar results have been obtained from analysis of primary DC isolated from *irf-3* deficient mice: LPS-stimulated induction of ISRE-regulated cytokines IFNβ, IP-10 and IL-15 were impaired at the mRNA level in the absence of IRF-3. As a result, *irf3* deficient mice were resistant to fatal endotoxin shock induced by high dose intraperitoneal injection of LPS compared to their control littermates (428).

With respect to LPS signaling, data obtained in innate immune cells contrasts independent studies of IRF-3 activation in fibroblasts (354,412). In this context, LPS did not induce classical IRF-3 carboxy-terminal phosphorylation. Rather, amino-terminal phosphorylation mediated via a mitogen-activated protein kinase kinase kinase (MAPKKK)-related signaling pathway was observed in response to DNA damaging agents, stress inducers and LPS (412). The precise role of amino-terminal MAPKKK phosphorylation of IRF-3 is unclear, because it did not affect the transactivation capacity of IRF-3 with respect to the RANTES or IFNβ promoters (412). However, independent experiments characterizing phosphorylation of IRF-3 in the amino-terminal domain by the stress-activated DNA-dependent protein kinase (DNA-PK) at the T135 residue suggest that amino-terminal phosphorylation favors nuclear retention of IRF-3, an event which may complement carboxy-terminal phosphorylation events in the context of full IRF-3 activation (430).

2.2.4 The virus activated kinase (VAK)

Several biochemical characteristics of the virus-inducible VAK complex that phosphorylates IRF-3 and IRF-7 are evident. In addition to targeting key virus-specific residues in the carboxy-terminal domains of both IRF-3 and IRF-7, the serine/threonine kinase complex should be ubiquitous and constitutively expressed in latent cells.

Furthermore, the complex should be catalytically activated as an immediate early event in response to virus infection, independently of type I IFN signaling or *de novo* protein synthesis. Catalytic induction of VAK kinase activity should correlate with activation of the classical IKK complex responsible for NF-κB activation, as well as the c-jun kinase (JNK) that phosphorylates AP-1 proteins in response to virus infection or dsRNA treatment (353). However, VAK activity should be refractory to the broad array of NF-κB and AP-1 activators that do not induce type I IFN expression, or the anti-viral state that ensues.

Biochemical analysis of IRF-3 and IRF-7 activation indicates that pre-treatment with staurosporine, a broad-spectrum pharmacological kinase inhibitor, blocked IRF-7 phosphorylation by NDV infection (421). However, specific kinase inhibitors have not been identified, indicating that VAK may represent a novel and uncharacterized serine/threonine kinase (412,416,421). Interestingly, cellular pre-treatment with Geldanamycin inhibits virus-induced IRF-3 activation (416). Geldanamycin sequesters chaperone proteins such as Hsp90, which is a common structural/trafficking molecule for cellular kinase complexes including the classical IKK complex (83). Induction of IRF-3 phosphorylation by SV is sensitive to ribavirin, a selective inhibitor of the paramyxovirus RNA polymerase, which reflects a requirement for ongoing viral replication for VAK activation, particularly at low multiplicity of infection (MOI) (412,422). Similarly, pre-treatment with BAPTA-AM, an intracellular calcium-chelating agent, also blocked SV-induced phosphorylation of IRF-3 (412); although these results implicate a calcium-dependent pathway upstream of IRF-3 activation, like ribavirin BAPTA-AM may interfere with viral replication (B.R. tenOever, unpublished data). As treatment with dsRNA is sufficient to activate IRF-3 signaling, the serine threonine kinase PKR represents a prime candidate as a part of the VAK complex. However, analyses of cells derived from PKR deficient mice indicate that the enzymatic kinase activity of PKR is dispensable for activation of IRF-3/-IRF-7 signaling in response to virus infection (421), which is consistent for the essential role of PKR in type I IFN production in response to dsRNA treatment but not *de novo* virus infection (203,424). Similarly, an *in vitro* kinase assay approach applied in our laboratory ruled out the carboxy-terminal signal-responsive

domain of IRF-3 as a direct substrate for PKR (M. Servant, unpublished data). However, a role for PKR as an upstream activator of IRF-3 signaling may exist, because the serine/threonine kinase has been shown recently to associate with the TIR-adaptor molecule TRIF, which lies downstream of dsRNA/TLR3 signaling within the MyD88-independent pathway that leads to IRF-3 activation and type I IFN induction (431).

2.3 The lymphoid/myeloid-specific IRF-4 transcription factor

Although the best characterized members of the IRF family IRF-1, IRF-2, IRF-3 and IRF-7 display a fairly ubiquitous pattern of expression in mammalian cells, expression of IRF-4/Pip/ICSAT/LSIRF is specific to the lymphoid and myeloid compartments of the immune system. IRF-4 plays an essential role in the homeostasis and function of mature lymphocytes in the periphery, and its expression is tightly regulated in primary T-lymphocytes. IRF-4 mRNA and protein levels are transiently induced following activation by antigen-mimetic stimuli such as TCR cross-linking or treatment with phorbol ester and calcium ionophore (PMA/ionomycin). However, IRF-4 is constitutively upregulated at the mRNA and protein levels in HTLV-I infected T-cells, as a direct gene target for the HTLV-I Tax oncoprotein.

2.3.1 Cloning and characterization of IRF-4

The structural and functional domains of the murine IRF-4 protein are summarized in Figure 9. IRF-4 was cloned in three independent contexts; in the effort to isolate factors binding to the murine immunoglobulin (Ig) light chain enhancer $E_{\lambda 2\text{-}4}$ (432), PU.1 interaction partner, Pip, was identified as a novel transcription factor possessing an IRF-like amino-terminal domain that bound to the light chain enhancer exclusively in association with the B-cell-specific Ets transcription factor PU.1 (433). Phosphorylation of PU.1 at S148 was required for PU.1-Pip interaction and subsequent binding of the heterodimer to the ISRE-like λB site present within the $E_{\lambda 2\text{-}4}$ Ig enhancer region (432). During the isolation of Pip, Matsuyama et al. cloned IRF-4 from murine spleen cells as a lymphoid specific IRF (LSIRF) expressed at all stages of B-cell development but only in mature, activated T-cells (434). In contrast to the situation for B-cells, in T-cells IRF-4 was found to bind autonomously to the ISRE element of the MHC class I promoter (434).

Figure 9. The lymphoid/myeloid-specific IRF-4 transcription factor IRF-4 has been described as both activator and repressor of gene transcription. The IRF-4 DNA binding domain (DBD) contains the conserved tryptophan repeat sequence (W) characteristic of all IRF proteins as well as the IRF association domain (IAD) involved in IRF homo- and hetero-dimerization. A transcriptional activation domain is located between aa138-450. The proline rich domain (Pro) between aa208-238 is 45% proline. An autoinhibiton domain between aa410-439 is essential for inhibiton of DNA binding and ternary complex formation with the Ets protein PU.1.

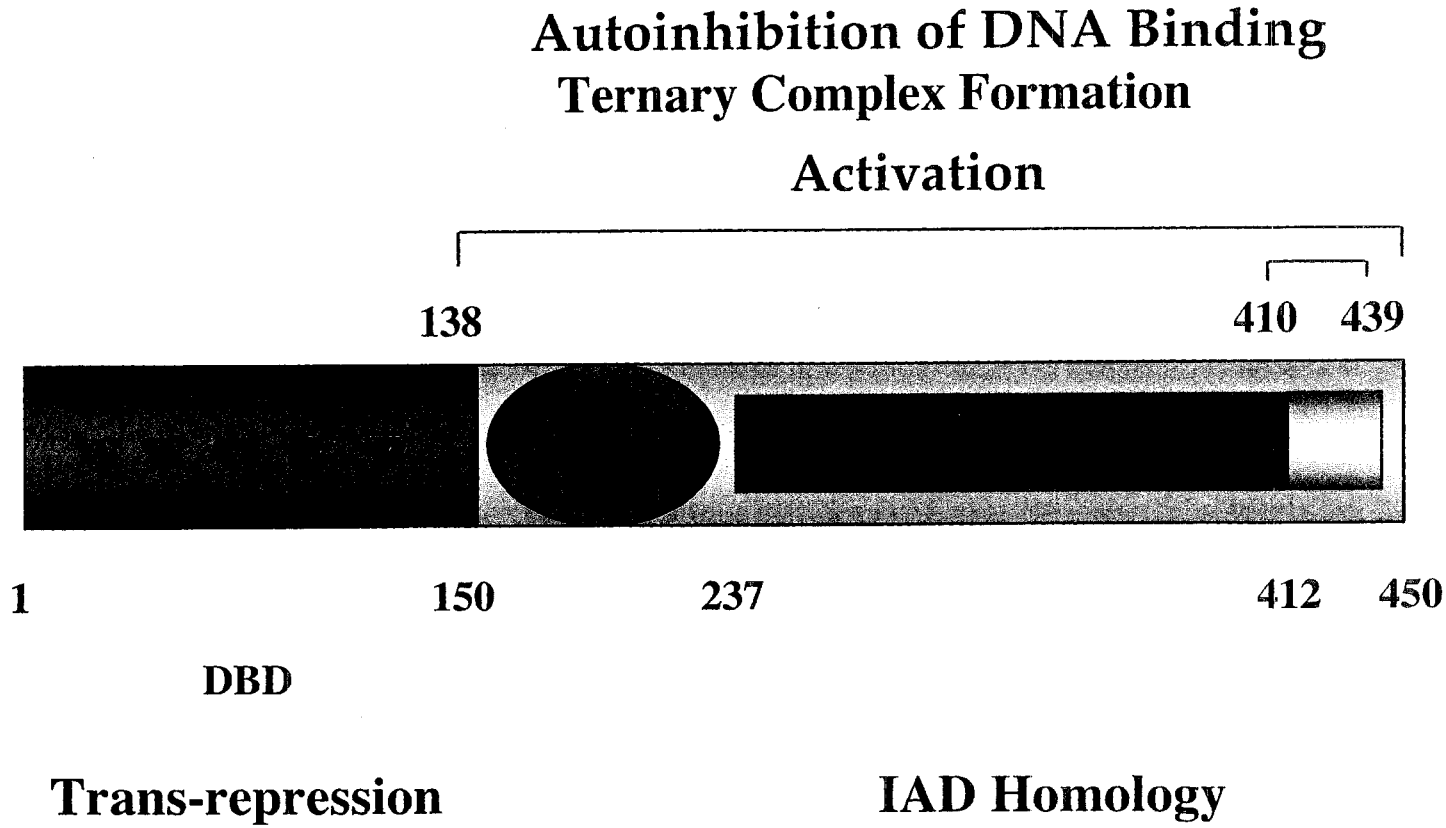
Autoinhibition of DNA Binding
Ternary Complex Formation
Activation
138
410
439
1
150
237
412
450
DBD
Trans-repression
IAD Homology

The IRF-4 mRNA message is inducible in primary T-lymphocytes by antigen-mimetic stimuli such as concanavalin A (conA) treatment, CD3/CD28 crosslinking and PMA stimulation, while treatment with type I and type II IFN or TNFα does not induce IRF-4 mRNA (434). Furthermore, conA-stimulated IRF-4 expression was found to be downregulated by pre-treatment with immunosuppressive drugs CsA or FK506, which block T-cell activation in part through inhibition of the calcium-sensitive regulatory phosphatase calcineurin (435). The inducibility of IRF-4 by T-cell-specific activation signals implied that this IRF subunit might function in the transduction of antigenic signals through the TCR.

A third group isolated the human homologue of Pip/LSIRF from an adult T-cell leukemia cell line as IRF-4/IFN consensus sequence-binding protein in ATL cell lines or activated T-cells (ICSAT) (436). Interestingly, IRF-4/ICSAT possesses a very different function compared to its murine counterpart. While PU.1-IRF-4 functions as a transactivator complex, IRF-4/ ICSAT repressed type I IFN- or IRF-1-induced gene activation in a manner that was reminiscent of IRF-2 (436). Expression of IRF-4/ICSAT is exclusive to the lymphoid and myeloid lineages, but is restricted to a specific subset of human T-cells: only T-lymphocytes stimulated by antigen or infected and transformed with the HTLV-I express IRF-4 (436). Jurkat T-cells transiently over-expressing HTLV-I Tax cDNA constitutively express the IRF-4 mRNA message, indicating that Tax activates the human IRF-4 promoter (436). Since the oncogenic potential of HTLV-I resides in the viral Tax oncoprotein, induction of IRF-4 expression by Tax is believed to represent a cellular target that may contribute to the development of HTLV-I-induced T-cell leukemogenesis (436).

2.3.2 Phenotype of the IRF-4 knockout

The importance of IRF-4 expression in the activation and proliferation of mature T-cells is underscored by the immunocompromised phenotype of mice deficient for IRF-4 expression (437). At 4 to 5 weeks, T- and B-cell distribution in the periphery was comparable in *irf4*-deficient mice compared to control littermates, but over time the IRF-4 KO animals gradually exhibited marked lymphadenopathy and splenomagaly. Although

the thymus of IRF-4-/- mice was normal at 10 to 15 weeks, the spleen was enlarged 3 to 5 fold and lymph nodes were approximately enlarged 10 fold compared to control littermates due to the increased levels of B-cells, CD4+ and CD8+ T-cells in these compartments. Significantly, B- and T-lymphocyte activation events and subsequent effector function in response to antigen stimulation were profoundly impaired in IRF-4-deficient lymphocytes; circulating serum immunoglobulin concentrations and humoral responses were dramatically reduced, and cytotoxic and cytotoxic T-lymphocyte (CTL)-mediated anti-viral and antitumor responses were absent in IRF-4 knockout mice (437). Early T-cell activation events such as intracellular calcium influx and expression of the CD25 and CD69 T-cell activation markers were intact in IRF-4-/- T-cells. These results suggest that IRF-4 functions during the later stages of T-cell activation, possibly at the level of integration of IL-2 growth factor signaling. This hypothesis was supported by the observation that diminished T-cell proliferation in IRF-4-deficient mice was not rescued by exogenous IL-2 administration (437). Thus, IRF-4 appears to be essential for the function and homeostasis of mature B- and T-lymphocytes in the periphery.

2.3.3 Oncogenic potential of IRF-4

The relationship between IRF-4 expression and oncogenicity is highlighted by the observation a proportion of patients with multiple myeloma (MM) exhibit a t(6;14)(p25;q32) chromosomal translocation that juxtaposes the immunoglobulin heavy-chain (IgH) promoter to the multiple myeloma 1 (MUM1) locus. The MUM1 locus at 6p25 is identical to the coding region of IRF-4. This chromosomal translocation involving the *irf4* gene may contribute to leukemogenesis, since MUM1/IRF-4 has oncogenic activity *in vitro* (438). The expression of the avian homologue of IRF-4 in primary Rat-1 fibroblasts resulted in morphological alterations, increased saturation density, proliferation, and life span, and promotion of growth in soft agar (438). Furthermore, IRF-4 and cooperated synergistically in the transformation of primary Rat-1 fibroblasts with v-Rel, the oncoprotein of the transforming avian reticuloendotheliosis virus. Antisense RNA to IRF-4 eliminated the formation of soft agar colonies induced by expression of v-Rel, which corresponded with reduced proliferation of v-Rel-transformed cells (438). Interestingly, exogenous expression of IRF-4 in v-Rel-transformed fibroblasts

decreased the production of type I IFN and suppressed the expression of ISG such as STAT1, JAK1, and 2'-5'-oligo(A) synthetase (438), suggesting that IRF-4 expression in conjunction with v-Rel facilitates cellular transformation by inhibiting the type I IFN antiproliferative pathway (438).

Transgenic mice overexpressing IRF-4/ICSAT have been generated, but IRF-4 overexpression alone was not sufficient to induce an ATL or MM-like phenotype in these mice (439). Production of IL-2 following stimulation with conA was significantly increased in transgenic mice compared to wild type controls, suggesting that IRF-4 overexpression may contribute to T-cell proliferation via control of IL-2 production (439). However, preliminary results obtained with IRF-4 transgenic mice must be interpreted with caution, because data obtained using the avian homologue of IRF-4 (438) suggests that IRF-4 may require additional factors to promote its oncogenic activity *in vivo* (289).

Specific Research Aims

The objective of this research was to characterize specific molecular mechanisms that regulate the activation of IRF signaling in response to virus infection. Initial studies examined a novel protein-protein interaction that regulates the activity of IRF-4 in T-cells infected and transformed with the HTLV-I retrovirus; subsequently, experiments were performed to identify protein-DNA interactions on the human IRF-4 promoter that are responsible for driving chronic IRF-4 expression in HTLV-I infected T-cells. These experiments identified several enhancer elements occupied by NF-κB/Rel subunits, which are chronically activated through classical IKK signaling in HTLV-I infected cells. The essential role of NF-κB/Rel proteins in the upregulation of IRF-4 gene transcription prompted further experiments to explore the role of IKK kinases in activation of NF-κB/Rel and IRF signaling, specifically through carboxy-terminal phosphorylation of transcription factors such as c-Rel, IRF-3 and IRF-7. These studies identified a novel physiological role specific to the IKK-related kinases IKKε and TBK-1: activation of the innate type I IFN anti-viral response through direct carboxy-terminal phosphorylation of IRF-3 and IRF-7. Subsequent experiments were performed to characterize the virus-inducible IKK-related pathway to IRF-3 and IRF-7 activation *in vitro* and *in vivo*, and define its importance for establishment of the cellular anti-viral state.

Chapter II

Materials and Methods

Chapter II

Materials and Methods

1. Cell culture and reagents

1.1 Cell lines

B-cell lines KR-12 (ATCC#CRL-8658, *homo sapiens* B lymphoblast), MC/CAR (ATCC#CRL-8083, *homo sapiens* B-lymphocyte plasmocytoma), Namalwa (ATCC#CRL-1432, *homo sapiens* Burkitt's Lymphoma), A20 (ATCC#TIB-208, *mus musculus*, B-lymphocyte reticulum cell sarcoma) and 70Z/3 (ATCC#TIB-158, *mus musculus* pre-B lymphoblast); T-cell lines Jurkat (ATCC#CRL-10915, *homo sapiens* T lymphoblast, acute T-cell lymphoma) and CEM (ATCC#CCL-119, *homo sapiens* T lymphoblast, acute lymphoblastic leukemia) were purchased from the American Type Culture Collection (ATCC). T-cell lines MT2 (#237, *homo sapiens*, human T-cell leukemia cells isolated from cord blood lymphocytes and co-cultured with cells from ATL patients), C8166 (#404, *homo sapiens*, HTLV-I transformed; HTLV-I infected cord blood lymphocytes banded on Percoll to obtain cells with increased production of HTLV-I), MT4 (#120, *homo sapiens*, HTLV-I transformed human T-cell cells isolated from patient with ATL), MoT (*homo sapiens*, HTLV-II transformed T-lymphocyte variant of hairy cell leukemia; (440)) and T4 (*homo sapiens* T lymphoblast, acute T-cell lymphoma (441)) were obtained from the National Institutes of Health (NIH) AIDS Research and Reference Reagent Program. The cell line BJAB (*homo sapiens* B-cell myeloma) was obtained from Dr. Jae U. Jung (Harvard Medical School, Harvard University, Cambridge, MA). All lymphocytic cell lines were maintained in RPMI 1640 (Canadian Life Technology, CLT) supplemented with 10% heat inactivated (HI) fetal bovine serum (FBS, GIBCO-BRL) and antibiotics, unless otherwise detailed by ATCC or NIH recommendations. ATCC293 cells (ATCC#CRL-1573, *homo sapiens* kidney, transformed with Adenovirus 5 DNA) and COS-7 cells (ATCC#CRL-1651, *cercopithecus aethips* (African Green Monkey), kidney, SV40 transformed) purchased from ATCC were maintained in DMEM medium (GIBCO-BRL) supplemented with 10% HI-FBS and antibiotics. ATCC A549 cells (ATCC#CCL-185, *homo sapiens* epithelial lung carcinoma) were maintained in F12K medium (GIBCO-BRL) supplemented with 10% HI-FBS and antibiotics. Control and TBK-1-/- MEFs were generated as previously

described (106), and maintained in MEM media (GIBCO-BRL) supplemented with 10% HI-FBS and antibiotics.

1.2 Isolation of primary T-lymphocytes

Primary human T-lymphocytes were isolated by Ficoll density gradient centrifugation from fresh sodium-citrate treated whole blood diluted 2X with phosphate-buffered saline (PBS) and overlaid in 30 mL aliquots over 15 mL Ficoll-Hypaque PLUS (Amersham Pharmacia) in 50 mL Falcon tubes. Following 25-minute centrifugation at 2000 rpm/20^{0}C without the brake, the ring of peripheral blood leukocytes (PBL) was extracted from the plasma-Ficoll interface. Pooled PBL fractions were incubated with RosetteSep T-cell enrichment cocktail (StemCell Technologies) at a final concentration of 20 μL/mL for 20 minutes at RT. Following a second Ficoll density gradient centrifugation to negatively select for CD3+ T-cells at the interface, the T-cell fraction was washed twice in PBS-2% non-HI FBS and maintained in RPMI 1640 medium with L-glutamine and sodium pyruvate (Sigma-Aldrich) supplemented with 1% human AB serum (GemCell Technology), HEPES (Sigma-Aldrich) and antibiotics. All experiments were performed within 48h of T-cell isolation.

PBL extracts from HAM/TSP, ATL patients and normal donors were obtained from Dr. Nazlim Azimi (National Cancer Institute, NIH, Bethesda, MD). All ATL patients possessed high leukemic T-cell counts (5-6 fold higher PBMC levels compared to normal donors), and at least 50% of peripheral T-lymphocytes displayed the ATL-associated CD4+CD8-CD25+ surface phenotype.

1.3 Biochemical reagents

For western blot analysis of IRF-4 expression in primary T-cells, PMA and ionomycin (Calbiochem) were used at a final concentration of 10 ηg/ml and 200 ηM, respectively. For *in vitro* kinase assays of classical and non-classical IKK kinase activity in Jurkat T-cells, PMA was used at a final concentration of 50 ηg/ml and TNFα (Calbiochem) was used at a final concentration of 10 μg/mL. Prior to PMA/ionomycin stimulation of primary T-cells, pre-treatment with FK506 (Sigma-Aldrich) was performed at a final

concentration of 1 mM for 1h. Doxycyclin (Dox) was used at a concentration of 1 μg/mL.

1.4 Transfection

Transfections using FuGene 6 reagent (Roche), LipofectAMINE Plus reagent (Invitrogen Life Technologies) and OligofectAMINE reagent (Invitrogen Life Technologies) were performed according to the manufacturer's specifications. Transient transfections using the calcium phosphate co-precipitation method were performed as previously described (398). dsRNA (polyI/polyC, Amersham-Pharmacia), prepared according to manufacturer's specifications and VSV ribonucleoprotein complex (RNP), prepared as previously described (442), were transfected into A549 cells using LipofecAMINE 2000 reagent (Invitrogen Life Technologies) according to manufacturer's specifications.

1.5 Virus infection

Sendai Virus (SV, a kind gift from Dr. Illka Julkenen, University of Helsinki, Finland) was used at a final concentration of 40 hemaglutinin units per mL (HAU/mL). Vesicular Stomatitis Virus (VSV, a kind gift from Dr. John Bell, University of Ottawa, Ontario) was used at the indicated multiplicity of infection (MOI), which corresponds to plaque forming units (pfu) per cell (pfu/cell). All SV and VSV infections were performed in the absence of serum for 1h following addition of virus to allow for viral adsorption; subsequently, the virus-containing supernatant was removed, cells were washed twice with PBS and fresh growth media was added for the indicated incubation time.

2. Plasmid construction

2.1 Luciferase reporter constructs

1.2-kbIRF-4PRO-PGL3B luc was generated by PCR amplification of the 1189 nucleotide upstream element corresponding to the human IRF-4 promoter (443) from genomic ATCC293 DNA based on the Genbank sequence #U52683 using specific primers (upstream primer 5'-GAGCTCATGAAAATCCCTGGTCCAC-3' and downstream primer 5'-AGATCTTGAGGGCAGCGGTGGGTCCC-3'). The promoter fragment was sub-cloned into *SacI/BglII* digested luciferase reporter plasmid pGL3 Basic (pGL3B, Promega). The following 5' promoter deletions were generated by restriction enzyme

digestion of 1.2-kbIRF-4PRO-pGL3B: *NotI/SmaI* (1.0-kb); *NotI/HindIII* (0.6-kb); *NotI/PstI* (0.4-kb); *NotI/StyI* (0.2-kb); *NotI/StuI* (0.08-kb).

Plasmids carrying point mutations in the κB1 and Sp1 sites were generated by *in vitro* site-directed mutagenesis using 1.2-kbIRF-4PRO-PGL3B as the template. Sub cloning of PCR-amplified fragments into *SacI/BglII* digested pGL3B was followed by *NotI/HindI* digestion to obtain a 0.6-kb promoter fragment. The κB1 site was mutated to 5'-CTCTGCAAAGCGtcGaaCCCTTCGCACCAG-3' (nucleotides in lowercase represent point mutations), and the Sp1 site was mutated to 5'-CACCAGATTCaaGaTACTACAaGaaCaaCATTTCaaGaaCTGGaaACATCGCTGCAA GTT-3'. ΔCD28RE was generated by a *PstI/StyI* digestion of 0.6-kbIRF-4PRO-pGL3B.

κBm RANTES-pGL3B (403), IFNA4-pGL3B (402) and IFNB-pGL3B (402) reporter constructs, which correspond to the human RANTES, human type I IFNα4 and human type I IFNβ promoters, respectively, have been described previously.

2.2 Expression vectors

HA epitope tagged wild type and mutant murine IRF-4 plasmid constructs IRF-4(aa1-439), IRF-4(aa1-419), IRF-4(aa1-410), IRF-4(aa1-150) and IRF-4Δ150-410 (433) were a kind gift from Dr. Harinder Singh (University of Chicago, Chicago, IL). FLAG epitope tagged murine IRF-4 plasmid constructs IRF-4(aa1-340), IRF-4(aa1-237), IRF-4(aa150-237), IRF-4(aa150-340) and IRF-4(aa150-410) as well as Myc epitope tagged human FKBP52 wild type and FKBP52(aa1-243) and FKBP52(aa233-459) plasmid constructs were generated as described previously (444).

Mammalian expression plasmids pCMV4-Tax WT, pCMV4-M22 and pCMV4-M47, encoding wild type and two mutant forms of the HTLV-I Tax protein (257) were provided by Dr. W.C Greene (Gladstone Institute, San Francisco, CA). pCMV4-NF-ATpXS (286), encoding a truncated, constitutively active form of NF-ATp, was provided by Dr. S.C Sun (Penn State University, Hershey, PA).

Human IKKε cDNA was PCR amplified from a Human T-cell Leukemia Virus I transformed T-cell line (SLB-1) cDNA library (Clontech) using specific primers (upstream primer 5'-GAATTCGATGCAGAGCACAGCCAATTACCCGT-3' and downstream primer 5'-GATCTTCAGACATCAGGAGGTGCTGGGACT-3'). Human TBK-1 cDNA was obtained from Origene Technology and PCR amplified for subcloning (upstream primer 5'-GCGGCCGCGATGCAGAGCACTTCTAATCATC-3' and downstream primer 5'-TCTAGAGCTAAAGACAGTCAACGTTGC-3'). IKKε cDNA was digested with *EcoRI/BglII*, TBK-1 was digested with *NotI/XbaI*, and each was cloned directionally into the corresponding restriction sites of the pCDNA3.1 mammalian expression vector (Invitrogen) with either a FLAG or Myc epitope tag inserted before the multi-cloning site. Dominant negative IKKε(K38A) and TBK-1(K38A) constructs were generated by site directed mutagenesis using overlap PCR followed by directional cloning into pCDNA3.1 (Invitrogen) with either a FLAG or Myc epitope tag using the same sites as for wild type constructs. IKKε(1-361) was created through digestion of pcDNA 3.1FLAG-IKKε with *XhoI/XbaI*, followed by Klenow treatment and re-ligation of the construct. pRevTre (rtTA-responsive vector, Clontech) encoding FLAG-IKKε was obtained by *NheI/EcoRV* digestion of pcDNA3.1FLAG-IKKε, followed by Klenow treatment and nondirectional cloning into *EcoRV* digested pRevTre.

Plasmids encoding NIK, Myc-IKKα, FLAG-IKKβ, FLAG-IRF-3 (398), FLAG-IRF-7 (420), GFP-IRF3 (398) and GFP-IRF-7 (420) mammalian expression vectors have been described previously. All expression plasmids were sequenced and verified for expression by transfection into ATCC293 cells followed by western blot using protein-specific antisera in addition to epitope-specific antisera.

2.3 GST fusion vectors

Vectors encoding GST-IκBα(aa1-55) and GST-2NIκBα(aa1-55) (445), and GST-IRF-3(aa380-427) (411,422) and GST-IRF-7(aa468-503) (420) fusion constructs have been previously described. GST fusion constructs corresponding to the c-Rel TD were PCR-amplified from full-length human c-Rel cDNA (66). GST-c-RelTD(aa422-588) (upstream primer 5'-GATTTAAATGCTTCTAATGCT–3' and downstream primer

5'–TACAAAATGCTGCATCTATAT–3'), GST-c-RelTD(A)(aa422-472) (upstream primer 5'-GATTTAAATGCTTCTAATGCT–3' and downstream primer 5'–TTAACTGCTGGTGTCATCATA-3'), GST-c-RelTD(B)(aa473-528) (upstream primer 5'– GACAGCATGGGAGAGACTG–3' and downstream primer 5'–TTACTCAAATGCATCTGATTGTGA–3') and GST-c-RelTD(C)(aa529-588) (upstream primer 5'–GGATCTGACTTCAGTTGTG–3' and downstream primer 5'–TACAAAATGCTGCATCTATAT–3'). The fragments were digested with *BamHI/EcoRI* and cloned directionally into the corresponding restriction sites of the pGEX-4T2 GST fusion vector (Clonetech).

3. Protein analysis

3.1 Specific antisera

Primary antisera and the corresponding dilutions used in western blot analysis for one dimensional SDS-PAGE: anti-HA (HA-7 mouse monoclonal, Sigma; 1μg/mL), anti-Myc (9E10 mouse monoclonal, a kind gift from Dr. Stephane Richard, McGill University, Montreal; 1μg/mL), anti-FLAG (M2 mouse monoclonal, Sigma; 1 μg/mL), anti-IRF-4 (sc-6059 M47 goat polyclonal, Santa Cruz Biotechnology; 1μg/mL), anti-FKBP52 (Biomol, 1 μg/mL), anti-Tax (rabbit polyclonal, a kind gift from Dr. W.C Greene; 1/10 000), anti-IRF-3 (sc-9082 FL-425 rabbit polyclonal, Santa Cruz Biotechnology; 1 μg/mL), anti-IRF-3 S396 phosphospecific (HIS503 rabbit polyclonal (415); 1/5000), anti-ISG56 (rabbit polyclonal, a kind gift from Dr. Ganes C. Sen, Lerner Research Institute, Cleveland Clinic; 1/1000), anti-IKKε/TBK (IMG-270 mouse monoclonal, Imgenex; 1 μg/mL), anti-VSV (rabbit polyclonal, a kind gift from Dr. John Bell, University of Ottawa; 1/1000), anti-IKKβ (mouse monoclonal, Alexis; 1 μg/mL) and anti-actin (mouse monoclonal, Sigma;1/10 000), anti-mIRF-3 (51-3200 rabbit polyclonal, Zymed; 1 μg/mL).

3.2 Whole cell extracts and SDS-PAGE

For preparation of whole cell extracts (WCE), cells were washed twice in cold PBS and lysed at 4°C for 30 minutes in a buffer containing 10mM Tris-HCl (pH 8.0), 60 mM KCl, 1mM ethylene diamine tetraacetic acid (EDTA), 1 mM dithiothreitol (DTT), 0.5%

Nonidet P-40 (NP-40), 0.5 mM phenylmethlysulfonyl fluoride (PMSF), 10 mM sodium orthovanadate, leupeptin (10 μg/ml), pepstatin (10 μg/ml) and aprotinin (10 μg/ml). Following a 20 minute centrifugation at 14 000 rpm at 4°C to remove cellular debris, equal amounts of WCE were fractionated by sodium dodecyl sulfate-polyacrylamide gel electrophoresis (SDS-PAGE). After transfer, the Hybond nitrocellulose membrane (Amersham, Cleveland, Ohio) was blocked in 5% milk dissolved in Tris-buffered saline-Tween 20 1% (TBS-T) for 1h. The membrane was incubated with primary antisera diluted in 5% milk/TBS-T or 5% BSA/TBS-T (IRF-3 serine 396 phosphospecific antisera) at room temperature (RT) for 2h or overnight at 4°C. After four 5-minute washes in TBS-T, membranes were incubated with a peroxidase-conjugated secondary antibody. Reaction was visualized with enhanced chemiluminescence detection system as detailed by manufacturer (Amersham).

3.3 Co-immunoprecipitation

For *in vivo* co-immunoprecipitation experiments, WCE were prepared as detailed above and immunoprecipitated with 1 μg of specific antisera cross-linked to 30 μL protein Sepharose G beads with dimethyl pimelidate (DMP, Sigma). Antisera used for co-immunoprecipitation were directed against Myc (9E10 mouse monoclonal, Dr. Stephane Richard), IRF-4 (sc-6059 M47 goat polyclonal, Santa Cruz Biotechnology), FKBP52 (Biomol) and Tax (rabbit polyclonal, Dr. W.C Greene). All co-immunoprecipitations were performed overnight at 4°C. Immune complexes were washed four times in lysis buffer and resolved by SDS-PAGE followed by western blotting with specific antisera as detailed above.

4. Transient co-expression and reporter gene assay

Exponentially growing Jurkat and MT2 cells (10^6) were transfected by FuGene 6 transfection reagent (Roche) with 25 ηg of pRLTK normalizing plasmid (*renilla* luciferase for internal control) and 0.2 μg of luciferase reporter plasmid (firefly luciferase, experimental reporter) per transfection. Expression plasmids were added in 3-fold molar excess and empty vector was added to each sample to bring the total amount of DNA to 2.0 μg per transfection. Sub confluent ATCC293, A549 or control and TBK-/-

MEFs cells in 35mm tissue culture dishes were transfected with 20 ηg of pRLTK normalizing plasmid (*renilla* luciferase for internal control), 100 ηg of pGL3 reporter (firefly luciferase, experimental reporter) by the calcium phosphate co-precipitation method (ATCC293), LipofectAMINE2000 (A549) or FuGene6 (control and TBK-/- MEFs). Up to 800 ηg of expression plasmid and empty vector was added to each sample to bring the total amount of DNA to 0.5 μg per transfection. Cells were harvested 46h (Jurkat and MT2) or 24h (ATCC293, A549, control and TBK-/- MEFs) post-transfection, lysed in 100 μL passive lysis buffer (Promega) and assayed for dual-luciferase activity using 5 μL of lysate according to manufacturers instructions (Promega). All firefly luciferase values were normalized to *renilla* luciferase to control for transfection efficiency, and results shown represent the average of at least three independent experiments.

5. *In vitro* kinase assay

5.1 Preparation of recombinant GST fusion peptides

Escherichia coli (E. Coli) strain Rossetta (Invitrogen) were transformed with different expression plasmids encoding GST fusion peptides and streaked for single colonies. Single colonies were amplified overnight in a culture volume of 2 mL of Luria Broth (LB) at 37°C. Following overnight incubation, culture was diluted 1/100 and incubated at 37°C until optical density (OD) read 0.6 at 600 ηM. Bacteria were then stimulated with isopropyl-β-D-thiogalactopyranoside (IPTG) at a concentration of 1 mM for 3h at 37°C. Bacterial pellet was lysed in PBS 1% Triton X-100, sonicated for 5 sets of 30 second pulses at 30% efficiency and centrifuged for 15 minutes at 10 000 rpm/4°C. Bacterial lysate was incubated with glutathione sepharose beads (Pharmacia) for 30 minutes at RT, washed 4 times with PBS 0.1% Triton-X and eluted in 3 batches in 1 mL of elution buffer (150 mM NaCl, 50 mM Tris (pH 7.5), 20 mM glutathione).

5.2 Immunoprecipitation

Immunoprecipitations for *in vitro* kinase assay were performed by incubating WCE (150-400 μg) for a total of 4h at 4°C with protein A or protein G sepharose beads (Amersham Pharmacia, Sweden) pre-coupled to specific antisera directed against IKKγ (rabbit

polyclonal, Santa Cruz Biotechnology), Myc (9E10 mouse monoclonal, Dr. Stephane Richard), FLAG (M2 mouse monoclonal, Sigma), IKKε (Q-15 goat polyclonal, Santa Cruz Biotechnology) or TBK-1 (rabbit polyclonal, a kind gift from Dr. Tom Maniatis, Harvard University, Cambridge). The pre-coupling reaction was performed by incubation of 0.5-1 μg specific antisera per 30 μL packed sepharose beads for 2h at 4°C in TNET buffer (50 mM TRIS pH 7.4, 100 mM NaCl, 1 mM EDTA pH 8.0, 0.5% NP-40 and 1% BSA).

5.3 Endogenous kinase assay

For classical IKK kinase assays, 500 μg WCE was incubated with anti-IKKγ-coupled protein A sepharose beads. For IKKε kinase assays, 500 μg WCE was incubated with anti-IKKε-coupled protein A sepharose beads. For TBK-1 kinase assays, 200 μg WCE was incubated with anti-TBK-1-coupled protein A sepharose beads. IKK immunocomplexes were washed twice in lysis buffer and twice in a standard IKK kinase buffer (20 mM HEPES, 10 mM $MgCl_2$, 0.1 mM sodium orthovanadate, 20 mM β-glycerophosphate, 10 mM p-nitrophenylphosphate (PNPP), 1 mM DTT and 50 mM NaCl). Kinase reaction was performed by incubation of immunocomplexes with 1X kinase buffer, 10 μCi [γ-^{32}P]-ATP, 1mM ATP and a specific GST substrate at 30°C for 30 minutes in a 40 μL volume. Following fractionation of samples by 10% SDS-PAGE, the upper half of the gel was transferred to a nitrocellulose membrane and western blotted for immunoprecipitated kinase; the lower half of the gel was stained with Coomassie blue for 15 minutes, destained in 10% methanol/10% acetic acid for 1 hour, soaked in 2% glycerol for 30 minutes, dried and exposed to Biomax XR film (Kodak).

5.4 Whole cell extract kinase assay

Subconfluent ATCC293 cells were transected with 12.0 μg total DNA (12.0 μg empty pcDNA3.0, 4.0 μg pcDNA3.0 IKKα, -β or -ε and 8.0 μg empty pcDNA3.0, 4.0 μg IKKε and 8.0 μg pcDNA3.0 IKKε(K38A)) using FuGene 6 transfection reagent (Roche) as detailed by the manufacturer. WCE (2.0 μg) were incubated with 2.0 μg GST substrate and subjected to *in vitro* kinase assay as described above.

5.5 *In vitro* transcription/translation coupled kinase assay

In vitro transcription and translation was performed using the TNT Quick Coupled Reticulocyte System (Promega) as detailed by manufacturer. Following immunoprecipitation of rabbit reticulocytes with anti-FLAG-coupled protein G sepharose beads (pcDNA3.0, pcDNA3.0 IKKβ, pcDNA3.0 IKKε and pcDNA3.0 IKKε(K38A)) or anti-Myc-coupled protein G sepharose beads (pcDNA3.0 IKKα), immune complexes were washed 4 times in kinase buffer containing 250 mM NaCl and *in vitro* kinase assay was performed as described above using 2.0 μg GST, GST-IRF-3(aa380-427), GST-IRF-7(aa468-503), or GSTIκBα(aa1-55) as substrate for 50 minutes at 30°C.

5.6 Recombinant protein *in vitro* kinase assay

For preparation of purified recombinant IKKε and TBK-1, 15cm tissue culture plates were seeded with $2x10^7$ SF9 insect cells (BD Bioscience) per plate. Fresh TMN-FH medium (BD Bioscience) containing 10% HI-FBS was added to make up a final volume of 30 ml per plate. SF9 cells were infected with a high-titer stock solution of recombinant baculoviruses (constructed by Dr. Lin, integrated with human TBK-1 and IKKi cDNA, minimum titer $1X10^8$ virus particles/ml). Enough inoculum was added to achieve an MOI greater than 1.0. Following incubation at 27°C for 3 days, the cells were harvested by spinning down the cells at 2500 rpm for 10 minutes. Following resuspension of the cell pellet with 1 ml of cold lysis buffer (50mM Tris pH 7.5, 650mM NaCl, 5% Triton-X100, 50mM NaF, 50mM NaPi pH 7.5, 50mM NaPPi pH 7.5), the lysate was incubated on ice for 1h and centrifuged at 13 000 rpm for 30 minutes. Supernatant was incubated with HIS-binding beads (Novogene, 0.5 ml supernatant per 50 μl beads) pre-equilibrated with His-binding buffer for 1h at 4C. Beads were washed with His-washing buffer 3 times, and recombinant proteins were eluted in His-eluting buffer for 30 minutes at 4C. 500 ηg of control and purified kinase extract was used in a standard IKK *in vitro* kinase assay as described above.

6. *In vivo* genomic footprinting

For *in vivo* methylation by dimethyl sulfate (DMS, Aldrich Chemical, Milwaukee, WI), exponentially growing MT2 or Jurkat T-cells (10^8) were harvested and resuspended in

RPMI 1640 -10% heat inactivated FBS supplemented with 20 mM HEPES (pH 7.3). Methylation reaction was performed in the presence of 10 µl/ml of concentrated DMS for 1 minute at RT. Reaction was stopped by two washes with ice-cold PBS containing 2% β-mercaptoethanol. Genomic DNA extraction was performed as previously described (66). To obtain naked DNA, cells were first lysed to extract genomic DNA and then submitted to DMS treatment for 30 seconds. Genomic DNA resuspended in 200 µl H_2O was treated with 20 µl of piperidine (Aldrich) for 30 minutes at 90 °C to cleave methylated G (or A) residues. For each sample, 5 µg of DMS-treated, piperidine-cleaved genomic DNA was used for ligation-mediated PCR (LM-PCR) using Vent DNA polymerase (New England Biolabs, Mississauga, Canada), as described elsewhere (446,447). To ensure elongation of different fragment sizes, PCR amplification step was 2 minutes for the first cycle and was progressively increased to 10 minutes in the last cycle, with a total of 18 cycles. A third primer was radiolabelled by end labeling using T4 polynucleotide kinase (Amersham) and [γ-^{32}P]-ATP (ICN Pharmaceuticals). Two more PCR cycles were performed to labeled elongated DNA.

Each reaction product was phenol-chloroform extracted and ethanol precipitated prior to electrophoresis on a 7.5 % Explorer sequencing gel (Baker, Phillipsburg, NJ) in 1X TBE at 65 W. Reactions were visualized by autoradiography using Biomax MR films (Kodak, Rochester, NY). For the LM-PCR, several sets of primers were used. For analysis of the non-coding strand of the –600 to –400 region of the IRF-4 promoter, primer 1, 5'-GTCACTTCAATTCACCAGC-3', Tm 58° C; primer 2, 5'-GCAAAAGGATGTAAGCATGTCAGACACG-3', Tm 63° C; primer 3: 5'-GTAAGCATGTCAGACACGCAGAGACAGTATTTG-3', Tm 65 °C. For analysis of the non-coding strand of the –460 to –260 region of the IRF-4 promoter, primer 4, 5'-GTGATGGCCTTGCCGA-3', Tm 60° C; primer 5, 5'-GCAACCTCCACCTCCAGTTCTCTT-3', Tm 63 °C; primer 6, 5'-ACCTCCAGTTCTCTTTGGACCATTCCTCC-3', Tm 66 °C. Results shown represent at least three independent experiments.

7. Electromobility shift assay (EMSA)

7.1 Oligonucleotide probes

Complimentary oligonucleotides for EMSA probes were obtained from GIBCO BRL/Life Technologies. 20 μg of each complimentary oligonucleotide were mixed together, heated at 85°C for 5 minutes, and cooled down slowly to RT overnight to favor proper annealing of complimentary strands. The resulting double stranded probes were gel purified from a 1X TBE (50 mM Tris-HCl pH 8.0, 50 mM Boric Acid, 1 mM EDTA) 15% polyacrylamide gel (19:1 crosslink) and eluted in TE (10 mM Tris-HCl pH 8.0, 1 mM EDTA) by shaking overnight at 4°C. Probes were end-labeled with [γ-^{32}P]-ATP (Mandel) using T4 polynucleotide kinase. Unincorporated nucleotides and salts were removed by passing the labeled reaction through G-25 or G-50 micro-spin column (Amersham Pharmacia).

Oligonucleotide probes (mutations indicated in bold):

NF-AT consensus: 5'-CGC CCA AAG AGG AAA ATT TGT TTC ATA-3'

NF-AT mutant: 5'-CGC CCA AAG **CTT** AAA ATT TGT TTC ATA-3'

Sp1 consensus: 5'-ATT CGA TCG GGG CGG GGC GAG C-3'

Sp1 mutant: 5'-ATT CGA TCG **GTT** CGG GGC GAG C-3'

κB1: 5'- CTC TGC AAA GCG AAG TCC CCT TCG CAC-3'

NF-2/Sp1:5'-TGG CCA GGG CGG GAA ATG GGG GGC GTG TAG CGG-3'

CD28RE: 5'-GCC CTT CGC GGG AAA CGG CCC CAG TGA CAG TCC CCG AGG CGG-3'

IRF-7 BS1: 5'-GAAAGTGAACGC-3'

ISRE ISG15: 5'-ATCGGAAAGGGAAACCGAAACTGAAGCC-3'

7.2 Nuclear extracts

Crude nuclear extracts were prepared from 10^7 cells washed in cold Buffer A (10 mM HEPES pH 7.9, 1.5 mM $MgCl_2$, 10 mM KCl, 0.5 mM DTT, 0.5 mM PMSF), then resuspended in 10 μL Buffer A/0.5%NP-40 for 10-minutes on ice. Samples were centrifuged for 10 minutes at 10 000 rpm/4°C, and supernatant containing the cytoplasmic fraction was removed. Nuclear pellets were resuspended in 20 μL cold

Buffer B (20 mM HEPES pH 7.9, 0.42 M NaCl, 1.5 mM $MgCl_2$, 0.2 mM EDTA, 25% glycerol, 0.5 mM DTT, 0.5 mM PMSF, 5 μg/mL leupeptin, 5 μg/mL pepstatin, 5 μg/mL aprotinin, 0.5 mM spermidine and 0.15 M spermine) for 10 minutes on ice. Following centrifugation at 10 000 rpm/4°C, nuclear extracts were diluted 5-fold in Buffer C (20 mM HEPES pH 7.9, 0.2 mM EDTA, 50 mM KCl, 20% glycerol 0.5 mM DTT and PMSF).

7.3 Binding reaction and antibody supershift

For NF-κB, NF-AT and Sp1, the binding reaction was carried out in a 20 μl final volume in a binding buffer containing 20 mM HEPES pH 7.9, 5% glycerol, 0.1 M KCl, 0.2 mM EDTA pH 8.0, 0.2 mM ethylene glycol-bis(β-aminoethyl-ether)-N,N,N',N'-tetraacetate (EGTA) pH 8.0 and 1 μg of poly(dI-dC) using 5-10 μg of protein extract. For IRF-3 and IRF-7, the binding reaction was carried out in a 20 μl final volume in a binding buffer containing 10 mM Tris-Cl pH 7.5, 1 mM EDTA, 50 mM NaCl, 2 mM DTT, 5% glycerol, 0.5% NP-40, 1 μg bovine serum albumin (BSA) and 1 μg of poly(dI-dC) using 5-10 μg of protein extract. Antibody supershifts were performed for 15 minutes at RT using 1 μg of specific antisera directed against p65 (sc-372 C-20 rabbit polyclonal, Santa Cruz Biotechnology), p50 (sc-1190 C-19 goat polyclonal, Santa Cruz Biotechnology), c-Rel (sc-71 C rabbit polyclonal, Santa Cruz Biotechnology), Sp1 (sc-59 PEP 2 rabbit polyclonal, Santa Cruz Biotechnology), NF-ATx/NF-AT4 (sc-1152 C-20 goat polyclonal, Santa Cruz Biotechnology), NF-ATc/NF-AT2 (MA3-024 mouse monoclonal, Affinty Bioreagents), IRF-7 (sc-9083 H-246 rabbit polyclonal, Santa Cruz Biotechnology), IRF-3 (sc-9082 FL-425 rabbit polyclonal, Santa Cruz Biotechnology), FLAG (M2 mouse monoclonal, Sigma) or control rabbit, goat or mouse serum. 1 μL of a 1:10 dilution of antisera directed against NF-ATp/NF-AT1 (06-348 rabbit polyclonal, Upstate Biotechnology) was also used. For oligonucleotide competitions, a 100-fold molar excess of unlabelled probe was added to the binding reaction for 10 minutes prior to the addition of the labeled probe. Protein/DNA complexes were resolved on 5% polyacrylamide-0.5X Tris-borate-EDTA (TBE) gels and exposed to Biomax XR film (Kodak) overnight at -80°C.

8. Formaldehyde cross-linking and chromatin immunoprecipitation (chIP)

Formaldehyde cross-linking and chromatin immunoprecipitation procedure was modified from the protocol reported by Boyd et al (448). Exponentially growing Jurkat or MT2 cells (2 x 10^7) were treated with formaldehyde (Fischer Scientific), which was added directly to the growth medium at a final concentration of 1% at RT with stirring. The reaction was stopped after 10 minutes by addition of glycine at a final concentration of 0.125 M. Suspension cells were harvested, washed twice in ice cold PBS and lysed in SDS lysis buffer (Upstate Biotechnology) on ice for 10 minutes. DNA was sonicated to an average length of 600 base pairs using 5 sets of 10-second pulses at 30% lysate was removed for 10% input control. Lysates were diluted five fold in IP buffer (Upstate Biotechnology) and precleared for 1h at 4°C with 80 mL of a 50 % salmon sperm DNA/protein A agarose slurry (Upstate Biotechnology). Immunoprecipitations were carried out by the addition of 4 μg of mouse monoclonal anti-c-Rel (Santa Cruz), rabbit polyclonal anti-p50 (Santa Cruz), rabbit polyclonal anti-Sp1 (Santa Cruz), rabbit polyclonal anti-NF-ATp (Upstate Biotechnology), rabbit polyclonal anti-IRF3 (Santa Cruz) or no antibody overnight at 4°C with rotation. A secondary rabbit anti-mouse antibody was added to the c-Rel sample 2h before collection of immune complexes with 60 μL slurry for 1 hour at 4°C. Immune complexes were washed for 5 minutes in Low Salt Buffer (Upstate Biotechnology), High Salt Buffer (Upstate Biotechnology, LiCl Wash Buffer (Upstate Biotechnology) and twice in TE followed by elution of protein/DNA complexes in 1% SDS and 0.1 M $NaHCO_3$. Protein/DNA crosslinks were reversed by addition of NaCl at a final concentration of 200 mM and incubation at 65°C for 4 hours. Following proteinase K treatment, samples were extracted with phenol/chloroform/isoamyl alcohol and precipitated at -20°C overnight with 95% ethanol/0.5M sodium acetate and 20 μg glycogen. DNA pellets were resuspended in 50 μL TE and PCR was performed in the linear range of amplification using primers specific to the human IRF-4 promoter, corresponding to a 250bp region containing the κB1, NF-1/Sp1 and CD28RE sites: primer 1: 5'-GCAACCTCCACCTCCAGTTCTCTTTG-3'; primer 2: 5'-TTCGGGGACTGTCACTGGGGCCGT-3'.

9. Fluorescent microscopy

To analyze the subcellular localization of IRF-3 and IRF-7 proteins, GFP-IRF-3 and GFP-IRF-7 expression plasmids (2.5 μg) were transiently transfected into subconfluent COS-7 cells by LipofectAMINE (Invitrogen Life Technology) together with expression plasmids (2.5 μg) encoding IKKε, IKKε(K38A), TBK-1, and TBK-1(K38A). At 24h post-transfection, GFP fluorescence was analyzed in living cells with a Leica fluorescence microscope and photographed at 400x. Cells positive for GFP expression were counted, and fluorescence was considered nuclear if a greater than 2-fold level of fluorescence was localized in the nucleus.

10. RNA interference

RNA duplexes were synthesized with 2-nt (2'deoxy) uridine 3' overhangs directed against nucleotides 1472 to 1492 for TBK-1 (AAGCGGCAGAGUUAGGUGAAUUAAA) and 1611 to 1631 for IKKε (AAGAAGCAUCCAGCAGAUUCAUUAA) (Dharmacon Research). A control RNA oligonucleotide (AACAUAGCGUCCUUGAUCACAUUAA) was also synthesized. A549 lung epithelial cells were split at 1.5 x 10^5 cells/well in 6 well dishes 24h prior to infection in the absence of antibiotics. Oligonucleotides (20 μl of 20 mM control oligonucleotides and 10 μl of 20 mM for each of TBK-1 and IKKε) were transfected with OligofectAMINE (Invitrogen Life Technology) as per manufacturers' instructions. VSV infections were performed at MOI 100 and coordinated to harvest simultaneously at 72h post-oligonucleotide transfection for each time point.

11. Anti-viral assay

ATCC293 cells were transfected with 10.0 μg of GFP, FLAG-IKKε, or FLAG-IKKε(K38A) and either IRF-3 or IRF-3ΔN with FuGene6 24h prior to VSV infection. VSV was used at an MOI of 5.0 and supernatant was harvested at 1, 3, 6, 9, and 12h post infection. WCE (80 μg) was resolved on a 7.5% SDS-PAGE gel and analyzed with anti-FLAG (M2), IRF-3 (sc-9082), anti-VSV, anti-ISG56, and anti-actin. Virus titers from 293 cell infections were determined from 1:10^6 dilutions of the ATCC293 supernatant seeded onto confluent plates of Vero cells in triplicate. At 1h post infection, supernatant

was removed and 3% methylcellulose was overlayed. At 3 days post infection, overlay was removed; cells were fixed with 4% formaldehyde for 1h, and stained with 0.2% crystal violet in 20% methanol. Plaque assays were counted, averaged, and multiplied by the dilution factor to determine viral titer as pfu/mL.

Chapter III

Activation of IRF-4 in HTLV-I transformed T-cells

IRF-4 is a lymphoid/myeloid-specific member of the IRF family of transcription factors that plays an essential role in the proliferative capacity of mature B- and T-lymphocytes stimulated by antigen. In resting T-lymphocytes expression of IRF-4 is tightly regulated, and is limited to transient induction following activation through the TCR. However, IRF-4 is constitutively upregulated at the mRNA and protein levels in CD4+ T-cells infected with HTLV-I, as a direct gene target for the Tax oncoprotein. In this study we describe a novel interaction between IRF-4 and the immunophilin FKBP52, which results in post-translational modulation of IRF-4 activity. We demonstrate that chronic IRF-4 expression in HTLV-I infected T-cells is associated with a leukemic phenotype, and examine the mechanisms by which continuous production of IRF-4 is achieved. These experiments constitute the first detailed analysis of the transcriptional regulation of the human IRF-4 promoter within the context of HTLV-I infection and transformation of CD4+ T-lymphocytes.

Chapter III

Activation of IRF-4 in HTLV-I transformed T-cells

1. Post-translational regulation of IRF-4 by the immunophilin FKBP52

As a lymphoid/myeloid-restricted member of the IRF transcription factors, IRF-4 expression is fundamental for the homeostasis and effector function of mature lymphocytes (437). In addition to regulated expression in B-cells at various stages of development, IRF-4 overexpression is observed in all HTLV-I-transformed T-cell lines (432-434,436,449,450). A yeast two hybrid screen performed by Dr. Yäel Mamane identified a novel interaction between IRF-4 and the FK506-binding protein 52 (FKBP52) (444), a member of the immunophilin family of chaperone proteins that possesses intrinsic peptidyl-prolyl isomerase (PPIase) activity (451-453). Since full-length IRF-4 is intrinsically active for transcription, the bait utilized was IRF-4(aa150-410), which comprises the proline-rich domain and carboxy-terminal IAD domain of IRF-4 (433,454). Out of 10^6 clones screened, 2/10 clones that were positive in the yeast two-hybrid corresponded to full-length human FKBP52 (444). Further studies indicated that IRF-4 binding to FKBP52 precipitates a novel post-translational modification of IRF-4, which affects its transcriptional activity. Specifically, the IRF-4-FKBP52 association results in structural modification of IRF-4, through peptidyl-prolyl isomerization within the IRF-4 proline rich domain, which inhibits IRF-4 DNA binding and transactivation potential. FKBP52 modification of IRF-4 is dependent on the functional PPIase activity of FKBP52, as treatment with the CsA analogue ascomycin, an inhibition of FKBP52 enzymatic activity, abolishes the inhibitory effects of the FKBP52-IRF-4 interaction (444).

1.1 Mapping the interaction domain between IRF-4 and FKBP52

Figure 10A is a schematic representation of human FKBP52, which contains three FKBP-like domains: domain 1 possesses intrinsic PPIase activity and an FK506 recognition/binding site, domain 2 provides binding sites for ATP and GTP, and domain 3 contains the tetratricopeptide repeats (TPR) responsible for association with chaperone molecules such as Hsp90 (452,455). To localize the specific region interacting with IRF-4, FKBP52 was truncated to an amino-terminal fragment N-FKBP52(aa1-243), which

Figure 10. An interaction between IRF-4 and FKBP52 (A) FKBP52 possesses three functional domains. FKBP-like domain 1 contains PPIase activity (aa1-148); FKBP-like domain 2 contains the ATP/GTP binding site (aa148-267); 3 tetratricopeptide repeats (aa267-389) mediate protein-protein interactions. **(B, C, D)** The proline-rich region of IRF-4 (aa150-237) interacts with the tetratricopeptide repeats of FKBP52 (aa233-459). COS-7 cells were transfected with Myc-FKBP52 and FLAG or HA-IRF-4 constructs (15.0 μg each) and WCE (300 μg) were immunoprecipitated (IP) with anti-Myc antibody 9E10 (anti-Myc); immunoprecipitated complexes were resolved by 15% SDS-PAGE and immunoblotted (IB) with anti-FLAG antibody to detect FLAG-IRF-4 expression (in upper panels B and C), anti-HA antibody for IRF-4 (upper panel D). The membranes were reprobed with anti-Myc to verify protein expression and successful IP (lower panels). WCE (30 μg) were used as input and extract from untransfected COS-7 cells (300 μg) was immunoprecipitated with anti-Myc as control IP. **(E)** Schematic summary of the IRF-4 interaction domains with full length FKBP52. The 150-237 construct could not be stably expressed as a tagged peptide and was not tested directly, hence the parentheses. Domains of IRF-4: DNA binding domain with tryptophan repeats (DBD; aa1-150), the proline-rich region (Pro; aa150-237), the IRF association domain (IAD; aa237-410) and the carboxy-terminal autoinhibition element (AIE; aa410-450) are illustrated.

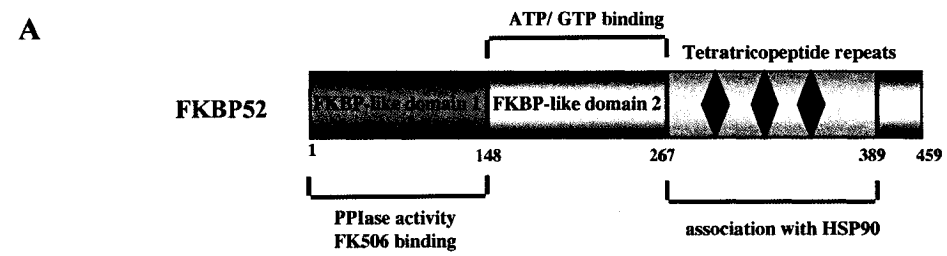
A
ATP/ GTP binding
Tetratricopeptide repeats
FKBP52
FKBP-like domain 2
1
148
267
389
459
PPIase activity
FK506 binding
association with HSP90

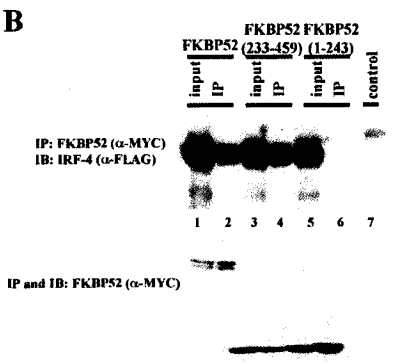
B
FKBP52
FKBP52 (233-459)
FKBP52 (1-243)
input
IP
control
IP: FKBP52 (α-MYC)
IB: IRF-4 (α-FLAG)
1 2 3 4 5 6 7
IP and IB: FKBP52 (α-MYC)


C
IRF-4 1-237
IRF-4 1-340
IRF-4 1-410
IRF-4 150-340
IRF-4 150-410
input
IP
control
IP: FKBP52 (α- MYC)
IB: IRF-4 (α- FLAG)
48
36
28
34
28
21
IP and IB: α-FKBP52 (MYC)
1 2 3 4 5 6 7 8 9 10 11 12

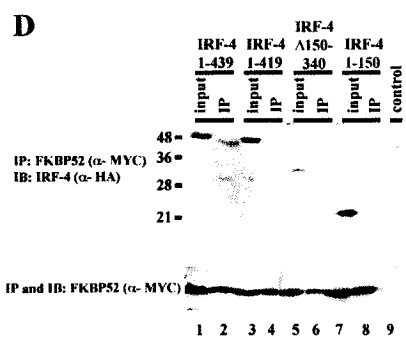
D
IRF-4 1-439
IRF-4 1-419
IRF-4 Δ150-340
IRF-4 1-150
input
IP
control
48
36
28
21
IP: FKBP52 (α- MYC)
IB: IRF-4 (α- HA)
IP and IB: FKBP52 (α- MYC)
1 2 3 4 5 6 7 8 9

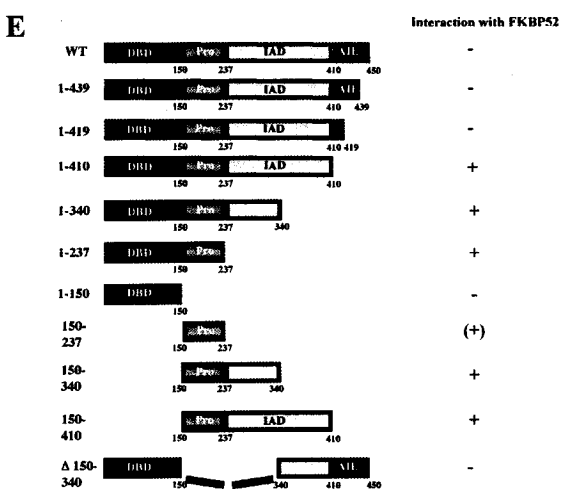
E
Interaction with FKBP52
WT
1-439
1-419
1-410
1-340
1-237
1-150
150-237
150-340
150-410
Δ 150-340
DBD
Pro
IAD
NTL
-
-
-
+
+
+
-
(+)
+
+
-

retains domains 1 and 2, and a carboxy-terminal fragment ΔN-FKBP52(aa233-459), which retains the TPR in domain 3 (Fig. 10A). Each FKBP52 construct expressed as a Myc-tagged fusion protein was co-transfected with FLAG-IRF-4(aa150-410) into COS-7 cells, and WCE were immunoprecipitated with anti-Myc antisera (Fig. 10B). Resolution of the immunoprecipitates by one-dimensional SDS-PAGE followed by western blot with anti-FLAG revealed that IRF-4(aa150-410) co-precipitated with full length and ΔN-FKBP52(aa233-459) (Fig. 10B, upper panel, lanes 2 and 4), but not with N-FKBP52(aa1-243) (Fig. 10B, upper panel, lane 6). The lower panels of Figure 10B, C and D are western blot control for Myc-FKBP52 expression and immunoprecipitation. These results confirm the interaction between FKBP52 and IRF-4, and delineate the TPR region within domain 3 of FKBP52 as the IRF-4 association domain.

To localize the region of IRF-4 that interacts with the TPR domain of FKBP52, wild type and deletions of IRF-4 fused to a FLAG epitope tag were co-transfected into COS-7 cells with full length Myc-tagged FKBP52. WCE were co-immunoprecipitated with anti-Myc antisera followed with resolution by one-dimensional SDS-PAGE and western blot (Fig. 10C). These experiments demonstrate that full length FKBP52 co-precipitated with IRF-4(aa1-237), IRF-4(aa1-340), IRF-4(aa1-410), IRF-4(aa150-340) and IRF-4(aa150-410) (Fig. 10C, upper panel, lanes 2, 4, 6, 9 and 11, respectively), which indicates that the interaction domain lies within the amino-terminal aa1-237 region of IRF-4. Significantly, FKBP52 did not co-precipitate with IRF-4(aa1-150) (Fig. 10D, upper panel, lane 8) or with an IRF-4 mutant containing an internal deletion of aa 150-340 (Fig. 10D, upper panel, lane 6). Interestingly, addition of the carboxy-terminal residues beyond aa410 of IRF-4 abolished the FKBP52 interaction in transfected COS-7 cells (Fig. 10D, upper panel, lanes 2 and 4). In this context, the conformation of IRF-4 may be inaccessible to FKBP52 because of structural constraints imposed by the carboxy-terminal autoinhibition element (AIE) of IRF-4 (Fig. 10E), which folds back on the amino-terminal DBD (432,433). The results of the domain interaction studies are summarized schematically in Figure 10E. Based on these results, the proline-rich region of IRF-4(aa150-237) appears to be the minimal region required for interaction with FKBP52. However, despite repeated efforts, this domain could not be stably expressed as a tagged fusion peptide,

and could not be tested directly (Y. Mamane and S. Sharma, data not shown). Hence the parenthesis in Figure 10E.

1.2 FKBP52 interacts with IRF-4 in HTLV-I infected T-cells

Based on the inability of full-length IRF-4 to interact with FKBP52 in transfected COS-7 cells, co-immunoprecipitation experiments were performed to investigate the interaction of endogenous IRF-4 and FKBP52 in lymphocytic cell lines (Fig. 11). Two chronically HTLV-I infected T-cell lines C8166 and MT2 and a chronically HTLV-II infected T-cell line MoT, which overexpress IRF-4 at the protein level (Fig. 11A, upper panel, lanes 1-3), were analyzed by co-immunoprecipitation experiments. Five B-cell lines A20, KR-12, MC/CAR, 70Z and Namalwa, which express variable amounts of IRF-4 at the protein level (Fig. 11B, first panel, lanes 1-5 respectively), were also analyzed. Two T-cell lines T4 and Jurkat, which do not express IRF-4 (Fig. 11A, upper panel, lane 4 and 11B, first panel, lane 6), were used as negative controls. The levels of endogenous FKBP52 were comparable in all cell lines (Fig. 11A, bottom panel and 11B, third panel). Immunoprecipitation using an anti-FKBP52 antibody revealed that endogenous IRF-4 co-precipitated with endogenous FKBP52 in all IRF-4-expressing cells as a consequence of the level of IRF-4 expression (Fig. 11A, middle panel, lanes 1-3 and 11B, second panel, lanes 1-5). Taken together, these results demonstrate that the FKBP52-IRF-4 interaction, which is mediated through the proline rich region of IRF-4 and the TPR domain of FKBP52, occurs *in vivo* in IRF-4-expressing B- and T-lymphocytes.

2. Deregulation of IRF-4 expression in HTLV-I transformed T-cells

Although IRF-4 expression is tightly regulated in resting primary T-cells (432-434,436,449,450), IRF-4 mRNA and protein levels are upregulated in HTLV-I infected T-cells as a direct gene target for the HTLV-I Tax oncoprotein (436,449,450). In this study we examine the mechanism by which continuous IRF-4 production is achieved in HTLV-I infected T-lymphocytes. These experiments constitute the first detailed analysis of IRF-4 transcriptional regulation in the context of HTLV-I infection and transformation.

Figure 11. Endogenous interactions between IRF-4 and FKBP52 in B-cells and HTLV-I transformed T-cells (**A**) C8166, MT2, T4 and MO-T WCE (500 μg) were immunoprecipitated (IP) with anti-FKBP52, and complexes were resolved on 10% SDS-PAGE then immunoblotted (IB) using anti-IRF-4 antibody (middle panel) and FKBP52 antibody (lower panel). Input extracts consisted of 50 μg of WCE (upper panel). Control IP was performed by incubating WCE (500 μg) with normal precleared mouse serum (data not shown). (**B**) A20, KR-12, MC/CAR, 70Z/3, Namalwa and Jurkat WCE (500 μg) were immunoprecipitated (IP) with anti-FKBP52 antibody; complexes were run on 10% SDS-PAGE and immunoblotted using anti-IRF-4 antibody (second panel) and anti-FKBP52 antibody (fourth panel). Input extracts consisted of 50 μg of WCE (first and third panels).

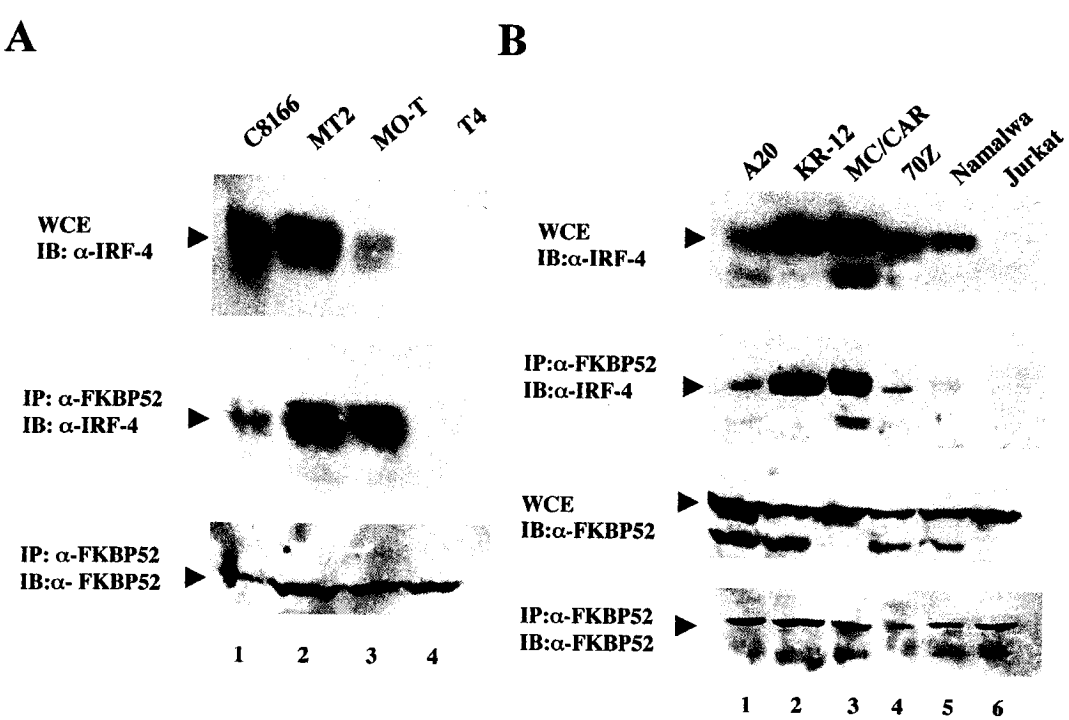
A
C8166
MT2
MO-T
T4
WCE
IB: α-IRF-4
IP: α-FKBP52
IB: α-IRF-4
IP: α-FKBP52
IB:α- FKBP52
1 2 3 4
B
A20
KR-12
MC/CAR
70Z
Namalwa
Jurkat
WCE
IB:α-IRF-4
IP:α-FKBP52
IB:α-IRF-4
WCE
IB:α-FKBP52
IP:α-FKBP52
IB:α-FKBP52
1 2 3 4 5 6

2.1 Differential IRF-4 expression patterns in T-lymphocytes

Initial experiments sought to establish a pattern of IRF-4 expression in T-lymphocytes by western blot analysis of WCE derived from primary T-cells, HTLV-I-infected T-cell lines and peripheral blood lymphocytes (PBL) isolated from HTLV-I infected patients. Figure 12A demonstrates that IRF-4 protein expression was not detectable in resting primary T-lymphocytes (Fig. 12A, upper panel, lane 1), but was inducible by antigen-mimetic PMA/ionomycin stimulation after 3h (Fig. 12A, upper panel, lanes 2-6), as detected using antisera against IRF-4. Furthermore, induction of IRF-4 expression by PMA/ionomycin stimulation in primary T-lymphocytes was inhibited by a 1h pre-treatment with the immunosuppressive drug FK506 (Fig. 12A, upper panel, lane 8).

Constitutive overexpression of IRF-4 was detectable by western blot analysis of WCE derived from the chronically infected, HTLV-I transformed T-cell lines MT2, C8166 and MT4 (Fig. 12B, upper panel, lanes 1-3), whereas IRF-4 was not expressed in control Jurkat, CEM or T4 T-cells (Fig. 12B, lanes 4-6). Anti-CD3/CD28 crosslinking, PMA/ionomycin or conA treatment did not further increase the IRF-4 levels in the HTLV-I transformed T-cell lines, indicating that IRF-4 was maximally expressed in these cells (S. Sharma, data not shown). Western blot analysis of WCE derived from PBL isolated from HTLV-I infected donors revealed that overexpression of IRF-4 was detectable in samples drawn from acute ATL patients (Fig. 12C, upper panel, lanes 2-6), but undetectable in samples drawn from non-leukemic donors (Fig. 12C, upper panel, lane 1). Although a single HAM/TSP sample is shown in Fig. 12, a total of 11 individual HAM/TSP samples were evaluated by western blot, and all were negative for IRF-4 expression (S. Sharma, data not shown). These results demonstrate that in T-lymphocytes, transient and inducible IRF-4 expression is associated with antigen or antigen-mimetic stimulation; however, chronic IRF-4 expression is associated with HTLV-I infection and development of acute ATL.

Figure 12. Differential IRF-4 expression in T-lymphocytes WCE were prepared from (**A**) primary human T-lymphocytes, (**B**) HTLV-I infected MT2, C8166 and MT4 or control Jurkat, CEM and T4 T cell lines and (**C**) PBL isolated from patients with ATL or HAM/TSP. Primary T lymphocytes were stimulated for various time hours (h) with 10 ηg/mL PMA and 200 ηmol ionomycin. Pre-treatment with FK506 was carried out at a final concentration of 1 μM for 1h prior to PMA/ionomycin stimulation. WCE (A) 25 μg, (B) 40 μg and (C) 100 μg were resolved by 10% SDS-PAGE and analyzed by western blotting with anti-IRF-4 and anti-actin antibodies.

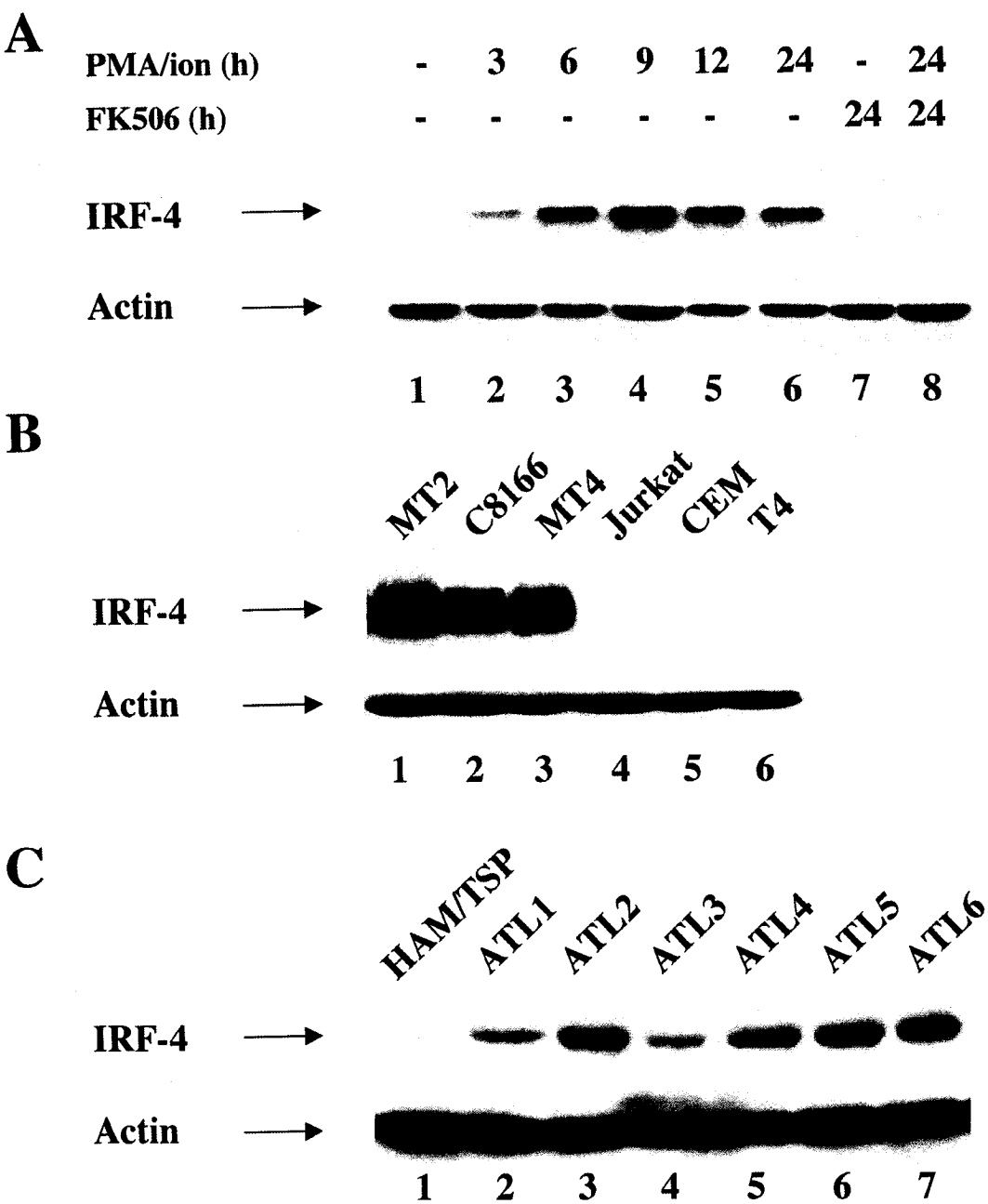
A
PMA/ion (h) - 3 6 9 12 24 - 24
FK506 (h) - - - - - - 24 24
IRF-4
Actin
1 2 3 4 5 6 7 8
B
MT2
C8166
MT4
Jurkat
CEM
T4
IRF-4
Actin
1 2 3 4 5 6
C
HAM/TSP
ATL1
ATL2
ATL3
ATL4
ATL5
ATL6
IRF-4
Actin
1 2 3 4 5 6 7

2.2 HTLV-I responsive domains within the IRF-4 promoter

The 1189 nucleotide sequence upstream from the transcriptional start site of the human IRF-4 gene comprises the human IRF-4 promoter (443). To study transcriptional regulation of IRF-4 in HTLV-I infected T-cells, this sequence was PCR-amplified from genomic ATCC293 DNA using the specific primers described in Chapter II. To identify HTLV-I-responsive regulatory regions within the human IRF-4 promoter sequence, full length and a series of 5' promoter deletions subcloned upstream of a luciferase reporter gene were transfected into chronically HTLV-I infected MT2 T-cells (Fig. 13). Compared to the activity of the full-length promoter construct in MT2 cells, a deletion from -617 to -367 nucleotides reduced relative luciferase activity by approximately one-half (Fig. 13, compare 1.2 kb and 0.6 kb to 0.4 kb). Subsequent removal of the -367 to -209 and -209 to -79 nucleotides abolished IRF-4 promoter activation, as compared to the activity of the full length promoter construct in MT2 cells (Fig. 13, compare 0.2 kb and 0.08 kb with 1.2 kb, respectively). Based on these results, it was concluded that transcriptional activation of the IRF-4 gene in HTLV-I infected T-cells is mediated by regulatory elements located within the -617 to -209 region of the human IRF-4 promoter.

2.3 Sequence analysis of the HTLV-I-responsive promoter region

To further analyze the HTLV-I-responsive region of the IRF-4 promoter, sequence evaluation and transcription factor binding site analysis was performed for the -700 to -200 sequence using the TRANSFAC database and MatInspector Binding Site Analysis software. Schematic representation of the HTLV-I-responsive region of the human IRF-4 promoter is shown in Figure 14, where consensus DNA binding elements are boxed. Several putative consensus binding sites are represented, which are specific to the FK506-sensitive NF-κB or NF-AT transcription factors (Fig. 14, κB1, κB2 and NF-1, NF-2 and NF-3, respectively), as well as a T-cell-specific enhancer termed the CD28RE, which is recognized by both NF-κB and NF-AT proteins (286,287,456,457) (Fig. 14, CD28RE). The HTLV-I-responsive region of the IRF-4 promoter also contains consensus recognition sites for transcription factors such as Ets and AP-1 (Fig. 14).

Figure 13. Analysis of HTLV-I responsive domains within the human IRF-4 promoter Full length (1.189 kb) and 5' deletions of the human IRF-4 promoter used in luciferase analysis of IRF-4 promoter activity in MT2 cells are represented. MT2 cells (10^6) were transfected using FuGene 6 transfection reagent with 0.2 μg of each reporter construct and 25 ηg of pRLTK *renilla* luciferase normalizing vector. Empty pFLAG-CMV-2 vector was added to each sample to bring the total amount of DNA to 2.0 μg per sample. Cells were assayed for luciferase activity at 46h post-transfection; percentages represent luciferase units corrected for transfection efficiency by *renilla* luciferase expression relative to luciferase activity of the full length 1.2 kb promoter in MT2 cells. Results presented are representative of at least 3 independent experiments.

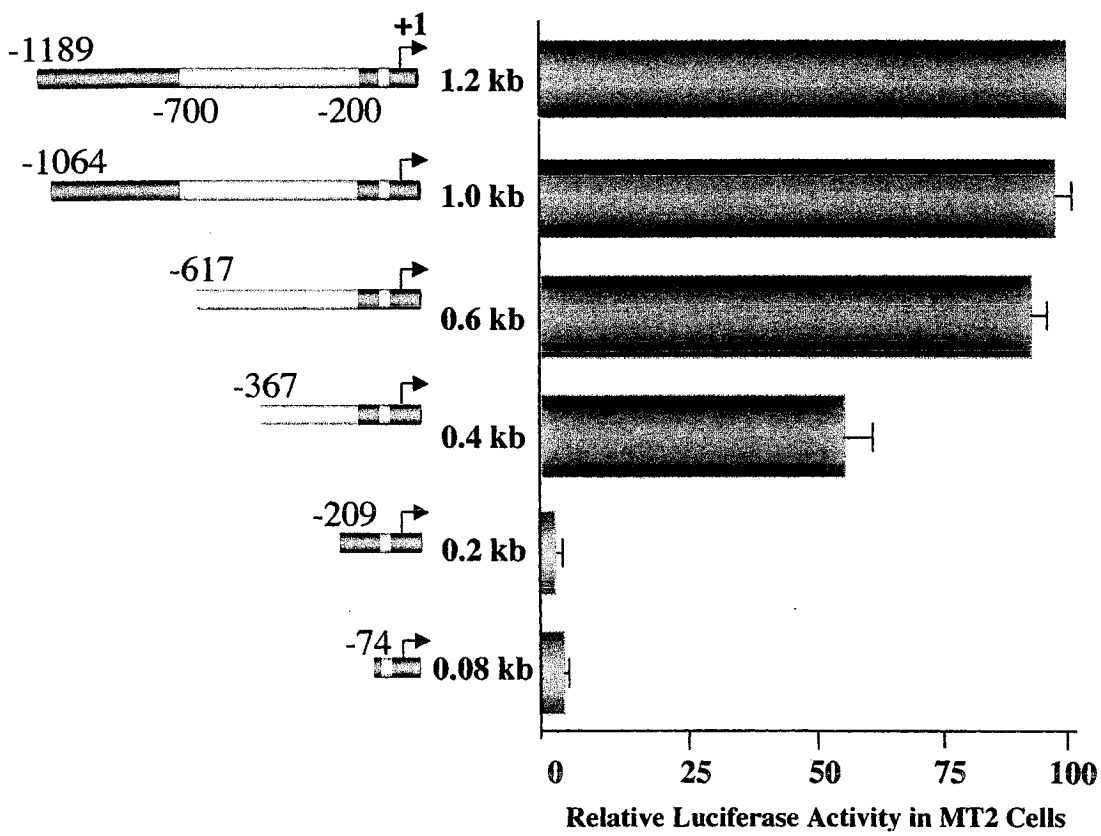
+1
-1189
-700
-200
1.2 kb
-1064
1.0 kb
-617
0.6 kb
-367
0.4 kb
-209
0.2 kb
-74
0.08 kb
0
25
50
75
100
Relative Luciferase Activity in MT2 Cells

Figure 14. Schematic representation of the IRF-4 promoter The sequence of the HTLV-I-responsive -200 to -700 region of the IRF-4 promoter. Major consensus binding sites for NF-κB (κB1and κB2), NF-AT (NF-1, NF-2 and NF-3), AP-1 and Ets-1 transcription factors and CD28-response element (CD28RE) are boxed. Transcription factor binding sites were determined by searching against the TRANSFAC database using MatInspector algorithm. Sequences used as probes for EMSA are indicated in bold. Arrows correspond to primers used in genomic footprinting experiments. Primers 1, 2 and 3 and 4, 5 and 6 were designed to analyse the -600 to -400 and -460 to -260 regions of the promoter, respectively.

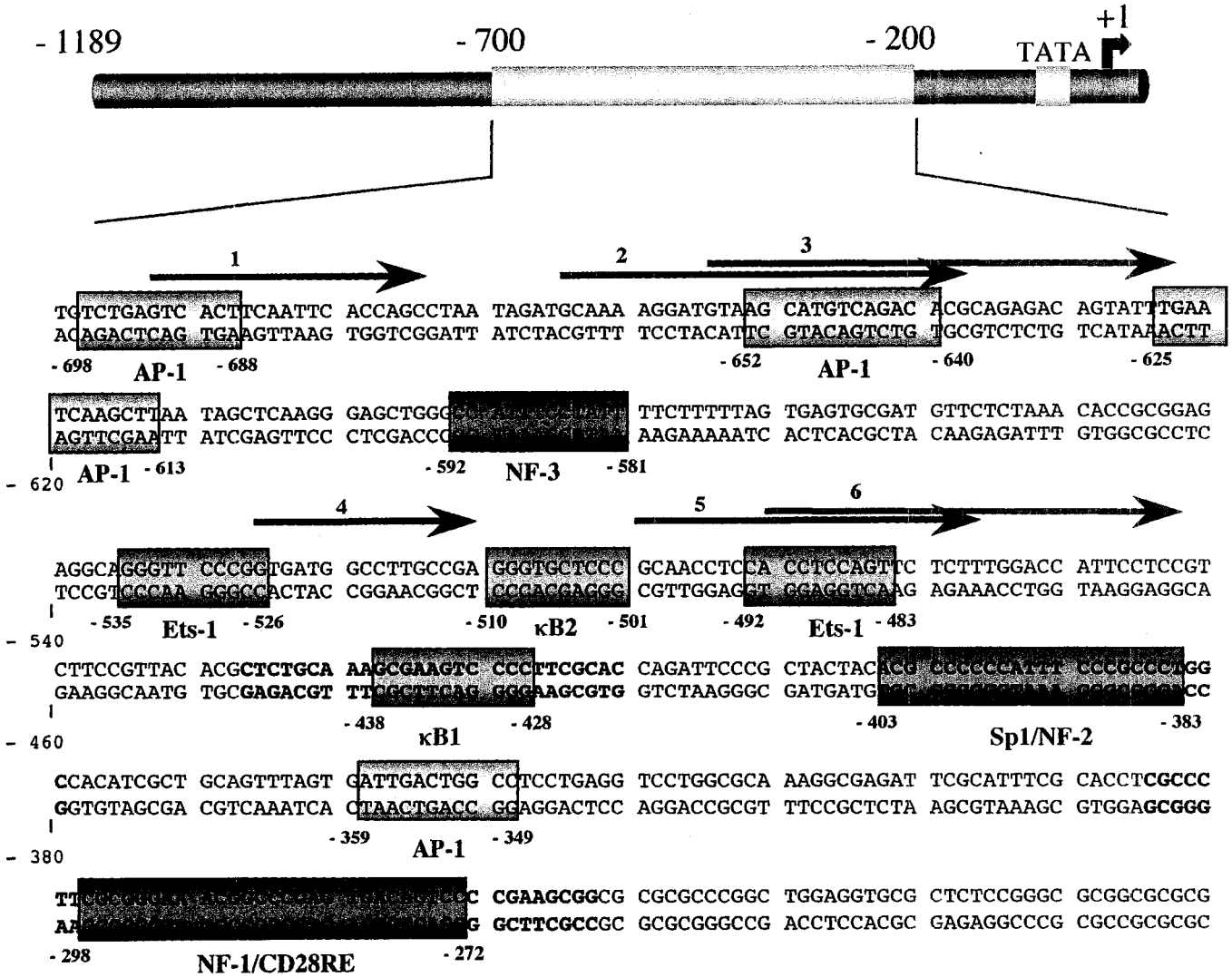
- 1189
- 700
- 200
TATA
+1
1
2
3
AP-1
AP-1
NF-3
4
5
6
Ets-1
κB2
Ets-1
κB1
Sp1/NF-2
AP-1
NF-1/CD28RE

3. Chronic NF-κB and NF-AT signaling in HTLV-I transformed T-cells

It has previously been shown that activation of classical NF-κB signaling in HTLV-I infected T-cells occurs at the level of Tax interaction with the IKKγ/NEMO subunit of the classical IKK complex (269-273,458,459); furthermore, T-cell lines expressing Tax are characterized by constitutively dephosphorylated, activated NF-AT proteins (285). A role for the NF-κB and NF-AT transcription factors in the regulation of gene expression during the course of HTLV-I infection has previously been established through analysis of IL-2 promoter activation (287,460,461).

3.1 Classical NF-κB activation in HTLV-I transformed T-cells

To assess the status of classical NF-κB signaling in HTLV-I transformed T-cells, the catalytic activity of the classical IKK complex was analyzed by *in vitro* kinase assay of endogenous IKK complexes isolated from control Jurkat and HTLV-I transformed T-cells using IKKγ/NEMO-specific antisera (Fig. 15A). Substrates for *in vitro* kinase analysis of purified IKK complexes corresponded to the signal-responsive domain of IκBα (49-51) fused to GST (Fig. 15A, GST-IκBα, lanes 1-5), or a S32/S36A-substituted IκBα fusion peptide (Fig. 15A, GST-2NIκBα, lanes 6-10). As demonstrated in Fig. 15A, enzymatic activation of the classical IKK complex was inducible in Jurkat T-cells treated with PMA (Fig. 15A, compare lanes 1 and 2), but was constitutively elevated in chronically HTLV-I infected MT2, C8166 and MT4 cells (Fig. 15A, lanes 3-5). Phosphorylation of the peptide substrate was specific for the signal-responsive residues of IκBα, as no phosphorylation was detectable using the 2NIκBα substrate (Fig. 15A, lanes 6-10). Next, co-immunoprecipitation assays were performed in Jurkat and MT2 cells (Fig. 15B). As previously demonstrated (272-274), immunoprecipitation using Tax-specific antisera resulted in co-precipitation of endogenous IKKγ/NEMO from HTLV-I infected MT2 cells (Fig. 15B, lane 4) but not control Jurkat T-cells (Fig. 15B, lane 2). Together, these results confirm that constitutive activation of classical NF-κB signaling in HTLV-I transformed T-cells occurs through direct modulation of classical IKK complex by the Tax oncoprotein.

Figure 15. Activation of NF-κB in HTLV-I infected T-cells (A) WCE (500 μg) from control Jurkat or PMA-treated Jurkat (50 ηg/ml for 15 minutes) and HTLV-I infected MT2, C8166 and MT4 T-cell lines were immunoprecipitated (IP) with antisera directed against IKKγ/NEMO. Immunoprecipitates were incubated in kinase reaction buffer with 10 μCi [γ-^{32}P]-ATP for 30 minutes at 30°C. Substrates for the kinase reactions were GST-IκBα(aa 1-55) (lanes 1-4) or GST-2NIκBα(aa 1-55) with S32/S36A substitutions, which cannot be phosphorylated by IKK (lanes 5-8). **(B)** Jurkat (lane 2) and MT2 (lane 4) WCE (1 mg) were immunoprecipitated (IP) with antisera directed against Tax. Immunocomplexes were resolved by 8% SDS-PAGE and immunoblotted with anti-IKKγ (lower panel) or anti-Tax (upper panel).

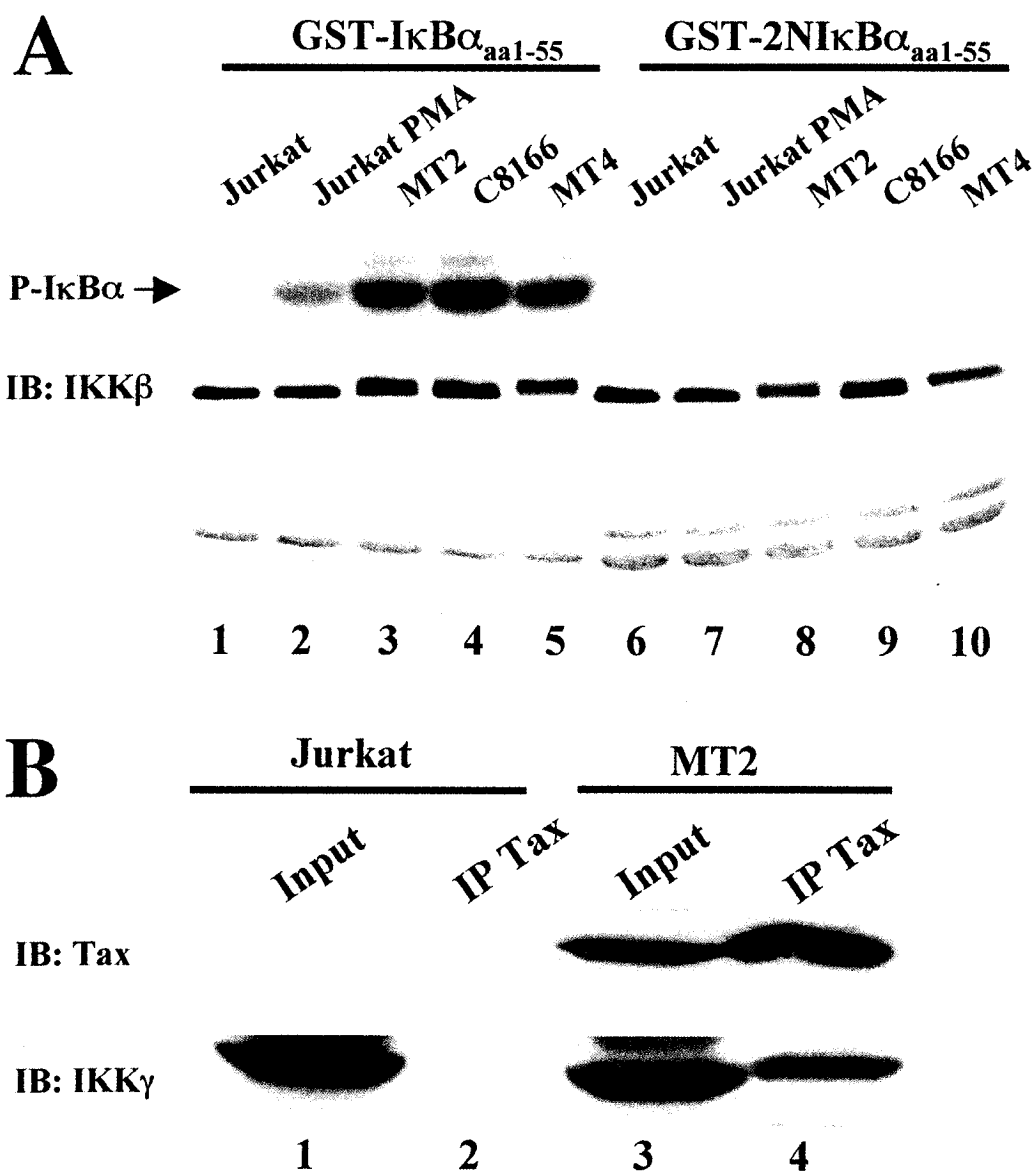
A
GST-IκBα aa1-55
GST-2NIκBα aa1-55
Jurkat
Jurkat PMA
MT2
C8166
MT4
Jurkat
Jurkat PMA
MT2
C8166
MT4
P-IκBα
IB: IKKβ
1 2 3 4 5 6 7 8 9 10
B
Jurkat
MT2
Input
IP Tax
Input
IP Tax
IB: Tax
IB: IKKγ
1 2 3 4

3.2 Activation of NF-AT proteins in HTLV-I transformed T-cells

To analyze activation of NF-AT signaling in HTLV-I transformed T-cells, nuclear extracts from MT2 cells and WCE from ATL donor PBL (ATL2, Fig. 12C, lane 3) were analyzed for NF-AT DNA binding activity by electromobility shift assay (EMSA) (Fig. 16A and 16B, respectively). A protein-DNA complex bound to the NF-AT consensus site probe was detectable in MT2 and ATL2 extracts (Fig. 16A and 4B, lane2), but not in control Jurkat extracts (Fig. 16A and 4B, lane 1). Antibody supershifts performed to identify subunit composition revealed that the HTLV-I-specific complexes contained subunits NF-ATp (NF-AT1/NF-ATc2) (10) in MT2 extracts, (Fig. 16A, lane 4) and NF-ATp and NF-ATc (NF-AT2/NF-ATc1) (10) in ATL2 extracts (Fig. 16B, lanes 3 and 4). The binding specificity of protein complexes associated with the NF-AT consensus probe was confirmed by a competition using 100-fold molar excess of unlabelled NF-AT consensus oligonucleotide (Fig. 16A and 16B, lane 11), but not the corresponding probe mutated in NF-AT-specific residues (Fig. 16A and 16B, lane 12). Thus, in HTLV-I transformed T-cells MT2 and ATL2, in constitutive activation of NF-AT signaling is also observed.

4. Regulatory elements driving IRF-4 transcription

Subsequent experiments sought to analyze the contribution of chronic NF-κB and NF-AT activation in HTLV-I transformed T-cells to transcriptional activation of the human IRF-4 promoter. An *in vivo* genomic footprinting approach coupled with *in vitro* EMSA experiments and luciferase assay were used to study protein-DNA interactions within the -600 to -200 region of the IRF-4 promoter in HTLV-I transformed T-cells compared to control T-cells. A detailed description of specific primers used for *in vivo* footprinting and oligonucleotide DNA probes used in EMSA is detailed in Chapter II and Figure 14.

4.1 Analysis of the κB1 and κB2 sites

The contribution of NF-κB signaling to activation of the HTLV-I-responsive region of the IRF-4 promoter was studied by *in vivo* genomic footprinting studies, as detailed in Chapter II. Primers were designed to analyze *in vivo* protein-DNA interactions in the -600 to -400 region of the IRF-4 promoter, which contains two putative consensus binding

Figure 16. Activation of NF-AT in HTLV-I infected T-cells (**A**) Nuclear extracts (3.0 μg) from control T4 (lane 1) and MT2 (lanes 2-12) cells and (**B**) WCE (5.0 μg) from control (lane 1) and ATL-derived PBL (lanes 2-12) were incubated with a radiolabeled oligonucleotide probe corresponding to a consensus NF-AT binding site, as described in Chapter II. Arrows indicate the positions of the inducible protein-DNA complexes. Antibody supershift was carried out using 1.0 μg each of anti-NF-ATc (lanes 3, 6, 8 and 9), anti-NF-ATx (lanes 5, 7, 8 and 9) or control serum (lane 10), or 1 μL of a 1:10 dilution of anti-NF-ATp (lanes 4, 6, 7 and 9). Cold oligonucleotide competitions were carried out using a 100-fold molar excess of NF-AT consensus (lane 11) or NF-AT mutant consensus (lane 12).

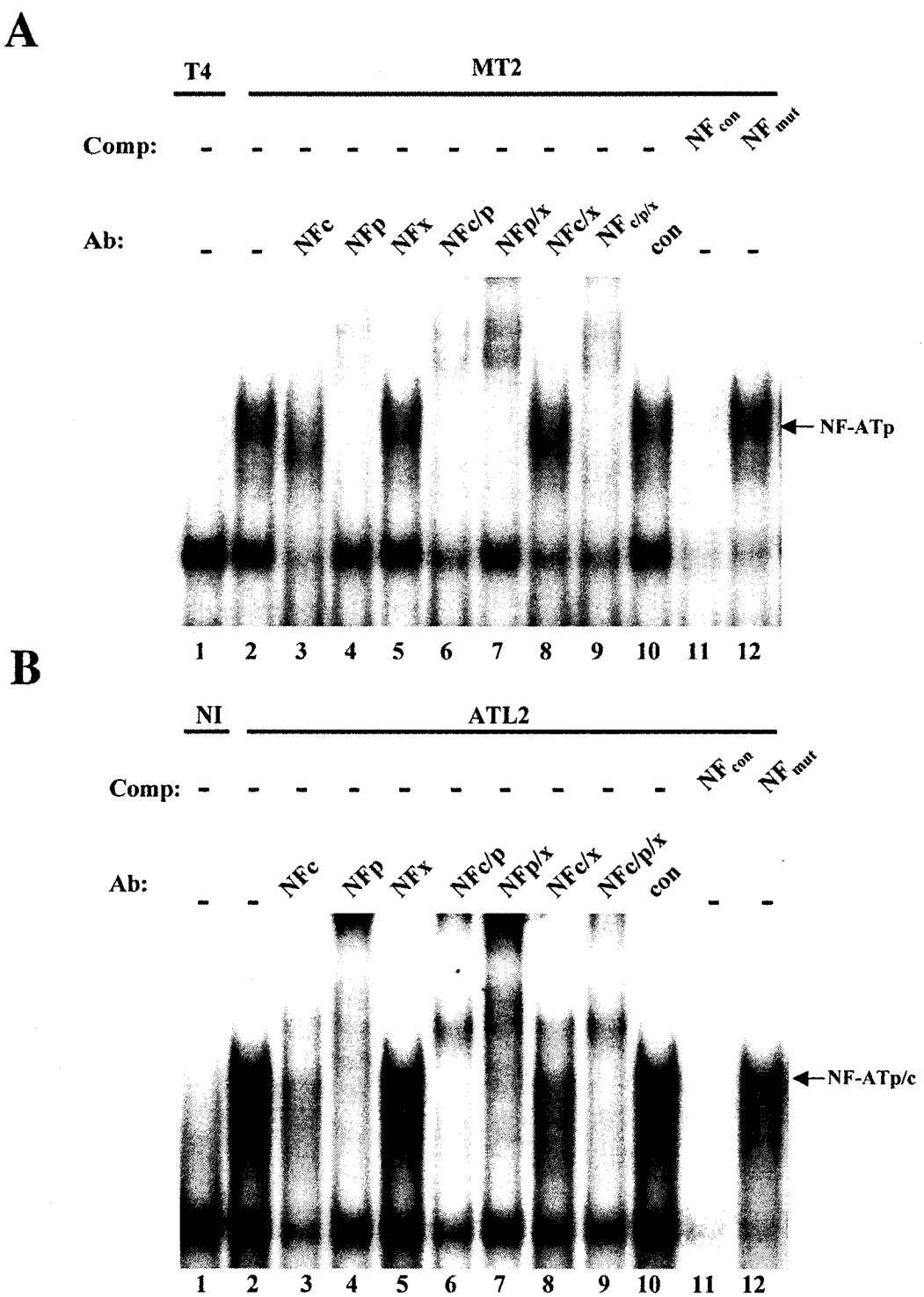
A
T4
MT2
Comp:
NF con
NF mut
Ab:
NFc
NFp
NFx
NFc/p
NFp/x
NFc/x
NF c/p/x
con
NF-ATp
1 2 3 4 5 6 7 8 9 10 11 12
B
NI
ATL2
Comp:
NF con
NF mut
Ab:
NFc
NFp
NFx
NFc/p
NFp/x
NFc/x
NFc/p/x
con
NF-ATp/c
1 2 3 4 5 6 7 8 9 10 11 12

sites for NF-κB transcription factors, κB1 and κB2 (Fig. 14, primers 1, 2 and 3). The footprinting analysis was performed on the non-coding strand, because the κB1 and κB2 sites are G-rich on this strand (Fig. 14). *In vivo* genomic footprinting analyses detected a methylation protection of the κB1 site in MT2 cells, but not in control Jurkat T-cells (Fig. 17A, compare lanes 1 and 3). Specifically, comparison of the *in vivo* and naked DNA pattern obtained from MT2 cells revealed a decrease in methylation of the -429G, -430G and -431G residues (Fig. 17A, lanes 2 and 3), suggesting *in vivo* protein occupancy of these residues in MT2 cells. Modifications with respect to the methylation pattern within the κB1 site of the IRF-4 promoter were quantified by densitometric scanning, which is shown in the top right panel of Fig. 17A. Arrows indicate the position of the three G residues showing decreased methylation *in vivo* in MT2 cells but not naked DNA or control Jurkat cells. In contrast, no occupancy of the κB2 site was observed by *in vivo* genomic footprinting analysis (Fig. 17A, lanes 2 and 3), or by additional *in vitro* EMSA experiments in Jurkat or MT2 cells (S. Sharma, data not shown).

Interestingly, analysis of this region using primers 1, 2 and 3 showed *in vivo* modification at the consensus Ets-1 binding site at position -483 to -492 (Fig. 14). Specifically, hypermethylation of the -487G and -493G residues that flank the Ets-1 binding site was observed in MT2 but not Jurkat T-cells (Fig. 17A, compare lanes 2 and 3), suggesting protein occupancy between these residues in MT2 cells. Densitometric scanning of hypermethylation at the Ets-1 binding site of the IRF-4 promoter is represented by the bottom right panel of Fig. 15A, where the arrows represent specific G residues showing increased methylation *in vivo* in MT2 cells.

To identify specific proteins occupying the κB1 site of the IRF-4 promoter in HTLV-I infected T-cells, EMSA experiments were performed using a probe corresponding to the κB1 site, spanning to the -447 to -421 region of the human IRF-4 promoter (Fig. 14). A protein complex bound to κB1 was identified in nuclear extracts derived from MT2 cells (Fig. 17B, upper panel, lane 2) and WCE derived from ATL PBL (Fig. 17B, lower panel, lane 2) but not control Jurkat or T4 extracts (Fig. 17B, upper and lower panels, lane 1). Antibody supershift analyses demonstrated that anti-c-Rel antibodies supershifted

Figure 17. Binding to the κB1 site of the IRF-4 promoter in HTLV-I infected T-cells

(A) *In vivo* genomic footprinting of the noncoding strand of the -600 to -400 region of the IRF-4 promoter. Putative NF-κB binding sites, κB1 and κB2, are indicated with the Ets-1 binding site. Arrows indicate G residues protected or hypermethylated *in vivo* in MT2 cells compared to control lanes. Methylation patterns observed in the -600 to -400 region of the IRF-4 promoter were analyzed by densitometric scanning, using a Hewlett-Packard Scan Jet 4c scanner and NIH Image 1.60 software. Arrows pointing up or down represent increased or decreased *in vivo* methylation on G residues in MT2 cells. Sequence of the scanned region and position of the methylated G residues in capital letters are indicated below each graph. **(B)** [Upper panel] Nuclear extracts (3.0 μg) from Jurkat (lane 1) and MT2 (lanes 2-6) cells and [lower panel] WCE (5.0 μg) from control (lane 1) and ATL-derived PBL (lane 2-6) were incubated with radiolabeled oligonucleotide probes corresponding to the κB1 site of the IRF-4 promoter (Fig. 14). Arrows indicate the positions of inducible and nonspecific (NS) complexes. Antibody supershift was carried out using 1 μg of anti-c-Rel (lane 3), anti-p65 (lane4), anti-p50 (lane 5) or control serum (lane 6). **(C)** Jurkat T-cells (10^6) were transfected with 0.2 μg of 0.6-kb4PRO-pGL3B, 25 ηg of pRLTK *renilla* luciferase normalizing vector and a threefold molar excess of NIK, Tax WT, Tax M47 or Tax M22. Empty pFLAG-CMV2 plasmid was added to each transfection to bring total DNA per sample to 2.0. Luciferase activity was assessed 46h post-transfection. Fold induction was calculated relative to reporter gene expression in the presence of empty vector after correction for transfection efficiency by *renilla* luciferase. Results presented are representative of at least 3 independent experiments.

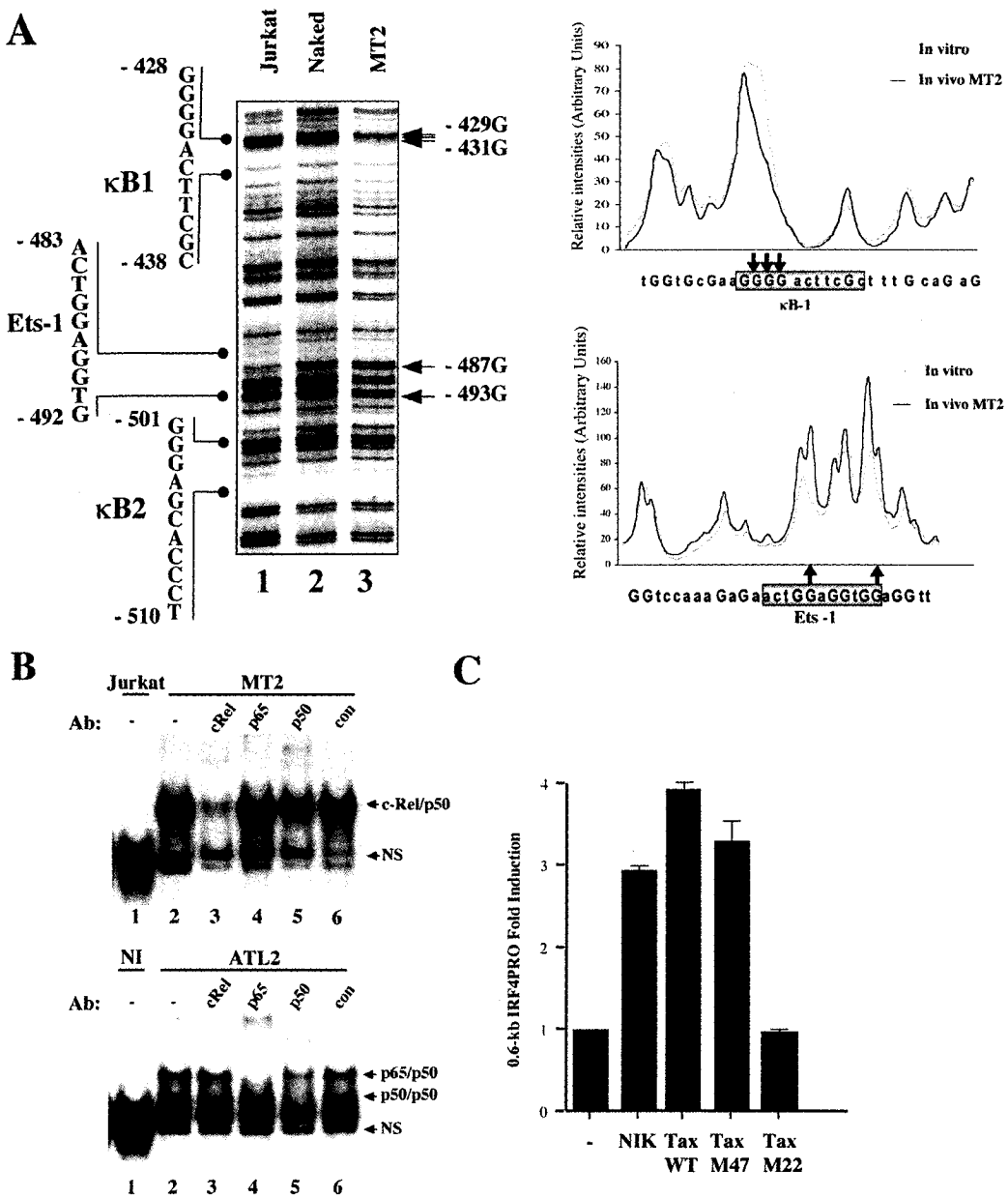
A
Jurkat
Naked
MT2
- 428
GGGGACTTTCCGC
κB1
- 438
- 483
ACTGGAGGGTG
Ets-1
- 492
- 501
GGGAGCACCCCT
κB2
- 510
- 429G
- 431G
- 487G
- 493G
1 2 3
Relative intensities (Arbitrary Units)
In vitro
In vivo MT2
tGGtGcGaaGGGGactt cGct t t G caG aG
κB-1
GGtccaaa GaGaactGGaGGtGGaGG tt
Ets -1
B
Jurkat
MT2
Ab: - - cRel p65 p50 con
c-Rel/p50
NS
1 2 3 4 5 6
NI
ATL2
Ab: - - cRel p65 p50 con
p65/p50
p50/p50
NS
1 2 3 4 5 6
C
0.6-kb IRF4PRO Fold Induction
- NIK Tax WT Tax M47 Tax M22

the majority of the upper κB1 complex in MT2 cells. (Fig. 17B, upper panel, lane 3). Additional supershifts with anti-p50 revealed that this upper complex was a heterodimer of p50 and c-Rel (Fig. 17B, upper panel, lane 5). In ATL2 extracts, the upper complex did not react with anti-c-Rel antibodies (Fig 17B, lower panel, lane 3), but was specifically supershifted with a combination of anti-p65 and anti-p50 antibodies (Fig 17B, lower panel, lanes 5 and 6). Therefore, in ATL2 extracts the upper protein complex binding to κB1 represents a p65/p50 heterodimer, while the middle complex represents a p50 homodimer. Complex NS was designated nonspecific, based on the failure of 100-fold molar excess of cold κB1 probe to specifically compete for the complex formation (S. Sharma, data not shown). κB1 EMSA was also performed using WCE from primary human T-lymphocytes, which demonstrated inducible binding to the κB1 site upon T-cell stimulation with PMA/ionomycin (S. Sharma, data not shown). Together, these data demonstrate that *in vivo* occupancy of the consensus κB1 site in HTLV-I transformed T-cells correlates with binding of NF-κB subunits c-Rel, p65 and p50 to κB1 *in vitro*. Therefore, the κB1 site within the HTLV-I-responsive region of the IRF-4 promoter represents a functional NF-κB binding site.

The requirement for NF-κB signaling in transactivation of the IRF-4 promoter was further investigated by luciferase assay performed in Jurkat T-cells (Fig. 17C). Transfection of NIK resulted in 3-fold induction of the 0.6-kb IRF-4 promoter construct (Fig. 17C). Similarly, transfection with HTLV-I Tax stimulated IRF-4 promoter activity approximately 4-fold. (Fig. 17C). Tax M47, a specific mutant for CREB/ATF activation (257), retained the ability to transactivate 0.6-kbIRF-4PRO-LUC to wild type levels (Fig. 17C). In contrast, Tax M22, a specific mutant for NF-κB activation (257), failed to activate the 0.6-kb IRF-4 promoter in Jurkat T-cells (Fig. 17C). Taken together, these results show that constitutive *in vivo* and *in vitro* occupancy of the κB1 site by NF-κB subunits in HTLV-I infected T-cells is consistent with reporter gene experiments, which implicate activation of NF-κB signaling as an essential component of IRF-4 promoter activation by Tax.

4.2 Analysis of the Sp1/NF-2 site

A second set of primers was designed for *in vivo* genomic footprinting analysis of the non-coding strand of the -260 to -460 region of the IRF-4 promoter. This region contains the CD28RE/NF-1, Sp1/NF-2 and AP-1 consensus binding sites (Fig. 14, primers 4, 5 and 6). Using these primers, protection of several G residues within and adjacent to the Sp1/NF-2 site (-385G to -413G) was observed in MT2 cells compared to naked control DNA (Fig. 18A, lanes 2 and 3). Protection of the -388G, -396G to -398G, -402G, -410G, -412G and -413G residues within and around the Sp1/NF-2 site was specific to HTLV-I transformed cells, and was not detected in control Jurkat T-cells (Fig. 18A, compare lanes 1 and 3). The MT2-specific changes in methylation within this site are represented by densitometric scanning (Fig. 18A, right panel), with arrows indicating the eight G residues within and adjacent to NF-2/Sp1 that exhibit decreased *in vivo* methylation in MT2 cells.

To identify the composition of the protein complex(es) inducing methylation protection within and surrounding the Sp1/NF-2 site, EMSA analysis was performed using an oligonucleotide probe corresponding to the -413 to -378 region of the IRF-4 promoter (Fig. 14). Two novel protein complexes binding to the Sp1/NF-2 probe were detected in MT2 nuclear extracts compared to control T4 extracts (Fig. 18B, lanes 1 and 2). Binding to the Sp1/NF-2 site was specifically decreased by addition of a 100-fold molar excess of Sp1 consensus oligonucleotide to the binding reaction (Fig. 18B, lane 6), while competition with the corresponding oligonucleotide mutated in the Sp1-specific residues abolished the inhibitory effect (Fig. 18B, lane 7). Antibody supershift confirmed that the Sp1/NF2 complex was specifically displaced by anti-Sp1 antisera (Fig. 18B, lanes 3 and 4). The Sp1/NF2-specific protein-DNA complexes were not displaced by heterologous NF-AT or Ets oligonucleotides, nor were they supershifted with antibodies against NF-AT or Ets proteins (S. Sharma, data not shown). EMSA using the Sp1/NF-2 probe was also performed using WCE from primary ATL2 PBL, with results that confirmed Sp1 binding to the Sp1/NF2 site in ATL extracts (Fig. 18B, lanes 10 and 12). These data demonstrate that constitutive occupancy of the Sp1/NF2 region of the IRF-4 promoter in

Figure 18. Binding to the Sp1/NF-2 site of the IRF-4 promoter in HTLV-I infected T-cells **(A)** *In vivo* genomic footprinting of the noncoding strand of the -460 to -260 region of the IRF-4 promoter. Putative NF-AT binding sites NF-1, NF-2 and NF-3 are indicated. Methylation patterns observed in the -460 to -260 region of the IRF-4 promoter were analyzed by densitometry scanning. Arrows pointing up or down represent specific increased or decreased *in vivo* methylation on G residues in MT2 cells. The sequence of the scanned region and the position of methylated G residues in capital letters are indicated below each graph. **(B)** [Right Panel] Nuclear extracts (1.0 μg) from Jurkat (lane 1) and MT2 (lanes 2-7) cells and [left panel] WCE from control (lane 8) and ATL derived PBL (lanes 9-13) were incubated with radiolabeled oligonucleotide probes corresponding to the Sp1/NF-2 site of the IRF-4 promoter (Fig. 14). Arrows indicate the positions of the inducible protein-DNA complexes. Antibody supershift was carried out using 1 μg of anti-Sp1 (lanes 4 and 12) or control antisera (lanes 3 and 13), and cold oligonucleotide competitions were carried out using a 100-fold molar excess of Sp1/NF-2 (lane 5), Sp1 consensus (lanes 6 and 10) or Sp1-mutant consenus (lanes 7 and 11).

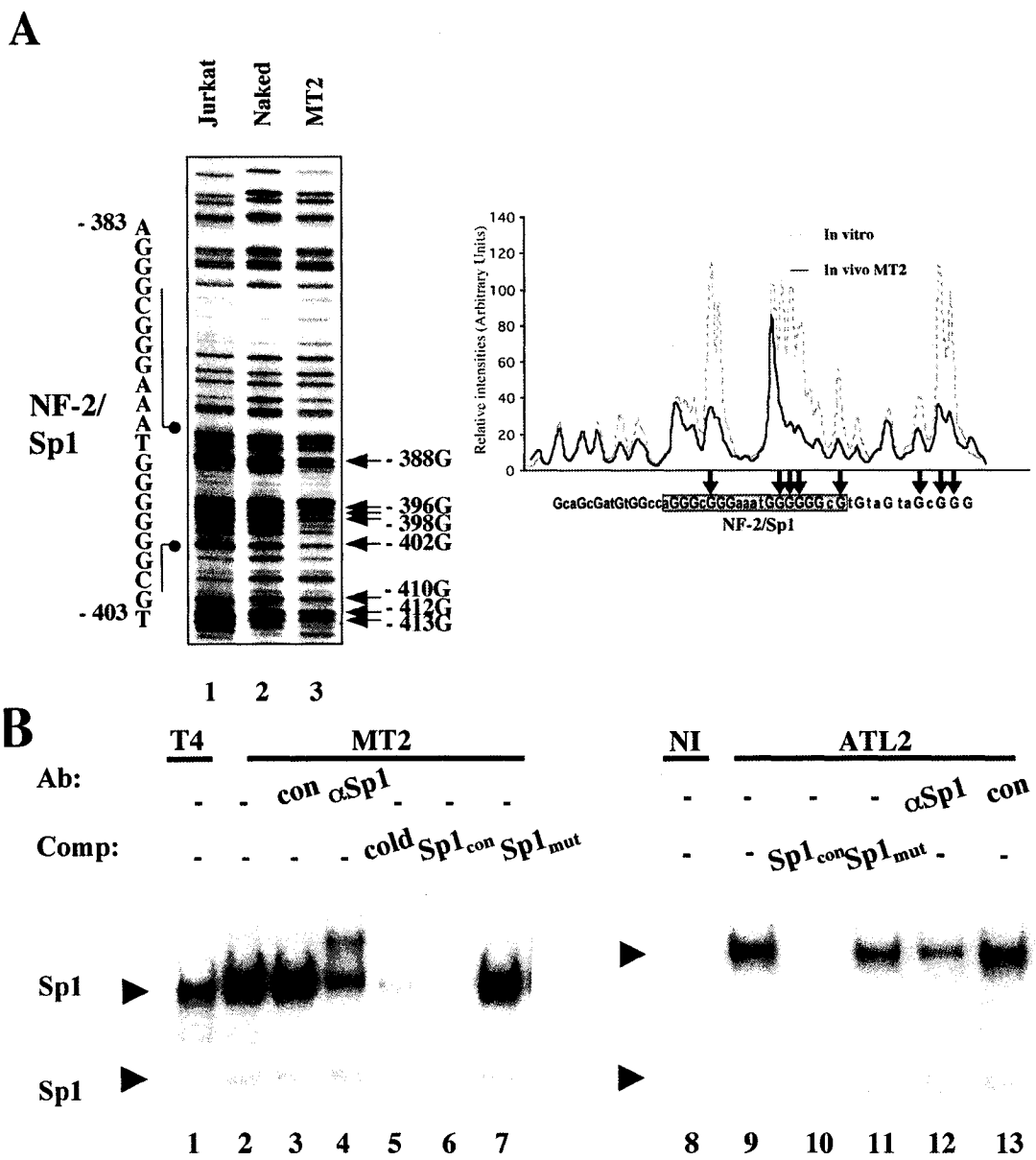
A
Jurkat
Naked
MT2
- 383
NF-2/
Sp1
- 403
- 388G
- 396G
- 398G
- 402G
- 410G
- 412G
- 413G
1 2 3
In vitro
In vivo MT2
Relative intensities (Arbitrary Units)
GcaGcGatGtGGcc
tGtaG taGcGGG
NF-2/Sp1
B
T4
MT2
NI
ATL2
Ab:
con
αSp1
αSp1
con
Comp:
cold
Sp1con
Sp1mut
Sp1con
Sp1mut
Sp1
Sp1
1 2 3 4 5 6 7 8 9 10 11 12 13

HTLV-I cells is mediated through Sp1 binding to two adjacent Sp1 binding sites (Fig. 14).

4.3 Analysis of the CD28RE site

Reporter gene assays performed in MT2 cells indicated that the CD28RE might contribute to IRF-4 promoter activation in HTLV-I infected cells, because deletion of the –367 to –209 nucleotides decreased IRF-4 promoter activity in MT2 cells (Fig. 13). CD28RE enhancers play an important role in gene regulation during the T-cell activation response (462,463); through binding of different transcriptional activators, including NF-κB, NF-AT and fos/jun (AP-1) proteins (286,287,456,457,464), CD28RE activate lymphoid-specific genes such as IL-2, GM-SCF and CD40L, (465-467). For example, the IL-2 CD28RE enhancer is a direct target for HTLV-I Tax-mediated transactivation (287).

Consistent hypermethylation of -270G residue adjacent to the CD28RE site was observed in MT2 cells, but not in Jurkat T-cells, suggesting binding of one or several transcription factors near this site (Fig. 19A, lane 3). Hypermethylation of the IRF-4 promoter adjacent to CD28RE site was quantified by densitometric scanning (Fig. 19A, right panel), where the arrow represents the -270 G residue and demonstrates a reproducible increase in methylation that is specific to MT2 cells. Further analysis of the coding strand would have been necessary to provide a detailed characterization of promoter occupancy in the CD28RE region (including the NF-1 site) of the IRF-4 promoter by *in vivo* genomic footprinting. However, PCR amplification was not successful using anti-sense primers due to the fact that this highly GC rich region impaired PCR mediated elongation. Because of the low abundance of G residues in the non-coding strand of the CD28RE site, no modification of the methylation pattern was detected in either Jurkat T-cells or in MT2 cells (Fig. 19A, lanes 1 and 3) compared to naked DNA.

EMSA analysis using the CD28RE site (Fig. 14, -305 to -263) as a probe detected protein binding in nuclear extracts derived from HTLV-I infected MT2 cells but not control Jurkat cells (Fig. 19B, compare lanes 1 and 2). Supershift analysis using NF-κB-specific antisera identified c-Rel and p50 (Fig. 19B, lanes 3 and 4) but not p65 (Fig. 19B, lane

Figure 19. Binding to the CD28RE site of the IRF-4 promoter in HTLV-I infected T-cells (**A**) *In vivo* genomic footprinting of the noncoding strand of the -460 to -260 region of the IRF-4 promoter. The position of the CD28RE is indicated and arrows indicate hypermethylated G residues. Methylation patterns observed in the CD28RE region of the IRF-4 promoter are represented by densitometric scanning. Arrows pointing up or down represent increased or decreased *in vivo* methylation on G residues in MT2 cells. The sequence of the scanned region, where the methylated G residues are in capital letters, is indicated below each graph. (**B**) Nuclear extracts (10 μg) from Jurkat (lane 1) or MT2 (lanes 2-10) cells were incubated with radiolabelled oligonucleotide probes corresponding to the CD28RE site of the IRF-4 promoter (Fig. 14). Arrows indicate the positions of the inducible protein-DNA complexes. Supershift analysis was carried out using 1.0 μg of anti-c-Rel (lane 3), anti-p50 (lane 4), anti-p65 (lane 5), anti-NF-ATc (lane 9) and anti-NF-ATx (lane 10) antibodies or 1 μl of a 1:10 dilution of anti-NF-ATp (lane 8). (C) Jurkat T-cells (10^6) were transfected with 0.2 μg of 0.4-kb4PRO-pGL3B, 25 ηg of pRLTK *renilla* luciferase normalizing vector and a threefold molar excess of NIK, NF-ATpXS, NIK + NF-ATpXS, Tax WT, Tax M47 or Tax M22. Empty pFLAG-CMV2 vector was added to each transfection to bring total DNA per sample to 2.0 μg. Cells were assayed for luciferase activity at 46h post-transfection. Fold induction was calculated relative to reporter gene expression in the presence of empty vector after correction for transfection efficiency by *renilla* luciferase. Results presented are representative of at least 3 independent experiments.

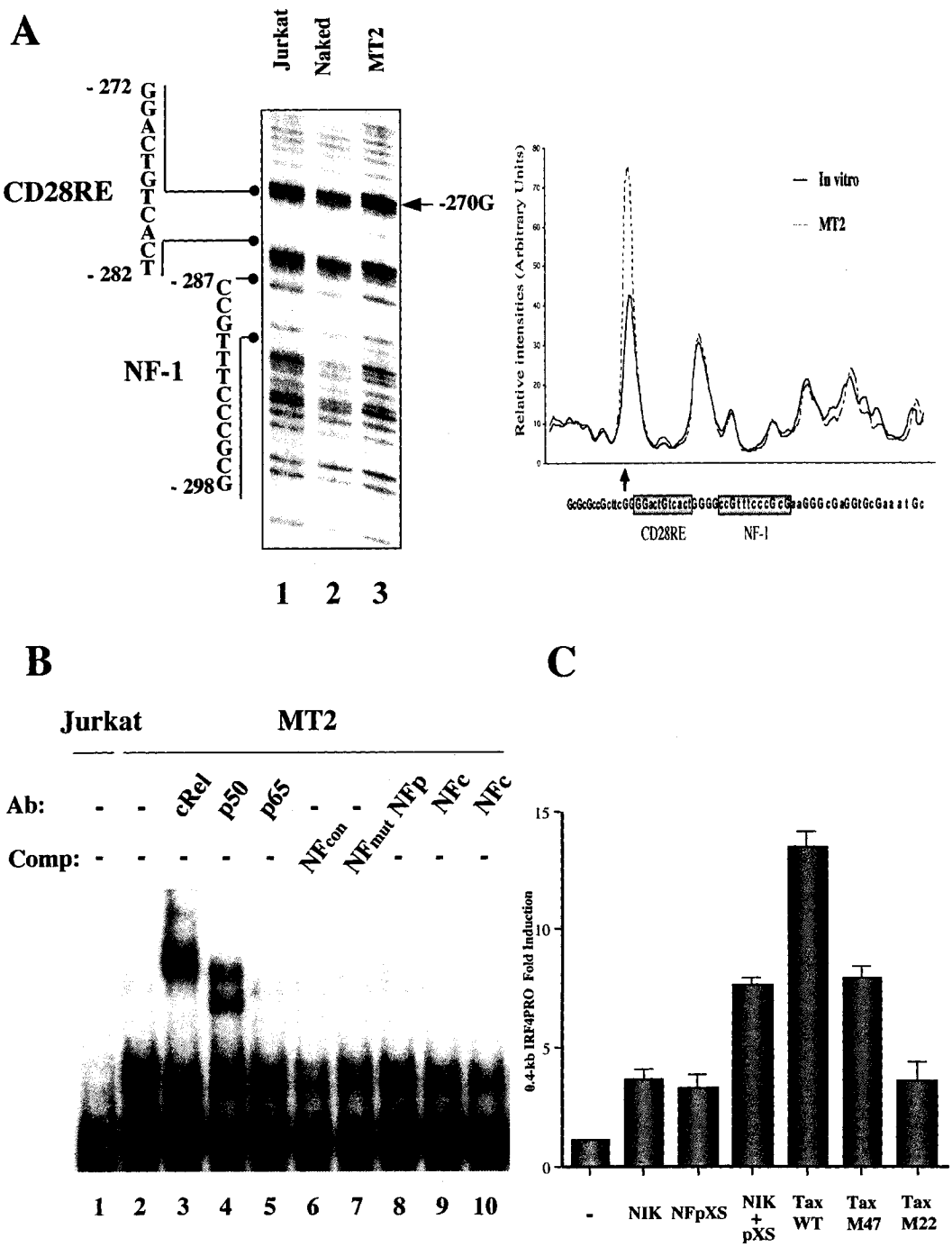
A
Jurkat
Naked
MT2
- 272
GGACTGTCACT
CD28RE
- 282
- 287
CCGTTTCCCGCG
NF-1
- 298G
-270G
1 2 3
In vitro
MT2
Relative intensities (Arbitrary Units)
GcGcGccGcttcGGGGactGtcactGGGGccGttTcccGcGaaGGGcGaGGtGcGaa a t Gc
CD28RE
NF-1
B
Jurkat
MT2
Ab: - - cRel p50 p65 - - NFp NFc NFc
Comp: - - - - - NFcon NFmut - - -
1 2 3 4 5 6 7 8 9 10
C
0.4-kb IRF4PRO Fold Induction
15
10
5
0
-
NIK
NFpXS
NIK + pXS
Tax WT
Tax M47
Tax M22

5) binding to CD28RE in MT2 extracts. Since the CD28RE binds several transcription factors, further competition analyses were performed. Addition of 100-fold molar excess of a consensus NF-AT oligonucleotide (Fig. 19B, lane 6) but not the mutant oligonucleotide (Fig. 19B, lane 7) to the binding reaction reduced protein occupancy of the CD28RE in MT2 nuclear extracts. Supershift with NF-AT-specific antibodies identified NF-ATp bound to the CD28RE in MT2 cells (Fig. 19B, lane 8). Protein binding to the IRF-4 CD28RE was not reactive to antibody supershift using AP-1, Sp1 or Ets antisera (S. Sharma, data not shown). Together, these data indicate that the IRF-4 CD28RE binds NF-κB subunits (c-Rel and p50) and NF-AT subunits (NF-ATp) in HTLV-I infected cells *in vitro*. CD28RE-specific EMSA demonstrated inducible and specific binding detectable in WCE stimulated with PMA/ionomycin, suggesting that the IRF-4 CD28RE is occupied in primary, activated T-lymphocytes (S. Sharma, data not shown). In addition, extensive EMSA experiments were performed using DNA probes corresponding to each putative transcription factor consensus site identified by sequence analysis of the -367 to -209 region of the IRF-4 promoter (Fig. 13). In accordance with *in vivo* footprinting data, novel protein-DNA complexes were not detectable on any of these sites when comparing control Jurkat or T4 cell extracts to MT2 or ATL2 cell extracts (S. Sharma, data not shown).

To further examine NF-κB and NF-AT activation of the IRF-4 promoter the 0.4-kb IRF-4 promoter, lacking the κB1 and Sp1 elements while retaining the CD28RE, was analyzed by luciferase co-expression studies in Jurkat T-cells (Fig. 19C). These studies demonstrated that an IRF-4 promoter construct containing CD28RE was activated 4-fold as a result of NIK overexpression in Jurkat cells (Fig. 19C). Expression of a constitutively active mutant of NF-ATp, NF-ATpXS (286) with the 0.4-kb IRF-4 promoter resulted in a 3-fold induction of IRF-4 promoter activity (Fig. 19C). Co-expression of NIK and NF-ATpXS resulted in a 7-fold induction of the 0.4-kb IRF-4 promoter fragment (Fig. 19C). With respect to HTLV-I Tax expression, transfection of wild type Tax and Tax M47 resulted in 14-fold and 8-fold induction of the 0.4-kb IRF-4 promoter construct, respectively (Fig. 19C). Expression of Tax M22 induced the 0.4-kb IRF-4 promoter approximately 3-fold. Taken together, these results demonstrate that that

NF-κB and NF-AT proteins synergize to stimulate an IRF-4 promoter construct containing the CD28RE element.

4.4 κB1 and CD28RE are required for Tax-induced IRF-4 promoter activation

To analyze the requirement for the κB1, Sp1 and CD28RE enhancer elements in Tax-mediated activation of the IRF-4 promoter, additional luciferase experiments were performed to quantify Tax-mediated activation of 0.6-kb IRF-4 promoter constructs containing specific mutations or deletions. Transfection of Tax with the wild type promoter resulted in a 4-fold induction (Fig. 20A). Specific mutation of κB1 abolished IRF-4 promoter activity in response to Tax expression in Jurkat T-cells (Fig. 20A), which confirmed previous luciferase experiments demonstrating a requirement for NF-κB signaling in Tax-mediated IRF-4 activation (Fig. 15C). Specific mutation of the Sp1 site reduced IRF-4 promoter activation to one-fourth the level of wild type activation in response to Tax expression (Fig. 20A). Like κB1, deletion of the CD28RE abrogated Tax-induced IRF-4 promoter activity (Fig. 20A). Taken together, luciferase data demonstrates that activation of the IRF-4 promoter by the HTLV-I Tax protein requires transactivation from the κB1 and CD28RE, but not the Sp1 sites of the human IRF-4 promoter.

To confirm constitutive occupancy of the κB1, Sp1/NF-2 and CD28RE elements of the IRF-4 promoter in HTLV-I infected cells, *in vivo* formaldehyde crosslinking and chromatin immunoprecipitation (chIP) assays were performed in MT2 cells (Fig. 20B, upper panel) and control Jurkat cells (Fig. 20B, lower panel) treated with formaldehyde to cross-link DNA-associated proteins in the nucleus (448). A 250-bp sequence spanning the κB1 to the CD28RE sites of the IRF-4 promoter was PCR-amplified from DNA sequences isolated with antisera specific to NF-ATp, c-Rel, p-50 and Sp1 proteins (Fig. 20B, lanes 4-7), to a degree significantly above control IRF-3 antibody or no antibody samples (Fig. 20B, lanes 2 and 4). Immunoprecipitation of the 250-bp regulatory sequence of the IRF-4 promoter was specific to MT2 cells, which indicates that the κB1, Sp1/NF-2 and CD28RE sites are constitutively occupied in HTLV-I-infected cells. A

Figure 20. Requirement of κB1 and CD28RE for Tax-mediated transactivation of the IRF-4 promoter (A) Wild type and mutant constructs used in luciferase analysis of Tax-induced IRF-4 promoter activity are represented. Jurkat T-cells (10^6) were transfected with 0.2 μg of 0.6-kb4PRO-pGL3B wild type (lanes 1 and 2), 0.6-kb4PROκB1$_{mut}$-pGL3B (lane 3), 0.6-kb4PROSp1$_{mut}$-pGL3B (lane 4) and 0.6-kb4PROΔCD28RE –pGL3B (lane 5). 25 ηg of pRLTK *renilla* luciferase normalizing vector and a threefold molar excess of Tax WT (lanes 2-5) were added with pFLAG-CMV2 vector to bring total DNA per sample to 2.0 μg. Luciferase activity was assayed 46h post-transfection. Fold induction was calculated relative to the reporter gene expression in the presence of empty vector after correction for transfection efficiency by *renilla* luciferase. Results are representative of at least 3 independent experiments. **(B)** Antibodies against NF-ATp, c-Rel, p50 and Sp1 enrich IRF-4 promoter sequences in ChIP assay. Proteins cross-linked to DNA by formaldehyde treatment in control Jurkat (lower panel) and MT2 (upper panel) cells were immunoprecipitated with antibodies (4 μg) specific to IRF-3 (lane 3), NF-ATp (lane 4), c-Rel (lane 5), p50 (lane 6) and Sp1 (lane 7). Precipitated DNA was analyzed by PCR for the presence of the proximal IRF-4 promoter region, spanning the CD28RE to the κB1 site, by specific primers detailed in Chapter II. Amplification products were analyzed on a long range sequencing gel and visualized by autoradiography. **(C)** [Upper] Organization of regulatory domains within the -500 to -200 region of the IRF-4 promoter, including the κB1 to κB2, Ets-1, Sp1 and CD28RE, is shown at the top. [Lower] In HTLV-I infected cells, constitutive binding is observed at the κB1, Ets-1, Sp1 and CD28RE sites, corresponding to p50/p65 or p50/c-Rel binding to κB1, Sp1 binding to two adjacent Sp1 sites and p50/c-Rel and NF-ATp binding to the CD28RE.

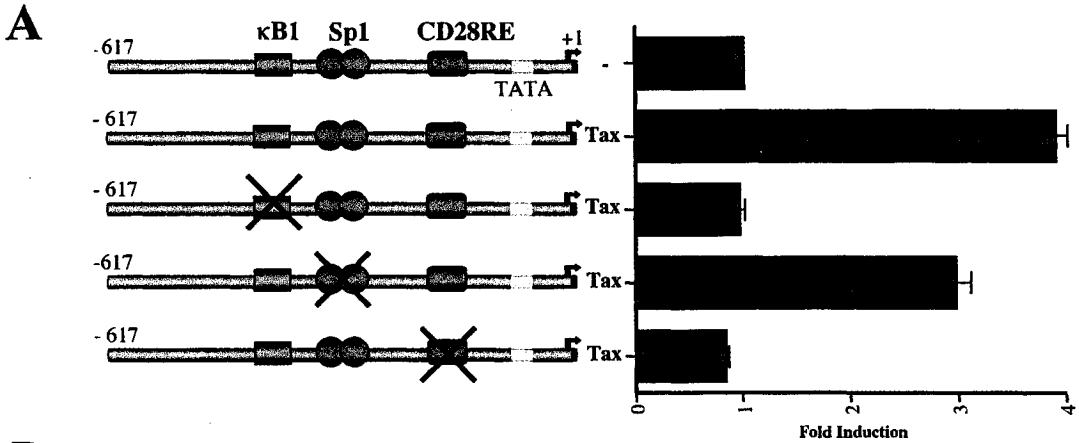
A
κB1
Sp1
CD28RE
-617
+1
TATA
-
Tax
Tax
Tax
Tax
0
1
2
3
4
Fold Induction

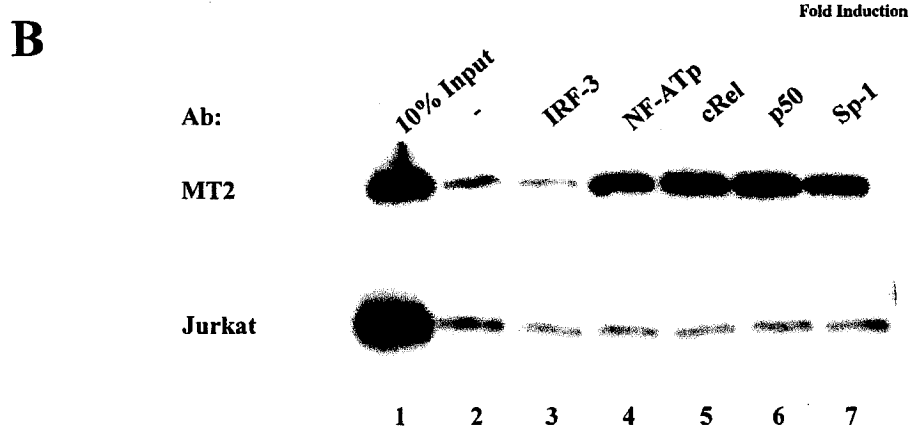
B
Ab:
10% Input
-
IRF-3
NF-ATp
cRel
p50
Sp-1
MT2
Jurkat
1
2
3
4
5
6
7
Primers: IRF-4 promoter

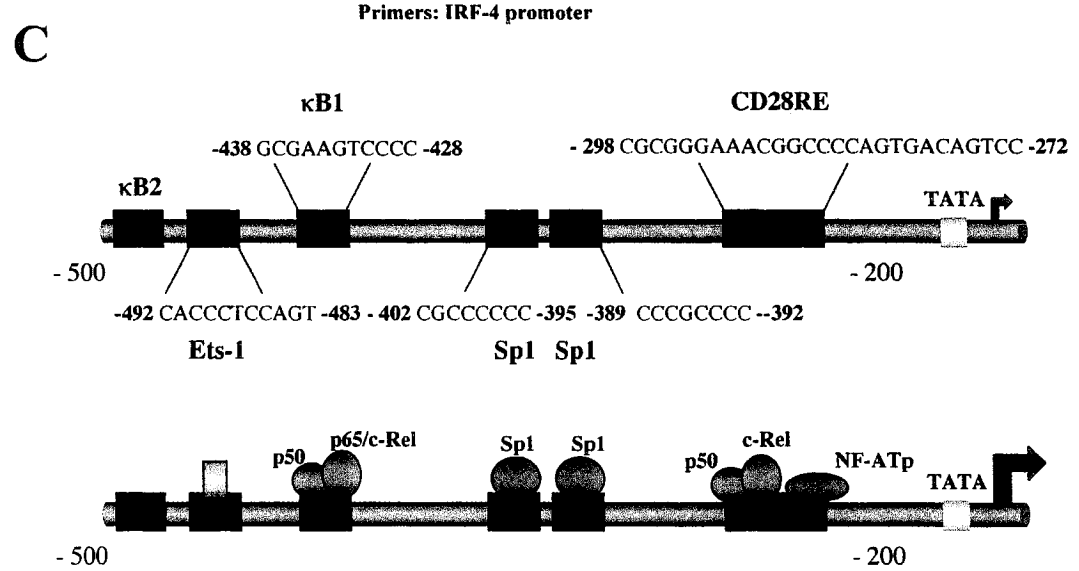
C
κB1
CD28RE
-438 GCGAAGTCCCC -428
- 298 CGCGGGAAACGGCCCCAGTGACAGTCC -272
κB2
TATA
- 500
- 200
-492 CACCCTCCAGT -483 - 402 CGCCCCCC -395 -389 CCCGCCCC --392
Ets-1
Sp1 Sp1
p50
p65/c-Rel
Sp1
Sp1
p50
c-Rel
NF-ATp
TATA
- 500
- 200

schematic representation of human IRF-4 promoter activation in HTLV-I-infected T-cells is summarized by Figure 20C.

Chapter IV

Activation of IRF-3 and IRF-7 signaling by an IKK-related pathway: establishment of the anti-viral state

Initial studies focused on the transcriptional regulation of IRF-4 in HTLV-I infected T-cells. These studies demonstrated that the classical IKK pathway to NF-κB activation is essential for IRF-4 promoter activation by the viral Tax protein. Subsequent experiments sought to identify additional regulatory components of IRF-4 signaling in HTLV-I infected cells. The IKK kinase family has been recently expanded to include two additional members; TBK-1 and IKKε promote activation of NF-κB signaling independently of IκB phosphorylation. Preliminary evidence suggests that these IKK-related kinases regulate transcription factors at the level of carboxy-terminal phosphorylation, an event associated with enhanced transcriptional activation of both NF-κB and IRF subunits.

Chapter IV

Activation of IRF-3 and IRF-7 signaling by an IKK-related pathway: establishment of the anti-viral state

1. Cloning and characterization of the IKK-related kinases

IKKε is an IKK-related kinase that displays limited structural and sequence homology to the classical IKK kinases IKKα and IKKβ (Fig. 4) (103,104,107). However, biochemical and genetic analyses of IKKε and the closely related TBK-1 indicate that, unlike the classical IKK kinases, the IKK-related kinases function independently of IκB phosphorylation and degradation (102,106,109). Initial experiments were performed to analyze the role of IKK-related kinases in direct carboxy-terminal phosphorylation of NF-κB subunits, an event that enhances their transactivation potential (120,121,123). For these studies, human IKKε cDNA was amplified from an HTLV-I transformed T-cell cDNA library using the specific primers described in Chapter II; human TBK-1 cDNA was subsequently obtained from OriGENE technologies, and sub-cloned as detailed in Chapter II. Wild type IKKε and TBK-1 and dominant negative, kinase dead mutants containing a critical K38A substitution in the ATP binding pocket (103,104) were expressed as either a Myc or FLAG epitope-tagged fusion protein.

Previous studies characterize IKKε as a lymphoid-specific kinase induced by PMA but not TNFα stimulation of T-lymphocytes (104). To functionally analyze IKKε, Jurkat T-cells were transiently transfected with the FLAG-IKKε expression vector; 48h post-transfection, samples were left untreated or stimulated with TNFα or PMA for 5 and 15 minutes, respectively (Fig. 21A). An anti-FLAG monoclonal antibody was used to immunoprecipitate IKKε from untreated and TNF or PMA-stimulated WCE. Catalytic kinase activity of the IKKε-associated immunocomplexes was analyzed by a standard IKK *in vitro* kinase assay using peptide substrates corresponding to GST-IκBα(aa1-55) (Fig. 21A, lanes 1-3), which has previously been demonstrated an *in vitro* substrate for IKKε at S36 (103,104), and GST-2NIκBα(aa1-55) (Fig. 21A, lanes 4-6) as a negative control. As previously reported (104), IKKε immunocomplexes isolated from Jurkat T-cells displayed a catalytic activity that was induced in response to PMA treatment (Fig.

Figure 21. IKKε phosphorylates the carboxy-terminal of c-Rel *in vitro* (**A**) Jurkat T-cells (10^7) were transfected with FLAG-IKKε expression plasmid (10.0 μg) using FuGene 6 transfection reagent. 36h post-transfection, cells were left untreated (-) or stimulated with TNFα for 5 minutes (TNF) or PMA for 15 minutes (PMA). WCE were immunoprecipited (IP) with anti-FLAG antisera, and immunoprecipiates were incubated in kinase reaction buffer with 10 μCi [γ-^{32}P]-ATP for 30 minutes at 30°C. Peptide substrates corresponded to GST-IκBα(aa 1-55) (lanes 1-3) or GST-IκBα2N(aa 1-55) (lanes 4-6). Following resolution by 10% SDS-PAGE, the upper half of gel was immunoblotted (IB) with anti-FLAG; after Coomassie blue staining to control substrate loading (Coomassie), the lower half of gel was visualized by autoradiography (middle panel, position of phosphorylated IκBα is indicated). (**B**) Schematic representation of human c-Rel. Carboxy-terminal transactivation domain (TD, aa422-588) is represented. TD contains three putative IKK phosphoacceptor sites (uppercase and underlined) within subdomains A(aa422-472), B(aa472-528) and C(aa473-522). (**C**) ATCC293 cells were transfected with FLAG-IKKε or FLAGIKKβ expression plasmids (5.0 μg). 16h post-transfection, WCE were immunoprecipitated (IP) with anti-FLAG antisera. Immunoprecipitates were incubated in kinase reaction buffer with 10 μCi [γ–^{32}P]-ATP for 15 minutes at 30°C. Following resolution by 10% SDS-PAGE., the upper half of the gel was immunoblotted (IB) with anti-FLAG; the lower half was visualized by autoradiography (lower panel, position of phosphorylated substrates are indicated). Substrates corresponded to GST, GST-IκBα(aa 1-55), GST-IκBα2N(aa 1-55), GST-c-RelTD(aa 422-588), GST-c-RelTD(A), GST-c-RelTD(B) and GST-c-RelTD(C).

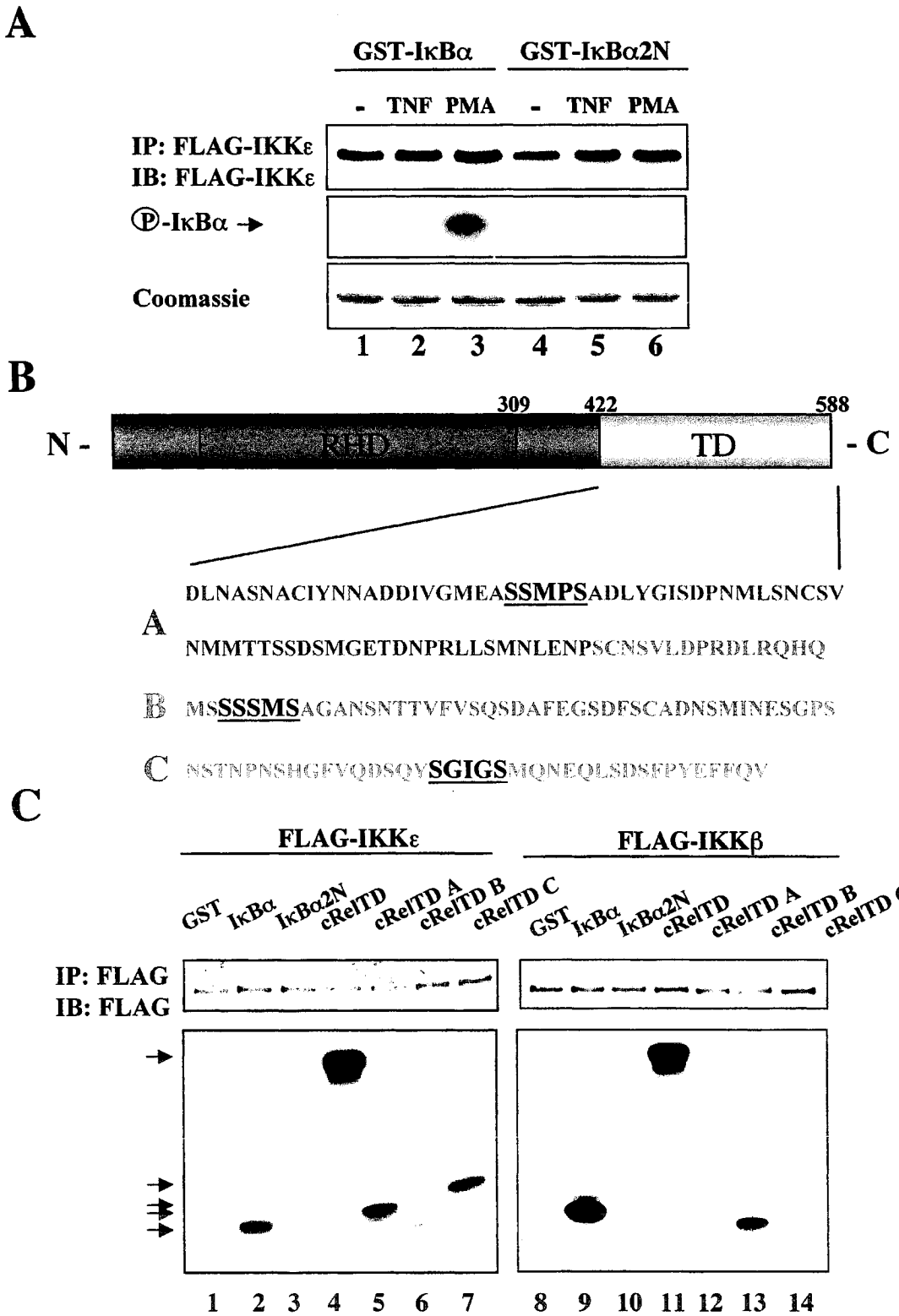
A
GST-IκBα
GST-IκBα2N
- TNF PMA - TNF PMA
IP: FLAG-IKKε
IB: FLAG-IKKε
Ⓟ-IκBα
Coomassie
1 2 3 4 5 6
B
309
422
588
N -
RHD
TD
- C
DLNASNACIYNNADDIVGMEASSMPSADLYGISDPNMLSNCSV
A
NMMTTSSDSMGETDNPRLLSMNLENPSCNSVLDPRDLRQHQ
B MSSSSMSAGANSNTTVFVSQSDAFEGSDFSCADNSMINESGPS
C NSTNPNSHGFVQDSQYSGIGSMQNEQLSDSFPYEFFQV
C
FLAG-IKKε
FLAG-IKKβ
GST IκBα IκBα2N cRelTD cRelTD A cRelTD B cRelTD C
GST IκBα IκBα2N cRelTD cRelTD A cRelTD B cRelTD C
IP: FLAG
IB: FLAG
1 2 3 4 5 6 7 8 9 10 11 12 13 14

21A, lane 3) but not TNFα treatment (Fig. 21A, lane 2). Furthermore, IKKε-mediated phosphorylation of the GST-IκBα substrate was specific to the signal-responsive residues, as the GST-2NIκB αpeptide was not phosphorylated by IKKε-immunocomplexes derived from PMA-treated cells (Fig. 21A, compare lanes 3 and 6).

1.1 IKKε phosphorylates the carboxy terminal of c-Rel

Further experiments were performed to examine the capacity of IKKε to potentiate NF-κB-driven transcription through carboxy-terminal phosphorylation of the c-Rel transcription factor. Displaying a pattern of expression that is similar to IKKε in cells of the lymphoid lineage (2,103,104), c-Rel contains a serine-rich carboxy-terminal transactivation domain (TD) that represents a signal-responsive phosphoaceptor domain in response to CD28 cross-linking and PMA treatment (120-122). Sequence analysis was performed with respect to the c-Rel TD (aa422-588), which identified three potential IKKε phosphoacceptor sites (103,104) located within a canonical MAPK/IKK consensus SXXXS motif (Fig. 21B).

To determine whether the PMA-activated IKKε kinase mediates phosphorylation of carboxy-terminal residues within the c-Rel TD, ATCC293 cells were transfected with FLAG-IKKε (Fig. 21C, right panel). 16h post-transfection, WCE were prepared and immunoprecipitated with anti-FLAG antisera to isolate IKKε-specific immunocomplexes. Immunoprecipitates were subject to a standard IKK *in vitro* kinase assay using peptide substrates corresponding to GST, GST-IκBα(aa1-55), GST-c-RelTD(aa488-522), which represents the entire carboxy-terminal transactivation domain, as well as three smaller peptides designated GST-c-RelTD(A)(aa422-472), GST-c-RelTD(B)(aa473-522) and GST-c-RelTD(C)(aa523-588), each containing a single SXXXS motif (Fig. 21B). *In vitro* kinase analysis indicated that the IKKε-associated kinase activity specifically phosphorylated GST-IκBα(Fig. 21C, left panel, compare lanes 2 and 3), but also the carboxy-terminal of c-Rel (Fig. 21C, left panel, lanes 4, 5 and 7).

Previous data suggests that the IKK-related kinases IKKε and TBK-1 function independently of the classical IKK kinases IKKα and IKKβ (102,104,106). Although each IKK subset can preferentially target a SXXXS recognition motif *in vitro*, the IKK-related kinases display unique substrate specificities and kinetic properties when compared to the classical IKK kinases (110,468). To determine if IKKε-mediated phosphorylation of c-Rel occurs independently of the classical IKK complex, ATCC293 cells were transfected with FLAG-IKKβ (Fig. 21C, right panel) and analyzed by *in vitro* kinase assay using peptide substrates corresponding to GST, GST-IκBα, GST-c-RelTD and GST-c-Rel(A)(aa422-572), GST-c-RelTD(B)(aa473-522) and GST-c-RelTD(C)(aa423-588). While FLAG-IKKε immunoprecipitates preferentially targeted serine residues within TD peptides (A) and (C) (Fig. 21C, left panel, lanes 5 and 7), FLAG-IKKβ immunoprecipitates preferentially targeted the c-Rel TD for phosphorylation within peptide (B) (Fig. 21C, right panel, lane 6). These results demonstrate that expression of IKKε or IKKβ induces phosphorylation of c-Rel in the carboxy-terminal signal responsive domain. However, IKKε and IKKβ display a different preference for substrate recognition with respect to phosphoacceptor sites within the c-Rel TD.

2. The IKK-related kinases phosphorylate the carboxy terminal of IRFs

The type I IFN response is a fundamental component of innate immunity: upon virus infection, rapid induction of type I IFN transcription is signaled via post-translational modification of cellular transcription factors belonging to the NF-κB, ATF-2/c-Jun, and IRF families (352,353). These latent, early-response transcription factors are primarily activated as a consequence of phosphorylation events by regulatory kinase components of the anti-viral signaling network. Although activation of the NF-κB and ATF-2/c-Jun pathways is well characterized, signal transduction cascades from virus infection to IRF activation are not as well delineated.

The IRF-3 and IRF-7 transcriptional program is often induced in conjunction with NF-κB signaling in response to pathogen recognition. As a result, IRF and NF-κB proteins often function in a cooperative manner to promote transcription from immune response

promoters containing functional ISRE and κB sites, such as those of the type I IFNβ and RANTES genes (321,400,403,469). Virus-inducible phosphorylation events mediated by an unidentified virus activated kinase (VAK) complex control IRF-3 (393,397,399,412,414) and IRF-7 activation (410,420,421). Although intense research by several groups, including our own laboratory, have focused on identifying the regulatory kinase components directly upstream of IRF-3 and IRF-7 activation, the identity of VAK has remained elusive (208,289,412,421).

A yeast two-hybrid screen performed in the lab by Dr. R. Lin previously identified an interaction between IRF-3 and the carboxy-terminal domain of the IKKα subunit of the classical IKK complex(R. Lin, unpublished results). Based on the ability of IKK kinases to (1) mediate carboxy-terminal phosphorylation of transcription factors such as c-Rel (Fig. 21C, left panel) and (2) associate with IRF-3 in a yeast two hybrid assay, it was of interest to explore the role of IKK subunits in carboxy-terminal phosphorylation and IRF-3 and IRF-7.

2.1 *In vitro* phosphorylation of IRF-3 and IRF-7

To determine whether IKK subunits could induce carboxy-terminal phosphorylation of IRF-3 and IRF-7, control plasmid and plasmids encoding Myc-IKKα, FLAG-IKKβ, FLAG-IKKε and FLAG-TBK1 were expressed in ATCC293 cells (Fig. 22A). 16h post-transfection WCE were prepared and used in a standard IKK *in vitro* kinase assay. Figure 22A demonstrates that only WCE derived from IKKε or TBK-1-expressing cells possessed an intrinsic kinase activity capable of inducing phosphorylation of a peptide substrate corresponding to the carboxy-terminal signal responsive domain of IRF-3 (398,422) fused to GST, GST-IRF-3(aa380-427) (Fig. 22A, lanes 11 and 14). Phosphorylation of IRF-3 by IKKε or TBK-1 transfection was specific for the virus-responsive phosphoacceptor residues with the IRF-3 carboxy-terminal, because a GST-IRF-3 peptide substrate mutated in the critical virus-responsive serine-threonine cluster II residues (398,422), GST-IRF-3(5A)(aa380-427), was not specifically phosphorylated in response to IKKε or TBK-1 overexpression (Fig. 22A, lanes 12 and 15). Furthermore,

Figure 22. IKKε phosphorylates the carboxy-terminal of IRF-3 and IRF-7 *in vitro*

(A) ATCC293 cells were transfected with control or IKKα, IKKβ, IKKε, or TBK-1 expression plasmids (5.0 μg) using FuGene 6 transfection reagent. 24h post-transfection, WCE (2.0 μg) were incubated in kinase reaction buffer with 10 μCi [γ-^{32}P]-ATP for 30 minutes at 30°C using GST, GST-IRF-3(aa380-427) or GST-IRF-3(5A)(aa380-427 with alanine substitutions at positions S396, S398, S402, T404 and S405) as peptide substrates. **(B)** Plasmids encoding control, FLAG-IKKε or FLAG-TBK-1 (1.0 μg) were transcribed and translated *in vitro* and immunoprecipitated with anti-FLAG; immunoprecipitates were incubated in kinase reaction buffer with 10 μCi [γ-^{32}P]-ATP for 50 minutes at 30°C using GST, GST-IκBα(aa1-55), GST-IRF-3(aa380-427) and GST-IRF-7(aa468-503) as peptide substrates. Following resolution of kinase reactions by 10% SDS-PAGE, gels were stained with Coomassie blue to control substrate loading (Coomassie), and visualized by autoradiography (upper panel, positions of phosphorylated substrates are indicated). In (A), a non-specific band was phosphorylated in all lanes containing the 5A substrate; this band does not migrate to the position of the 5A substrate.

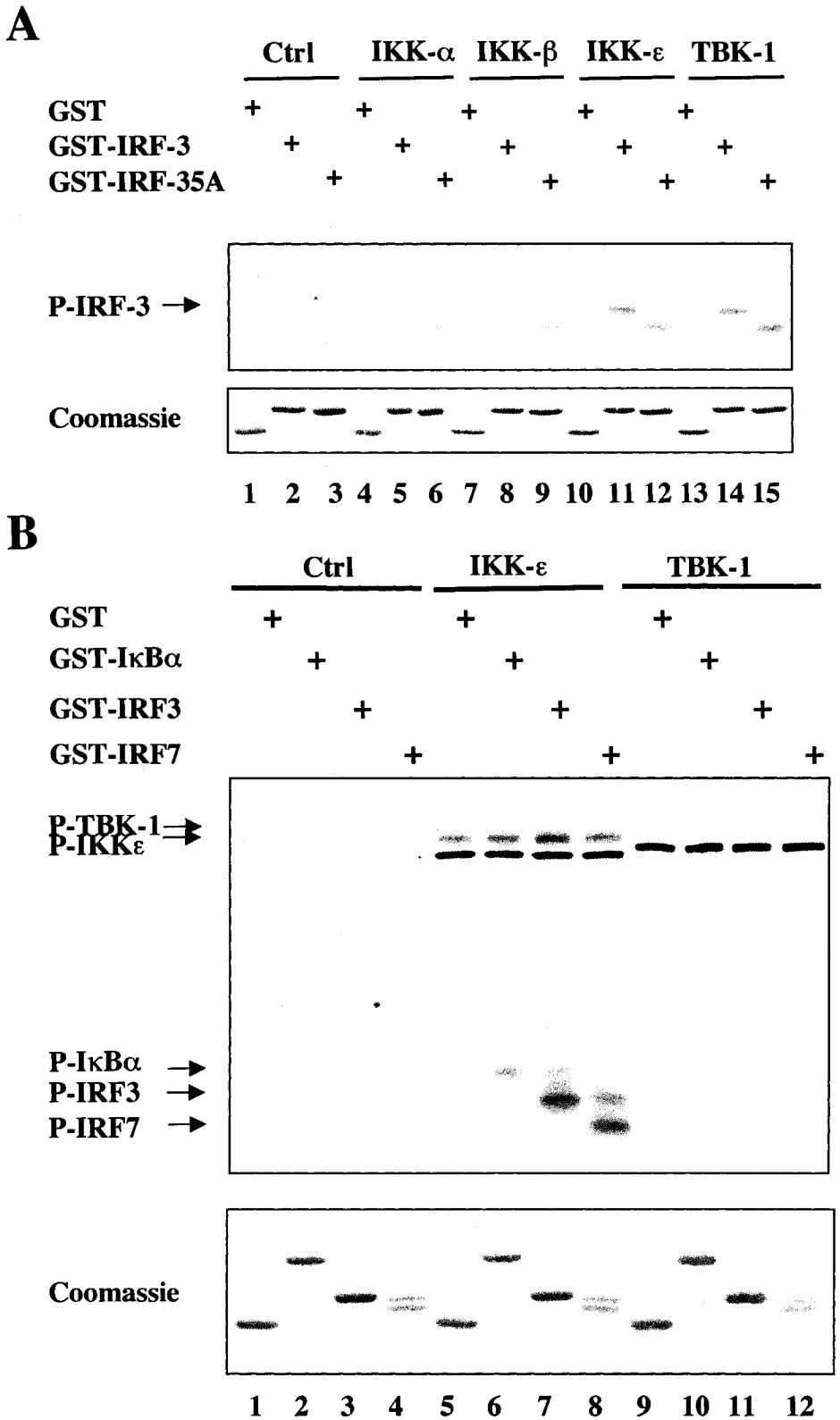
A
Ctrl
IKK-α
IKK-β
IKK-ε
TBK-1
GST
GST-IRF-3
GST-IRF-35A
P-IRF-3
Coomassie
1 2 3 4 5 6 7 8 9 10 11 12 13 14 15
B
Ctrl
IKK-ε
TBK-1
GST
GST-IκBα
GST-IRF3
GST-IRF7
P-TBK-1
P-IKKε
P-IκBα
P-IRF3
P-IRF7
Coomassie
1 2 3 4 5 6 7 8 9 10 11 12

the catalytic activity of IKKε and TBK-1 was required for IRF-3 carboxy-terminal phosphorylation, as expression of kinase dead IKKε(K38A) or TBK-1(K38A) not only failed to induce phosphorylation of GST-IRF-3, but blocked wild type IKKε or TBK-1-induced GST-IRF-3 phosphorylation (S. Sharma, data not shown).

Next, to determine if IKKε or TBK-1 directly phosphorylate IRF-3 and the closely related IRF-7 (289) within the signal responsive carboxy-terminal domain, empty vector (Fig. 22B, lanes 1-4), FLAG-IKKε (Fig. 22B, lanes 5-8) and FLAG-TBK-1 (Fig. 22B, lanes 9-12) transcribed and translated *in vitro* in a rabbit reticulocyte background were immunoprecipitated using anti-FLAG antisera. Immunoprecipitates were subjected to standard IKK *in vitro* kinase assay using fusion peptide substrates that corresponded to GST alone (Fig. 22B, lanes 1, 5 and 9), GST- IκBα(aa1-55)(Fig. 22B, lanes 2, 6 and 10),GST-IRF-3(aa380-427) (Fig. 22B, lanes 3, 7 and 11) and GST-IRF-7(aa468-503) (Fig. 22B, lanes 4, 8 and 12). Figure 22B demonstrates that IKKε directly phosphorylated the GST-IRF-3 and GST-IRF-7 substrates (Fig. 22B, lanes 7 and 8) in addition to the GST-IκBα substrate (Fig. 21B, lane 6), but not GST alone (Fig. 22B, lane 5).

Interestingly, TBK-1 transcribed and translated *in vitro* was not enzymatically active, as evidenced by the failure of TBK-1 to phosphorylate the GST-IκBα positive control (Fig. 22B, lane 10). This result was not precipitated by interference of FLAG epitope, because TBK-1 transcribed and translated with a Myc epitope tag or no tag at all was also devoid of catalytic activity *in vitro* (S. Sharma, data not shown). Due to the requirement for post-translational modification(s) not available in rabbit reticulocyte preparations but essential to the enzymatic activity of TBK-1, analysis of IRF phosphorylation by TBK-1 could not be performed. However, based on the *in vitro* kinase data presented in Figure 22 it can be concluded that, in contrast to the classical kinases IKKα and IKKβ, expression of the non-classical kinases IKKε and TBK-1 activates a kinase activity that targets the carboxy-terminal IRF-3 *in vitro*. Significantly, IRF-3 phosphorylation by IKKε and TBK-1 was specific for the carboxy-terminal serine/threonine cluster II residues that have been shown to be critical for virus-induced IRF-3 activation (398). Finally, with respect to

IKKε, phosphorylation of IRF-3 and IRF-7 within the carboxy-terminal signal response domain is a direct event.

2.2 *In vivo* phosphorylation of IRF-3 and IRF-7

Within the context of *de novo* virus infection, carboxy-terminal hyperphosphorylation of IRF-3 and IRF-7 is associated with the appearance of slowly migrating forms of IRF-3 (393,396,398,399) and IRF-7 (299,410,421) when resolved by one-dimensional 7.5% SDS-PAGE followed by western blot detection. As demonstrated in Figure 23A, western blot analysis of WCE derived from Jurkat T-cells infected with SV at a titer of 40 HAU/mL for various time points demonstrates that conversion of latent IRF-3 forms I and II to hyperphosphorylated forms III and IV (412) began approximately 6h post SV infection (Fig. 23A, upper panel, lanes 3-8). The appearance of hyperphosphorylated IRF-3 correlates with induction of the translational inhibitor ISG56 (320), an immediate early response gene which is directly induced by activated IRF-3 (317) (Fig. 23A, middle panel, lanes 4-8). Western blot for actin was performed as a loading control (Fig. 23A, lower panel).

To evaluate the capacity of non-classical IKK kinases to mediate IRF-3 and IRF-7 phosphorylation *in vivo*, FLAG-IKKε was co-expressed with FLAG-IRF-3 in Vero cells utilizing a Tet-inducible expression system. 48h post-transfection, WCE were prepared and analyzed by 7.5% SDS-PAGE followed with detection by western blot (Fig. 23B). Doxycyclin (Dox)-induced IKKε protein expression, which was detected using anti-FLAG antibody at 180 minutes post-induction (Fig. 23B, first panel, lane 4), correlated with the appearance of the slowly migrating forms III and IV of IRF-3, as detected using an antibody against full length IRF-3 (Fig. 23B, second panel, lanes 4 and 5) as well as one specifically recognizing phosphorylation at S396, a modification that has been demonstrated to be critical for physiological IRF-3 activation in response to virus infection (415) (Fig. 23B, third panel, lanes 4 and 5).

In a similar experiment, co-transfection of FLAG-IKKε (Fig. 23C, left panel) or FLAG-TBK-1 (Fig. 23C, right panel) with FLAG-IRF-3 or FLAG-IRF-7 in ATCC293 cells

Figure 23. IKKε and TBK-1 induce IRF-3 and IRF-7 phosphorylation *in vivo* (A) **(B)** Vero cells were co-transfected an rtTA-expressing vector (pRevTetOn, 3.0 μg) and Tet-inducuible FLAG-IKKε expression vector (pRevTreFLAG-IKKε, 3.0 μg) and Myc-IRF-3 expression vector (4.0 μg) using FuGene 6 transfection reagent. 24h post-transfection, cells were treated with doxycycline (Dox, 1 μg/mL) for 0 to 360 min. WCE (75 μg) were resolved by 7.5% SDS-PAGE and analyzed by western blot with anti-IKKε, anti-Myc and anti-IRF-3 Ser396 phosphospecific antisera. (C) ATCC293 cells transfected with expression vectors encoding FLAG-IRF-3 (1.0 μg) or FLAG-IRF-7 (1.0 μg) in the absence (lanes 1 and 3) or presence (lanes 2 and 4) of (A) FLAG-IKKε (4.0 μg) or (B) FLAG-TBK-1 (4.0 μg) by calcium phosphate co-precipitation. 24h post-transfection, WCE (50 μg) were resolved by 7.5% SDS-PAGE and analyzed by western blot with anti-FLAG antibody. The positions of IRF-3, IRF-7, IKKε and TBK-1 are indicated.

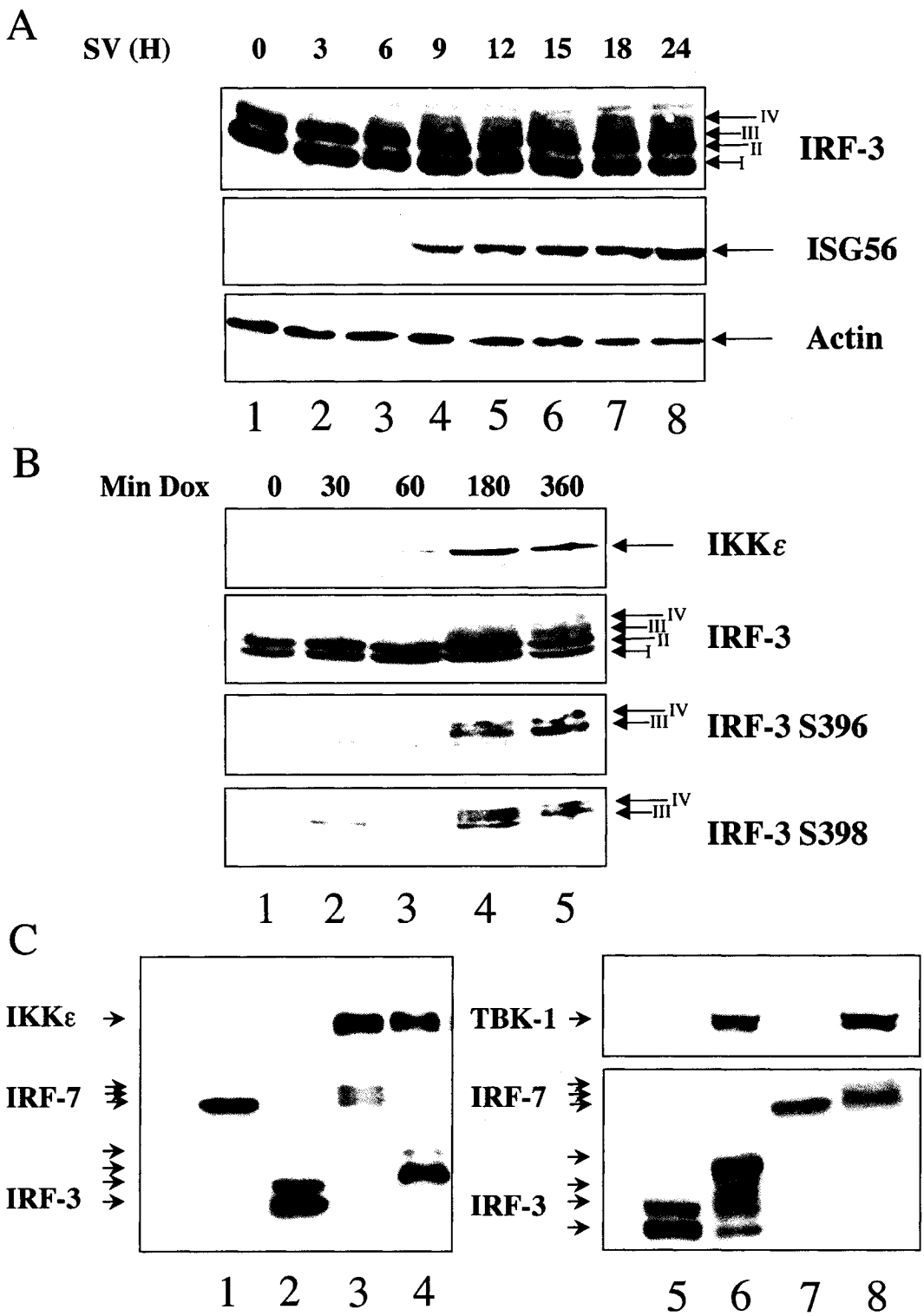
A
SV (H)
0 3 6 9 12 15 18 24
IV
III
II
I
IRF-3
ISG56
Actin
1 2 3 4 5 6 7 8
B
Min Dox
0 30 60 180 360
IKKε
IRF-3
IRF-3 S396
IRF-3 S398
1 2 3 4 5
C
IKKε
IRF-7
IRF-3
TBK-1
IRF-7
IRF-3
1 2 3 4
5 6 7 8

induced IRF hyperphosphorylation *in vivo*, as evidenced by one-dimensional 7.5% SDS-PAGE followed by anti-FLAG western blot detection of the slowly migrating IRF phosphoforms (Fig. 23B, compare lanes in left and right panels). In accordance with *in vitro* kinase data, these results demonstrate that the IKK-related kinases IKKε and TBK-1 target the carboxy-terminal of IRF-3 and IRF-7 *in vitro* and *in vivo*. Hyperphosphorylation of IRF-3 and IRF-7 in the carboxy-terminal, a modification that is associated with activation of these transcription factors in the context of virus infection (393,396,398,399,410), is detectable *in vivo* using one-dimensional 7.5% SDS-PAGE to resolve the slowly migrating phosphoforms of IRF-3 and IRF-7 induced in response to IKKε and TBK-1 expression.

3. IKK-related kinases mediate IRF-3 and IRF-7 activation

During virus infection, carboxy-terminal phosphorylation activates IRF-3/IRF-7 signaling. To determine if carboxy-terminal phosphorylation of IRF-3 and IRF-7 by IKKε and TBK-1 is sufficient to induce the IRF-3/-7 transcriptional program, functional assays were performed to analyze IRF-3 and IRF-7 nuclear accumulation, DNA binding and transcriptional capacity in response to expression of the IKK-related kinases IKKε and TBK-1.

3.1 Cytoplasmic to nuclear translocation IRF-3 and IRF-7

Fluorescent microscopy was performed to monitor the subcellular localization of fusion proteins, consisting of IRF-3 or IRF-7 fused to green fluorescent protein (GFP), in response to IKKε or TBK-1 expression in COS-7 cells (Fig. 24). When co-transfected with control empty vector, each transcription factor localized predominantly to the cytoplasm (Fig. 24A and B, left panel). When either IKKε (Fig. 24A, middle panel) or TBK-1 (Fig. 24B, middle panel) was co-transfected with GFP-IRF-3 or GFP-IRF-7 fusion proteins, approximately 35% of IRF-3 and 95% of IRF-7 was translocated to the nucleus. Intact IKKε and TBK-1 kinase activity was required to induce nuclear accumulation of GFP-IRF-3 and IRF-7, because expression of kinase dead IKKε(K38A) (Fig. 24A, right panel) or TBK-1(K38A) (Fig. 24A, right panel) not only failed to induce

Figure 24. IKKε and TBK-1 induce IRF-3 and IRF-7 nuclear translocation Subcellular localization of IRF-3 or IRF-7 was analyzed in COS-7 cells transfected using LipoefectAMINE Plus transfection reagent with GFP-IRF-3 or GFP-IRF-7 (2.5 μg) in the presence of (A) pcDNA3.1 (2.5 μg, left), IKKε (2.5 μg, middle) or IKKε(K38A) (2.5 μg, right) and (B) pcDNA3.1 (2.5 μg, left), TBK-1 (2.5 μg, middle) or TBK-1(K38A) (2.5 μg, right). Fluorescence was quantified in living cells 24h post transfection at magnification 400x.

A

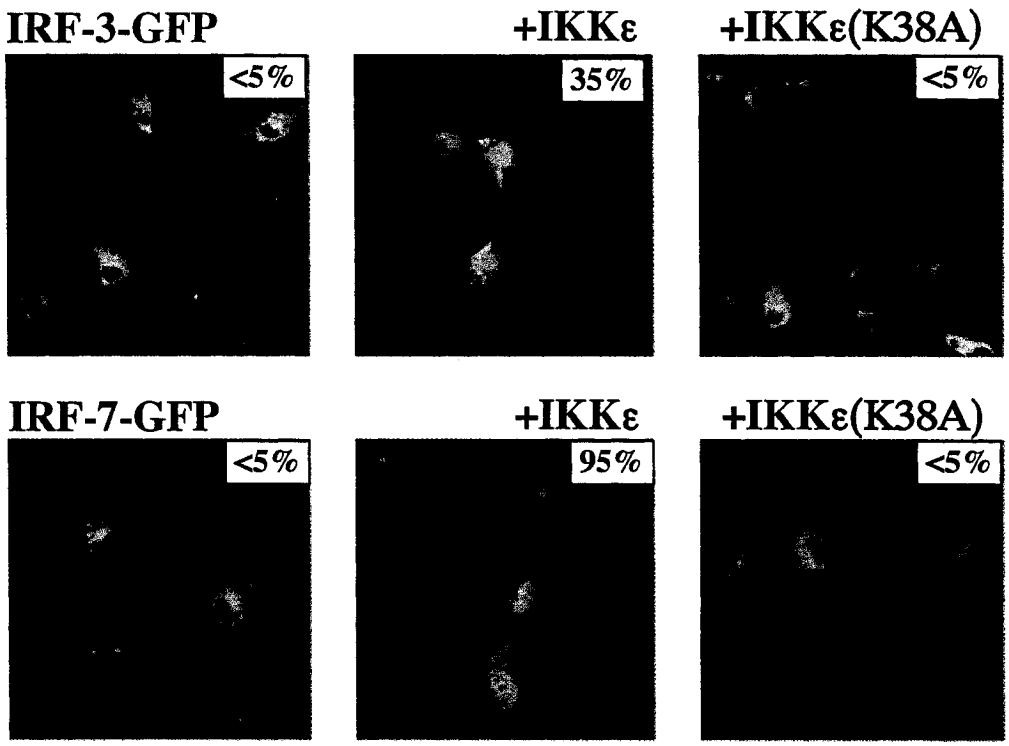
IRF-3-GFP
<5%
+IKKε
35%
+IKKε(K38A)
<5%
IRF-7-GFP
<5%
+IKKε
95%
+IKKε(K38A)
<5%

B

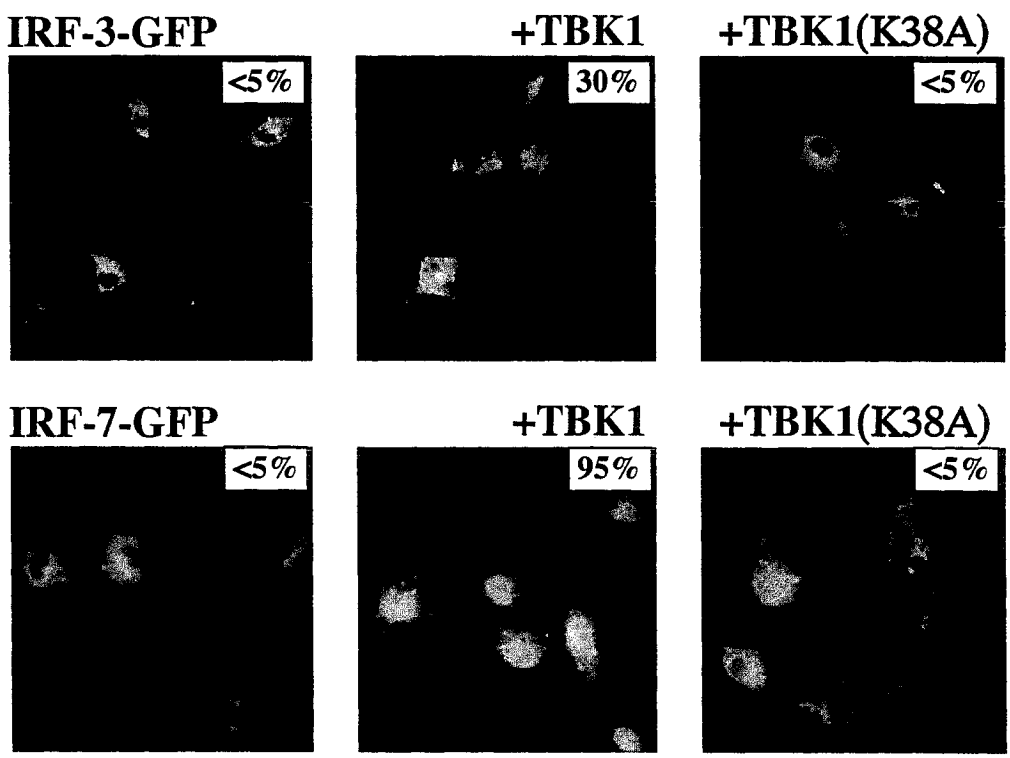
IRF-3-GFP
<5%
+TBK1
30%
+TBK1(K38A)
<5%
IRF-7-GFP
<5%
+TBK1
95%
+TBK1(K38A)
<5%

significant IRF-3 or IRF-7 nuclear accumulation, but in fact seemed to exclude it. Based on these data, it can be concluded that overexpression of either IKKε or TBK-1 is sufficient to induce IRF-3 and IRF-7 cytoplasmic to nuclear translocation.

3.2 Induction of IRF-3 and IRF-7 DNA binding

To determine if IRF-3 and IRF-7 nuclear accumulation induced by IKKε or TBK-1 phosphorylation are associated with functional DNA binding activity, EMSA analyses were performed using oligonucleotide probes that correspond to previously characterized binding sites for IRF-7 (402) (Fig. 25A, IRF-7 BS-1) and IRF-3 (393) (Fig. 25B, ISG15 ISRE). EMSA analysis of nuclear extracts derived from ATCC293 cells co-transfected with IKKε and IRF-7 detected the formation of an inducible protein-DNA complex (Fig. 25A, compare lanes 1 and 3) that co-migrated with a complex detected from nuclear extracts transfected with IRF-7 and subsequently infected with SV (Fig. 25A, compare lanes 2 and 3). The IKKε-inducible complex was specifically supershifted by anti-IRF-7 antibody (Fig. 25A, lane 4) but not anti-IRF-3 or control antisera (Fig. 25A, lanes 5 and 6, respectively).

Expression of IKKε with IRF-3 also resulted in the formation of a protein-DNA complex using the ISG15 ISRE probe (Fig. 25B, compare lanes 1 and 3) that co-migrated with a SV-inducible band (Fig. 25B, compare lanes 2 and 3). The complex was supershifted using anti-IRF-3 or anti-FLAG antibody (Fig. 25B, lanes 11 and 12), but not anti-IRF-7 or control antisera (Fig. 25B, lanes 4 and 7, respectively). Taken together, these experiments demonstrate that phosphorylation by IKKε or TBK-1 of IRF-3 and IRF-7 induces cytoplasmic to nuclear translocation and DNA binding.

3.3 IKKε and TBK-1 stimulate type I IFN transcription

To examine the ability of IKKε and TBK-1 to stimulate ISRE-driven, IRF-dependent type I IFN gene expression, reporter gene analyses were performed to analyze luciferase expression driven by the ISRE-dependent IFNA4 and IFNB promoters (402). Co-expression of IKKε with IRF-7, which is not expressed at the basal level in ATCC293 cells, resulted in a 2000-fold stimulation of the IRF-7-responsive IFNA4 promoter, which

Figure 25. IKKε and TBK-1 induce IRF-3 and IRF-7 DNA binding ATCC293 cells were transfected with expression plasmids encoding FLAG-IRF-7 (5.0 μg) or FLAG-IRF-3 (1.0 μg) in the absence or presence of Myc-IKKε (5.0μg) by the calcium phosphate co-precipitation method. 24h post-transfection, nuclear extracts (10.0μg) were assayed for DNA binding capacity of **(A)** IRF-7 and **(B)** IRF-3 in response to IKKε expression was examined by EMSA using IRF-7 binding site 1 (IRF-7BS1) and the ISG15 ISRE, respectively, as radiolabeled oligonucleotide probes. Specific and non-specific antibodies (1.0 μg) were used to identify IRF-3 or IRF-7 specific complexes by supershift. Protein-DNA complexes corresponding to IRF-7 or IRF-3 are indicated (*) with supershifted complexes (**).

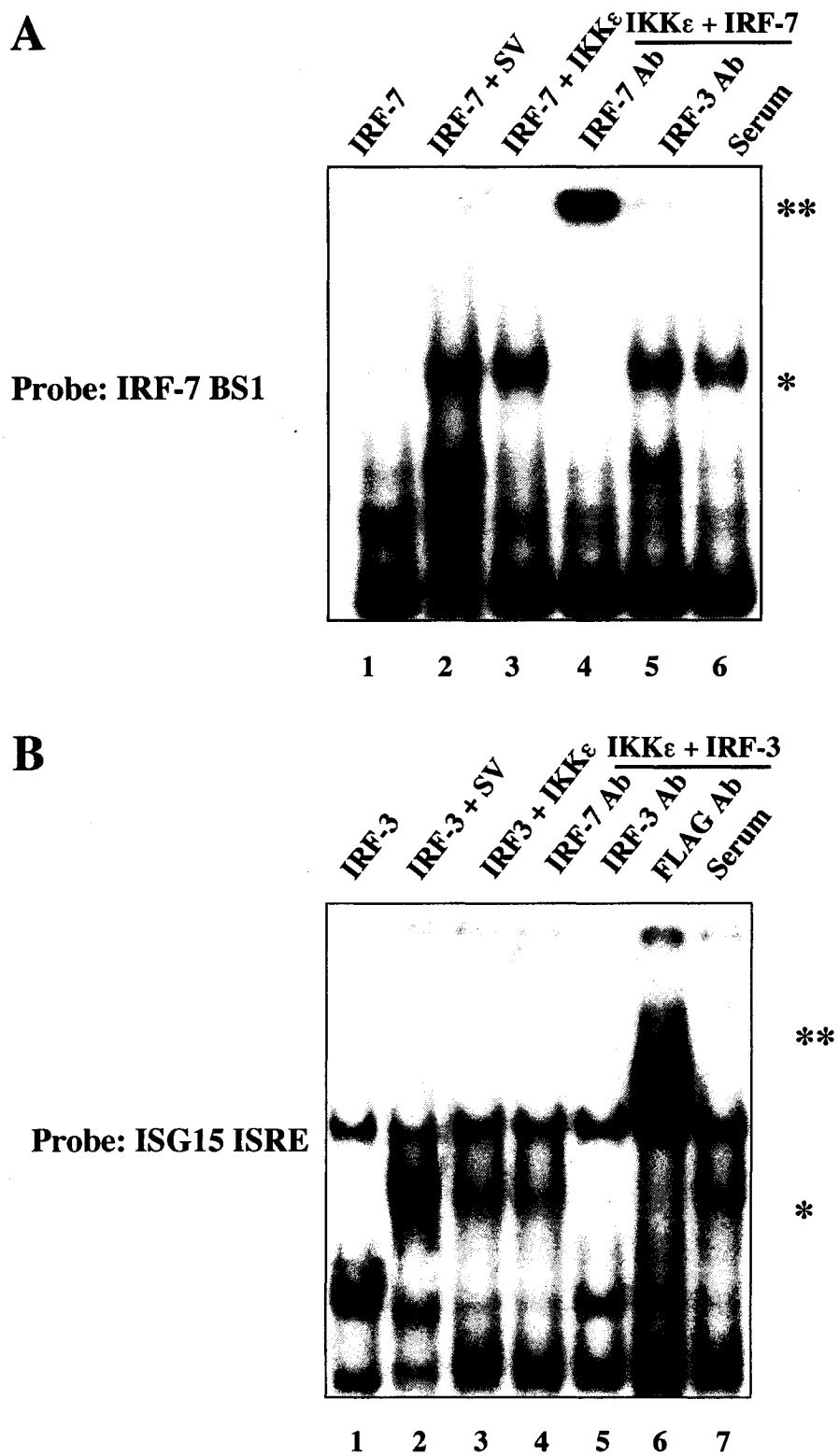
A
IRF-7
IRF-7 + SV
IRF-7 + IKKε
IKKε + IRF-7
IRF-7 Ab
IRF-3 Ab
Serum
**
*
Probe: IRF-7 BS1
1 2 3 4 5 6
B
IRF-3
IRF-3 + SV
IRF3 + IKKε
IKKε + IRF-3
IRF-7 Ab
IRF-3 Ab
FLAG Ab
Serum
**
*
Probe: ISG15 ISRE
1 2 3 4 5 6 7

was normalized as fold induction relative to luciferase expression in the absence of IKKε and IRF-7 transfection (Fig. 26A).

The IFNB reporter was likewise responsive to IKKε expression, resulting in a 40-fold stimulation of the reporter gene (Fig. 26B). Virus infection alone or virus infection in addition to IKKε expression resulted in a 60-fold stimulation of the IFNB promoter construct, an effect that was blocked by co-expression of a dominant negative IRF-3 that lacks the amino-terminal DNA binding domain (IRF-3ΔN) (399) (Fig. 26B). Furthermore, activation of the IFNA4 promoter by IRF-7 and IKKε was blocked by either IKKε(K38A) or a dominant negative carboxy-terminal truncation of IKKε(1-361) (103) (Fig. 26C).

The capacity of each IKK kinase to stimulate reporter constructs was further investigated; When IKKα, IKKβ, IKKε, TBK-1 and NIK were co-expressed with the IFNA4 promoter together with IRF-7, only IKKε and TBK-1 activated the IFNA4 promoter (Fig. 26D). In contrast, each kinase induced a 10- to 40-fold stimulation of a NF-κB-dependent reporter construct (R. Lin, data not shown). Taken together, these results demonstrate that IRF-7 and IRF-3 stimulate the IFNA4 and IFNB promoters in an IKKε and TBK-1-dependent manner.

4. IKK-related kinases are essential to establish the anti-viral state *in vivo*

Preliminary experiments suggest that IκBα is a substrate for the IKK-related kinases *in vitro* (103,104). However, analysis of MEFs derived from mice deficient in TBK-1 or IKKε yielded unexpected results: signal-induced phosphorylation and degradation of IκBα were intact in TBK-1-/- and IKKε-/- cells (106,109). Further experiments were performed to analyze the physiological requirement of endogenous IKKε and TBK-1 expression for activation of the IRF-3 and IRF-7 in response to virus infection. Specific interfering RNA oligonucleotides (RNAi) were designed to downregulate TBK-1 and IKKε expression in human cell lines, as detailed in Chapter II.

Figure 26. Activation of IRF-regulated IFN promoters by IKKε and TBK-1
ATCC293 cells were transfected by the calcium phosphate co-precipitation method with pRLTK *renilla* luciferase normalizing plasmid (20 ηg), a luciferase reporter plasmid containing the IFNB or IFNA4 promoters (0.1 μg) and expression plasmids encoding control, IKKε, IRF-7, IRF-3ΔN, IKKε(K38A), IKKε(1-361), IKKα, IKKβ, TBK-1 or NIK (0.2-0.8 μg). **(A)** and **(B)** 8h post-transfection, cells were infected with Sendai virus at 40 HAU/ml or left uninfected. Luciferase activity was analyzed 24h post-transfection as fold activation relative to the basal level of reporter gene in the presence of control vector after normalization with co-transfected *renilla* luciferase. **(C)** Fold activation of IFNA4 in the presence of IKKε and IRF-7 is plotted as 100; the relative luciferase activity in the presence of increasing amounts (0.2-0.8 μg) of IKKε(K38A) or IKKε(1-361) is expressed as a fraction of 100. **(D)** Luciferase activities were calculated as per panel **A** and **B**, with fold activation relative to the basal level of the IFNA4 promoter in the presence of IRF-7. All values represent the average of 3 experiments, performed in duplicate with variability shown by error bars.

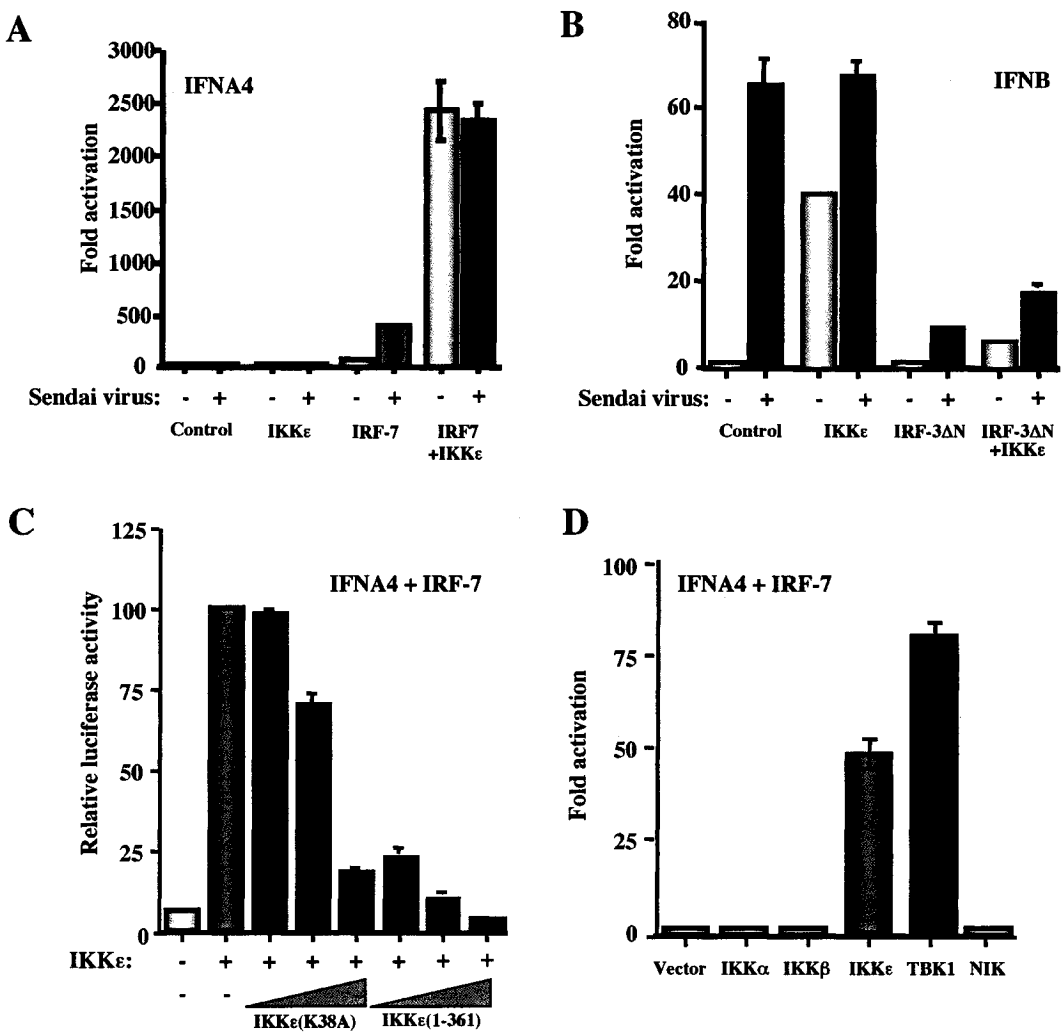
A
IFNA4
Fold activation
3000
2500
2000
1500
1000
500
0
Sendai virus: - + - + - + - +
Control
IKKε
IRF-7
IRF7 +IKKε
B
IFNB
Fold activation
80
60
40
20
0
Sendai virus: - + - + - + - +
Control
IKKε
IRF-3ΔN
IRF-3ΔN +IKKε
C
IFNA4 + IRF-7
Relative luciferase activity
125
100
75
50
25
0
IKKε: - + + + + + + +
- -
IKKε(K38A)
IKKε(1-361)
D
IFNA4 + IRF-7
Fold activation
100
75
50
25
0
Vector
IKKα
IKKβ
IKKε
TBK1
NIK

4.1 Downregulation of IKKε and TBK1 abolishes virus activation of the IRF-3 and IRF-7 transcriptional program

To analyze the requirement for IKK-related kinase activity in virus activation of the IRF-3 and IRF-7 anti-viral pathway, lung epithelial A549 cells were transfected with control or TBK-1 and IKKε-specific RNAi oligonucleotides (Fig. 27). Specific RNAi-mediated knockdown of TBK-1 and IKKε expression eliminated IKKε expression and blocked 70-75% of TBK-1 expression, as detected by western blot analysis (Fig. 27A, first panel, lanes 5-8). 48h post-transfection, control RNAi-treated (Fig. 27A, lanes 1-4) and TBK-1 and IKKε-specific RNAi-treated cells were left unstimulated (Fig. 27A, lanes 1 and 5) or infected with VSV at MOI 100 for the indicated time points (Fig. 27A, lanes 204 and 6-8). In RNAi-treated A549 cells, knockdown of IKKε and TBK-1 expression resulted in an inhibition of endogenous IRF-3 phosphorylation in response to VSV infection (Fig. 27A, compare lanes 3 and 4 to lanes 7 and 8). Inhibition of IRF-3 phosphorylation as a result of TBK-1 and IKKε downregulation correlated with reduced expression of the IRF-3 responsive ISG56 gene (Fig. 27A, compare lanes 3 and 4 to lanes 7 and 8). Similarly, in luciferase assay experiments, induction of the IFNA4 promoter by endogenous IRF-7 was also decreased in RNAi-treated A549 cells (Fig. 27B, compare RNAi control to RNAi IKKε + TBK-1). These results demonstrate that IKK-related kinase modification of IRF-3 and IRF-7 is required for physiological activation of the IRF-3 and IRF-7 signaling pathway in response to virus infection.

4.2 IKKε and TBK-1 exert a global anti-viral effect

To assess the anti-viral effect of the TBK-1/IKKε-dependent pathway to IRF-3 and IRF-7 activation, experiments were performed to monitor the replication of VSV in the absence or presence of IKKε expression (Fig. 28). IKKε or IKKε(K38A) were co-expressed with either wild type IRF-3 or IRF-3ΔN in ATCC293 cells; 16h post-transfection, cells were infected with VSV at an MOI of 5 pfu/cell, and the supernatant was collected post-infection at various time points to quantify VSV titer by standard plaque assay in Vero cells. As demonstrated in Figure 28A, IKKε overexpression decreased VSV replication in ATCC293 cells by 4 logs compared to the control plasmid, from 10^{10} logs to 10^{6} logs (Fig. 28A). Blocking type I IFN/ISG induction by expression of dominant negative IRF-

Figure 27. IKKε and TBK-1 are required for virus activation of the IRF-3/-7 transcriptional program (**A**) RNAi-mediated silencing of TBK-1 and IKKε expression in lung epithelial A549 cells. A549 cells were transfected with control or TBK-1 and IKKε-specific RNAi oligonucleotides using OligofectAMINE reagent. 48h post-transfection, RNAi-treated cells were infected with VSV MOI 100, and harvested at 0, 2, 4, and 6h post-infection. WCE (30 μg) were analysed by western blot using antibodies against TBK-1, IKKε, IRF-3, IRF-3 S396, ISG56, VSV N protein, and actin. (**B**) A549 cells transfected with control or TBK-1 and IKKε-specific RNAi oligonucleotides for 48h and subsequently transfected with IFNA4-pGL3 (0.1 μg) and pRLTK *renilla* luciferase normalizing plasmid (20 ηg). 6h post-transfection, cells were infected with VSV (MOI 10) and harvested 12h post infection. Relative luciferase activity is represented relative to the basal level of reporter gene in the presence of control vector after normalization with co-transfected *renilla* luciferase.

A

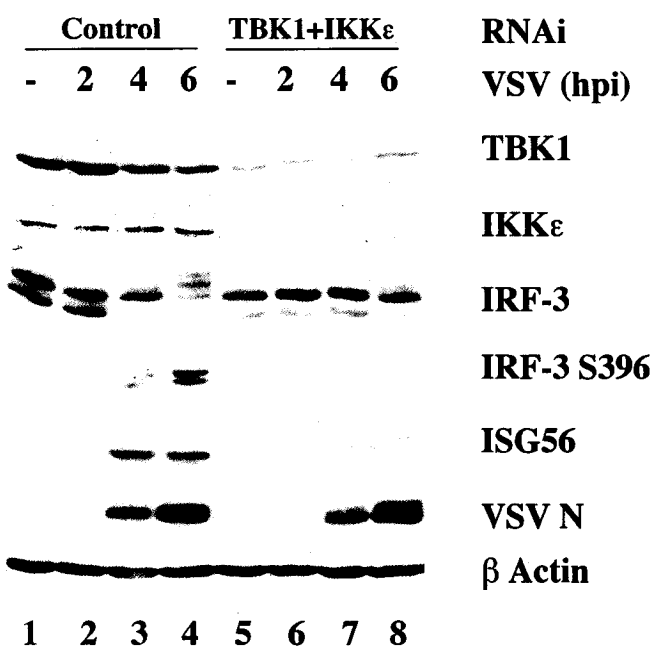
Control
TBK1+IKKε
RNAi
- 2 4 6 - 2 4 6
VSV (hpi)
TBK1
IKKε
IRF-3
IRF-3 S396
ISG56
VSV N
β Actin
1 2 3 4 5 6 7 8

B

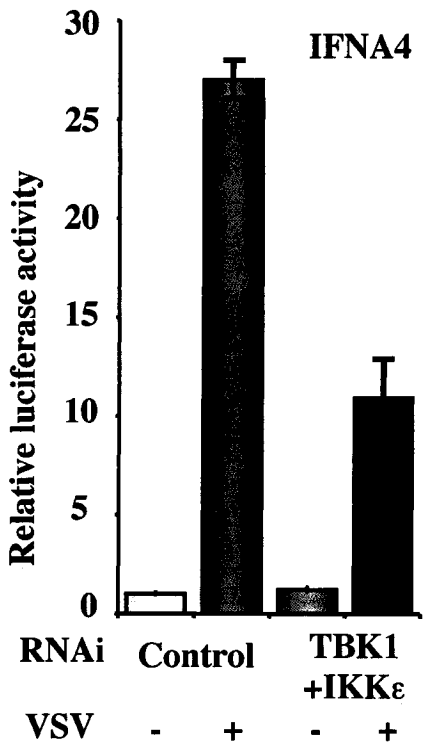
IFNA4
Relative luciferase activity
30
25
20
15
10
5
0
RNAi
Control
TBK1
+IKKε
VSV
- + - +

Figure 28. IKKε and TBK-1 mediate establishment of the IRF-dependent anti-viral state (**A**) ATCC293 cells were co-transfected with pEGFP, IKKε, or IKKε(K38A) (10.0 μg) and either IRF-3 (1.0 μg) or IRF-3ΔN (5.0 μg) by the calcium phosphate co-precipitation method. 24h post transfection, cells were infected with VSV (MOI 100) and supernatants were analyzed for virus production. Supernatants from transfected cells were quantified for VSV replication using a standard plaque assay at the indicated time points. Plaques were counted and titers calculated as plaque forming units per ml (pfu/mL). Left panel: (pEGFP+IRF-3; ●); (IKKε+IRF-3; ▲); (IKKε (K38A)+IRF-3; ■); (Right Panel: (pEGFP+IRF-3ΔN; O); (IKKε+IRF-3ΔN; Δ); (IKKε(K38A)+IRF-3ΔN; □). (**B**) WCE (80 μg) from the 12h post-infection time point in were analysed by 7.5% SDS-PAGE followed by western blot using antibodies against FLAG, IRF-3, VSV N, ISG56, and actin.

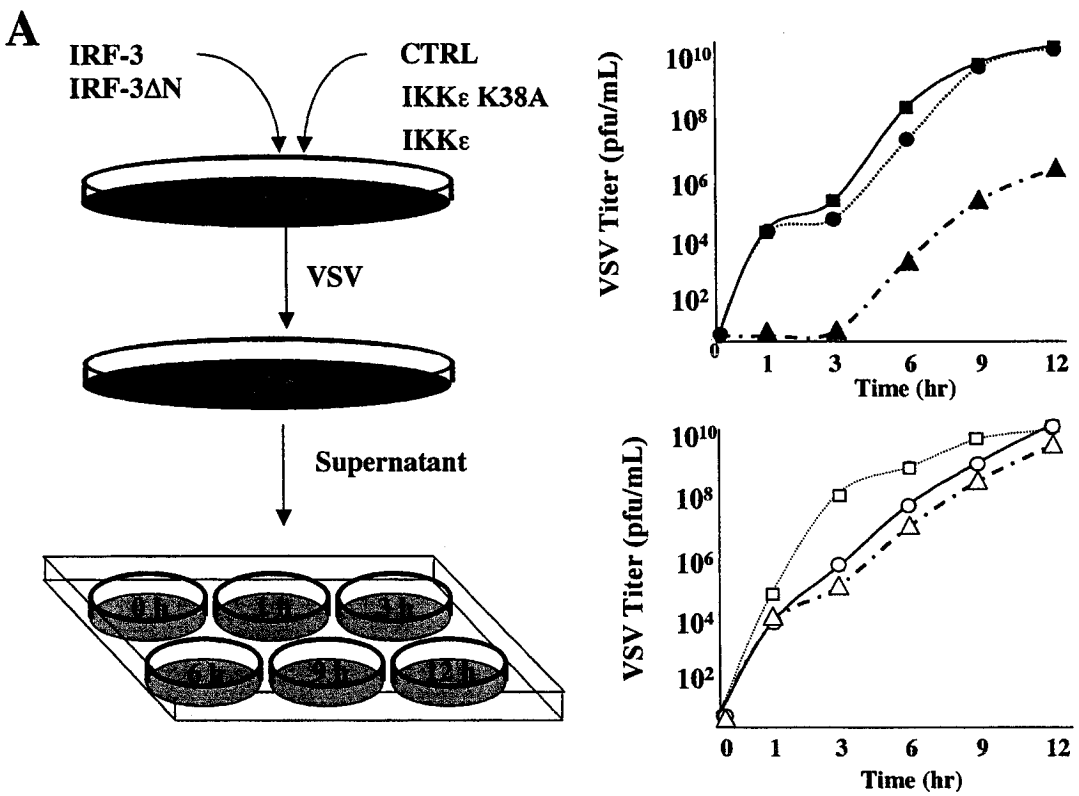
A
IRF-3
IRF-3ΔN
CTRL
IKKε K38A
IKKε
VSV
Supernatant
VSV Titer (pfu/mL)
Time (hr)
B
IRF-3 wt
IRF-3 ΔN
IKKε wt
IKKε K38A
IKKε wt
IKKε K38A
VSV
Flag-IKKε
IRF-3
IRF-3 ΔN
VSV N
ISG56
Beta Actin
1 2 3 4 5 6 7 8

3ΔN (399) restored VSV titer to 10^{10} pfu/ml, which demonstrates that the anti-viral activity of IKKε is dependent on IRF-3 expression in ATCC293 cells (Fig. 28B). Western blot analysis confirmed that IKKε expression induced ISG56 expression while inhibiting VSV replication, as demonstrated by the decrease in expression of the VSV nucleocapsid (N) protein (Fig. 28D, lane 3); in contrast, expression of IRF-3ΔN permitted viral replication in the presence of IKKε (Fig. 28D, lane 7). An identical experiment performed with TBK-1 yielded similar results (B.R. tenOever, data not shown). Thus, engagement of the anti-viral program through IKKε or TBK-1 was sufficient to induce interferon-stimulated genes and inhibit *de novo* VSV replication in tissue culture conditions. These results emphasize the importance of the IKK-related in mediating the anti-viral effects of IRF-dependent signaling.

Chapter V

Biochemical and genetic analysis of the IKK-related kinases

Identification of IRF-3 and IRF-7 as physiological targets of the IKK-related kinases assigns a novel role for TBK-1 and IKKε, and identifies two regulatory components of an anti-viral signaling pathway that has until recently been poorly defined. Upon establishment of the essential role for IKK-related kinases in the activation IRF-3 and IRF-7 phosphorylation within the carboxy-terminal, further experiments were performed to characterize the IKK-related pathway to IRF-3 and IRF-7 activation. Specifically, detailed analyses of TBK-1 and IKKε enzymatic activation was performed using both *in vitro* and *in vivo* model systems.

Chapter V

Biochemical and genetic analysis of the IKK-related kinases

1. TBK-1 and IKKε are virus-activated kinases

Induction of the enzymatic activity of TBK-1 and IKKε in response to virus infection had not been directly demonstrated in previous experiments, so *in vitro* kinase assay experiments were performed to monitor the catalytic activity of IKK-related kinases in virus-infected cells. The BJAB B-lymphocyte cell line was chosen as a model to examine virus-inducible of the IKK-related activation, because lymphocytes express both TBK-1 and IKKε at the basal level(103,104). Similar to the IRF-7 expression pattern (289), constitutive IKKε expression is absent in non-lymphoid cells but is inducible by virus infection, dsRNA, LPS (108,109) and expression of the HTLV-I Tax protein (S. Sharma, data not shown), in part through an NF-κB-dependent mechanism (108,109).

1.1 The IKK-related kinase complex is responsive to virus infection

For analysis of IKK-related kinase activation in virus infected cells, BJAB B-lymphocytes were left untreated (Fig. 29, lane 1) or infected with VSV MOI 10 for 6h (Fig. 29, lane 2). WCE were immunoprecipitated with IKKε-specific antisera, and IKKε immunoprecipitates were subjected to standard a IKK *in vitro* kinase assay. As demonstrated in Figure 29, only IKKε immunoprecipitates isolated from VSV-infected cells phosphorylated peptide substrates corresponding to GST-IRF-3(aa380-427) and GST-IRF-7(aa468-503) (Fig. 29, first and second panels, lane 2) but not GST alone (S. Sharma, data not shown). Interestingly, western blot analysis of IKKε-immunoprecipitates revealed that *in vivo*, endogenous TBK-1 co-precipitated with endogenous IKKε in control and VSV-infected BJAB cells (Fig. 29, third panel, lanes 1 and 2). Furthermore, virus-inducibility of the kinase complex correlated with the appearance of hyperphosphorylated forms III and IV of IRF-3, as shown by one one-dimensional 7.5% SDS-PAGE and western blot analysis of WCE using anti-IRF-3 antisera (Fig. 29, panel four). These results demonstrate that the catalytic activity of the endogenous IKK-related complex, in which IKKε and TBK-1 stably associate as a heterodimer *in vivo*, is activated in response to virus infection. Furthermore, virus-

Figure 29. IKKε and TBK-1 form a virus activated kinase complex WCE (500 μg) from control (lane 1) or VSV infected (MOI 10, lane 2) BJAB B-lymphocytes were immunoprecipitated (IP) with anti-IKKε antisera. IKKε immunoprecipitates were incubated in kinase buffer with 10μCi [γ-^{32}P]-ATP for 30 minutes at 30°C, with peptide substrates corresponding to GST-IRF-3(aa380-427) (first panel) and GST-IRF-7(aa468-503) (second panel). Following resolution by 10% SDS-PAGE, the upper half of the gel was immunoblotted (IB) with antisera against IKKε and TBK-1 (third panel); the lower half of the gel was visualized by autoradiography (first and second panel, positions of phosphorylated GST-IRF-3, GST-IRF-7 and non-specific (NS) complexes are indicated). WCE (50 μg) were also resolved by 7.5% SDS-PAGE and immunoblotted with anti-IRF-3 antisera (panel four). Positions of forms I, II, III and IV of IRF-3 are indicated.

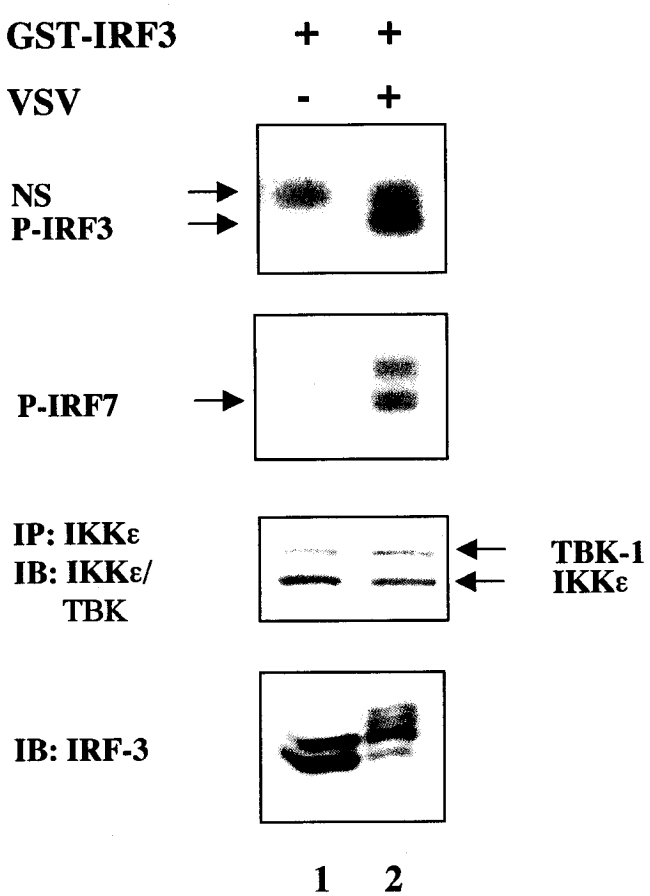
GST-IRF3 + +
VSV - +
NS
P-IRF3
P-IRF7
IP: IKKε
IB: IKKε/
TBK
TBK-1
IKKε
IB: IRF-3
1 2

inducible activation of the IKK-related complex correlates with the appearance *in vivo* of hyperphosphorylated and activated forms III and IV of IRF-3 in virus-infected cells.

1.2 Viral by-products dsRNA and RNP activate TBK1 and IKKε

Further experiments sought to examine the capacity of different molecular components of the virus life cycle to induce IRF-3 and IRF-7 signaling through the IKKε and TBK-1 pathway. Several studies have documented the role of viral dsRNA (393) and the Paramyxovirus N protein (415,422), a component of the genomic viral RNA:nucleocapsid complex (ribonucleoprotein or RNP), as virus-specific activator molecules of IRF-3 and IRF-7 signaling and the anti-viral state that ensues. In contrast to Paramyxoviruses such as MeV and SV, for Rhabdoviruses such as VSV, RNP formation cannot be mimicked *in vivo* by overexpression of the N protein alone (442). Consequently, in contrast to the Measles N protein, overexpression of VSV N protein alone fails to induce carboxy-terminal phosphorylation of IRF-3, presumably through lack of spontaneous RNP formation ((422) and B.R. tenOever, data not shown). However, isolation of intact RNP structures has been described through *de novo* purification from whole VSV virions (442), which provides an alternative method to evaluate whether VSV RNP represents a viral motif capable of IRF-3 and IRF-7 activation through induction of TBK-1 or IKKε kinase activity.

To compare IRF-3 activation by dsRNA and RNP treatment to a *de novo* VSV infection, lung epithelial A549 cells were infected with VSV MOI 10 or transfected with viral components dsRNA (polyI:polyC) or RNP complexes, and harvested 6h post treatment. WCE were analyzed by 7.5% SDS-PAGE followed by western blot with antisera specific to IRF-3, IRF-3 S396 phosphospecific, IRF-1 and ISG56 (Fig. 30A, first to fourth panels). Virus infection, as well as treatment with either dsRNA or VSV RNP induced IRF-3 carboxy-terminal phosphorylation, a result that was corroborated through the use of the S396 phosphospecific antibody (415) (Fig. 30A, first and second panels, lanes 2-4). IRF-3 activation by all three stimuli was associated with ISRE-dependent upregulation of interferon stimulated genes ISG56 and IRF-1 at the protein level (Fig. 30A, third and fourth panels, lanes 2-4); in fact, the levels of both IRF-1 and ISG56

Figure 30. VSV induced IRF activation is mimicked by dsRNA or RNP transfection (**A**) A549 cells were treated with vector, vector and VSV (MOI 10), dsRNA or RNP for 6h. WCE (50 μg) was analyzed by 7.5% SDS-PAGE and immunoblotted for IRF-3, IRF-3 S396, IRF-1, ISG56, VSV antisera, or actin as indicated. (**B**) Standard plaque assay of Vero cells treated with vector, VSV (1:100 000 dilution), or RNP (1:100 dilution), overlayed with 1% methylcellulose, and stained with 0.4% crystal violet 3 days post treatment. (**C**) WCE (5.0 μg) from (A) were used to analyze IRF-3 binding activity by EMSA using the ISRE of the ISG15 as an oligonucleotide probe. Arrows indicate positions of protein-DNA complexes.

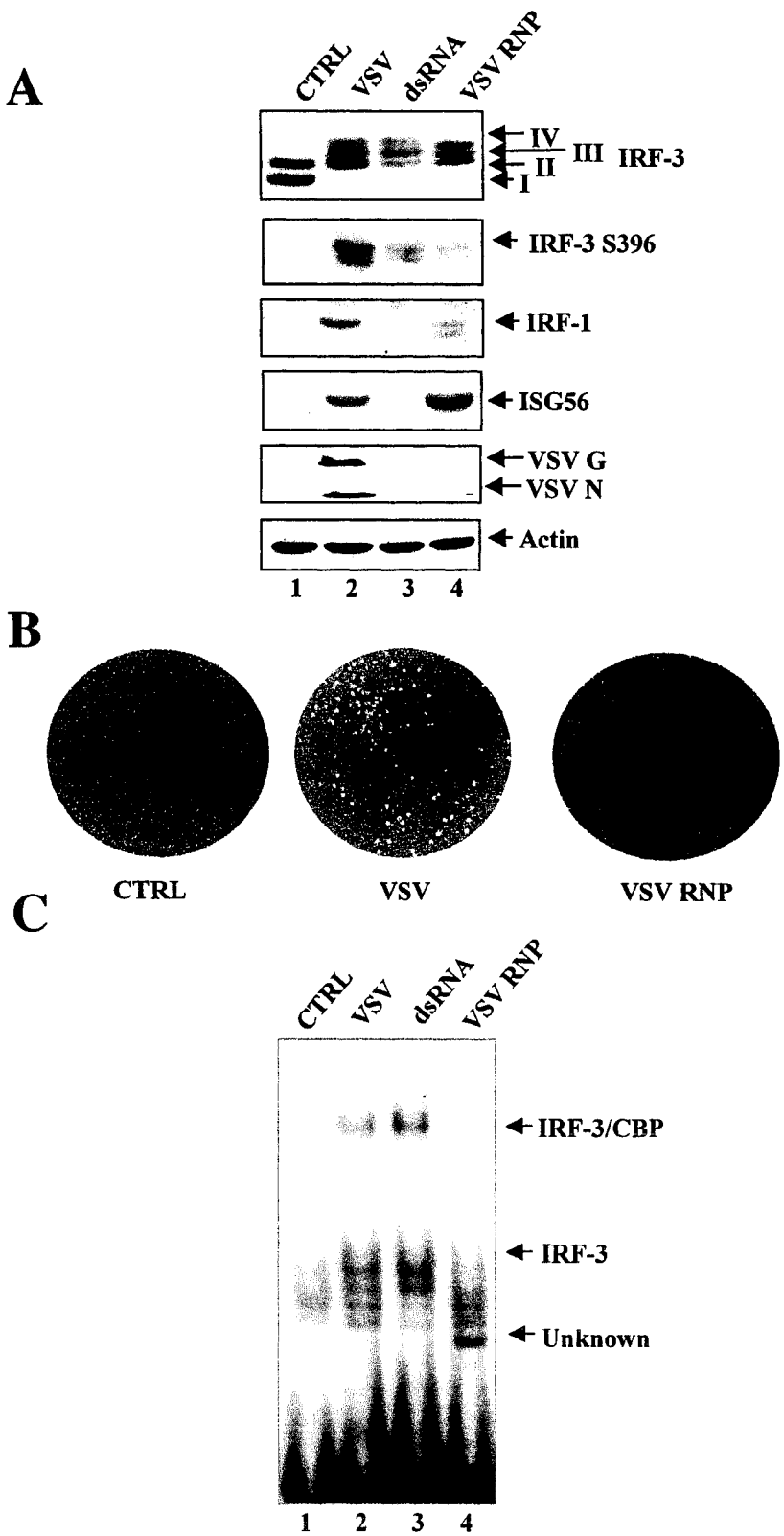
A
CTRL
VSV
dsRNA
VSV RNP
IV
III
II
I
IRF-3
IRF-3 S396
IRF-1
ISG56
VSV G
VSV N
Actin
1 2 3 4
B
CTRL
VSV
VSV RNP
C
CTRL
VSV
dsRNA
VSV RNP
IRF-3/CBP
IRF-3
Unknown
1 2 3 4

induced in response to VSV RNP were above those observed with either VSV infection or dsRNA treatment. To ensure that transfection of VSV RNP does not induce active VSV replication, WCE were western blotted with antisera directed against VSV. These results demonstrate that only *de novo* VSV infection induced expression of the transcription and translation machinery necessary for viral replication, and that purified VSV RNP complexes are transcriptionally inert.

Additionally, VSV RNP preparations were evaluated for infectivity using standard plaque assay, which confirms that in contrast to VSV virions, VSV RNP complexes do not induce plaque formation (Fig. 30B). To further compare VSV, dsRNA and RNP, WCE were analyzed in a DNA binding assay using the ISG15 ISRE (Fig. 30C). As expected, IRF-3 and IRF-3/CBP complexes are detectable in all three conditions (Fig. 30C, lanes 2-4). Curiously, RNP treatment induced the binding of an unknown DNA binding factor that could not be identified by supershift analysis with either IRF-1, IRF-3, IRF-7, or IRF-9 antibodies (B.R. tenOever, data not shown). Taken together, these data demonstrate that both dsRNA and RNP represent isolated viral components that stimulate innate anti-viral immune responses through activation of IRF-3 signaling.

To establish whether stimulation by dsRNA or VSV RNP induces IRF-3 phosphorylation through activation of the IKK-related complex, *in vitro* kinase assays were performed to analyze the catalytic activity of endogenous TBK-1 immunoprecipitates from A549 cells infected with VSV MOI 10 or treated with dsRNA or VSV-RNP for different time points (Fig. 31). Compared to LipofectAMINE 2000 transfection alone (Fig. 31, control, upper panel, lanes 1-6), all three stimuli induced TBK-1 kinase activity in A549 cells, as demonstrated by the specific phosphorylation of a GST-IRF-3(aa380-427) peptide substrate incubated with TBK-1 immunoprecipitates in the presence of [γ-^{32}P]-ATP (Fig. 31, upper panel, lanes 10-12, 13-18 and 22-24). The same experiment performed using GST and GST-IRF-3(5A) substrates did not show detectable phosphorylation by TBK-1 immunoprecipitates (S. Sharma, data not shown). Western blot analysis of TBK-1 immunoprecipitates demonstrated that comparable amounts of TBK-1 were immunoprecipitated in the relevant reactions (Fig. 31, middle panel). For all

Figure 31. VSV, dsRNA and RNP stimulate IRF-3 through TBK-1 activation WCE (150 μg) from lung epithelial A549 cells treated from 1-6h with vector alone (control, lanes 1-6), vector and VSV (VSV MOI 10, lanes 7-12), dsRNA (4.0 μg, polyI/polyC, lanes 13-18) or RNP (4.0 μg, VSV RNP, lanes 19-24) were immunoprecipitated (IP) with anti-TBK-1 antisera. Endogenous TBK-1 immunoprecipitates were incubated in kinase buffer in the presence of 10 μCi [γ-^{32}P]-ATP for 30 minutes at 30°C with a peptide substrate corresponding to GST-IRF-3(aa380-427). Following resolution by 10% SDS-PAGE, the lower half of the gel was visualized by autoradiography (first panel, position of phosphorylated GST-IRF-3 (aa380-427) is indicated). The upper half of the gel was transferred to nitrocellulose membrane and blotted (IB) with anti-TBK-1. WCE used for *in vitro* kinase assay (50 μg) were resolved by 7.5% SDS-PAGE and blotted with anti-IRF-3 (third panel). Positions of forms I, II, III and IV of IRF-3 are indicated.

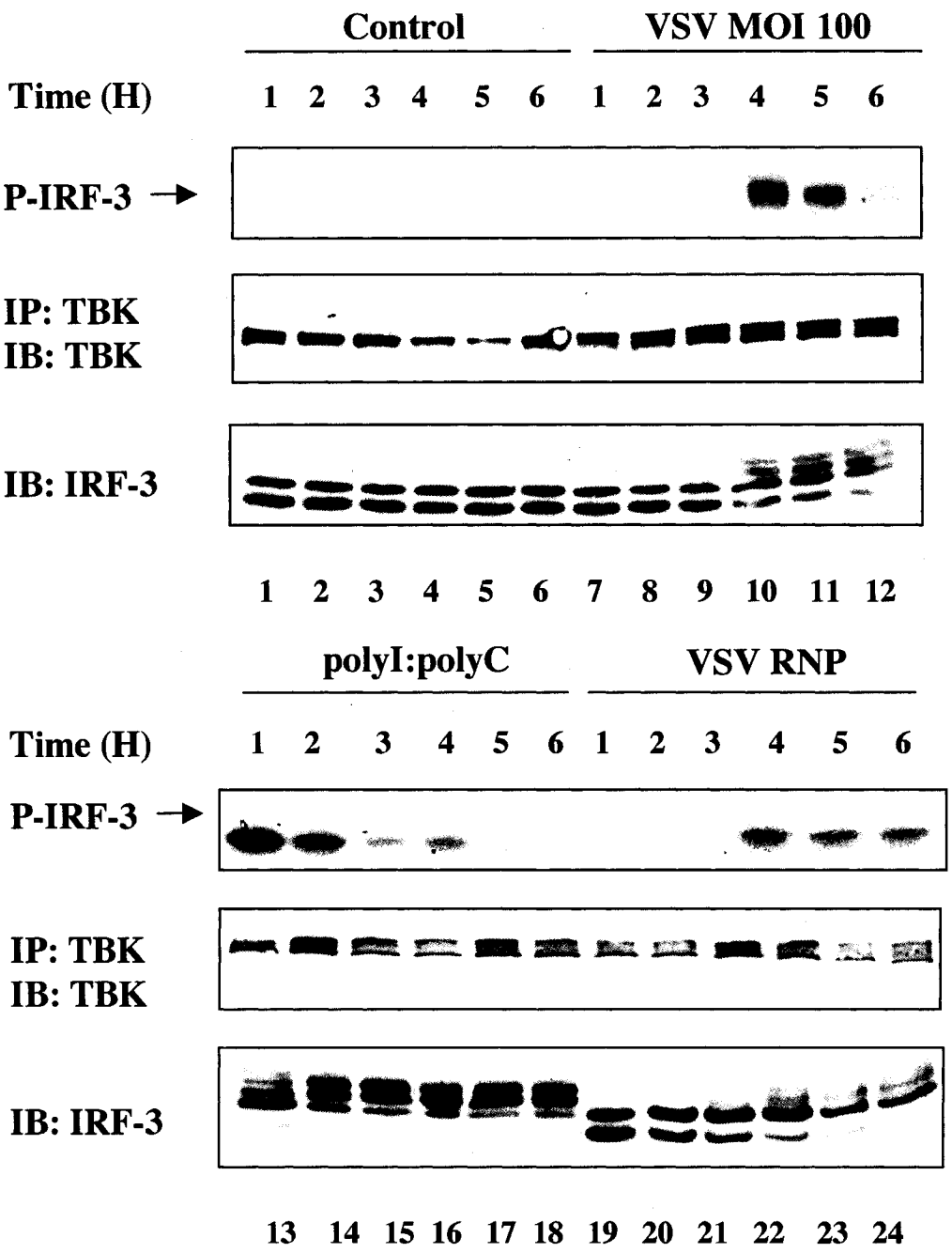
Control
VSV MOI 100
Time (H)
1 2 3 4 5 6 1 2 3 4 5 6
P-IRF-3
IP: TBK
IB: TBK
IB: IRF-3
1 2 3 4 5 6 7 8 9 10 11 12
polyI:polyC
VSV RNP
Time (H)
1 2 3 4 5 6 1 2 3 4 5 6
P-IRF-3
IP: TBK
IB: TBK
IB: IRF-3
13 14 15 16 17 18 19 20 21 22 23 24

three stimuli, induction of TBK-1 kinase activity *in vitro* correlated with the appearance of hyperphosphorylated forms III and IV of IRF-3 *in vivo*, as detected by one-dimensional 7.5% SDS-PAGE followed by western blot using antisera against IRF-3 (Fig. 31, lower panel).

There were notable differences with respect to the kinetics of TBK-1 activation; polyI/polyC treatment resulted in rapid induction of TBK-1 kinase activity, with phosphorylation of the GST-IRF-3 substrate detectable as early as 1h post dsRNA treatment (Fig. 31, upper panel, lane 13). However, VSV infection and VSV-RNP treatment activated TBK-1 at delayed kinetics, which was detectable by *in vitro* kinase assay at 4h post stimulation (Fig. 31, upper panel, lanes 10 and 22, respectively). Taken together, these results suggest that both dsRNA and RNP treatment alone are sufficient to mimic virus infection with respect to activation of IRF-3; furthermore, the significant difference in TBK-1 activation kinetics observed between the two different treatment suggests that dsRNA and RNP signaling represent two distinct pathways that converge upstream of IRF-3 and IRF-7 at the level of TBK-1 kinase activation.

2. Characterization of IRF phosphorylation by IKKε and TBK-1

2.1 Mapping IKK-related phosphoacceptor sites within IRF-3

In contrast to IKKε, TBK-1 produced by *in vitro* transcription and translation in a rabbit reticulocyte background was not enzymatically active (Fig. 22B, lane 10). To circumvent this problem, recombinant kinases were purified from SF9 insect cells infected with baculoviruses engineered to express either IKKε or TBK-1 fused to a His-epitope tag. To compare the catalytic activity of TBK-1 with IKKε, purified recombinant TBK-1 and IKKε were examined by *in vitro* kinase assay using a series of wild type and serine/threonine to alanine GST fusion proteins corresponding to the carboxy-terminal of IRF-3(aa380-427).

Figure 32A is a schematic representation of the IRF-3 carboxy-terminal, which contains several serine and threonine residues within the aa380-427 region that represent putative targets for the IKK-related kinases. Previous biochemical analysis has implicated seven

Figure 32. Mapping IKKε and TBK-1 phosphoacceptor sites within IRF-3 (**A**) Schematic representation of IRF-3. Positions of the DNA binding domain (DBD), nuclear localization sequence (NLS), nuclear export sequence (NES), Proline rich domain (Pro), IRF interaction domain (IAD) and regulatory domain (RD) are indicated. The RD(aa380-427) contains seven potential virus-inducible phosphoacceptor serine or threonine (S/T) residues organized into cluster I (aaS385/385) and cluster II (aaS396-S405). Nomenclature of WT (WT) and alanine (A) mutants of GST-IRF-3(aa380-427) substrates used in *in vitro* kinase assays are detailed. (**B**) Recombinant TBK-1 (0.5 μg, lanes 1-7) and IKKε (0.5 μg, lanes 8-14) purified from baculovirus-infected SF9 insect cells was incubated in kinase buffer in the presence of 10 μCi [γ-^{32}P]-ATP for 30 minutes at 30°C with WT and S/T to A mutants of GST-IRF-3(aa380-427) peptide substrates. Following resolution by 10% SDS-PAGE, the gel was stained visualized by autoradiography; positions of phosphorylated GST-IRF-3 are indicated.

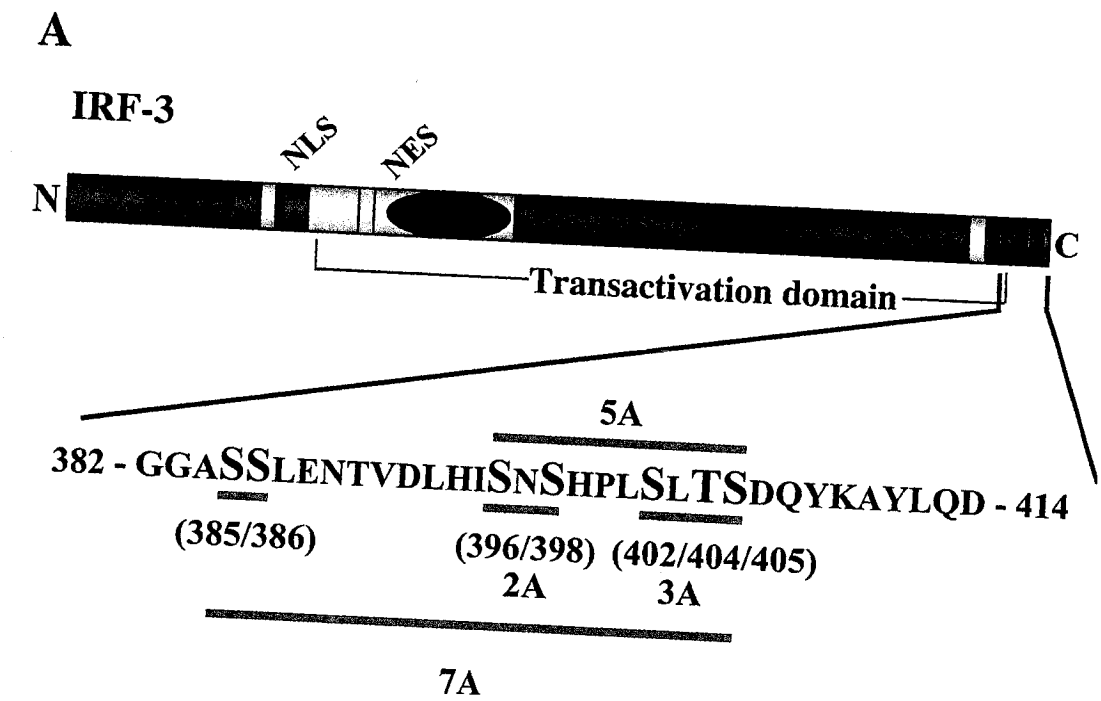
A
IRF-3
NLS
NES
N
C
Transactivation domain
5A
382 - GGASSLENTVDLHISNSHPLSLTSDQYKAYLQD - 414
(385/386)
(396/398)
2A
(402/404/405)
3A
7A

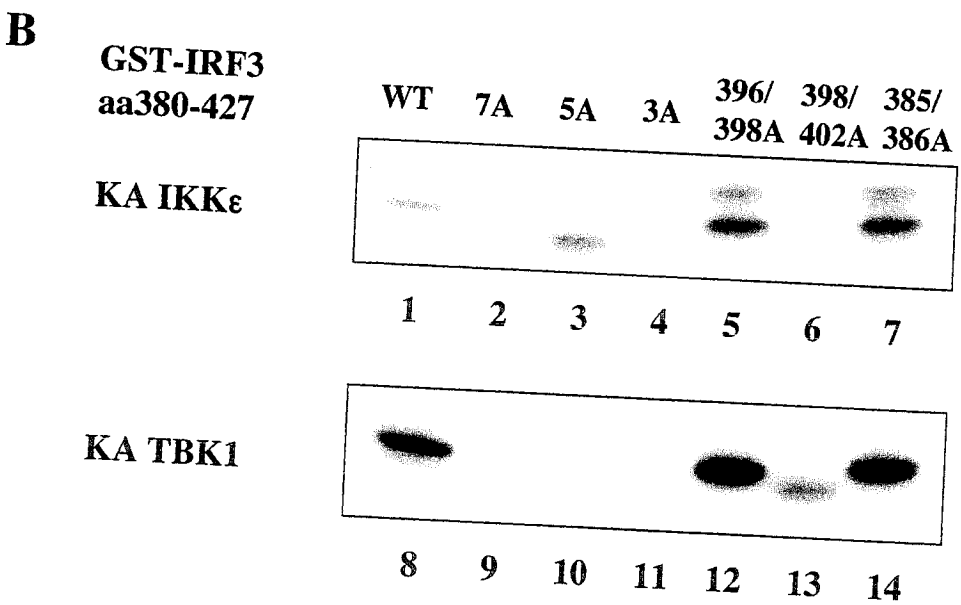
B
GST-IRF3
aa380-427
WT
7A
5A
3A
396/
398A
398/
402A
385/
386A
KA IKKε
1
2
3
4
5
6
7
KA TBK1
8
9
10
11
12
13
14

of these carboxy-terminal residues as phosphoacceptor sites important for activation of IRF-3 in response to virus infection (396,398,411,413-415); these seven residues are indicated in uppercase characters (Fig. 32A). The seven residues are grouped into two distinct clusters, a 2-residue 385/386 cluster I at the amino-terminal of the IRF-3 TD, and a 5-residue 396-405 cluster II at the carboxy-terminal of the TD (Fig. 32A).

To analyze which site(s) within the IRF-3 carboxy-terminal domain are directly targeted for phosphorylation by the IKK-related kinases, six different GST-IRF-3(aa380-427) peptide mutants were constructed using *in vitro* site-directed mutagenesis to introduce specific serine or threonine to alanine (S-T/A) mutations. The nomenclature used for these IRF-3 carboxy-terminal mutants is detailed in Figure 32A. Equal amounts of recombinant IKKε or TBK-1 purified from baculovirus-infected SF9 cells were used in a standard *in vitro* kinase assay using the wild type and six serine to alanine mutant GST-IRF-3(aa380-427) peptides for substrates (Fig. 32B). As demonstrated in Figure 32B, both TBK-1 and IKKε directly phosphorylated IRF-3 within the carboxy-terminal (Fig. 32B, lanes 1 and 8). In fact, GST-IRF-3(aa380-427) is a better substrate for TBK-1, as evidenced by an increased level of GST-IRF-3 phosphorylation induced by TBK-1 compared to IKKε (Fig. 32B, compare lanes 1 and 8).

Analysis of GST-IRF-3 S-T/A mutant peptides revealed that the IKK-related kinases exhibited an identical pattern with respect to direct IRF-3 carboxy-terminal phosphorylation (Fig. 32B, compare lanes 1-7 to 8-14). Mutation of the seven critical carboxy-terminal residues abolished direct IRF-3 phosphorylation by IKKε and TBK-1 (Fig. 32A, 7A, lanes 2 and 9), a result that confirms the specificity of the IKK-related kinases for the seven critical virus-responsive residues within the IRF-3 carboxy-terminal. Mutation of the 5-residue S-T carboxy-terminal cluster II residues to alanine diminished the majority of phosphorylation by IKKε and TBK-1 (Fig. 32B, 5A, lanes 3 and 10), indicating that the 396-405 cluster II residues, as opposed to the 385/386 cluster I residues, are the primary targets for direct IKKε and TBK-1 phosphorylation.

A specific mutation of S402A within the 5S/T cluster resulted in a loss of the majority of IRF-3 phosphorylation by TBK-1 and IKKε (Fig. 32B, 7A, 5A, 3A and 398/402A, lanes 4, 6, 10 and 12). The position of S402 as the second residue within a MAPK/IKK SXXXS aa recognition motif (Fig. 32A) is consistent with the target motif that has previously been documented for the IKK-related kinases for the amino-terminal domain of IκBα (103,104,110,468). Taken together, these results demonstrate that the IKK related kinases display an identical substrate specificity with respect to carboxy-terminal residues within IRF-3, although phosphorylation of GST-IRF-3(aa380-427) is more efficient by TBK-1. Both kinases primarily target the virus-responsive 5-residue cluster II sequence that lies between aa396-405. Furthermore, a mutation of S402A abolishes the majority of direct TBK-1 and IKKε phosphorylation within the IRF-3 carboxy-terminal, indicating that S402 serves as an important site for direct IKK-related IRF-3 carboxy-terminal phosphorylation.

2.2 Mapping IKK-related phosphoacceptor sites within IRF-7

The regulatory element within the carboxy-terminal of IRF-7 spanning aa468 to 491 contains numerous serine residues that represent potential phosphoacceptor sites that may be important for IRF-7 activation. Functional analyses of wild type and a series of serine to phosphomimetic glutamic acid (Fig. 33A and 33B) and serine to alanine (Fig. 33C) IRF-7 constructs were performed using IFNA4 promoter-driven luciferase activity as a measurement of IRF-7 transactivation capacity.

Figure 33 demonstrates differential induction of the IFNA4 promoter in response to phosphomimetic serine to glutamic acid mutants (S/D) of IRF-7 expressed alone (Fig. 33A) or in response to SV infection (Fig. 33B). Expression of wild type IRF-7 did not significantly transactivate the IFNA4 promoter construct in the absence of virus infection (Fig. 33A, IRF-7 wt). However, substitution of 4 serines present within the IRF-7 aa475-479 carboxy-terminal cluster with phosphomimetic glutamic acid residues generated a constitutively active form of IRF-7 that transactivated IFNA4 approximately 800-fold in the absence of stimulation (Fig. 33A, D475-479). Likewise, partial phosphomimetic substitutions within the 475-479 cluster generated active forms of IRF-7 (Fig. 33, top

Figure 33. Functional analysis of IRF-7 phosphomimetic mutants ATCC293 cells were transfected by the calcium phosphate co-precipitation method with pRLTK *renilla* luciferase reporter plasmid (20 ηg), luciferase reporter plasmid containing the IFNA4 promoter (0.1 μg) and either control or wild type (WT) and a series of serine to aspartic acid (D) mutants (**A**) and (**B**), or a series of serine to alanine (A) (**C**) IRF-7 expression plasmids. 8h post-transfection, cells were left untreated (**A**) or infected with SV at 40 HAU/ml (**B**) and (**C**). Luciferase activity was analyzed 24h post-transfection as fold induction relative to the basal level of reporter gene in the presence of control vector after normalization with co-transfected *renilla* relative light units. Values represent the average of 3 independent experiments, performed in duplicate with variability shown by error bars.

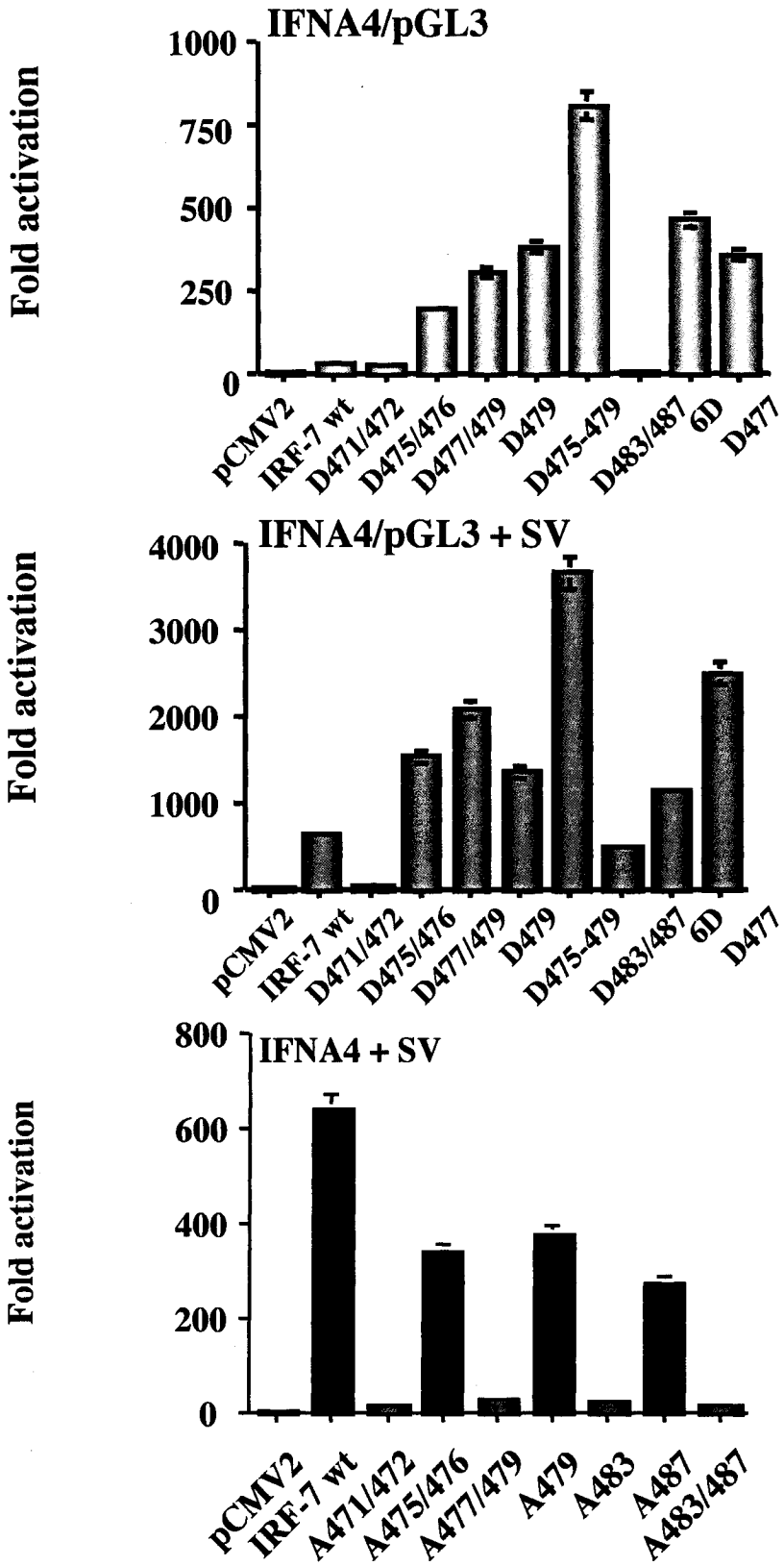
IFNA4/pGL3
Fold activation
1000
750
500
250
0
pCMV2
IRF-7 wt
D471/472
D475/476
D477/479
D479
D475-479
D483/487
6D
D477
IFNA4/pGL3 + SV
Fold activation
4000
3000
2000
1000
0
pCMV2
IRF-7 wt
D471/472
D475/476
D477/479
D479
D475-479
D483/487
6D
D477
IFNA4 + SV
Fold activation
800
600
400
200
0
pCMV2
IRF-7 wt
A471/472
A475/476
A477/479
A479
A483
A487
A483/487

panel, D475-476, D477/79, D479, 6D, and D477); however, in the absence of stimulation, no partial mutant was as active as D475-479 IRF-7.

As expected, SV infection augmented relative fold induction of the IFNA4 promoter in response to IRF-7 expression (Fig. 33, IRf-7 wt, compare fold induction in A and B panels). In a virus-infected background, S/D mutation of the 475-479 cluster also generated the most potent transactivator (Fig. 33, middle panel, D475-479). Although partial substitutions within this cluster were not as efficient as the full substitution with respect to IFNA4 transactivation, (Fig. 33B, D475-476, D477/79, D479, 6D, and D477), specific substitutions at positions 477 or 479 precipitated higher transactivation potential than substitutions at 475/476 in the presence of SV infection (Fig. 33B, compare D477/479 and D477 with D475/476). Virus infection activated wild type IRF-7 and as well as the S483/487D mutant to similar levels (Fig. 33B, IRF-7 wt and D483/487). Interestingly, mutation of S471/472D generated a catalytically inactive form of IRF-7 that was unresponsive to SV infection (Fig. 33B, D471/472). This result is reminiscent to similar data obtained with S385/386D mutants of IRF-3, which are also catalytically inactive (414).

Next, the transactivation capacity of IRF-7 constructs containing serine to alanine (S/A) mutations within the carboxy-terminal domain was analyzed using IFNA4 promoter luciferase (Fig. 33C). Although all S/A substitutions tested by this method displayed a decreased transactivation capacity compared to wild type IRF-7, S/A mutation of three distinct clusters within the IRF-7 carboxy-terminal completely abolished SV-induced activation of the IFNA4 promoter by IRF-7 (Fig. 33C, A471/472, A477/479 and A483/487), indicating that serine clusters 471/472, 477/489 and 483/487 are essential for activation of latent IRF-7 by virus infection.

To determine which IRF-7 carboxy-terminal residues are directly targeted by purified IKK-related kinases, peptide substrates corresponding to wild type and eight serine to alanine mutants of GST-IRF-7(aa468-503) were analyzed by *in vitro* kinase assay (Fig. 34). Organization of the IRF-7 carboxy-terminal is represented in Figure 34A, with a

description of the wild type and serine to alanine (S/A) mutant GST fusion peptides. As demonstrated in Figure 34B, GST-IRF-7(aa468-503) is phosphorylated to a higher degree by TBK-1 compared to IKKε (Fig. 34B, compare lanes 1 and 8); moreover, both kinases exhibit an identical specificity with respect to direct IRF-7 carboxy-terminal phosphorylation (Fig. 34B, compare lanes 1-9 to lanes 10-18). Mutation of 6 residues within the aa475-487 domain abolished TBK-1 and IKKε-mediated phosphorylation of IRF-7 (Fig. 34B, lanes 2 and 11). Similarly, a S477/479A mutation decreased the majority of direct IRF-7 phosphorylation by IKKε and TBK-1 (Fig. 34B, lanes 5 and 10), while a mutation of S479A reduced phosphorylation by approximately 50%. Based on these results, it can be concluded that the S477/479 cluster within the carboxy-terminal domain of IRF-7 is the primary candidate for phosphorylation by IKKε and TBK-1. These results are in accordance with luciferase analysis of IRF-7 mutants, which indicate that phosphorylation at the 477/479 cluster is associated with increased IRF-7 transcriptional activity in response to virus infection. The position of S479 within the IRF-7 carboxy-terminal is consistent with the SXXXS consensus motif; however, S479A mutation does not completely abolish direct phosphorylation of TBK-1 and IKKε, presumably due to phosphorylation at S477.

3. Analysis of TBK-1 knockout cells

Mice deficient for TBK-1 expression have been generated, but initial studies focused on characterization of the phenotype with respect to NF-κB signaling (106). Following characterization of TBK-1 as a component of the VAK complex responsible for virus-inducible activation of IRF-3 and IRF-7 (470,471), it was of interest to examine the phenotype of MEFs derived from TBK-1 deficient mice with respect to virus-inducible IRF activation and signaling in response to virus infection.

3.1 IKKε functionally compensates for lack of TBK-1 expression

To ascertain whether IRF-3 activation was decreased or impaired in the absence of TBK-1 expression, control TBK-1+/+ or KO TBK-1-/- MEFs (106) were infected with VSV MOI 10 or transfected with dsRNA, and harvested 0, 3, 6, and 9h post-induction.

Figure 34. Mapping IKKε and TBK-1 phosphoacceptor sites within IRF-7 (A) Schematic representation of IRF-7. Positions of the DNA binding domain (DBD), constitutive activation domain (CAD), virus activation domain (VAD), regulatory domain (RD) and nuclear export signal (NES) are indicated. The RD(aa461-491) contains nine potential virus-inducible phosphoacceptor serine (S) residues organized into cluster I (aaS471/S472) and cluster II (aaS475-S477) and cluster III (aaS483-S87). Nomenclature for serine to alanine (A) GST-IRF-7(aa468-503) peptide substrate used in *in vitro* kinase assay is detailed. **(B)** Recombinant TBK-1 (0.5 μg, lanes 1-9) and IKKε (0.5 μg, lanes 10-17) extracts purified from baculovirus-infected SF9 insect cells was incubated in kinase buffer with 10 μCi [γ-^{32}P]-ATP for 30 minutes at 30°C with peptide substrates corresponding to WT and S/A mutants of GST-IRF-7(aa468-503). Following resolution by 10% SDS-PAGE, the gel was visualized by autoradiography; positions of phosphorylated GST-IRF-7 are indicated.

A

IRF-7

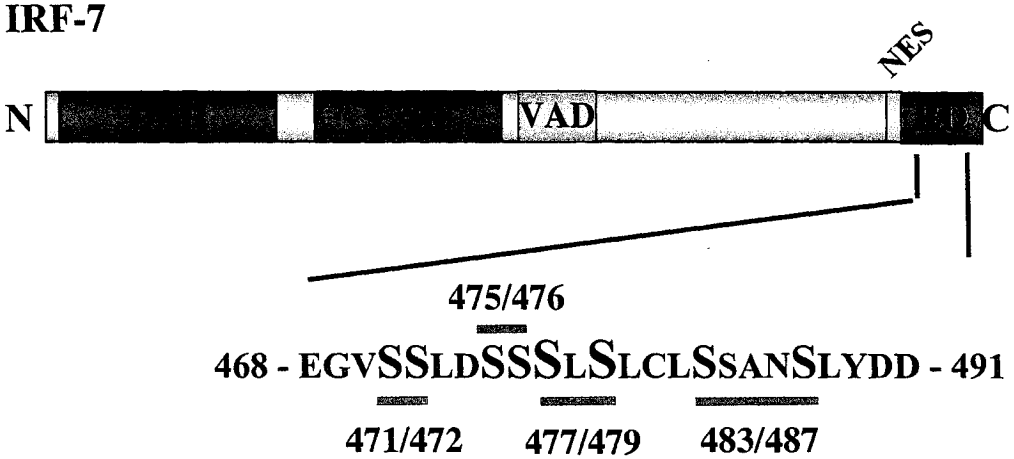
NES
N
VAD
C
475/476
468 - EGVSSLDSSSLSLCLSSANSLYDD - 491
471/472
477/479
483/487

B

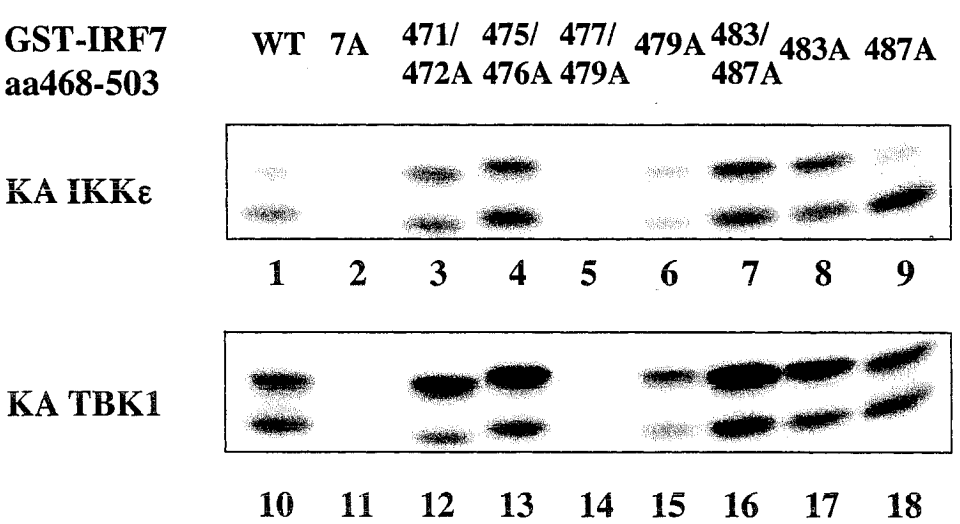
GST-IRF7
aa468-503
WT
7A
471/ 472A
475/ 476A
477/ 479A
479A
483/ 487A
483A
487A
KA IKKε
1 2 3 4 5 6 7 8 9
KA TBK1
10 11 12 13 14 15 16 17 18

Western blot analysis of WCE derived from control TBK-1+/+ MEFs (Fig. 35A, middle panel) demonstrated that IRF-3 carboxy-terminal phosphorylation occurred within 6h of VSV infection and within 3h of dsRNA treatment (Fig. 35A, upper panel, lanes 3 and 6). Interestingly, TBK-1-/- MEFs with infected with VSV or treated with dsRNA also demonstrated intact IRF-3 carboxy-terminal phosphorylation, with a kinetics that was delayed compared to wild type cells (Fig. 35B, upper panel, compare to Fig. 35A, upper panel). Western blot was performed to analyze the expression of IKKε at the protein level in TBK-1+/+ and TBK-1-/- MEFs, which demonstrated that IKKε was expressed at the protein level in these cells, and inducible in response to VSV infection and dsRNA treatment (Fig. 35A and B, bottom panels).

To determine if deficiency of TBK-1 affects IRF-dependent gene transcription, the transactivation potential of IRF-3 was analyzed in control and TBK-1-/- MEFs in response to virus infection or dsRNA treatment using a luciferase reporter construct corresponding to the ISRE-driven RANTES promoter that is specifically mutated in the NF-κB-responsive sites (κBm RANTES, Figure 35C) (403). However, κBm RANTES luciferase activity was below the detection limit in both TBK-1+/+ and TBK-1-/- MEFs in response to dsRNA treatment, which yielded values too low to be statistically analyzed following standardization with a control *renilla* reading (R. Lin, data not shown). However, stimulation with VSV at a low MOI (MOI 0.1) induced greater than 9 fold response over basal activity of the κBm RANTES promoter in TBK-1+/+ MEFs, whereas TBK-1-/- MEFs demonstrated decreased promoter activity to below 4 fold (Fig. 35C). These results suggest that loss of TBK-1 expression decreases the transcriptional activity of IRF-3 following virus infection. However, the response is not completely lost, a result that is in accordance with the delay observed for IRF-3 phosphorylation detected by western blot analysis.

To evaluate IRF-7-dependent transcription, the IFNA4 luciferase reporter construct was transfected in the absence and presence of IRF-7 into wild type and TBK-1-/- MEFs, then infected with VSV (MOI 0.1) or treated with dsRNA for 16 hours (Fig. 35D). VSV infection and dsRNA treatment increased the luciferase activity of the IFNA4

Figure 35. TBK-1-/- MEFs demonstrate functional compensation by IKKε expression (**A**) C57/BL WT MEFs were treated with VSV (MOI 10) or dsRNA (4.0 μg) for 0, 3, 6, and 9h. WCE (55 μg) was resolved by 7.5% SDS-PAGE and immunoblotted with murine IRF-3, TBK-1 and IKKε antisera. (**B**) C57/BL MEFs disrupted in TBK-1 gene expression were analyzed as (**A**). (**C**) C57/BL TBK-1+/+ and TBK-1-/- were transfected with a pRLTK *renilla* luciferase normalizing plasmid (20 ηg) and a luciferase reporter plasmid encoding the κBm RANTES or IFNA4 promoter (0.1 μg) with IRF-7 (0.2 μg). 16h post-transfection, cells were left unstimulated or treated with VSV (MOI 0.1) or dsRNA (1.0 μg) for 16h. Luciferase activities for all of the above were expressed as fold activation relative to the basal level of the promoter in the presence of control vector after normalization to co-transfected *renilla* luciferase; values represent the average of 2 experiments, performed in duplicate.

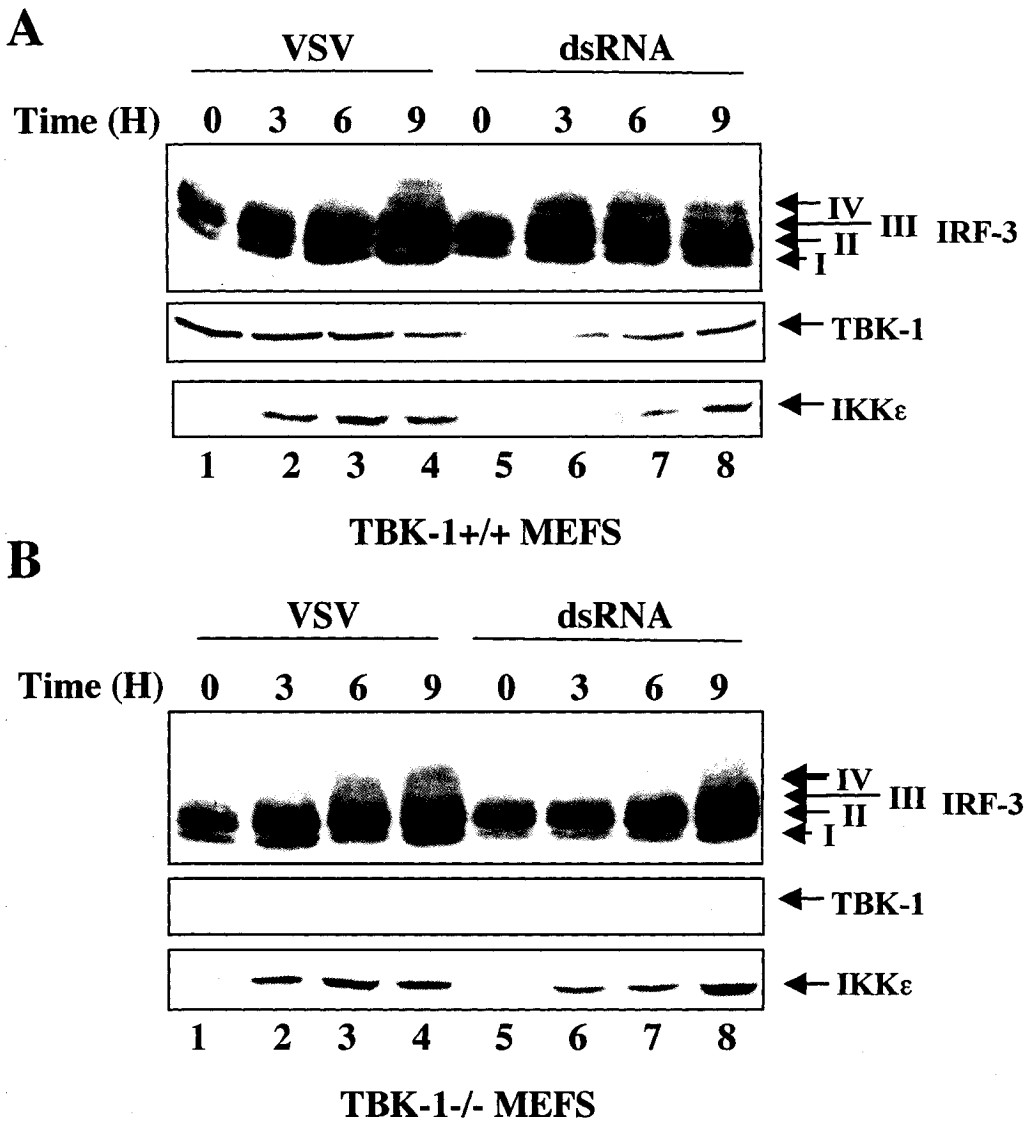
A
VSV
dsRNA
Time (H) 0 3 6 9 0 3 6 9
IV
III
II
I
IRF-3
TBK-1
IKKε
1 2 3 4 5 6 7 8
TBK-1+/+ MEFS
B
VSV
dsRNA
Time (H) 0 3 6 9 0 3 6 9
IV
III
II
I
IRF-3
TBK-1
IKKε
1 2 3 4 5 6 7 8
TBK-1-/- MEFS

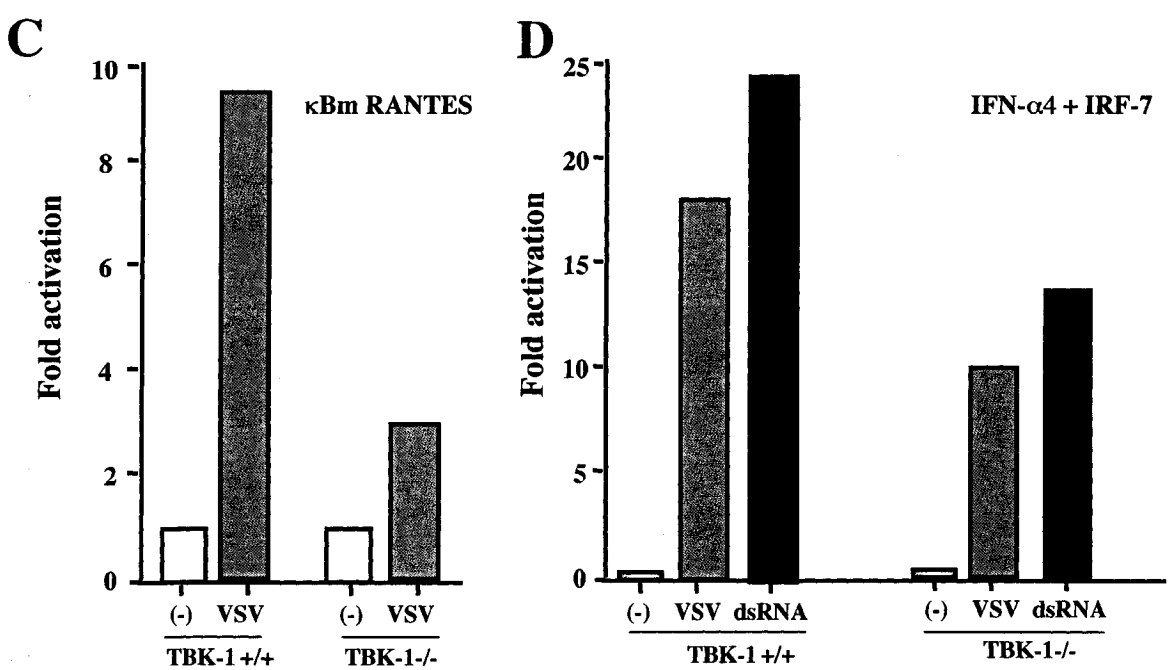
C
κBm RANTES
Fold activation
10
8
6
4
2
0
(-) VSV
TBK-1 +/+
(-) VSV
TBK-1-/-
D
IFN-α4 + IRF-7
Fold activation
25
20
15
10
5
0
(-) VSV dsRNA
TBK-1 +/+
(-) VSV dsRNA
TBK-1-/-

promoter 18- and 24- fold, respectively. The same experiment performed in TBK-1-/- MEFs demonstrated that the transcriptional response of the IFNA4 promoter to VSV infection and dsRNA treatment was diminished compared to control MEFs, to levels of 11 and 13 fold induction, respectively. Taken together, these data suggest that TBK-1 expression is required for full induction of both IRF-3 and IRF-7 transcriptional activity in response to physiological inducers such as virus infection and dsRNA treatment. However, the residual activation of IRF-3 and IRF-7 in the absence of TBK-1 is likely the result of compensation by expression of IKKε in TBK-/- MEFs, which demonstrates identical substrate specificity for the carboxy-termini of both IRF-3 (Fig. 32B) and IRF-7 (Fig. 34B) to TBK-1 *in vitro*, and is transcriptionally induced in response to viral infection and dsRNA treatment (Fig. 35A and 35B).

Chapter VI

Discussion

Chapter VI

Discussion

1. FKBP52 modulates IRF-4 activity by a functional interaction

Human IRF-4 was originally isolated, in part, from HTLV-I-infected ATL cell lines (436). The high levels of constitutive IRF-4 protein expression in HTLV-1 infected ATL cells are exceptional, as T-lymphocytes normally express IRF-4 in an inducible and transient manner in response to antigenic stimulation (432,434,436,449,450). To examine IRF-4 regulation in HTLV-I infected T-cells, initial studies characterized a novel interaction between IRF-4 and the immunophilin FKBP52 (444). Co-immunoprecipitation studies delineated that the proline rich region of IRF-4 (aa150-237) and the carboxy-terminal tetratricopeptide repeats of FKBP52 are the minimal domains required for the interaction. Furthermore, the association of FKBP52 with IRF-4 inhibited IRF-4-PU.1 binding to the IgLλ enhancer Eλ2-4 and IRF-4 interaction with the ISRE element from the ISG15 promoter *in vitro*, which resulted in an inhibition of IRF-4 transactivation capacity (444). Inhibition of IRF-4 DNA binding required functional FKBP52 PPIase activity, since the PPIase inhibitor ascomycin restored IRF-4 binding in the presence of FKBP52. Based on these observations, we conclude that the functional FKBP52/IRF-4 interaction alters the conformation of IRF-4 by *cis-trans* isomerization of proline residues within the IRF-4 proline rich domain. This modification appears to convert IRF-4 from a DNA binding configuration that activates IRF-4-driven gene expression, to a closed conformation that no longer interacts with enhancer DNA. Ascomycin relieves the inhibition catalyzed by FKBP52, by abrogating the PPIase activity of the immunophilin (444).

Previous structural analysis using deletion mutants of murine IRF-4 revealed the presence of a carboxy-terminal segment (aa410-450) that is important for autoinhibition of ternary complex formation with PU.1 and DNA (433). Consistent with these observations, in transfected COS-7 cells the IRF-4-FKBP52 interaction was only detected upon removal of this carboxy-terminal autoinhibition domain. The conformation of full length IRF-4 may be inaccessible to FKBP52 because of structural constraints imposed by the carboxy-terminal autoinhibition element, which folds back on the amino-terminal DBD.

However, in contrast to transfected COS-7 cells, the IRF-4 interaction with FKBP52 was readily detectable *in vivo* in all human B-cells and HTLV-I infected T-cells expressing IRF-4. These results suggest that the conformation of IRF-4, hence the interaction with FKBP52, may be differentially regulated in lymphoid versus non-lymphoid cells: in contrast to COS-7 cells, in B-cells and HTLV-I infected T-cells, IRF-4 appears to exist in an open conformation capable of interaction with FKBP52.

Several physiological roles have been ascribed to immunophilins, including binding and sequestration of calcineurin, protein folding and assembly, protein trafficking as well as direct regulation of protein activity (455,472). The PPIase activity of FKBP52 is essential for inhibition of IRF-4 DNA binding, because inhibition of FKBP52 PPIase activity by ascomycin abolished the negative effects of the immunophilin on IRF-4 function (444). *Cis* prolines are important to protein structural integrity by introducing bends within proteins. During protein synthesis, the peptide bonds on the amino side of proline residues are found in the open *trans* conformation. When the three-dimensional structure was determined, 15% of these bonds were in the alternate *cis*-conformation (455,472). Enzymes with PPIase activity such as FKBP52 catalyze the *cis-trans* inter-conversion, a modification that would otherwise occur slowly. Immunophilins target specific proline residues preceded by a bulky hydrophobic residue for *cis-trans* isomerization (473). Within IRF-4, several clustered prolines preceded by hydrophobic residues within the proline rich domain are available for peptidyl-prolyl isomerization by FKBP52 (Fig. 36A). In the model illustrated in Figure 36B, we propose that FKBP52 can act as a chaperone that escorts IRF-4 into the nucleus. During transport or once in the nucleus, FKBP52 would alter IRF-4 conformation through proline isomerization, thereby sequestering IRF-4. The interaction with the proper transcriptional partner such as PU.1 would alleviate this inhibitory effect and permit DNA binding and transcriptional modulation of target genes.

Another member of the immunophilin family, the human cyclophilin Cyp-40, was shown to regulate the transcriptional activity of the c-Myb transcription factor by interfering with the capacity of c-Myb to bind DNA (474). Interestingly, the oncogenic form of v-

Figure 36. A functional interaction with FKBP52 regulates IRF-4 activity (**A**) PPIase activity of FKBP52 catalyzes *cis-trans* isomerization of specific proline residues. Peptide bonds on the amino side of proline residues are mainly found in *trans* at equilibrium; introduction of the *cis* conformation catalyzed by PPIase activity. Amino acids preceeding A_{-1} and following the proline residue A_{-2} are linked to polypeptide chains (adapted from). Residues within the IRF-4 proline rich domain (aa150-237) that may serve as targets for FKBP52 PPIase activity. (**B**) Model describing potential functions of FKBP52 in nuclear transport/chaperone function, *cis-trans* isomerization and regulation of IRF-4 function, including DNA binding and transcriptional potential. DBD, DNA binding domain; IAD, IRF association domain; Pro, proline rich region; diamond, tetratricopeptide repeats.

A

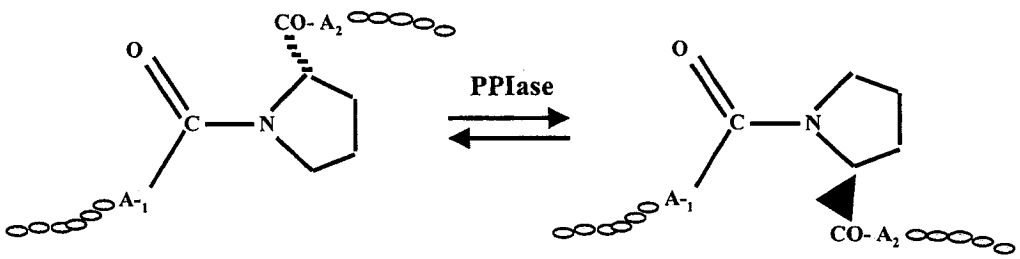

trans proline

cis proline

150 PYPMT<u>AP</u>YGS<u>LP</u>AQQVHNYM<u>MP</u>PHDRSWR
DY<u>AP</u>DQSHPE<u>IP</u>YQ<u>CP</u>VTFGPRGHHWQGPS
CENGCQVTGTFYAC<u>AP</u>PESQ<u>AP</u>G<u>IP</u>IEPSIRS 237

B

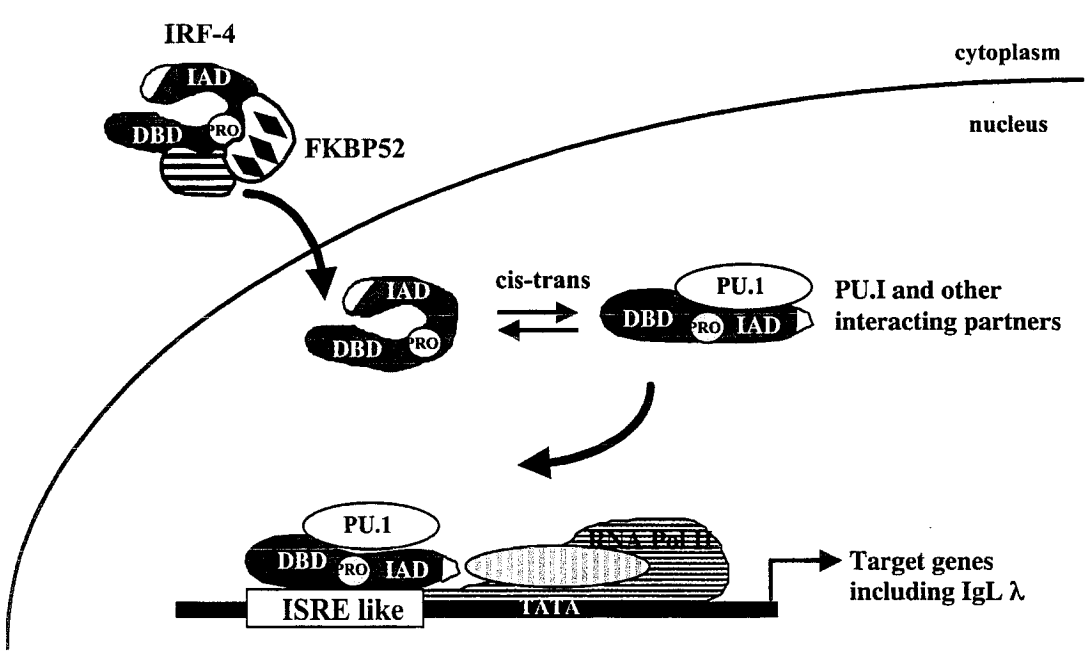

Myb evaded this inhibition of DNA binding (475). Point mutations and deletions in v-Myb that contributed to oncogenic potential also abrogated the cyclophilin-mediated inhibition of DNA binding of v-Myb. By analogy with c-Myb and Cyp-40, IRF-4 interacts with the immunophilin FKBP52, which inhibits its DNA binding activity and transactivation potential in a PPIase-dependent fashion. IRF-4 has shown to be a dichotomous regulator, as it specifically stimulates transcription in conjunction with PU.1 but represses ISRE-driven transcription in the absence of PU.1 (433,436). Thus, during lymphocyte activation and differentiation, IRF-4 appears to function both as an activator to promote B cell-specific gene expression and as a repressor to inhibit the antiproliferative effects of type I IFN in B- and T- cells. As an endogenous FKBP52-IRF-4 interaction is detectable in HTLV-I-transformed T-cells, it would be interesting to examine the functional consequences of the interaction with respect to T-cell-specific IRF-4 target gene expression in HTLV-I infected cells.

2. Regulation of IRF-4 expression in HTLV-I transformed T-cells

Detailed analysis was performed to elucidate the mechanisms that govern human IRF-4 promoter activation in T-cells infected and transformed with HTLV-I (450). These experiments demonstrate that HTLV-I Tax-driven IRF-4 gene expression is achieved through recruitment of transcriptional activators to three sites within the -617 to -209 region of the human IRF-4 promoter, specifically the κB1, Sp1 and CD28RE enhancer elements. Furthermore, the κB1 and CD28RE sites are essential for Tax-mediated transactivation of the human IRF-4 promoter in T-cells.

Gene knockout analysis has underscored the essential role of classical NF-κB activation in regulation of the IRF-4 gene. There is a marked phenotypic similarity between mice deficient in expression of c-Rel (27) and IRF-4 (437) with respect to specific defects in the adaptive immune response. The IRF-4 gene is essential for the function and homeostasis of mature B- and T-lymphocytes in the periphery (437). Specifically, the lymphocyte population was severely impaired at the level of late stage activation events downstream of TCR engagement. IRF-4-/- T-lymphocytes exhibited reduced proliferation and cytokine production in response to activators such as anti-CD3

stimulation, conA or bacterial superantigen staphylococcal enterotoxin A (SEA) treatment. Although levels of secreted IL-2 were slightly impaired in activated IRF-4-/- T-cells, proliferation and growth factor secretion could not be restored by exogenous IL-2 treatment, which suggests that IRF-4 may be involved in the integration of the IL-2 signaling response (437). Similarly, mice deficient for c-Rel expression display defects in development of appropriate adaptive immunity, because mature B- and T-cells in the periphery were unresponsive to mitogenic stimuli (27). Further analyses of lymphocytes derived from c-Rel-deficient mice indicated that expression of c-Rel was essential for IRF-4 production in primary B- and T-lymphocytes (476), as induction of IRF-4 was completely abolished in c-Rel-/- T-lymphocytes in response to CD3/CD28 cross-linking or PMA treatment. A direct role for c-Rel in transcription of the IRF-4 gene is attributed to the presence of two functional c-Rel binding sites within the murine IRF-4 promoter (476). Our data extend these studies to the human model by establishing the essential role of classical NF-κB signaling for activation of the human IRF-4 promoter in HTLV-I-infected, leukemic ATL cells. Tax-mediated activation of the classical IKK complex in HTLV-I transformed cells correlates with constitutive *in vivo* occupancy at the κB1 site of the IRF-4 promoter, which is not occupied in control, unstimulated T-cells. Furthermore, abrogation of IRF-4 promoter activity in response to Tax M22 expression or mutation of the κB1 site indicates that NF-κB-driven transcription is absolutely required for Tax-mediated IRF-4 gene induction in HTLV-I infected T-lymphocytes.

Recent identification and characterization of the non-canonical NF-κB pathway raises some interesting questions with respect to IRF-4 promoter activation by the Tax oncoprotein. Constitutive processing of the NF-κB2 precursor p100 to p52 is characteristic of HTLV-I infected T-cells (268). It has been demonstrated that the non-canonical NF-κB pathway is constitutively active in HTLV-I infected cells, through a NIK and IKKα-dependent processing of p100 that promotes continuous production of mature p52 (195,196,268). This event is directly promoted by Tax, which physically recruits IKKα to p100 and thereby triggers the phosphorylation-dependent ubiquitination and processing of p100 (268). A role for non-canonical NF-κB signaling in activation of the IRF-4 promoter is underscored by the results obtained with co-transfection of NIK

with the IRF-4 promoter luciferase reporter construct in Jurkat T-cells; NIK overexpression, a potent activator of the non-canonical NF-κB pathway (195), transactivated the HTLV-I-responsive -600 to -200 region of the IRF-4 promoter. Although *in vitro* EMSA analysis using antibodies specific to p52 and RelB did not detect binding of this complex to κB1 or CD28RE in cell extracts derived from HTLV-I transformed cells (S. Sharma, data not shown), further experiments analyzing p52/RelB binding to the IRF-4 promoter should be performed using *in vivo* systems. For example, detailed analysis of NF-κB signaling in maturing DC show that rapidly activated dimers of p65/p50 or c-Rel/p50 are gradually replaced by slowly activated dimers of p52/RelB on a subset of NF-κB promoters, as detected by *in vivo* chIP analyses (9). Since different NF-κB dimers possess different transcriptional capacities at each given promoter, this type of dimer exchange allows for fine-tuning of the NF-κB-driven transcriptional response over time. Furthermore, the insensitivity of p52/RelB to the IκB inhibitors ensures that dimer exchange contributes to sustained activation of selected NF-κB target genes in spite of NF-κB-driven resynthesis of IκBα (9). These studies emphasize the fact that regulation of a given NF-κB target gene cannot be accounted for by virtue of *in vitro* binding studies alone; rather, the context of the natural promoter rather than the isolated κB1 site itself is the major determinant for NF-κB subunit specificity (9). This observation is significant for interpretation of *in vitro* EMSA studies using the κB1 site of the IRF-4 promoter, which represents a canonical NF-κB consensus site that binds both c-Rel and p65 when in isolation *in vitro*. Analyses of hematopoietic cells derived from c-Rel deficient mice have underscored the fact that despite the ability of p65 to efficiently bind c-Rel enhancer elements *in vitro*, specific deficiencies in transcription of endogenous c-Rel-dependent genes, including IRF-4 itself (476), are not compensated by nuclear p65 complexes *in vivo* (27-29).

The CD28RE site of the IRF-4 promoter is a complex and diverse regulatory element; our results which characterize the IRF-4 CD28RE as a Tax-responsive enhancer constitutively occupied in HTLV-I-transformed T-cells *in vivo* are consistent with previous studies examining HTLV-I-associated occupancy of the IL-2 CD28RE (287).

The CD28RE is essential for IL-2 production in response to CD3/CD28 stimulation, and functions as a Tax-responsive element for HTLV-I-induced IL-2 upregulation during early stages of virus infection (287). A variety of distinct transcriptional regulatory proteins have been reported to bind CD28RE; in the present study, the IRF-4 CD28RE interacted with c-Rel and p50, as demonstrated through EMSA analysis and *in vivo* chromatin immunoprecipitation (chIP) in HTLV-I infected MT2 cells. Furthermore, we have correlated constitutive NF-AT DNA binding activity in the MT2 cell line and primary leukemic ATL cells with chronic occupancy of the IRF-4 CD28RE by the NF-ATp subunit in HTLV-I infected cells *in vivo*. Overexpression of NF-ATp in Jurkat T-cells synergizes with NIK to activate the CD28RE of the human IRF-4 promoter in reporter gene assay, indicating that both the NF-κB and NF-AT signaling pathways are involved in IRF-4 transactivation through CD28RE. The involvement of NF-AT transcription factors, specifically the NF-ATp subunit, for IRF-4 promoter activation is highlighted by genetic KO of NF-AT proteins; interestingly, lymphocytes derived from DKO mice deficient in expression of NF-ATp and NF-ATx, two subunits that are activated in response to stable Tax expression in Jurkat T-cells (285), display reduced IRF-4 expression ((477) and L. Glimcher, personal communication).

Deregulation of cellular gene expression by the HTLV-I Tax oncoprotein is required during the early stages of the retroviral life cycle to establish a productive infection. As a result, HTLV-I infection of mature CD4+ T-lymphocytes directly precipitates transcriptional upregulation of numerous cellular genes whose function is associated with T-cell activation and proliferation, including IL-2, the high affinity IL-2 receptor chain α (IL-2Rα), IL-15, c-fos and Fas ligand (211,212,478). The classical example of this phenomenon is HTLV-I-associated induction of T-cell growth factors such as IL-2 and IL-15, a hallmark of the early phase of HTLV-I infection (228). Tax-dependent IL-2 and IL-15 production is believed to initiate an autocrine/paracrine loop that drives polyclonal proliferation of T-cells within the HTLV-I microenvironment. Growth factor-dependent T-cell proliferation during the early stages of infection is believed to facilitate the accumulation of multiple genetic mutations that ultimately contribute to the transition from immortalization to transformation (211,212,478,479).

Regulation of the IRF-4 gene in T-lymphocytes displays striking similarities with that of the IL-2 promoter; IRF-4 expression is inducible in response to stimuli that mimic TCR engagement by antigen, such as PMA/ionomycin, conA or anti-CD3/CD28 treatment (436,449,450). Induction of IRF-4 expression in primary T-cells is also blocked by treatment with the immunosuppressive drug FK506, which suggests that changes in intracellular calcium concentration - an early feature of T-cell activation - is required for IRF-4 induction (436,450). The parallels between IL-2 and IRF-4 expression imply that their continuous production within the context of HTLV-I infection may involve common mechanisms. Like IL-2, IRF-4 expression in HTLV-I transformed cells dependent on Tax expression, and transient transfection of the *tax* gene induces low levels of IRF-4 expression in Jurkat T-cells (436). In this study, we have demonstrated that Tax expression stimulates transcriptional activation of the HTLV-I-responsive -617 to -209 region of the human IRF-4 promoter in Jurkat T-cells; the mechanism involves the κB1, Sp1 and CD28RE sites of the IRF-4 promoter.

We have characterized chronic IRF-4 overexpression as a specific marker for the ATL phenotype in the context of HTLV-I infection. In fact, high-level IRF-4 expression has since been proposed to represent a specific marker for the acute stage of ATL, which represents the most aggressive point of the disease (480). Continuous production of IRF-4 in HTLV-I transformed cells implicates IRF-4 as a component of viral pathogenesis with respect to ATL development. A role for IRF-4 expression in the development of certain lymphomas is further emphasized through a link to multiple myeloma (MM), a hyperproliferative disorder of terminally differentiated B-cells (481,482). MM has been associated with a t(6;14)(p25;q32) translocation that juxtaposes the immunoglobulin heavy chain locus (IgH) regulatory region to the IRF-4 coding sequence. As a result, MUM/IRF-4 is overexpressed, an event that has been implicated in leukemogenesis since IRF-4 overexpression is capable of synergizing with the v-Rel oncogene to transform Rat-1 fibroblasts *in vitro* (438). Studies examining the physiological role of IRF-4 in T-cells are consistent with such an interpretation. Chronic Tax-driven IRF-4 expression in HTLV-I-infected cells implies a role for IRF-4 in reprogramming T-cell gene expression.

Studies focused on elucidating IRF-4 target genes in T-lymphocytes have been performed through cDNA microarray analysis of a Jurkat T-cell line engineered to stably express IRF-4 (483). These experiments confirm that IRF-4 functions as a global repressor of gene transcription in T-lymphocytes; furthermore, chronic overexpression of IRF-4 in T-cells is associated with down-regulation of genes involved in apoptosis, cell cycle control, DNA repair and immune recognition (483). Detailed analysis of cyclin B1 promoter regulation in HTLV-I-transformed and IRF-4-expressing T-cells demonstrated that the cyclin B1 levels are decreased by IRF-4 expression at the mRNA and protein levels (483). Decreased expression of cyclin B1 as a direct consequence of IRF-4-mediated transcriptional repression has been proposed to destabilize cell cycle control, which may contribute to the formation the atypical, multi-nucleated phenotype of ATL cells. A schematic model of IRF-4 expression in the context of HTLV-I infection and transformation of mature CD4+ T-lymphocytes is detailed in Figure 37.

3. Pathogen-induced signaling into the IKK-related complex

Following establishment of the classical IKK pathway as a direct activator of IRF-4 signaling in T-cells infected and transformed by HTLV-I, further experiments examined the contribution of the IKK-related kinases to activation of NF-κB and IRF signaling through carboxy-terminal phosphorylation of the transcription factors c-Rel, IRF-3 and IRF-7. Although the functional implications of *in vitro* phosphorylation of c-Rel by IKKε remains to be characterized, these studies demonstrate that activation of the IKK-related kinases is necessary and sufficient to induce the full spectrum of IRF-3 and IRF-7 activation, as evidenced by induction of the nuclear localization, DNA binding and transactivation capacity of IRF-3 and IRF-7 *in vivo* in cells overexpressing TBK-1 or IKKε. Both kinases directly phosphorylated IRF-3 and IRF-7 at key resides within their carboxy-terminal signal-responsive domain, which is consistent with the fact that intact TBK-1 and IKKε kinase activity was required to activate IRF-3 and IRF-7 signaling. Significantly, expression of the IKK-related kinases was essential to initiate IRF signaling in response to *de novo* virus infection, as evidenced by the reduction of virus-inducible IRF-3 phosphorylation and IRF-dependent gene expression exhibited by human cell lines treated with RNAi directed against IKKε and TBK-1. Furthermore, expression

Figure 37. Activation of IRF-4 in HTLV-I infected T-cells HTLV-I infection of susceptible CD4+ T-cells results in expression of the Tax oncoprotein; Tax initiates activation of NF-κB signaling through direct interaction with the IKKγ/NEMO component of the classical IKK complex. Activation of NF-AT signaling occurs through Tax-mediated upregulation of intracellular calcium concentration, which activates the phosphatase calcineurin. Chronic activation of the NF-κB and NF-AT pathways results in constitutive occupancy of the κB1 and CD28RE regulatory enhancer elements of the human IRF-4 promoter by NF-κB (c-Rel, p50) and NF-AT (NF-ATp) subunits, which drives over-expression of IRF-4 in HTLV-I infected T-cells. Constitutive expression of IRF-4 in CD4+ T-cells is associated with a global repression of gene transcription. IRF-4-mediated repression of genes regulating cell cycle control, apoptosis and DNA repair may contribute to the emergence of a leukemic phenotype in HTLV-I-infected cells.

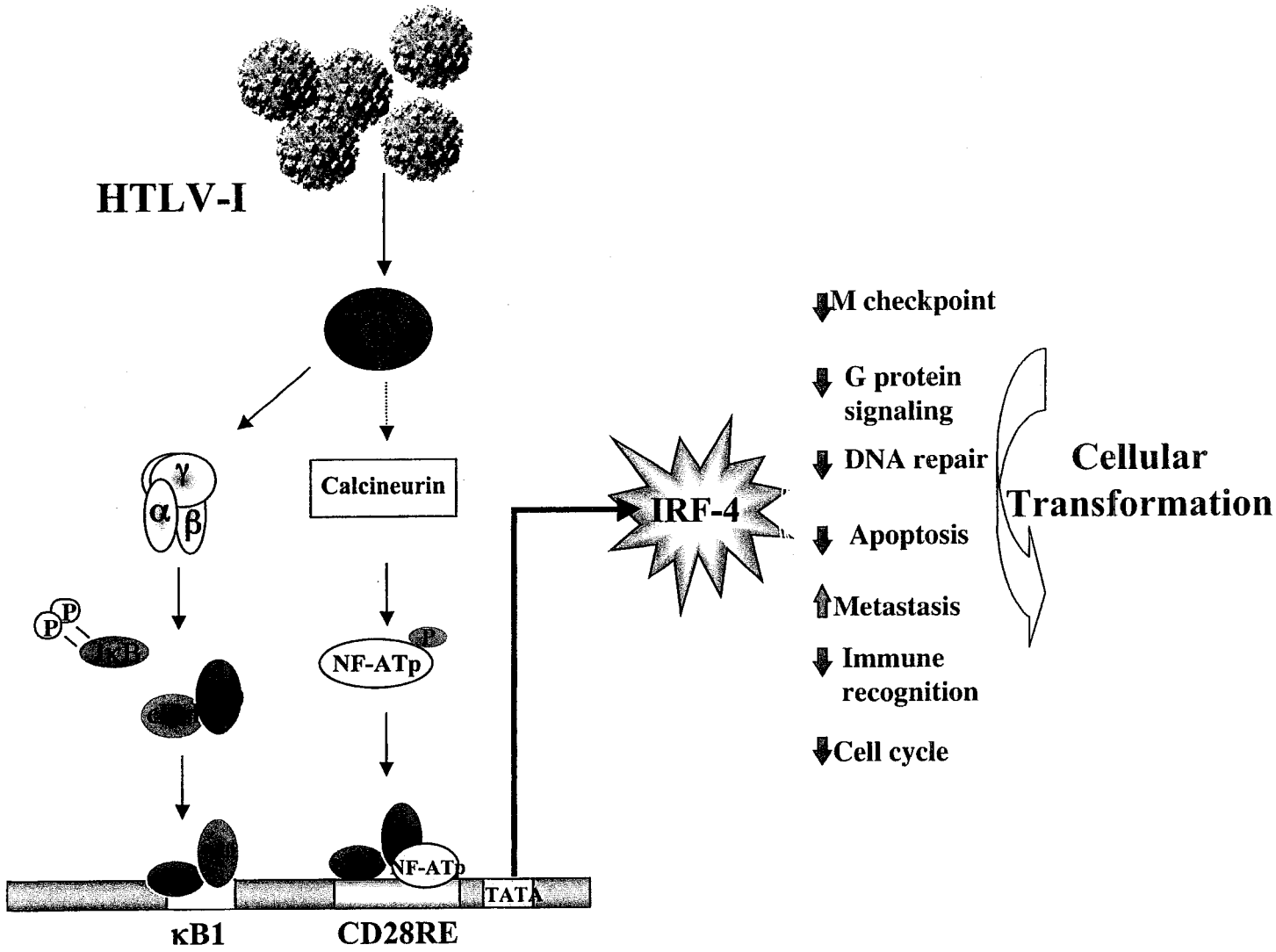
HTLV-I
γ
α
β
Calcineurin
IRF-4
M checkpoint
G protein signaling
DNA repair
Apoptosis
Metastasis
Immune recognition
Cell cycle
Cellular Transformation
P
P
IκB
NF-ATp
NF-ATp
TATA
κB1
CD28RE

of the IKK-related kinases precipitated an IRF-3-dependent anti-viral activity *in vivo*, through IKKε and TBK-1-mediated inhibition of *de novo* VSV replication.

The catalytic activity of the IKK-related kinase complex is inducible in response to cellular detection of *de novo* virus infection, or virus-associated antigens such as synthetic dsRNA (polyI/polyC) or purified RNP complexes. Once the viral threat has been detected, activation of the IKKε and TBK-1 kinase complex precipitates a cellular anti-viral state through activation of IRF-3 and IRF-7 signaling, which stimulates the expression of immune response genes such as the type I IFNs, and the signaling cascade that ensues. Intense study in the field of innate immune signaling through the germline-encoded TLRs has yielded further insight into placement of the IKK-related pathway to IRF-3/IRF-7 activation in the network of cellular signal transduction. IKK-related signaling is placed downstream of dsRNA/TLR3 signaling into type I IFN production (471), within the MyD88-independent pathway regulated by the TLR-associated TIR adaptor molecule TRIF/TICAM-1 (156-158,168,471). The TRIF adaptor directly interacts with TBK-1 (159,168), an event that requires intact TBK kinase activity and results in the post-translational modification of TRIF by phosphorylation (168). Interestingly, the domain of TRIF that associates with TBK-1 is in close proximity to the TRAF6 interaction domain of TRIF, a region that is required to activate classical IKK/NF-κB signaling downstream of dsRNA/TLR3 engagement (168). Based on these results, it can be concluded that MyD88-independent signaling from TLR3 bifurcates into two distinct pathways downstream of the TRIF/TICAM-1 adaptor: a TRAF6-dependent cascade that leads to classical IKK/NF-κB activation and transcriptional upregulation of pro-inflammatory genes such as IL-6, IL1β and TNFα, as well as a second IKKε/TBK-1-dependent cascade that feeds directly into IRF-3/IRF-7 activation and production of TLR3-specific genes such as the type I IFN, RANTES and IP-10 cytokines (166,168,471).

Although dsRNA/TLR3 signaling into IRF-3 and IRF-7 activation via the IKK-related pathway represents a fundamental and evolutionarily conserved mechanism for type I IFN production in mammalian cells, TLR3 engagement by dsRNA (165) is not the sole

trigger of VAK activation in the context of a *de novo* virus infection. Recent experiments using primary DC isolated from *tlr3-/-* mice demonstrate that there is not a significant reduction in the levels of type I IFN produced in response to dsRNA treatment by *tlr3-/-* cells compared to wild type controls (484). Similarly, studies performed in our lab indicate that IRF-3 and IRF-7 activation, as evidenced by detection of *in vivo* carboxy terminal phosphorylation as well as by transactivation of IRF-dependent target genes such as IFNA4, are intact in response to *de novo* virus infection and dsRNA or RNP transfection in MEFs derived from *tlr3-/-* mice (B.R. tenOever and S. Sharma, data not shown). The implications of these results do not detract from the significance of innate immune activation of the anti-viral response via TLR3 signaling; rather, these data confirm the existence of TLR3-independent pathways to innate immune activation and type I IFN production via IRF-3 and IRF-7 activation in both immune and epithelial cells.

A notable difference in the delivery method for dsRNA with respect to these studies may account for the distinct phenotypes observed in *tlr3-/-* cells treated with dsRNA. Studies of TLR3-dependent signaling via dsRNA performed by Alexopoulou et al. (165) have used a cellular overlay method to deliver the dsRNA stimulus. This method favors dsRNA signaling from the cell surface, and excludes efficient delivery of dsRNA inside the cell. In contrast, studies performed by Diebold et al. (484) and in our lab have applied transfection as a means to efficiently deliver dsRNA both extra- and intracellularly. Our data suggests that the two pathways are distinct: dsRNA/TLR3 signaling may represent an extracellular detection system for viral dsRNA, while intracellular dsRNA detection may represent an entirely distinct pathway that signals independently of TLR3 into VAK-mediated activation of the IRF-3 and IRF-7 cascade. For example, RNP complexes isolated from whole VSV virions activate IRF-3 signaling through the IKK-related pathway; the delayed kinetics of IKK-related activation by RNP compared to the rapid kinetics of activation via dsRNA suggest that, unlike dsRNA, RNP does not signal through the extracellular environment but must be delivered inside the cell to activate innate immune responses. In this regard, RNP represents a TLR3-independent intracellular mimic of virus infection, as it is actively produced within virus-infected cells as a life cycle intermediate of viral replication. However, as the TIR adaptor molecule

TRIF directly interacts with the IKK-related complex through TBK-1 (159,168) it will be of interest to determine if TLR3-independent intracellular signaling to IRF-3 and IRF-7 activation requires TRIF, which may be redundant to both TLR3-dependent and TLR3-independent pathways to type I IFN induction. Analysis of VAK activation in response to *de novo* virus infection and dsRNA or RNP treatment in cells derived from TRIF-deficient mice (166) should provide this answer.

Recent data implicates TBK-1 and IKKε as essential regulators of IRF-3 and IRF-7 activation of type I IFN production in response to LPS signaling through TLR4. The mechanism also involves the MyD88-independent pathway, which is dependent on the adaptor TRIF (156-158), as well as another recently identified TIR domain adaptor molecule called TRAM/TICAM-2 (159,160). The pathway has been well described in innate immune cells such as macrophages and DC, but the relevance of this cascade remains to be characterized in fibroblasts. The distinction is important, because previous studies had not established a firm link between LPS treatment and activation of IRF-3 target genes in a fibroblast model (412,415). However, the discrepancy may reflect the cell type the specificity of TLR4 cellular localization; recent experiments applying a flow cytometry approach to examine the localization of TLR4 in immune and non-immune cells using permeabilized or non-permeabilized cell extracts demonstrate that innate immune cells such as macrophages constitutively express TLR4 at both the intra- and extracellular levels (485). In contrast, in pulmonary epithelial cells, expression of TLR4 was exclusive to the intracellular compartment. As a result of this differential expression pattern for TLR4, the downstream signaling events associated with LPS/TLR4 signaling were not as efficiently initiated in pulmonary epithelial cells compared to macrophages, and required significantly higher concentrations of LPS to elicit a TLR4-depedent immunological response in epithelial cells (485). This recent observation may explain the negative results obtained in earlier experiments examining IRF-3 activation in LPS-treated fibroblasts (412,415), which may not have applied high enough concentrations of LPS to efficiently elicit the intracellular LPS/TLR4 response.

Early research on the IKK-related kinases described an interaction between the I-TRAF/TANK adaptor molecule (112) with TBK-1 and IKKε (105,112,113,486). Although these initial studies suggest that interaction with I-TRAF/TANK regulates the catalytic activity of the IKK-related kinases, the functional relevance of the association has yet to be well characterized. The NAK Associated Protein 1 (NAP1), a homologue of I-TRAF/TANK, has also been demonstrated to directly interact with the IKK related kinases (487). Overexpression of NAP1 specifically enhanced cytokine induction of an NF-κB-dependent reporter gene, while *in vivo* depletion of NAP1 reduced NF-κB-dependent reporter gene expression and sensitized cells to TNFα-induced apoptosis (487). While these results define a role for NAP1 as an activator of IKK-related NF-κB signaling, the effect of NAP1 or I-TRAF/TANK association with IKKε and TBK-1 with respect to the IRF-3 and IRF-7 pathway has yet to be examined. It is possible that I-TRAF/TANK or NAP1, or perhaps both, regulate the IKK-related complex by through an essential adaptor function, much like the NEMO/IKKγ component of the classical IKK complex (81,82,98,99). Alternatively, either of these molecules may function as a cellular inhibitor of the IKK-related complex in the absence of virus infection. Further experiments should focus on elaborating the function of I-TRAF/TANK and NAP1 interactions with the IKK-related complex. In particular, a gene deletion or RNA interference approach might prove the most useful to examine the contribution of these proteins to the regulation of VAK activity in the absence or presence of virus infection.

4. Mapping virus-inducible phosphoacceptor sites within IRF-3 and IRF-7

Identification of the specific virus-responsive phosphoacceptor sites within the carboxy-terminal signal responsive regions of IRF-3 and IRF-7 has been the focus of significant effort and some controversy. Characterization of these sites is important, because it has implications for the development of efficient analytical reagents to monitor IRF-3 and IRF-7 activation *in vivo*. Activation of the IRF-3 and IRF-7 transcription factors within the context of pathogen infection represents an important marker for the development of an effective immune response, because IRF-3/IRF-7 signaling is absolutely required to initiate proper anti-viral immunity (321).

Extensive mutagenesis of the IRF-3 carboxy-terminal domain has been performed to ascertain which serine/threonine (S/T) sites are targeted during a virus infection. Mutation of the cluster I S386/386 to alanine (A) completely abolishes IRF-3 transcriptional activity in response to virus infection (414); however, mutation of S385/386 to a phosphomimetic aspartic acid (D) substitution that should mimic the effect of virus-inducible phosphorylation eliminates the transcriptional activity of IRF-3 (411). These results can be interpreted in a variety of ways. Phosphomimetic substitutions do not always yield a functional protein, as evidenced by the phenotype of TBK-1 or IKKε S172D phosphomimetics, which are catalytically inactive (103,104). However, this result may also indicate that the S385/386 cluster is important as a recognition domain involved in kinase binding, as opposed to a direct phosphoacceptor target.

Mutational analyses of the cluster II residues indicate that five S/T residues within this region (S396, S398, S402, T404 and S405) are important for virus-inducible IRF-3 activation (398,411). Alanine substitution of the five cluster II S/T, IRF-3(5A), renders the protein transcriptionally inert in response to virus infection (411). Significantly, mutation of the five cluster II residues to phosphomimetic glutamic acid, IRF-3(5D), generates a constitutive form of IRF-3 which efficiently transactivates IRF-3-depedent promoters (398,411) and stimulates cellular apoptosis in the absence of virus infection (418).

The three-dimensional crystal structure of the IRF-3 carboxy-terminal domain has recently been reported by two independent groups (417,488). A study by Qin et al. confirms earlier biochemical structure/function studies (411) that described a unique autoinhibitory mechanism for IRF-3 whereby amino- and carboxy-terminal autoinhibitory domains interact with the IAD to form a central hydrophobic core (411,488). The interaction buries several key residues within the IAD that are involved in dimerization of the active protein and are therefore required for nuclear accumulation, DNA binding and transactivation events. Virus-inducible, carboxy-terminal phosphorylation events abolish autoinhibitory interactions by introducing charge repulsions within this region, which unmasks the IAD active site and re-aligns the DNA

binding domain to form the transcriptionally active protein (488). Significantly, Qin et al. maintain that multiple serine/threonine phosphorylation events within the cluster I and cluster II residues are required for relief of latent IRF-3 autoinhibition.

A similar study by Takahasi et al. undertook an X-ray crystallography approach coupled with functional analysis by evaluation of the dimerization capacity to study the structure of the IRF-3 carboxy-terminal (417). These experiments also assert that phosphorylation of the carboxy-terminal directly precipitates IRF-3 dimerization, which generates an acidic pocket responsible for p300/CBP association. However, this group maintains that the cluster I residues, in particular the S386 residue, is the primary target for virus-inducible, as well as IKKε and TBK-1-mediated IRF-3 phosphorylation during the initial stages of activation, because the cluster I residues represent the most accessible amino acids in latent IRF-3 (417). In contrast, Qin et al. emphasize a sequential mechanism of IRF-3 carboxy-terminal phosphorylation: although the cluster I residues are significantly exposed in latent IRF-3, residues within both serine clusters I and II around the IAD are available and are required to serve as either kinase recognition or direct phosphoacceptor sites; the authors emphasize that sequential phosphorylation events within both clusters is necessary to elicit the complete unfolding and activation of IRF-3 (488). Interestingly, both groups observed that the carboxy-terminal of IRF-3 exhibits a similarity to the Mad homology 2 (MH2) domain of the Smad family of transcriptional regulator proteins, with respect to structural integrity and surface electrostatic potential. The authors conclude that this similarity suggests a common molecular mechanism of action among a superfamily of signaling mediators; although the IRF and Smad proteins are functionally independent, these results suggest that IRF-3 may have originated from the Smad transcription factors (417,488).

Our studies assessing the direct, *in vitro* phosphorylation capacity of purified recombinant IKKε and TBK with respect to the carboxy-terminal signal-responsive domains of both IRF-3 and IRF-7 demonstrate that the IKK-related kinases exhibit an identical specificity for phosphoacceptor sites within IRF-3 and IRF-7. With respect to IRF-3, our results are in accordance with a similar study undertaken by McWhirter et al

(489) which demonstrates that substitution of the five cluster II residues to alanine abolished the majority of direct IKK-related IRF-3 carboxy-terminal phosphorylation; the residual activity was completely removed by further alanine mutation of the cluster I S385/S386 residues. These results clearly demonstrate that the IKK-related kinases primarily target the cluster II S/T residues, at least for direct phosphorylation. Further mutational analysis of the residues within cluster II indicated that a minimal mutation of S402A within this region abolished most of IKK-related phosphorylation. These results are consistent with the documented consensus motif for the IKK-related kinases, which have previously been shown to phosphorylate the second serine residue within the SXXXS motif of IκBα *in vitro* (103,104). However, identification of S402 as a minimal phosphoacceptor site for the IKK-related kinases is inconsistent with previous observations that have characterized phosphorylation within cluster II at S396 and S398 to be essential for IRF-3 activation (415). Phosphorylation at S402 by the IKK-related kinases may represent the initial steps in virus-induced IRF-3 phosphorylation, which is a multi-step process (411,488). Virus-inducible phosphorylation at the S402 residue may represent a prelude to phosphorylation of the protein at other residues within cluster I or cluster II, either by the same regulatory kinases IKKε and TBK-1, or by another, as-yet-unidentified kinase component(s) of the IKK-related complex.

Phosphorylation of the IRF-7 carboxy-terminal by the IKK-related kinases directly targets two primary serine residues, S477 and S479. Mutation of both residues to alanine abolished IKK-related phosphorylation of the IRF-7 carboxy-terminal. These results are in accordance with functional analysis of IRF-7, which demonstrated that a S477/479D phosphomimetic mutation enhanced the transcriptional activity of IRF-7 for the IFNA4 promoter; similarly, mutation of these residues to alanine abolished the transactivation capacity of IRF-7 in response to SV infection. The S479 residue lies within the SXXXS consensus motif that has been previously described for the IKK-related kinases; however, *in vitro* kinase assays indicated that a S479A substitution only partially diminished direct IKK-related phosphorylation. This result suggests that direct phosphorylation at S479 by the IKK-related kinases, which does not fit with the canonical consensus motif, is a significant source of IKK-related IRF-7 phosphorylation. The diversity of substrate

recognition by the IKK-related kinases for the carboxy-terminal of IRF-7 suggests that there is still much to be learned about the enzymatic activity of IKKε and TBK-1. However, future studies examining the phosphorylation of IRF-3 and IRF-7 by the IKK-related kinases should focus on applying more sophisticated techniques that take into account the complex three-dimensional structure of these proteins. A significant limitation of *in vitro* kinase analyses using small, isolated peptide fragments to represent the larger protein substrate do not account for the conformational constraints imposed by amino acid interactions along the entire protein. Although this type of *in vitro* analysis has been elegantly applied to identify critical regulatory residues within relatively simple, small molecules such as IκBα, which lacks the complex organization imposed by a DNA binding and transactivation domain, proper analysis of IRF-3 and IRF-7 should take into account the physiological, three dimensional structure of the proteins.

5. Genetic knockout studies of TBK-1

Although TBK-1 and IKKε form a functional heterodimer *in vivo*, their differential expression of is thought to reflect a distinct, non-redundant role in the activation of IRF signaling (470). For example, TBK-1 is constitutively and ubiquitously expressed (106) and correlates with the expression of IRF-3 (391,398,401), while IKKε expression is inducible in non-hematopoietic cells in response to a variety of stimuli including LPS and phorbol ester (103,104,109); the expression pattern of IKKε is reminiscent to that of IRF-7, which is also regulated at the transcriptional level (299,407). Human cell lines treated with RNAi directed against both IKK-related kinases demonstrated that RNAi-mediated knockdown of TBK-1 and IKKε expression significantly reduced virus-inducible IRF-3 and IRF-7 activation, which was associated with a reduction in the transcription of anti-viral genes such as ISG56 and IFNα4 in response to virus infection. These results indicate that both IKK-related kinases are required for induction of the anti-viral genetic program through IRF-3 and IRF-7 activation.

Data presented on the analysis of MEFs derived TBK-1 KO mice complement similar studies documenting significant defects in IRF-3 signaling in the absence of TBK-1 expression (489). Our results extend these studies by demonstrating that IRF-3 and IRF-7

signaling are both impaired by the loss of TBK-1 activity; however, we have shown that the IRF-3/IRF-7 anti-viral response is not completely abolished in TBK-1 KO MEFs. The kinetics of dsRNA and virus-induced IRF-3 activation, as monitored by hyperphosphorylation of IRF-3 on one-dimensional 7.5% SDS-PAGE, were delayed in TBK-1-/- MEFs compared to wild type MEFs; furthermore, the delay of IRF-3 phosphorylation *in vivo* correlated with a 50-75% reduction in IRF-3 and IRF-7-dependent gene transcription in response to dsRNA treatment and virus infection, as measured by activation of the ISRE-driven RANTES and IFNA4 luciferase reporter genes. Interestingly, IKKε protein expression was detected in WT and TBK-1-/- MEFs in response to dsRNA treatment and virus infection. These data suggest that expression of IKKε compensates for the TBK-1 deficiency with respect to IRF-3/IRF-7 activation by virus, which is consistent with *in vitro* kinase data, which indicates that both kinases exhibit an identical pattern of phosphorylation with respect to residues within the carboxy-terminal domains of both IRF-3 and IRF-7. Taken together, these results suggest that the IKK-related kinases are functionally redundant with respect to virus-inducible IRF-3 and IRF-7 activation and induction of the anti-viral state in mammalian cells.

However, a distinct role for each IKK-related kinase in the regulation of the anti-viral type I IFN immune response should not be ruled out. The classical IKK kinases exhibit an identical substrate specificity with respect to IκB phosphorylation, but analysis of the phenotypes of IKKα and IKKβ KO mice has demonstrated distinct functions for each *in vivo*. For example, IKKβ can efficiently compensate for the loss of IKKα with respect to inducible activation of classical NF-κB signaling (94-96), while IKKα homodimers do not compensate for loss of IKKβ as efficiently (91-93). Homodimers of IKKα appear to play a more important role keratinocyte differentiation, as well as in regulation of the non-canonical NF-κB pathway of p100 processing to p52. Taken together, these results suggest that a thorough comparison of virus-inducible IRF-3/IRF-7 activation, type I IFN induction and the anti-viral immune response in mice harboring single and double deletions of the IKK-related kinases may ultimately yield more information on the distinct role of TBK-1 and IKKε during establishment of anti-viral immunity. In particular, a quantitative comparison of the kinetics of endogenous virus-inducible type I

IFN production and secretion by *tbk1*, *ikke* and DKO mice versus wild type controls would represent a means to efficiently compare the relative contribution of each IKK-related subunit to IRF activation. Furthermore, as the IRF-dependent pathway has been implicated in LPS signaling in innate immune cells, it would merit attention to examine the individual contribution of TBK-1 or IKKε kinase activity in activation of IRF-3/IRF-7 signaling in response to diverse and distinct stimuli.

6. Viral interference with the IKK-related pathway

As a central regulator of innate immune induction and development of efficient anti-viral immunity, it is not surprising that a wide variety of viral agents have been demonstrated to interfere with the type I IFN cascade at the level of IRF-3 and IRF-7 activation. For example, viral proteins such as Influenza A NS1, Adenovirus E1A, Ebola Virus VP35, and Vaccine Virus E3L block virus-induced IRF activation (353). Although the exact mechanism for many of these proteins remains to be fully elucidated, some generalizations can be made with respect to viral evasion of IRF-3/IRF-7 signaling. For example, many viruses bind and sequester the antigenic viral components required to activate IRF signaling. Influenza NS1 (490) and Vaccine Virus E3L (421) are dsRNA-binding proteins that are believed to sequester the dsRNA activator during virus infection. Similarly, Ebola VP35 sequesters RNP complexes during virus infection (491), presumably hiding them from the cellular detection machinery.

More recent experiments documenting the role of the HCV serine protease NS3/4A complex in mediating HCV pathogenesis demonstrate that IRF-3 phosphorylation in response to *de novo* virus infection is inhibited by stable expression of functional NS3/4A alone; as expected, NS3/4A-associated inhibition of IRF-3 carboxy-terminal phosphorylation is concordant with decreased promoter activation of ISRE-regulated anti-viral genes such as ISG54, ISG56 and RANTES (492). Disruption of NS3/4A protease enzymatic activity by mutation or administration of a peptidomimetic inhibitor restored IRF-3 activation in response to SV infection. Furthermore, dominant-negative (IRF-3ΔN) or constitutively active (IRF-3(5D)) IRF-3 mutants enhanced or suppressed HCV RNA replication in hepatoma cells, respectively, indicating that activation of the

IRF-3 cascade has a functional impact on the replication capacity of human pathogens such as HCV (492). Thus, within the context of HCV infection of mammalian cells, the NS3/4A protease represents a therapeutic target to restore IRF-3 activation and induction of the type I IFN anti-viral response for immune system control of HCV infection.

The IKK-related IRF-3/IRF-7 transcriptional program, represented schematically in Figure 38, confers specificity to the innate immune response, as it is related to but functionally distinct from the broad immunoregulatory function of the classical IKK/NF-κB pathway. For example, IRF-3 and IRF-7 signaling is rapidly activated by cellular detection of foreign pathogens, to elicit production of immediate early immune response genes such as type I IFNs, which establish a cellular genetic response designed to be hostile to pathogen replication. Furthermore, as a central mediator of immunomodulatory gene expression, IRF-3 has been demonstrated to have a tumor-suppressor activity *in vivo* (493,494); for example, with weakly antigenic tumors such as B16 melanoma, a retroviral gene transfer of IRF-3 mediated significant antitumor responses, as evidenced by a reduced rate of tumor growth in B16-inoculated mice. Biochemical analysis indicated that the reductions in tumor growth were accompanied by specific increases in the cytokine expression profile of RANTES, IP-10, TNFα, IL-6 and IFNβ at the mRNA levels (493,494), which established a novel role for IRF-3 activation as a potential molecular target for gene therapy of cancer.

Identification of IKKε and TBK-1 as components of the VAK complex controlling IRF-3/IRF-7 activation defines a critical missing link in the type I IFN paradigm, one which establishes a place for IRF-3 and IRF-7 signaling in the cellular anti-viral signaling network and generates a specific regulatory target to modulate this fundamental immunostimulatory cascade. These results have implications for the identification and characterization of pharmacological or biological activators of the TBK-1/IKKε pathway

Figure 38. Activation of NF-κB and IRF signaling by the IKK kinases Virus infection, dsRNA and LPS activate NF-κB and IRF transcription. Virus infection activates NF-κB and IRF signaling via TLR3-dependent and TLR3-independent mechanisms. TLR-independent activation of IRF may involve direct recognition of viral ribonucleoprotein (RNP) complexes by as-yet-unidentified signaling machinery in virus infected cells. Recognition of dsRNA by TLR3 activates a MyD88-independent pathway via the TIR domain adaptor molecule TRIF, which interacts with TRAF6 to activate the classical IKK complex (IKKα, IKKβ and IKKγ), or with TBK-1 to activate the IKK-related complex (TBK-1, IKKε and putative adaptor proteins NAP1 and I-TRAF). Similarly, recognition of LPS by TLR4 activates NF-κB and IRF through TRIF in conjunction with the TIR domain adaptor TRAM.

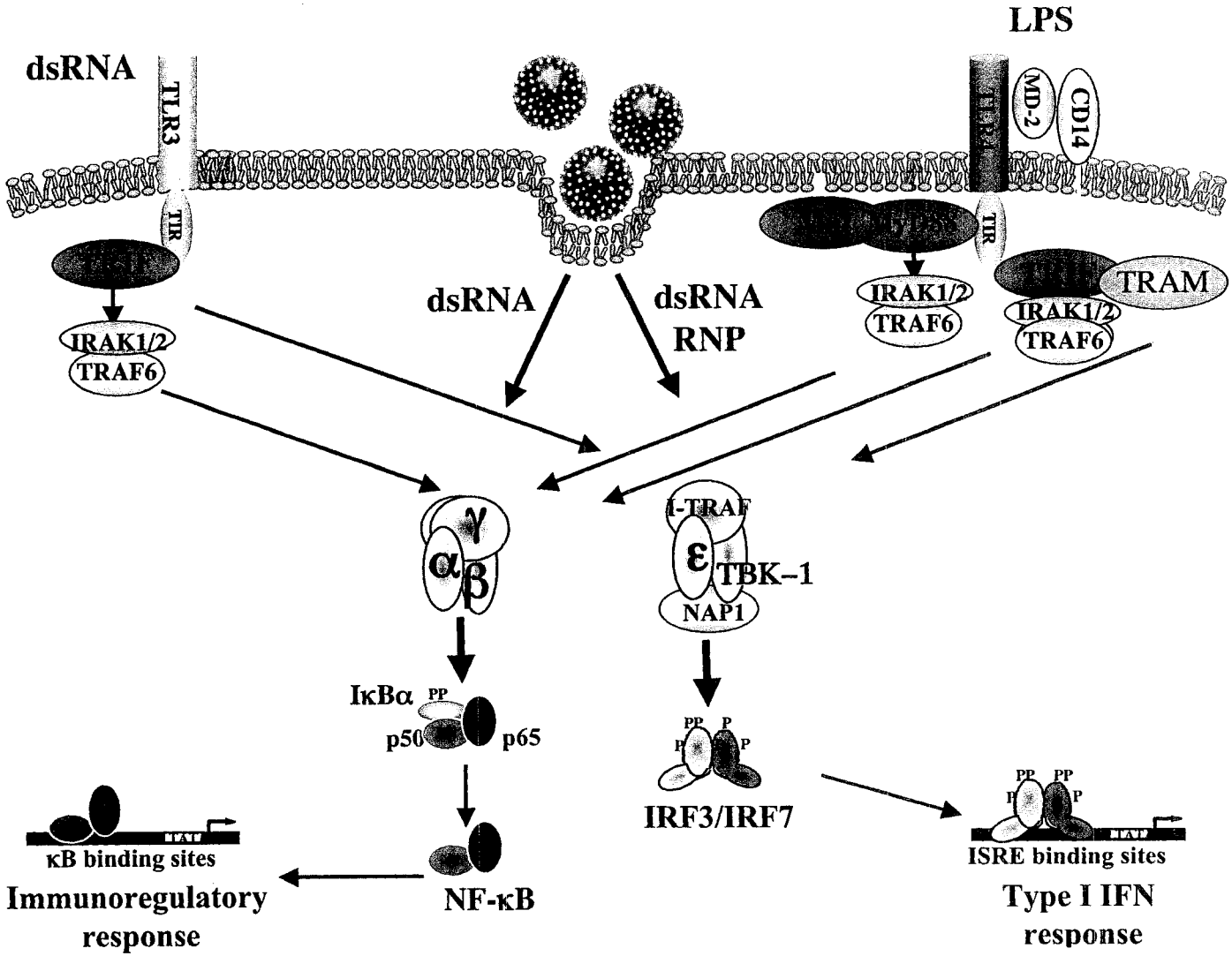
LPS
dsRNA
TLR3
TLR4
MD-2
CD14
TIR
TIR
TRAM
IRAK1/2
TRAF6
IRAK1/2
TRAF6
IRAK1/2
TRAF6
dsRNA
dsRNA
RNP
γ
α
β
ε
TBK–1
NAP1
IκBα
PP
p50
p65
IRF3/IRF7
κB binding sites
Immunoregulatory
response
NF-κB
ISRE binding sites
Type I IFN
response

to IRF-3/IRF-7 activation, which may prove to be an efficient cellular target for boosting host immunity to a broad array of human pathogens and disease.

Chapter VII

Contribution to Original Knowledge

Chapter VII

Contribution to original knowledge

The research presented within this document has contributed to the understanding of specific molecular mechanisms that regulate activation of the immune responsive IRF transcription factors in response to cellular infection by viral agents. These studies are some of the first biochemical and genetic evidence demonstrating that the NF-κB and IRF transcription factors not only act in synergy to activate gene expression during the course of the innate and adaptive immune responses, but are linked within the immune signaling network through regulation by IKK kinases. The candidate's major contributions are summarized as follows:

1. The candidate aided in the characterization of a novel and functional interaction that regulates DNA binding and subsequent transactivation potential of the lymphoid/myeloid-specific IRF-4 transcription factor, through elucidation of the specific domains involved in IRF-4/FKBP52 interaction and demonstration that this functional interaction has physiological relevance in B-cells and HTLV-I infected T-cells.

2. The candidate demonstrated that IRF-4 overexpression within the context of HTLV-I infection of T-cells is specifically associated with the ATL phenotype. Furthermore, the candidate performed the first detailed molecular analysis of the human IRF-4 promoter, through characterization of protein-DNA interactions that regulate IRF-4 transcriptional activation within the context of HTLV-I infection both *in vitro* and *in vivo*. These were the first experiments to demonstrate that IRF-4 expression is controlled by NF-κB and NF-AT transcription factors in HTLV-I infected cells.

3. The candidate was the first to identify components of the VAK complex that activates IRF-3/-7 anti-viral signaling by direct phosphorylation *in vitro* and *in vivo* within the carboxy-terminal domain. These experiments establish the first cellular components regulating the IRF-3 and IRF-7 pathway to type I IFN

transcription. The candidate subsequently participated in the first experiments that established the anti-viral capacity of the IKK-related TBK-1 and IKKε kinases, through IRF-3 and IRF-7-dependent activation of the type I IFN response.

4. Through detailed analysis of IRF-3 and IRF-7 activation by the IKK-related pathway, the candidate identified the first direct physiological target of the IKK-related kinases TBK-1 and IKKε. The candidate was also the first to characterize the specific phosphoacceptor sites within the carboxy termini of IRF-3 and IRF-7 that serve as direct substrates for the IKK-related kinases.

5. The candidate demonstrated that TBK-1 and IKKε form a functional heterodimeric kinase complex that is catalytically activated *in vivo* in response to virus infection or cellular stimulation with viral mimetics such as synthetic dsRNA or purified RNP complexes.

Chapter VIII

References

Chapter VIII

References

1. Ghosh S, May MJ, Kopp EB. 1998. NF-κB and Rel proteins: evolutionarily conserved mediators of immune responses. *Annu. Rev. Immunol.* 16: 225-60.

2. Caamano J, Hunter CA. 2002. NF-κB family of transcription factors: central regulators of innate and adaptive immune functions. *Clin. Microbiol. Rev.* 15: 414-29.

3. Hiscott J, Kwon H, Genin P. 2001. Hostile takeovers: viral appropriation of the NF-κB pathway. *J. Clin. Invest.* 107: 143-51.

4. Baldwin AS Jr. 1996. The NF-κB and IκB proteins: new discoveries and insights. *Annu. Rev. Immunol.* 14: 649-81.

5. Verma IM, Stevenson JK, Schwarz EM, Antwerp DV, Miyamoto S. 1995. Rel/NF-κB/IκB family: intimate tales of association and dissociation. *Genes Dev.* 9: 2723-35.

6. Baeuerle PA, Baltimore D. 1996. NF-κB: ten years after. *Cell* 87: 13-20.

7. Kunsch C, Ruben SM, Rosen CA. 1992. Selection of optimal κB/Rel DNA-binding motifs: interaction of both subunits of NF-κB with DNA is required for transcriptional activation. *Mol. Cell. Biol.* 12: 4412-21.

8. Lin R, Gewert D, Hiscott J. 1995. Differential transcriptional activation in vitro by NF-κB/Rel proteins. *J. Biol. Chem.* 270: 3123-31.

9. Saccani S, Pantano S, Natoli G. 2003. Modulation of NF-κB activity by exchange of dimers. *Mol. Cell* 11: 1563-74.

10. Rao A, Luo C, Hogan PG. 1997. Transcription factors of the NF-AT family: regulation and function. *Annu. Rev. Immunol.* 15: 707-47.

11. Nolan GP. 1994. NF-AT-AP-1 and Rel-bzip: hybrid vigor and binding under the influence. *Cell* 77: 795-8.

12. Steward R. 1987. Dorsal, an embryonic polarity gene in *Drosophila*, is homologous to the vertebrate proto-oncogene, c-Rel. *Science* 238: 692-4.

13. May MJ, Ghosh S. 1997. Rel/NF-κB and IκB proteins: an overview. *Semin. Cancer Biol.* 8: 63-73.

14. Blank V, Kourilsky P, Israël A. 1991. Cytoplasmic retention, DNA binding and processing of the NF-κB p50 precursor are controlled by a small region in its C-terminus. *EMBO J.* 10: 4159-67.

15. Fan C-M, Maniatis T. 1991. Generation of p50 subunit of NF-κB by processing of p105 through an ATP-dependant pathway. *Nature* 354: 395-8.

16. Bours V, Burd PR, Brown K, Villalobos J, Park S, Ryseck R-P, Bravo R, Kelly K, Siebenlist U. 1992. A novel mitogen-inducible gene product related to p50/p105-NF-κB participates in transactivation through a κB site. *Mol. Cell. Biol.* 12: 685-95.

17. Palombella VJ, Rando OJ, Goldberg AL, Maniatis T. 1994. The ubiquitin-proteosome pathway is required for processing the NF-κB1 precursor protein and the activation of NF-κB. *Cell* 78: 773-85.

18. Plaksin D, Baeuerle PA, Eisenbach L. 1993. KBF1 (p50 NF-κB homodimer) acts as a repressor of H-2K^b gene expression in metastatic tumor cells. *J. Exp. Med.* 177: 1651-62.

19. Grumont RJ, Richardson IB, Gaff C, Gerondakis S. 1993. Rel/NF-κB nuclear complexes that bind κB sites in the murine c-Rel promoter are required for constitutive c-Rel transcription in B-cells. *Cell Growth Diff.* 4: 731-43.

20. Bours V, Azarenko V, Dejardin E, Siebenlist U. 1994. Human RelB (I-Rel) functions as a κB site-dependent transactivating member of the family of Rel-related proteins. *Oncogene* 9: 1699-702.

21. Cogswell PC, Scheinman RI, Baldwin AS, Jr. 1993. Promoter of the human NF-κB p50/p105 gene. *J. Immunol.* 150: 2794-804.

22. Beg AA, Śha WC, Bronson RT, Ghosh S, Baltimore D. 1995. Embryonic lethality and liver degeneration in mice lacking the RelA component of NF-κB. *Nature* 376: 167-70.

23. Doi TS, Takahashi T, Taguchi O, Azuma T, Obata Y. 1997. NF-κB RelA-deficient lymphocytes: normal development of T-cells and B-cells, impaired production of IgA and IgG1 and reduced proliferative responses. *J. Exp. Med.* 185: 953-61.

24. Beg AA, Baltimore D. 1996. An essential role for NF-κB in preventing TNFα-induced cell death. *Science* 274: 782-4.

25. Doi TS, Marino MW, Takahashi T, Yoshida T, Sakakura T, Old LJ, Obata Y. 1999. Absence of TNF rescues RelA-deficient mice from embryonic lethality. *Proc. Natl. Acad. Sci. U. S. A.* 96: 2994-9.

26. Alcamo E, Hacohen N, Schulte LC, Rennert PD, Hynes RO, Baltimore D. 2002. Requirement for the NF-κB family member RelA in the development of secondary lymphoid organs. *J. Exp. Med.* 195: 233-44.

27. Kontgen F, Grumont RJ, Strasser A, Metcalf D, Li R, Tarlinton D, Gerondakis S. 1995. Mice lacking the c-Rel proto-oncogene exhibit defects in lymphocyte proliferation, humoral immunity, and IL-2 expression. *Genes Dev.* 9: 1965-77.

28. Gerondakis S, Strasser A, Metcalf D, Grigoriadis G, Scheerlinck J-PY, Grumont RJ. 1996. Rel-deficient T cells exhibit defects in production of IL-3 and GM-CSF. *Proc. Natl. Acad. Sci. U. S. A.* 93: 3405-9.

29. Grumont RJ, Rourke IJ, Gerondakis S. 1999. Rel-dependent induction of A1 transcription is required to protect B-cells from antigen receptor ligation-induced apoptosis. *Genes Dev.* 13: 400-11.

30. Burkly L, Hession C, Ogata L, Reilly C, Marconi LA, Olson D, Tizard R, Cate R, Lo D. 1995. Expression of RelB is required for the development of thymic medulla and dendritic cells. *Nature* 373: 531-6.

31. Weih F, Carrasco D, Durham SK, Barton DS, Rizzo CA, Ryseck R-P, Lira SA, Bravo R. 1995. Multiorgan inflammation and hematopoietic abnormalities in mice with a targeted disruption of RelB, a member of the NF-κB/Rel family. *Cell* 80: 331-40.

32. Beg AA, Baldwin S, Jr. 1993. The IκB proteins: multifunctional regulators of Rel/NF-κB transcription factors. *Genes Dev.* 7: 2064-70.

33. Naumann M, Nieters A, Hatada EN, Scheidereit C. 1993. NF-κB precursor p100 inhibits nuclear translocation and DNA binding of NF-κB/Rel factors. *Oncogene* 8: 2275-81.

34. Rice NR, MacKichan ML, Israel A. 1992. The precursor of NF-κB p50 has IκB-like functions. *Cell* 71: 243-53.

35. Waterfield MR, Zhang M, Norman LP, Sun SC. 2003. NF-κB1/p105 regulates lipopolysaccharide-stimulated MAP kinase signaling by governing the stability and function of the Tpl2 kinase. *Mol. Cell* 11: 685-94.

36. Lin X, Cunningham ET, Jr., Mu Y, Geleziunas R, Greene WC. 1999. The proto-oncogene Cot kinase participates in CD3/CD28 induction of NF-κB acting through the NF-κB-inducing kinase and IκB kinases. *Immunity* 10: 271-80.

37. Inoue JI, Kerr LD, Kakizuka A, Verma I. 1992. IkBg, a 70 kd protein identical to the C-terminal half of p110 NF-κB: a new member of the IκB family. *Cell* 68: 1109-20.

38. Liou H-C, Nolan GP, Ghosh S, Fujita T, Baltimore D. 1992. The NF-κB p50 precursor, p105, contains an internal IκB-like inhibitor that preferentially inhibits p50. *EMBO J.* 11: 3003-9.

39. Kerr LD, Duckett CS, Wamsley P, Zhang Q, Chiao P, Nabel G, McKeithan TW, Baeuerle PA, Verma IM. 1992. The proto-oncogene BCL-3 encodes an IκB protein. *Genes Dev.* 6: 2352-63.

40. Franzoso G, Bours V, Park S, Tomita-Yamaguchi M, Kelly K, Siebenlist U. 1992. The candidate oncoprotein BCL-3 is an antagonist of p50/NF-κB-mediated inhibition. *Nature* 359: 339-42.

41. Siebenlist U, Franzoso G, Brown K. 1995. Structure, regulation and function of NF-κB. *Annu. Rev. Cell. Biol.* 10: 405-55.

42. Whiteside ST, Israel S. 1997. IκB proteins: structure, function and regulation. *Cancer Biol.* 8: 75-82.

43. Beg AA, Ruben SM, Scheinman RI, Haskill S, Rosen CA, Baldwin AS, Jr. 1992. IκB interacts with the nuclear localization sequence of the subunits of NF-κB: a mechanism for cytoplasmic retention. *Genes Dev.* 6: 1899-913.

44. Huxford T, Huang D-B, Malek S, Ghosh G. 1998. The crystal structure of the IκBα/NF-κB complex reveals mechanisms of NF-κB inactivation. *Cell* 95: 759-70.

45. Huang TT, Kudo N, Yoshida M, Miyamoto S. 2000. A nuclear export signal in the N-terminal regulatory domain of IκBα controls cytoplasmic localization of inactive NF-κB/IκBα complexes. *Proc. Natl. Acad. Sci. U. S. A.* 97: 1014-9.

46. Johnson C, Van Antwerp D, Hope TJ. 1999. An N-terminal nuclear export signal is required for the nucleocytoplasmic shuttling of IκBα. *EMBO J.* 18: 6682-93.

47. Malek S, Chen Y, Huxford T, Ghosh G. 2001. IκBβ, but not IκBα, functions as a classical cytoplasmic inhibitor of NF-κB dimers by masking both NF-κB nuclear localization sequences in resting cells. *J. Biol. Chem.* 276: 45225-35.

48. Saccani S, Pantano S, Natoli G. 2001. Two waves of nuclear factor κB recruitment to target promoters. *J. Exp. Med.* 193: 1351-9

49. Chen Z, Hagler J, Palombella VJ, Melandri F, Scherer D, Ballard D, Maniatis T. 1995. Signal-induced site-specific phosphorylation targets IκBα to the ubiquitin-proteasome pathway. *Genes Dev.* 9: 1586-97.

50. Brown K, Gerstberger S, Carlson L, Franzoso G, Siebenlist U. 1995. Control of IκBα proteolysis by site-specific, signal-induced phosphorylation. *Science* 267: 1485-8.

51. Didonato J, Mercurio F, Rosette C, Wu-Li J, Suyang H, Ghosh S, Karin M. 1996. Mapping of the inducible IκB phosphorylation sites that signal its ubiquitination and degradation. *Mol. Cell. Biol.* 16: 1295-304.

52. Yaron A, Hatzubai A, Davis M, Lavon I, Amit S, Manning AM, Andersen JS, Mann M, Mercurio F, Ben-Neriah Y. 1998. Identification of the receptor component of the IκBα-ubiquitin ligase. *Nature* 396: 590-4.

53. Spencer E, Jiang J, Chen ZJ. 1999. Signal-induced ubiquitination of IκBα by the F-box protein Slimb/β-TrCP. *Genes Dev.* 13: 284-94.

54. Kroll M, Margottin F, Kohl A, Renard P, Durand H, Concordet JP, Bachelerie F, Arenzana-Seisdedos F, Benarous R. 1999. Inducible degradation of IκBα by the proteasome requires interaction with the F-box protein hβ–TrCP. *J. Biol. Chem.* 274: 7941-5.

55. Baldi L, Brown K, Franzoso G, Siebenlist U. 1996. Critical role for lysines 21 and 22 in signal-induced, ubiquitin-mediated proteolysis of IκBα. *J. Biol. Chem.* 271: 376-9.

56. Alkalay I, Yaron A, Hatzubai A, Orian A, Ciechanover A, Ben-Neriah Y. 1995. Stimulation-dependent IκBα phosphorylation marks the NF-κB inhibitor for degradation *via* the ubiquitin-proteasome pathway. *Proc. Natl. Acad. Sci. U. S. A.* 92: 10599-603.

57. Grisham MB, Palombella VJ, Elliott PJ, Conner EM, Brand S, Wong HL, Pien C, Mazzola LM, Destree A, Parent L, Adams J. 1999. Inhibition of NF-κB activation in vitro and in vivo: role of 26S proteasome. *Methods Enzymol.* 300: 345-63.

58. Brockman JA, Scherer DC, McKinsey TA, Hall SM, Qi X, Lee WY, Ballard DW. 1995. Coupling of a signal response domain in IκBα to multiple pathways for NF-κB activation. *Mol. Cell. Biol.* 15: 2809-18.

59. Brown K, Franzoso G, Baldi L, Carlson L, Mills L, Lin Y-C, Gerstberger S, Siebenlist U. 1997. The signal response of IκBα is regulated by transferable N- and C- terminal domains. *Mol. Cell. Biol.* 17: 3021-7.

60. Traenckner EBM, Pahl HL, Henkel T, Schmidt KN, Wilk S, Baeuerle PA. 1995. Phosphorylation of human IκBα on serines 32 and 36 controls IκBα proteolysis and NF-κB activation in response to diverse stimuli. *EMBO J.* 14: 2876-83.

61. Barroga CF, Stevenson JK, Schwarz EM, Verma IM. 1995. Constitutive phosphorylation of IκBα by CKII. *Proc. Natl. Acad. Sci. U.S.A.* 92: 7637-41.

62. Lin R, Beauparlant P, Makris C, Meloche S, Hiscott J. 1996. Phosphorylation of IκBα in the C-terminal PEST domain by CKII affects intrinsic protein stability. *Mol. Cell. Biol.* 16: 1401-9.

63. Beauparlant P, Lin R, Hiscott J. 1996. The role of the C-terminal Domain of IκBα in protein degradation and stabilization. *J. Biol. Chem.* 271, No 18: 10690-6.

64. Sun S-C, Ganchi PA, Ballard DW, Greene WC. 1993. NF-κB controls expression of inhibitor IκBα: evidence for an inducible autoregulatory pathway. *Science* 259: 1912-5.

65. Brown K, Park S, Kanno T, Franzoso G, Siebenlist U. 1993. Mutual regulation of the transcriptional activator NF-κB and its inhibitor, IκBα. *Proc. Natl. Acad. Sci. U.S.A.* 90: 2532-6.

66. Algarte M, Kwon H, Genin P, Hiscott J. 1999. Identification by in vivo genomic footprinting of a transcriptional switch containing NF-κB and Sp1 that regulates the IκBα promoter. *Mol. Cell. Biol.* 19: 6140-53.

67. Zabel U, Baeuerle PA. 1990. Purified human IκB can rapidly dissociate the complex of the NF-κB transcription factor with its cognate DNA. *Cell* 61: 255-65.

68. Arenzana-Seisdedos F, Turpin P, Rodriguez M, Thomas D, Hay RT, Virelizier J-L, Dargemont C. 1997. Nuclear localization of IκBα promotes active transport of NF-κB from the nucleus to the cytoplasm. *J. Cell Sci.* 110: 369-78.

69. Thompson JE, Phillips RJ, Erdjument-Bromage H, Tempst P, Ghosh S. 1995. IκB regulates the persistent response in a biphasic activation of NF-κB. *Cell* 80: 573-82.

70. Tran K, Merika M, Thanos D. 1997. Distinct functional properties of IκBα and IκBβ. *Mol. Cell. Biol.* 17: 5386-99.

71. Fenwick C, Na SY, Voll RE, Zhong H, Im SY, Lee JW, Ghosh S. 2000. A subclass of Ras proteins that regulate the degradation of IκB. *Science* 287: 869-73.

72. Beg AA, Sha WC, Bronson RT, Baltimore D. 1995. Constitutive NF-κB activation, enhanced granulopoiesis, and neonatal lethality in IκBα-deficient mice. *Genes Dev.* 9: 2736-46.

73. Cheng JD, Ryseck RP, Attar RM, Dambach D, Bravo R. 1998. Fucntional redundancy of the Nuclear Factor κB inhibitors IκBα and IκBβ. *J. Exp. Med.* 188: 1055-62.

74. Klement JF, Rice NR, Car BD, Abbondanzo SJ, Powers GD, Bhatt PH, Chen CH, Rosen CA, Stewart CL. 1996. IκBα deficiency results in a sustained NF-κB response and severe widespread dermatitis in mice. *Mol. Cel. Biol.* 16: 2341-9.

75. Israel A. 2000. The IKK complex: an integrator of all signals that activate NF-κB? *Trends Cell. Biol.* 10: 129-33.

76. DiDonato JA, Hayakawa M, Rothwarf DM, Zandi E, Karin M. 1997. A cytokine-responsive IκB kinase that activates the transcription factor NF-κB. *Nature* 388: 548-54.

77. Mercurio F, Zhu H, Murray BW, Shevchenko A, Bennett BL, Li JW, Young DB, Barbosa M, Mann M. 1997. IKK1 and IKK2: cytokine-activated IκB kinases essential for NF-κB activation. *Science* 278: 860-6.

78. Regnier CH, Song HY, Gao X, Goeddel DV, Cao Z, Rothe M. 1997. Identification and characterization of an IκB kinase. *Cell* 90: 373-83.

79. Woronicz JD, Gao X, Cao Z, Rothe M, Goeddel DV. 1997. IκB kinase-β: NF-κB activation and complex formation with IκB kinase-α and NIK. *Science* 278: 866-9.

80. Zandi E, Rothwarf DM, Delhase M, Hayakawa M, Karin M. 1997. The IκB kinase complex (IKK) contains two kinase subunits, IKKα and IKKβ, necessary for IκB phosphorylation and NF-κB activation. *Cell* 91: 243-52.

81. Yamaoka S, Courtois G, Bessia C, Whiteside ST, Weil R, Agou F, Kirk HE, Kay RJ, Israel A. 1998. Complementation cloning of NEMO, a component of the IKK complex essential for NF-κB activation. *Cell* 93: 1231-40.

82. Rothwarf DM, Zandi E, Natoli G, Karin M. 1998. IKKγ is an essential regulatory subunit of the IKK complex. *Nature* 395: 297-300.

83. Chen G, Cao P, Goeddel DV. 2002. TNF-induced recruitment and activation of the IKK complex require Cdc37 and Hsp90. *Mol. Cell* 9: 401-10.

84. Burke JR, Wood MK, Ryseck RP, Walther S, Meyers CA. 1999. Peptides corresponding to the N and C termini of IκBα, β, and ε as probes of the two catalytic subunits of IκB kinase, IKK-1 and IKK-2. *J. Biol. Chem.* 274: 36146-52.

85. Delhase M, Hayakawa M, Chen Y, Karin M. 1999. Positive and negative regulation of IκB kinase activity through IKKβ subunit phosphorylation. *Science* 284: 309-13.

86. Ling L, Cao Z, Goeddel DV. 1998. NF-κB-inducing kinase activates IKKα by phosphorylation of Ser-176. *Proc. Natl. Acad. Sci. U. S. A.* 95: 3792-7.

87. Nemoto S, DiDonato JA, Lin A. 1998. Coordinate regulation of IKK by mitogen-activated protein kinase kinase kinase 1 and NIK. *Mol. Cell. Biol.* 18: 7336-43.

88. Sun SC, Maggirwar SB, Harhaj E. 1995. Activation of NF-κB by phosphatase inhibitors involves the phosphorylation of IκBα at phosphatase 2A-sensitive sites. *J. Biol. Chem.* 270: 18347-51.

89. Prajapati S, Verma U, Yamamoto Y, Kwak YT, Gaynor RB. 2004. Protein Phosphatase 2Cβ Association with the IKK Complex Is Involved in Regulating NF-κB Activity. *J. Biol. Chem.* 279: 1739-46.

90. Li Q, Estepa G, Memet S, Israel A, Verma IM. 2000. Complete lack of NF-κB activity in IKK1 and IKK2 double-deficient mice: additional defect in neurulation. *Genes Dev.* 14: 1729-33.

91. Li Q, Van Antwerp D, Mercurio F, Lee KF, Verma IM. 1999. Severe liver degeration in mice lacking the IKK2 gene. *Science* 284: 321-5.

92. Tanaka M, Fuentes ME, Yamaguchi K, Durin MH, Dalrymple SA, Hardy KL, Goeddel DV. 1999. Embrionic lethality, liver degeneration, and impaired NF-κB activation in IKKβ deficient mice. *Immunity* 10: 421-9.

93. Li ZW, Chu W, Hu Y, Delhase M, Deerinck T, Ellisman M, Johnson R, Karin M. 1999. The IKKβ subunit of IKK is essential for NF-κB activation and prevention of apoptosis. *J. Exp. Med.* 189: 1839-45.

94. Hu Y, Baud V, Delhase M, Zhang P, Deerinck T, Ellisman M, Johnson R, Karin M. 1999. Abnormal morphogenesis but intact IKK activation in mice lacking the IKKα subunit of IκB kinase. *Science* 284: 316-20.

95. Li Q, Lu Q, Hwang JY, Buscher D, Lee KF, Izpisua-Belmonte JC, Verma IM. 1999. IKK1-deficient mice exhibit abnomal development of skin and skeleton. *Genes Dev.*13: 1322-8.

96. Takeda K, Takeuchi O, Tsujimura T, Itami S, Adachi O, Kawai T, Sanjo H, Yoshikawa K, Terada N, Akira S. 1999. Limb and skin abnormalities in mice lacking IKKα. *Science* 284: 313-6.

97. Hu Y, Baud V, Oga T, Kim KI, Yoshida K, Karin M. 2001. IKKα controls formation of the epidermis independently of NF-κB. *Nature* 410: 710-4.

98. Rudolph D, Yeh WC, Wakeham A, Rudolph B, Nallainathan D, Potter J, Elia AJ, Mak TW. 2000. Severe liver degeneration and lack of NF-κB activation in NEMO/IKKγ-deficient mice. *Genes Dev.* 14: 854-62.

99. Makris C, Godfrey VL, Krahn-Senftleben G, Takahashi T, Roberts JL, Schwarz T, Feng L, Johnson RS, Karin M. 2000. Female mice heterozygous for IKK γ/NEMO deficiencies develop a dermatopathy similar to the human X-linked disorder incontinentia pigmenti. *Mol. Cell* 5: 969-79.

100. Smahi A, Courtois G, Vabres P, Yamaoka S, Heuertz S, Munnich A, Israel A, Heiss NS, Klauck SM, Kioschis P, Wiemann S, Poustka A, Esposito T, Bardaro T, Gianfrancesco F, Ciccodicola A, D'Urso M, Woffendin H, Jakins T, Donnai D, Stewart H, Kenwrick SJ, Aradhya S, Yamagata T, Levy M, Lewis RA, Nelson

DL. 2000. Genomic rearrangement in NEMO impairs NF-κB activation and is a cause of incontinentia pigmenti. The International Incontinentia Pigmenti (IP) Consortium. *Nature* 405: 466-72.

101. Aradhya S, Woffendin H, Jakins T, Bardaro T, Esposito T, Smahi A, Shaw C, Levy M, Munnich A, D'Urso M, Lewis RA, Kenwrick S, Nelson DL. 2001. A recurrent deletion in the ubiquitously expressed NEMO (IKKγ) gene accounts for the vast majority of incontinentia pigmenti mutations. *Hum. Mol. Genet.* 10: 2171-9.

102. Peters RT, Maniatis T. 2001. A new family of IKK-related kinases may function as IκB kinase kinases. *Biochim. Biophys. Acta.* 1471: M57-62.

103. Shimada T, Kawai T, Takeda K, Matsumoto M, Inoue J, Tatsumi Y, Kanamaru A, Akira S. 1999. IKK-i, a novel lipopolysaccharide-inducible kinase that is related to IKK. *Int. Immunol.* 11: 1357-62.

104. Peters RT, Liao SM, Maniatis T. 2000. IKKε is part of a novel PMA-inducible IKK complex. *Mol. Cell* 5: 513-22.

105. Pomerantz JL, Baltimore D. 1999. NF-κB activation by a signaling complex containing TRAF2, TANK and TBK1, a novel IKK-related kinase. *EMBO J.* 18: 6694-704.

106. Bonnard M, Mirtsos C, Suzuki S, Graham K, Huang J, Ng M, Itie A, Wakeham A, Shahinian A, Henzel WJ, Elia AJ, Shillinglaw W, Mak TW, Cao Z, Yeh WC. 2000. Deficiency of T2K leads to apoptotic liver degeneration and impaired NF-κB-dependent gene transcription. *EMBO J.* 19: 4976-85.

107. Tojima Y, Fujimoto A, Delhase M, Chen Y, Hatakeyama S, Nakayama K, Kaneko Y, Nimura Y, Motoyama N, Ikeda K, Karin M, Nakanishi M. 2000. NAK is an IKK-activating kinase. *Nature* 404: 778-82.

108. Aupperle KR, Yamanishi Y, Bennett BL, Mercurio F, Boyle DL, Firestein GS. 2001. Expression and regulation of inducible IκB kinase (IKK-i) in human fibroblast-like synoviocytes. *Cell. Immunol.* 214: 54-9.

109. Kravchenko VV, Mathison JC, Schwamborn K, Mercurio F, Ulevitch RJ. 2003. IKKi/IKKε plays a key role in integrating signals induced by pro-inflammatory stimuli. *J. Biol. Chem.* 278: 26612-9.

110. Kishore N, Huynh QK, Mathialagan S, Hall T, Rouw S, Creely D, Lange G, Caroll J, Reitz B, Donnelly A, Boddupalli H, Combs RG, Kretzmer K, Tripp CS. 2002. IKK-i and TBK-1 are enzymatically distinct from the homologous enzyme IKK2: comparative analysis of recombinant human IKKi, TBK-1, and IKK2. *J. Biol. Chem.* 277: 13840-7.

111. Rothe M, Xiong J, Shu HB, Williamson K, Goddard A, Goeddel DV. 1996. I-TRAF is a novel TRAF-interacting protein that regulates TRAF-mediated signal transduction. *Proc. Natl. Acad. Sci. U. S. A.* 93: 8241-6.

112. Cheng G, Baltimore D. 1996. TANK, a co-inducer with TRAF2 of TNF- and CD 40L-mediated NF-κB activation. *Genes Dev.* 10: 963-73.

113. Nomura F, Kawai T, Nakanishi K, Akira S. 2000. NF-κB activation through IKKi-dependent I-TRAF/TANK phosphorylation. *Genes Cells* 5: 191-202.

114. Schmitz ML, Bacher S, Kracht M. 2001. IκB-independent control of NF-κB activity by modulatory phosphorylations. *Trends Biochem. Sci.* 26: 186-90.

115. Wang D, Baldwin AS, Jr. 1998. Activation of NF-κB-dependent transcription by TNFα is mediated through phosphorylation of RelA/p65 on serine 529. *J. Biol. Chem.* 273: 29411-6.

116. Sakurai H, Chiba H, Miyoshi H, Sugita T, Toriumi W. 1999. IκB kinases phosphorylate NF-κB p65 subunit on serine 536 in the transactivation domain. *J. Biol. Chem.* 274: 30353-6.

117. Sakurai H, Suzuki S, Kawasaki N, Nakano H, Okazaki T, Chino A, Doi T, Saiki I. 2003. TNFα-induced IKK phosphorylation of NF-κB p65 on serine 536 is mediated through the TRAF2, TRAF5, and TAK1 signaling pathway. *J. Biol. Chem.* 278: 36916-23.

118. Zhong H, Suyang H, Erdjument-Bromage H, Tempst P, Ghosh S. 1997. The transcriptional activity of NF-κB is regulated by the IκB-associated PKAc subunit through a cyclic AMP-independent mechanism. *Cell* 89: 413-24.

119. Okazaki T, Sakon S, Sasazuki T, Sakurai H, Doi T, Yagita H, Okumura K, Nakano H. 2003. Phosphorylation of serine 276 is essential for p65 NF-κB subunit-dependent cellular responses. *Biochem. Biophys. Res. Commun.* 300: 807-12.

120. Fognani C, Rondi R, Romano A, Blasi F. 2000. cRel-TD kinase: a serine/threonine kinase binding in vivo and in vitro c-Rel and phosphorylating its transactivation domain. *Oncogene* 19: 2224-32.

121. Martin AG, Fresno M. 2000. Tumor necrosis factor-α activation of NF-κB requires the phosphorylation of Ser-471 in the transactivation domain of c-Rel. *J. Biol. Chem.* 275: 24383-91.

122. Bryan RG, Li Y, Lai JH, Van M, Rice NR, Rich RR, Tan TH. 1994. Effect of CD28 signal transduction on c-Rel in human peripheral blood T-cells. *Mol. Cell Biol* 14: 7933-42.

123. Martin AG, San-Antonio B, Fresno M. 2001. Regulation of NF-κB transactivation. Implication of phosphatidylinositol 3-kinase and protein kinase C ζ in c-Rel activation by TNFα. *J. Biol. Chem.* 276: 15840-9.

124. Naumann M, Scheidereit C. 1994. Activation of NF-κB in vivo is regulated by multiple phosphorylations. *EMBO J.* 13: 4597-607.

125. Chen LF, Greene WC. 2003. Regulation of distinct biological activities of the NF-κB transcription factor complex by acetylation. *J. Mol. Med.* 81: 549-57.

126. Chen L, Fischle W, Verdin E, Greene WC. 2001. Duration of nuclear NF-κB action regulated by reversible acetylation. *Science* 293: 1653-7.

127. Chen LF, Mu Y, Greene WC. 2002. Acetylation of RelA at discrete sites regulates distinct nuclear functions of NF-κB. *EMBO J.* 21: 6539-48.

128. Kiernan R, Bres V, Ng RW, Coudart MP, El Messaoudi S, Sardet C, Jin DY, Emiliani S, Benkirane M. 2003. Post-activation turn-off of NF-κB-dependent transcription is regulated by acetylation of p65. *J. Biol. Chem.* 278: 2758-66.

129. Ashburner BP, Westerheide SD, Baldwin AS, Jr. 2001. The p65 (RelA) subunit of NF-κB interacts with the histone deacetylase (HDAC) corepressors HDAC1 and HDAC2 to negatively regulate gene expression. *Mol. Cell. Biol.* 21: 7065-77.

.130. Zhong H, May MJ, Jimi E, Ghosh S. 2002. The phosphorylation status of nuclear NF-κB determines its association with CBP/p300 or HDAC-1. *Mol. Cell* 9: 625-36.

131. Janeway C, Travera P. 1997. *Immunobiology: the immune system in health and disease*: Garland Publishing.

132. Janeway CA, Jr., Medzhitov R. 2002. Innate immune recognition. *Annu. Rev. Immunol.* 20: 197-216.

133. Akira S, Hemmi H. 2003. Recognition of pathogen-associated molecular patterns by TLR family. *Immunol. Lett.* 85: 85-95.

134. Zarember KA, Godowski PJ. 2002. Tissue expression of human Toll-like receptors and differential regulation of Toll-like receptor mRNAs in leukocytes in response to microbes, their products, and cytokines. *J. Immunol.* 168: 554-61.

135. Beutler B. 2000. Tlr4: central component of the sole mammalian LPS sensor. *Curr. Opin. Immunol.* 12: 20-6.

136. Beutler B, Poltorak A. 2001. The sole gateway to endotoxin response: how LPS was identified as TLR4, and its role in innate immunity. *Drug Metab. Dispos.* 29: 474-8.

137. Muta T, Takeshige K. 2001. Essential roles of CD14 and LPS-binding protein for activation of TLR2 as well as TLR4 reconstitution of TLR2- and TLR4-activation by distinguishable ligands in LPS preparations. *Eur. J. Biochem.* 268: 4580-9.

138. Nagai Y, Akashi S, Nagafuku M, Ogata M, Iwakura Y, Akira S, Kitamura T, Kosugi A, Kimoto M, Miyake K. 2002. Essential role of MD-2 in LPS responsiveness and TLR4 distribution. *Nat. Immunol.* 3: 667-72.

139. Beutler B, Rehli M. 2002. Evolution of the TIR, tolls and TLRs: functional inferences from computational biology. *Curr. Top. Microbiol. Immunol.* 270: 1-21.

140. Hultmark D. 1994. Macrophage differentiation marker MyD88 is a member of the Toll/IL-1 receptor family. *Biochem. Biophys. Res. Commun.* 199: 144-6.

141. Wesche H, Henzel WJ, Shillinglaw W, Li S, Cao Z. 1997. MyD88: an adapter that recruits IRAK to the IL-1 receptor complex. *Immunity* 7: 837-47.

142. Burns K, Martinon F, Esslinger C, Pahl H, Schneider P, Bodmer JL, Di Marco F, French L, Tschopp J. 1998. MyD88, an adapter protein involved in IL-1 signaling. *J. Biol. Chem.* 273: 12203-9.

143. Horng T, Barton GM, Medzhitov R. 2001. TIRAP: an adapter molecule in the Toll signaling pathway. *Nat. Immunol.* 2: 835-41.

144. Fitzgerald KA, Palsson-McDermott EM, Bowie AG, Jefferies CA, Mansell AS, Brady G, Brint E, Dunne A, Gray P, Harte MT, McMurray D, Smith DE, Sims JE, Bird TA, O'Neill LA. 2001. Mal (MyD88-adapter-like) is required for TLR4 signal transduction. *Nature* 413: 78-83.

145. Cao Z, Henzel WJ, Gao X. 1996. IRAK: a kinase associated with the IL-1 receptor. *Science* 271: 1128-31.

146. Muzio M, Ni J, Feng P, Dixit VM. 1997. IRAK (Pelle) family member IRAK-2 and MyD88 as proximal mediators of IL-1 signaling. *Science* 278: 1612-5.

147. Suzuki N, Suzuki S, Duncan GS, Millar DG, Wada T, Mirtsos C, Takada H, Wakeham A, Itie A, Li S, Penninger JM, Wesche H, Ohashi PS, Mak TW, Yeh WC. 2002. Severe impairment of IL-1 and TLR signalling in mice lacking IRAK-4. *Nature* 416: 750-6.

148. Cao Z, Xiong J, Takeuchi M, Kurama T, Goeddel DV. 1996. TRAF6 is a signal transducer for IL-1. *Nature* 383: 443-6.

149. Lee J, Mira-Arbibe L, Ulevitch RJ. 2000. TAK1 regulates multiple protein kinase cascades activated by bacterial LPS. *J. Leukoc. Biol.* 68: 909-15.

150. Takaesu G, Kishida S, Hiyama A, Yamaguchi K, Shibuya H, Irie K, Ninomiya-Tsuji J, Matsumoto K. 2000. TAB2, a novel adaptor protein, mediates activation of TAK1 MAPKKK by linking TAK1 to TRAF6 in the IL-1 signal transduction pathway. *Mol. Cell* 5: 649-58.

151. Takaesu G, Ninomiya-Tsuji J, Kishida S, Li X, Stark GR, Matsumoto K. 2001. IRAK leads to activation of TAK1 by inducing TAB2 translocation in the IL-1 signaling pathway. *Mol. Cell. Biol.* 21: 2475-84.

152. Qian Y, Commane M, Ninomiya-Tsuji J, Matsumoto K, Li X. 2001. IRAK-mediated translocation of TRAF6 and TAB2 in the IL-1-induced activation of NF-κB. *J. Biol. Chem.* 276: 41661-7.

153. Ninomiya-Tsuji J, Kishimoto K, Hiyama A, Inoue J, Cao Z, Matsumoto K. 1999. The kinase TAK1 can activate the NIK-IκB as well as the MAP kinase cascade in the IL-1 signaling pathway. *Nature* 398: 252-6.

154. Deng L, Wang C, Spencer E, Yang L, Braun A, You J, Slaughter C, Pickart C, Chen ZJ. 2000. Activation of the IκB kinase complex by TRAF6 requires a dimeric ubiquitin-conjugating enzyme complex and a unique polyubiquitin chain. *Cell* 103: 351-61.

155. Wang C, Deng L, Hong M, Akkaraju GR, Inoue J, Chen ZJ. 2001. TAK1 is a ubiquitin-dependent kinase of MKK and IKK. *Nature* 412: 346-51.

156. Yamamoto M, Sato S, Mori K, Hoshino K, Takeuchi O, Takeda K, Akira S. 2002. Cutting edge: a novel TIR domain-containing adapter that preferentially activates the IFNβ promoter in the TLR signaling. *J. Immunol.* 169: 6668-72.

157. Oshiumi H, Matsumoto M, Funami K, Akazawa T, Seya T. 2003. TICAM-1, an adaptor molecule that participates in TLR3-mediated IFNβ induction. *Nat. Immunol.* 4: 161-7.

158. Hoebe K, Du X, Georgel P, Janssen E, Tabeta K, Kim SO, Goode J, Lin P, Mann N, Mudd S, Crozat K, Sovath S, Han J, Beutler B. 2003. Identification of Lps2 as a key transducer of MyD88-independent TIR signalling. *Nature* 424: 743-8.

159. Fitzgerald KA, Rowe DC, Barnes BJ, Caffrey DR, Visintin A, Latz E, Monks B, Pitha PM, Golenbock DT. 2003. LPS-TLR4 signaling to IRF-3/7 and NF-κB involves the toll adapters TRAM and TRIF. *J. Exp. Med.* 198: 1043-5-5.

160. Oshiumi H, Sasai M, Shida K, Fujita T, Matsumoto M, Seya T. 2003. TIR-containing adapter molecule (TICAM)-2, a bridging adapter recruiting to toll-like receptor 4 TICAM-1 that induces IFNβ. *J. Biol. Chem.* 278: 49751-62.

161. Mink M, Fogelgren B, Olszewski K, Maroy P, Csiszar K. 2001. A novel human gene (SARM) at chromosome 17q11 encodes a protein with a SAM motif and

structural similarity to Armadillo/β-catenin that is conserved in mouse, Drosophila, and Caenorhabditis elegans. *Genomics* 74: 234-44.

162. Akira S, Hoshino K, Kaisho T. 2000. The role of TLRs and MyD88 in innate immune responses. *J. Endotoxin Res.* 6: 383-7.

163. Akira S, Hoshino K. 2003. MyD88-dependent and -independent pathways in TLR signaling. *J. Infect. Dis.* 187 Suppl 2: S356-63.

164. Kawai T, Adachi O, Ogawa T, Takeda K, Akira S. 1999. Unresponsiveness of MyD88-deficient mice to endotoxin. *Immunity* 11: 115-22.

165. Alexopoulou L, Holt AC, Medzhitov R, Flavell RA. 2001. Recognition of dsRNA and activation of NF-κB by TLR3. *Nature* 413: 732-8.

166. Yamamoto M, Sato S, Hemmi H, Hoshino K, Kaisho T, Sanjo H, Takeuchi O, Sugiyama M, Okabe M, Takeda K, Akira S. 2003. Role of adaptor TRIF in the MyD88-independent TLR signaling pathway. *Science* 301: 640-3.

167. Kawai T, Takeuchi O, Fujita T, Inoue J, Muhlradt PF, Sato S, Hoshino K, Akira S. 2001. LPS stimulates the MyD88-independent pathway and results in activation of IRF-3 and the expression of a subset of LPS-inducible genes. *J. Immunol.* 167: 5887-94.

168. Sato S, Sugiyama M, Yamamoto M, Watanabe Y, Kawai T, Takeda K, Akira S. 2003. TIR domain-containing adaptor inducing IFNβ(TRIF) associates with TRAF6 and TBK-1, and activates two distinct transcription factors, NF-κB and IRF-3, in the TLR Signaling. *J. Immunol.* 171: 4304-10.

169. Rosetto M, Engstrom Y, Baldari CT, Telford JL, Hultmark D. 1995. Signals from the IL-1 receptor homolog, Toll, can activate an immune response in a Drosophila hemocyte cell line. *Biochem. Biophys. Res. Commun.* 209: 111-6.

170. Gay NJ, Keith FJ. 1991. Drosophila Toll and IL-1 receptor. *Nature* 351: 355-6.

171. Tan KB, Harrop J, Reddy M, Young P, Terrett J, Emery J, Moore G, Truneh A. 1997. Characterization of a novel TNF-like ligand and recently described TNF ligand and TNF receptor superfamily genes and their constitutive and inducible expression in hematopoietic and non-hematopoietic cells. *Gene* 204: 35-46.

172. Harrington JR. 2000. SODD-silencer of death domains. *Stem Cells* 18: 388-9.

173. Takada H, Chen NJ, Mirtsos C, Suzuki S, Suzuki N, Wakeham A, Mak TW, Yeh WC. 2003. Role of SODD in regulation of TNF responses. *Mol. Cell. Biol.* 23: 4026-33.

174. Hsu H, Xiong J, Goeddel DV. 1995. The TNF receptor 1-associated protein TRADD signals cell death and NF-κB activation. *Cell* 81: 495-504.

175. Hsu H, Shu H, Pan M, Goeddel DV. 1996. TRADD-TRAF2 and TRADD-FADD interactions define two distinct TNF receptor 1 signal transduction pathways. *Cell* 84: 299-308.

176. Devin A, Cook A, Lin Y, Rodriguez Y, Kelliher M, Liu Z. 2000. The distinct roles of TRAF2 and RIP in IKK activation by TNF-R1: TRAF2 recruits IKK to TNF-R1 while RIP mediates IKK activation. *Immunity* 12: 419-29.

177. Zhang SQ, Kovalenko A, Cantarella G, Wallach D. 2000. Recruitment of the IKK signalosome to the p55 TNF receptor: RIP and A20 bind to NEMO (IKKγ) upon receptor stimulation. *Immunity* 12: 301-11.

178. Devin A, Lin Y, Yamaoka S, Li Z, Karin M, Liu Z. 2001. The α and β subunits of IκB kinase (IKK) mediate TRAF2-dependent IKK recruitment to tumor necrosis factor (TNF) receptor 1 in response to TNF. *Mol. Cell. Biol.* 21: 3986-94.

179. Leonard N, Chaggar R, Jones C, Takahashi M, Nikitopoulou A, Lakhani SR. 2001. Loss of heterozygosity at cylindromatosis gene locus, CYLD, in sporadic skin adnexal tumours. *J. Clin. Pathol.* 54: 689-92.

180. Poblete Gutierrez P, Eggermann T, Holler D, Jugert FK, Beermann T, Grussendorf-Conen EI, Zerres K, Merk HF, Frank J. 2002. Phenotype diversity in familial cylindromatosis: a frameshift mutation in the tumor suppressor gene CYLD underlies different tumors of skin appendages. *J. Invest. Dermatol.* 119: 527-31.

181. Trompouki E, Hatzivassiliou E, Tsichritzis T, Farmer H, Ashworth A, Mosialos G. 2003. CYLD is a deubiquitinating enzyme that negatively regulates NF-κB activation by TNFR family members. *Nature* 424: 793-6.

182. Kovalenko A, Chable-Bessia C, Cantarella G, Israel A, Wallach D, Courtois G. 2003. The tumour suppressor CYLD negatively regulates NF-κB signalling by deubiquitination. *Nature* 424: 801-5.

183. Grakoui A, Bromley SK, Sumen C, Davis MM, Shaw AS, Allen PM, Dustin ML. 1999. The immunological synapse: a molecular machine controlling T-cell activation. *Science* 285: 221-7.

184. Dustin ML, Cooper JA. 2000. The immunological synapse and the actin cytoskeleton: molecular hardware for T-cell signaling. *Nat. Immunol.* 1: 23-9.

185. Nakashima S. 2002. Protein kinase Cα (PKCα): regulation and biological function. *J. Biochem.* 132: 669-75.

186. Thome M. 2003. The immunological synapse and actin assembly: a regulatory role for PKCθ. *Dev. Cell* 4: 3-5.

187. Bauer B, Krumbock N, Ghaffari-Tabrizi N, Kampfer S, Villunger A, Wilda M, Hameister H, Utermann G, Leitges M, Uberall F, Baier G. 2000. T-cell expressed PKCθ demonstrates cell-type selective function. *Eur. J. Immunol.* 30: 3645-54.

188. Meller N, Elitzur Y, Isakov N. 1999. Protein kinase C θ (PKCθ) distribution analysis in hematopoietic cells: proliferating T-cells exhibit high proportions of PKCθ in the particulate fraction. *Cell. Immunol.* 193: 185-93.

189. Dienz O, Hehner SP, Droge W, Schmitz ML. 2000. Synergistic activation of NF-κB by functional cooperation between vav and PKCθ in T-lymphocytes. *J. Biol. Chem.* 275: 24547-51.

190. Sun Z, Arendt CW, Ellmeier W, Schaeffer EM, Sunshine MJ, Gandhi L, Annes J, Petrzilka D, Kupfer A, Schwartzberg PL, Littman DR. 2000. PKCθ is required for TCR-induced NF-κB activation in mature but not immature T-lymphocytes. *Nature* 404: 402-7.

191. Tao L, Wadsworth S, Mercer J, Mueller C, Lynn K, Siekierka J, August A. 2002. Opposing roles of serine/threonine kinases MEKK1 and LOK in regulating the CD28 responsive element in T-cells. *Biochem. J.* 363: 175-82.

192. Hehner SP, Hofmann TG, Ushmorov A, Dienz O, Wing-Lan Leung I, Lassam N, Scheidereit C, Droge W, Schmitz ML. 2000. Mixed-lineage kinase 3 delivers CD3/CD28-derived signals into the IKK complex. *Mol. Cell. Biol.* 20: 2556-68.

193. Lin L, DeMartino GN, Greene WC. 1998. Cotranslational biogenesis of NF-κB p50 by the 26S proteasome. *Cell* 92: 819-28.

194. Karin MB-NY. 2000. Phosphorylation meets ubiquitination: The control of NF-κB activity. *Ann. Rev. Immunol.* 18: 621-63.

195. Xiao G, Harhaj EW, Sun SC. 2001. NIK regulates the processing of NF-κB2 p100. *Mol. Cell* 7: 401-9

196. Senftleben U, Cao Y, Xiao G, Greten FR, Krahn G, Bonizzi G, Chen Y, Hu Y, Fong A, Sun SC, Karin M. 2001. Activation by IKKα of a second, evolutionary conserved, NF-κB signaling pathway. *Science* 293: 1495-9.

197. Yin L, Wu L, Wesche H, Arthur CD, White JM, Goeddel DV, Schreiber RD. 2001. Defective lymphotoxin-β receptor-induced NF-κB transcriptional activity in NIK-deficient mice. *Science* 291: 2162-5.

198. Schiemann B, Gommerman JL, Vora K, Cachero TG, Shulga-Morskaya S, Dobles M, Frew E, Scott ML. 2001. An essential role for BAFF in the normal development of B-cells through a BCMA-independent pathway. *Science* 293: 2111-4.

199. Claudio E, Brown K, Park S, Wang H, Siebenlist U. 2002. BAFF-induced NEMO-independent processing of NF-κB2 in maturing B-cells. *Nat. Immunol.* 3: 958-65.

200. Coope HJ, Atkinson PG, Huhse B, Belich M, Janzen J, Holman MJ, Klaus GG, Johnston LH, Ley SC. 2002. CD40 regulates the processing of NF-κB2 p100 to p52. *EMBO J.* 21: 5375-85.

201. Tewari M, Dixit VM. 1996. Recent advances in TNF and CD40 signaling. *Curr. Opin. Genet. Dev.* 6: 39-44.

202. Dejardin E, Droin NM, Delhase M, Haas E, Cao Y, Makris C, Li ZW, Karin M, Ware CF, Green DR. 2002. The lymphotoxin-β receptor induces different patterns of gene expression via two NF-κB pathways. *Immunity* 17: 525-35.

203. Kumar A, Yang YL, Flati V, Der S, Kadereit S, Deb A, Haque J, Reis L, Weissmann C, Williams BR. 1997. Deficient cytokine signaling in mouse embryo fibroblasts with a targeted deletion in the PKR gene: role of IRF-1 and NF-κB. *EMBO J.* 16: 406-16.

204. Gil J, Alcami J, Esteban M. 2000. Activation of NF-κB by the dsRNA-dependent protein kinase, PKR involves the IκB kinase complex. *Oncogene* 19: 1369-78.

205. Zamanian-Daryoush M, Mogensen TH, DiDonato JA, Williams BR. 2000. NF-κB activation by double-stranded-RNA-activated protein kinase (PKR) is mediated through NF-κB-inducing kinase and IκB kinase. *Mol. Cell. Biol.* 20: 1278-90.

206. Ishii T, Kwon H, Hiscott J, Mosialos G, Koromilas AE. 2001. Activation of the IKK complex by double- stranded RNA-binding defective and catalytic inactive mutants of the IFN-inducible protein kinase PKR. *Oncogene* 20: 1900-12.

207. Gil J, Rullas J, Garcia MA, Alcami J, Esteban M. 2001. The catalytic activity of dsRNA-dependent protein kinase, PKR, is required for NF-κB activation. *Oncogene* 20: 385-94.

208. Chu WM, Ostertag D, Li ZW, Chang L, Chen Y, Hu Y, Williams B, Perrault J, Karin M. 1999. JNK2 and IKKβ are required for activating the innate response to viral infection. *Immunity* 11: 721-31.

209. Senftleben U, Li ZW, Baud V, Karin M. 2001. IKKβ is essential for protecting T-cells from TNFα-induced apoptosis. *Immunity* 14: 217-30.

210. Boothby M, Mora AL, Scherer D, Brockman J, Ballard DW. 1997. Perturbation of the T-lymphocyte lineage in transgenic mice expressing a constitutive repressor of NF-kB. *J. Exp. Med.* 185: 1897-907.

211. Bex F, Gaynor RB. 1998. Regulation of gene expression by HTLV-I Tax protein. *Methods* 16: 83-94.

212. Sun SC, Ballard DW. 1999. Persistent activation of NF-κB by the Tax transforming protein of HTLV-1: hijacking cellular IKK. *Oncogene* 18: 6948-58.

213. Edlich RF, Arnette JA, Williams FM. 2000. Global epidemic of HTLV-I. *J. Emerg. Med.* 18: 109-19.

214. Eshima N, Tabata M, Okada T, Karukaya S. 2003. Population dynamics of HTLV-I infection: a discrete-time mathematical epidemic model approach. *Math. Med. Biol.* 20: 29-45.

215. Poiesz BJ, Ruscetti FW, Gazdar AF, Bunn PA, Minna JD, Gallo RC. 1980. Detection and isolation of type C retrovirus particles from fresh and cultured lymphocytes of a patient with cutaneous T-cell lymphoma. *Proc. Natl. Acad. Sci. U. S. A.* 77: 7415-9.

216. Poiesz BJ, Ruscetti FW, Mier JW, Woods AM, Gallo RC. 1980. T-cell lines established from human T-lymphocytic neoplasias by direct response to T-cell growth factor. *Proc. Natl. Acad. Sci. U. S. A.* 77: 6815-9.

217. Yoshida M, Miyoshi I, Hinuma Y. 1982. Isolation and characterization of retrovirus from cell lines of human ATL and its implication in the disease. *Proc. Natl. Acad. Sci. U. S. A.* 79: 2031-5.

218. Gessain A, Barin F, Vernant JC, Gout O, Maurs L, Calender A, de The G. 1985. Antibodies to HTLV-I in patients with tropical spastic paraparesis. *Lancet* 2: 407-10.

219. Bartholomew C, Blattner W, Cleghorn F. 1987. Progression to AIDS in homosexual men co-infected with HIV and HTLV-I in Trinidad. *Lancet* 2: 1469

220. Siekevitz M, Josephs SF, Dukovich M, Peffer N, Wong-Staal F, Greene WC. 1987. Activation of the HIV-1 LTR by T-cell mitogens and the transactivator protein of HTLV-I. *Science* 238: 1575-8.

221. Rosenblatt J, Wachsman W, Shimotohno K, Slamon D, Chen IS. 1984. The comparative molecular biology of HTLV-I and HTLV-II. *Princess Takamatsu Symp.* 15: 177-85.

222. Manel N, Kim FJ, Kinet S, Taylor N, Sitbon M, Battini JL. 2003. The ubiquitous glucose transporter GLUT-1 is a receptor for HTLV. *Cell* 115: 449-59.

223. Seiki M, Eddy R, Shows TB, Yoshida M. 1984. Nonspecific integration of the HTLV provirus genome into adult T-cell leukemia cells. *Nature* 309: 640-2

224. Seiki M, Hattori S, Hirayama Y, Yoshida M. 1983. HTLV-I: Complete nucleotide sequence of the provirus genome integrated in leukemia cell DNA. *Proc. Natl. Acad. Sci. U. S. A* 80: 3618-22.

225. Richardson JH, Edwards AJ, Cruickshank JK, Rudge P, Dalgleish AG. 1990. In vivo cellular tropism of HTLV-I. *J. Virol.* 64: 5682-7.

226. Newbound GC, Andrews JM, O'Rouke JP, Brady JN, Lairmore MD. 1996. HTLV-I Tax mediates enhanced transcription in $CD4^+$ T- lymphocytes. *J. Viro.* 70: 2101-6.

227. Cann A, Chen I. 1996. HTLV Types I and II. In *Fields Virology*, ed. B Fields, pp. 1849. Philadelphia: Lippincott-Raven.

228. Yoshida M. 2001. Multiple viral strategies of HTLV-1 for dysregulation of cell growth control. *Annu. Rev. Immunol.* 19: 475-96.

229. Kiyokawa T, Seiki M, Imagawa K, Shimizu F, Yoshida M. 1984. Identification of a protein (p40x) encoded by a unique sequence pX of HTLV-I. *Gann.* 75: 747-51.

230. Lee TH, Coligan JE, Sodroski JG, Haseltine WA, Salahuddin SZ, Wong-Staal F, Gallo RC, Essex M. 1984. Antigens encoded by the 3'-terminal region of HTLV-I: evidence for a functional gene. *Science* 226: 57-61.

231. Weiss RA, Schulz TF. 1990. Transforming properties of the HTLV-I *tax* gene. *Cancer Cells* 2: 281-3.

232. Wano Y, Feinberg M, Hosking JB, Bogerd H, Greene WC. 1988. Stable expression of the Tax gene of type I HTLV in human T-cells activates specific cellular genes involved in growth. *Proc. Natl. Acad. Sci. U. S. A.* 85: 9733-7.

233. Akagi T, Ono H, Shimotohno K. 1995. Characterization of T-cells immortalized by Tax1 of HTLV-I. *Blood* 86: 4243-9.

234. Pozzatti R, Vogel J, Jay G. 1990. HTLV-I Tax gene can cooperate with the Ras oncogene to induce neoplastic transformation of cells. *Mol. Cell. Biol.* 10: 413-7.

235. Tanaka A, Takahashi C, Yamaoka S, Nosaka T, Maki M, Hatanaka M. 1990. Oncogenic transformation by the tax gene of HTLV-I in vitro. *Proc. Natl. Acad. Sci. U. S. A.* 87: 1071-5.

236. Hinrichs SH, Nerenberg M, Reynolds RK, Khoury G, Jay G. 1987. A transgenic mouse model for human neurofibromatosis. *Science* 237: 1340-3.

237. Nerenberg M, Hinrichs SH, Reynolds RK, Khoury G, Jay G. 1987. The Tax gene of HTLV-I induces mesenchymol tumors in transgenic mice. *Science* 237: 1324-9.

238. Grossman WJ, Kimata JT, Wong F-H, Zutter M, Ley TJ. 1995. Development of leukemia in mice transgenic for the Tax gene of HTLV-I. *Proc. Natl. Acad. Sci. U. S. A.* 92: 1057-61.

239. Bex F, Murphy K, Wattiez R, Burny A, Gaynor RB. 1999. Phosphorylation of the HTLV-I transactivator Tax on adjacent serine residues is critical for Tax activation. *J. Virol.* 73: 738-45.

240. Beimling P, Moelling K. 1989. Isolation and characterization of the Tax protein of HTLV-I. *Oncogene* 4: 511-6.

241. Smith MR, Greene WC. 1992. Characterization of a novel nuclear localization signal in the HTLV-I tax transactivator protein. *Virology* 187: 316-20.

242. Sodroski JG, Rosen CA, Haseltine WA. 1984. *Trans*-acting transcriptional activation of the long terminal repeat of HTLV in infected cells. *Science* 225: 381-5.

243. Fujisawa J-I, Seiki M, Kiyokawa T, Yoshida M. 1985. Functional activation of the long terminal repeat of HTLV-I by a *trans*-acting factor. *Proc. Natl. Acad. Sci. U.S.A.* 82: 2277-81.

244. Lenzmeier BA, Giebler HA, Nyborg JK. 1998. HTLV-I Tax requires direct access to DNA for recruitment of CREB binding protein to the viral promoter. *Mol. Cell. Biol.* 18: 721-31.

245. Lenzmeier BA, Baird EE, Dervan PB, Nyborg JK. 1999. The Tax protein-DNA interaction is essential for HTLV-I transactivation *in vitro*. *J. Mol. Biol.* 291: 731-44.

246. Kwok RPS, Laurance ME, Lundblad RJ, Goldman PS, Shih H-M, Connor LM, Marriott SJ, Goodman RH. 1996. Control of cAMP-regulated enhancers by the viral transactivator Tax through CREB and the co-activator CBP. *Nature* 380: 642-6.

247. Bex F, Yin MJ, Burny A, Gaynor RB. 1998. Differential transcriptional activation by HTLV-I Tax mutants is mediated by distinct interactions with CBP and p300. *Mol. Cell. Biol.* 18: 2392-405,

248. Yoshida M. 1994. Mechanism of transcriptional activation of viral and cellular genes by oncogenic protein of HTLV-1. *Leukemia* 8: S51-S3.

249. Suzuki T, Uchida-Toita M, Yoshida M. 1999. Tax protein of HTLV-1 inhibits CBP/p300-mediated transcription by interfering with recruitment of CBP/p300 onto DNA element of E-box or p53 binding site. *Oncogene* 18: 4137-43.

250. Van Orden K, Nyborg JK. 2000. Insight into the tumor suppressor function of CBP through the viral oncoprotein Tax. *Gene Expr.* 9: 29-36.

251. Lemasson I, Nyborg JK. 2001. HTLV-I Tax repression of p73β is mediated through competition for the C/H1 domain of CBP. *J. Biol. Chem.* 276: 15720-7.

252. Mori N, Shirakawa F, Abe M, Kamo Y, Koyama Y, Murakami S, Shimizu H, Yamamoto K, Oda S, Eto S. 1995. HTLV-I Tax transactivates the IL-6 gene in human rheumatoid synovial cells. *J. Rheumatol.* 22: 2049-54.

253. Himes SR, Coles LS, Katsikeros R, Lang RK, Shannon MF. 1993. HTLV-1 Tax activation of the GM-CSF and G-CSF promoters requires the interaction of NF-κB with other transcription factor families. *Oncogene* 8: 3189-97.

254. Duyao MP, Kessler DJ, Spicer DB, Bartholomew C, Cleveland JL, Siekevitz M, Sonenshein GE. 1992. Transactivation of the c-Myc promoter by HTLV-I Tax is mediated by NF- κB. *J. Biol. Chem.* 267: 16288-91.

255. Kitajima I, Shinohara T, Bilakovics J, Brown DA, Xu X, Nerenberg M. 1992. Ablation of transplanted HTLV-I Tax-transformed tumors in mice by antisense inhibition of NF-κB. *Science* 258: 1792-5.

256. Lindholm PF, Tamami M, Makowski J, Brady JN. 1996. HTLV-I Tax activation of NF-κB: involvement of the protein kinase C pathway. *J. Virol.* 70: 2525-32.

257. Smith MR, Greene WC. 1990. Identification of HTLV-I tax trans-activator mutants exhibiting novel transcriptional phenotypes. *Genes Dev.* 4: 1875-85.

258. Trushin SA, Pennington KN, Carmona EM, Asin S, Savoy DN, Billadeau DD, Paya CV. 2003. PKCα acts upstream of PKCθ to activate IKK and NF-κB in T-lymphocytes. *Mol. Cell. Biol.* 23: 7068-81.

259. Lanoix J, Lacoste J, Pépin N, Rice NR, Hiscott J. 1994. Overproduction of NFKB2 (lyt-10) and c-Rel: a mechanism for HTLV-1 Tax-mediated trans-activation via the NF-κB signalling pathway. *Oncogene* 9: 841-52.

260. Hirai H, Suzuki T, Fujisawa J-I, Inoue J-I, Yoshida M. 1994. Tax protein of HTLV-I binds to the ankyrin motifs of inhibitory factor κB and induces nuclear translocation of transcription factor NF-κB proteins for transcriptional activtion. *Proc. Natl. Acad. Sci. U. S. A.* 91: 3584-8.

261. Suzuki T, Hirai H, Fujisawa J-I, Fujita T, Yoshida M. 1993. A trans-activator Tax of HTLV-I binds to NF-kB p50 and serum response factor (SRF) and associates with enhancer DNAs of the NF-κB site and CArG box. *Oncogene* 8: 2391-7.

262. Lacoste J, Lanoix J, Pépin N, Hiscott J. 1994. Interactions between HTLV-I Tax and NF-κB/Rel proteins in T-cells. *Leukemia* 8: S71-S6.

263. Suzuki T, Hirai H, Yoshida M. 1994. Tax protein of HTLV-I interacts with the Rel homology domain of NF-κB binding p65 and c-Rel proteins bound to the NF-κB binding site and activates transcription. *Oncogene* 9: 3099-105.

264. Beraud C, Sun SC, Ganchi P, Ballard DW, Greene WC. 1994. HTLV-I Tax associates with and is negatively regulated by the NF-κB2 p100 gene product: implications for viral latency. *Mol. Cell. Biol.* 14: 1374-82.

265. Hirai H, Fujisawa J-I, Suzuki K, Ueda K, Muramutsu M, Tsuboi A, Arai N, Yoshida M. 1992. Transcriptional activator Tax of HTLV-1 binds to the NF-κB precursor p105. *Oncogene* 7: 1737-42.

266. Gerritsen ME, Williams AJ, Neish AS, Moore S, Shi Y, Collins T. 1997. CREB-binding protein/p300 are transcriptional coactivators of p65. *Proc. Natl. Acad. Sci. U. S. A.* 7: 2927-32.

267. Perkins ND, Felzien LK, Betts JC, Leung K, Beach DH, Nabel GJ. 1997. Regulation of NF-κB by cyclin-dependent kinases associated with p300 coactivator. *Science* 275: 523-7.

268. Xiao G, Cvijic ME, Fong A, Harhaj EW, Uhlik MT, Waterfield M, Sun SC. 2001. Retroviral oncoprotein Tax induces processing of NF-κB2/p100 in T-cells: evidence for the involvement of IKKα. *EMBO J.* 20: 6805-15.

269. Geleziunas R, Ferrell S, Lin X, Mu Y, Cunningham ET, Jr., Grant M, Connelly MA, Hambor JE, Marcu KB, Greene WC. 1998. HTLV-I Tax induction of NF-κB involves activation of the IKKα and IKKβ cellular kinases. *Mol. Cell. Biol.* 18: 5157-65.

270. Chu Z-L, Didonato J, Hawiger J, Ballard DW. 1998. The Tax oncoprotein of HTLV-I associates with and persistently activates IκB kinases containing IKKα and IKKβ. *J. Biol. Chem.* 273: 15891-4.

271. Harhaj EW, Good L, Xiao G, Uhlik M, Cvijic ME, Rivera-Walsh I, Sun SC. 2000. Somatic mutagenesis studies of NF-κB signaling in human T-cells: evidence for an essential role of IKKγ in NF-κB activation by T-cell costimulatory signals and HTLV-I Tax protein. *Oncogene* 19: 1448-56.

272. Harhaj EW, Sun SC. 1999. IKKγ serves as a docking subunit of IKK and mediates interaction of IKK with HTLV-I Tax protein. *J. Biol. Chem.* 274: 22911-4.

273. Chu ZL, Shin YA, Yang JM, DiDonato JA, Ballard DW. 1999. IKKγ mediates the interaction of cellular IKK with the Tax transforming protein of HTLV-1. *J. Biol. Chem.* 274: 15297-300.

274. Jin DY, Giordano V, Kibler KV, Nakano H, Jeang KT. 1999. Role of adapter function in oncoprotein-mediated activation of NF-κB. HTLV-I Tax interacts directly with IKKγ. *J. Biol. Chem.* 274: 17402-5.

275. Serfling E, Berberich-Siebelt F, Chuvpilo S, Jankevics E, Klein-Hessling S, Twardzik T, Avots A. 2000. The role of NF-AT transcription factors in T-cell activation and differentiation. *Biochim. Biophys. Acta.* 1498: 1-18.

276. McCaffrey PG, Luo C, Kerppola TK, Jain J, Badalian TM, Ho AM, Burgeon E, Lane WS, Lambert JN, Curran T, et al. 1993. Isolation of the cyclosporin-sensitive T-cell transcription factor NFATp. *Science* 262: 750-4.

277. Shaw KT, Ho AM, Raghavan A, Kim J, Jain J, Park J, Sharma S, Rao A, Hogan PG. 1995. Immunosuppressive drugs prevent a rapid dephosphorylation of transcription factor NFAT1 in stimulated immune cells. *Proc. Natl. Acad. Sci. U. S. A.* 92: 11205-9.

278. Loh C, Carew JA, Kim J, Hogan PG, Rao A. 1996. T-cell receptor stimulation elicits an early phase of activation and a later phase of deactivation of the transcription factor NFAT1. *Mol. Cell. Biol.* 16: 3945-54.

279. Hemenway CS, Heitman J. 1999. Calcineurin. Structure, function, and inhibition. *Cell. Biochem. Biophys.* 30: 115-51.

280. Loh C, Shaw KT, Carew J, Viola JP, Luo C, Perrino BA, Rao A. 1996. Calcineurin binds the transcription factor NFAT1 and reversibly regulates its activity. *J. Biol. Chem.* 271: 10884-91.

281. Zhu J, McKeon F. 2000. Nucleocytoplasmic shuttling and the control of NF-AT signaling. *Cell. Mol. Life Sci.* 57: 411-20.

282. Ruff VA, Leach KL. 1995. Direct demonstration of NFATp dephosphorylation and nuclear localization in activated HT-2 cells using a specific NFATp polyclonal antibody. *J. Biol. Chem.* 270: 22602-7.

283. Oukka M, Ho IC, de la Brousse FC, Hoey T, Grusby MJ, Glimcher LH. 1998. The transcription factor NFAT4 is involved in the generation and survival of T-cells. *Immunity* 9: 295-304.

284. Peng SL, Gerth AJ, Ranger AM, Glimcher LH. 2001. NFATc1 and NFATc2 together control both T- and B-cell activation and differentiation. *Immunity* 14: 13-20.

285. Good L, Maggirwar SB, Harhaj EW, Sun SC. 1997. Constitutive dephosphorylation and activation of a member of the nuclear factor of activated T cells, NF-AT1, in Tax-expressing and HTLV-I-infected human T cells. *J. Biol. Chem.* 272: 1425-8.

286. Maggirwar SB, Harhaj EW, Sun SC. 1997. Regulation of the IL-2 CD28-responsive element by NF-ATp and various NF-κB/Rel transcription factors. *Mol. Cell. Biol.* 17: 2605-14.

287. Good L, Maggirwar SB, Sun S-C. 1996. Activation of the IL-2 gene promoter by HTLV-1 Tax involves induction of NF-AT complexes bound to the CD28RE. *EMBO J.* 15: 3744-50.

288. Bouchard MJ, Wang LH, Schneider RJ. 2001. Calcium signaling by HBx protein in HBV DNA replication. *Science* 294: 2376-8.

289. Taniguchi T, Ogasawara K, Takaoka A, Tanaka N. 2001. IRF family of transcription factors as regulators of host defense. *Annu. Rev. Immunol.* 19: 623-55.

290. Nguyen H, Hiscott J, Pitha PM. 1997. The growing family of IRF transcription factors. *Cytokine Growth Fact. Rev.* 8: 293-312.

291. Mamane Y, Heylbroeck C, Genin P, Algarte M, Servant MJ, LePage C, DeLuca C, Kwon H, Lin R, Hiscott J. 1999. IFN regulatory factors: the next generation. *Gene* 237: 1-14.

292. Medzhitov R, Janeway CA, Jr. 1998. Innate immune recognition and control of adaptive immune responses. *Semin. Immunol.* 10: 351-3.

293. Akira S, Takeda K, Kaisho T. 2001. Toll-like receptors: critical proteins linking innate and acquired immunity. *Nat. Immunol.* 2: 675-80.

294. Samuel CE. 2001. Antiviral actions of IFNs. *Clin. Microbiol. Rev.* 14: 778-809.

295. Huang Q, Liu D, Majewski P, Schulte LC, Korn JM, Young RA, Lander ES, Hacohen N. 2001. The plasticity of DC responses to pathogens and their components. *Science* 294: 870-5.

296. Stark GR, Kerr IM, Williams BRG, Silverman RH, Schreiber RD. 1998. How cells respond to IFNs. *Annu. Rev. Biochemis.* 67: 227-64.

297. Sen GC. 2001. Viruses and IFNs. *Annu. Rev. Microbiol.* 55: 255-81.

298. Roberts RM, Liu L, Guo Q, Leaman D, Bixby J. 1998. The evolution of the type I IFNs. *J. Interferon. Cytokine Res.* 18: 805-16.

299. Marie I, Durbin JE, Levy DE. 1998. Differential viral induction of distinct IFN-α genes by positive feedback through IRF-7. *EMBO J.* 17: 6660-9.

300. Isaacs A, Lindenmann J. 1957. Virus interference. I. The IFN. *Proc. R. Soc. Lond. B. Biol. Sci.* 147: 258-67.

301. Isaacs A, Lindenmann J, Valentine RC. 1957. Virus interference. II. Some properties of IFN. *Proc. R. Soc. Lond. B. Biol. Sci.* 147: 268-73.

302. Lindenmann J, Burke DC, Isaacs A. 1957. Studies on the production, mode of action and properties of IFN. *Br. J. Exp. Pathol.* 38: 551-62.

303. Muller U, Steinhoff U, Reis LF, Hemmi S, Pavlovic J, Zinkernagel RM, Aguet M. 1994. Functional role of type I and type II IFNs in antiviral defense. *Science* 264: 1918-21.

304. Hwang SY, Hertzog PJ, Holland KA, Sumarsono SH, Tymms MJ, Hamilton JA, Whitty G, Bertoncello I, Kola I. 1995. A null mutation in the gene encoding a type I IFN receptor component eliminates antiproliferative and antiviral responses to IFNs α and beta and alters macrophage responses. *Proc. Natl. Acad. Sci. U. S. A.* 92: 11284-8.

305. Der SD, Zhou A, Williams BRG, Silverman RH. 1998. Identification of genes differentially regulated by IFN α, β, or γ using oligonucleotide arrays. *Proc. Natl. Acad. Sci. U. S. A.* 95: 15623-8.

306. de Veer MJ, Holko M, Frevel M, Walker E, Der S, Paranjape JM, Silverman RH, Williams BR. 2001. Functional classification of IFN-stimulated genes identified using microarrays. *J. Leukoc. Biol.* 69: 912-20.

307. Geiss G, Jin G, Guo J, Bumgarner R, Katze MG, Sen GC. 2001. A comprehensive view of regulation of gene expression by dsRNA-mediated cell signaling. *J. Biol. Chem.* 30: 30.

308. Sen GC. 2000. Novel functions of IFN-induced proteins. *Semin. Cancer Biol.* 10: 93-101.

309. Rebouillat D, Hovanessian AG. 1999. The human 2'-5'-oligoadenylate synthetase family: IFN-induced proteins with unique enzymatic properties. *J. Interferon Cytokine Res.* 19: 295-308.

310. Sarkar SN, Ghosh A, Wang HW, Sung SS, Sen GC. 1999. The nature of the catalytic domain of 2'-5'-oligoadenylate synthetases. *J. Biol. Chem.* 274: 25535-42.

311. Dong B, Silverman RH. 1995. 2'-5'-oligoadenylate-dependent RNase molecules dimerize during activation by 2-5A. *J. Biol. Chem.* 270: 4133-7.

312. Clemens MJ, Elia A. 1997. The dsRNA-dependent protein kinase PKR: structure and function. *J. Interferon Cytokine Res.* 17: 503-24.

313. Ward SV, Samuel CE. 2002. Regulation of the IFN-inducible PKR kinase gene: the KCS element is a constitutive promoter element that functions in concert with the ISRE. *Virology* 296: 136-46.

314. Koromilas AE, Roy S, Barber GN, Katze MG, Sonenberg N. 1992. Malignant transformation by a mutant of the IFN-inducible dsRNA-dependent protein kinase PKR. *Science* 257: 1685-9.

315. Tan SL, Katze MG. 1999. The emerging role of the IFN-induced PKR protein kinase as an apoptotic effector: a new face of death? *J. Interferon Cytokine Res.* 19: 543-54.

316. Guo J, Peters KL, Sen GC. 2000. Induction of the human protein P56 by IFN, dsRNA, or virus infection. *Virology* 267: 209-19.

317. Grandvaux N, Servant MJ, tenOever B, Sen GC, Balachandran S, Barber GN, Lin R, Hiscott J. 2002. Transcriptional profiling of IRF-3 target genes: direct involvement in the regulation of ISG. *J. Virol.* 76: 5532-9.

318. Wathelet MG, Clauss IM, Content J, Huez GA. 1988. The ISG56 and ISG54 IFN-inducible human genes belong to the same gene family. *FEBS Lett.* 231: 164-71.

319. Guo J, Sen GC. 2000. Characterization of the interaction between the ISG P56 and the Int6 protein encoded by a locus of insertion of the mouse mammary tumor virus. *J. Virol.* 74: 1892-9.

320. Guo J, Hui DJ, Merrick WC, Sen GC. 2000. A new pathway of translational regulation mediated by eukaryotic initiation factor 3. *EMBO J.* 19: 6891-9.

321. Sato M, Suemori H, Hata N, Asagiri M, Ogasawara K, Nakao K, Nakaya T, Katsuki M, Noguchi S, Tanaka N, Taniguchi T. 2000. Distinct and essential roles of transcription factors IRF-3 and IRF-7 in response to viruses for IFNα/β gene induction. *Immunity* 13: 539-48.

322. Brinkmann V, Geiger T, Alkan S, Heusser CH. 1993. IFNα increases the frequency of IFNγ-producing human CD4+ T-cells. *J. Exp. Med.* 178: 1655-63.

323. Cella M, Salio M, Sakakibara Y, Langen H, Julkunen I, Lanzavecchia A. 1999. Maturation, activation, and protection of DC induced by dsRNA. *J. Exp. Med.* 189: 821-9.

324. Siegal FP, Kadowaki N, Shodell M, Fitzgerald-Bocarsly PA, Shah K, Ho S, Antonenko S, Liu YJ. 1999. The nature of the principal type 1 IFN-producing cells in human blood. *Science* 284: 1835-7.

325. Kadowaki N, Antonenko S, Lau JY, Liu YJ. 2000. Natural IFNα/β-producing cells link innate and adaptive immunity. *J. Exp. Med.* 192: 219-26.

326. Santini SM, Lapenta C, Logozzi M, Parlato S, Spada M, Di Pucchio T, Belardelli F. 2000. Type I IFN as a powerful adjuvant for monocyte-derived DC development and activity *in vitro* and in Hu-PBL-SCID mice. *J. Exp. Med.* 191: 1777-88.

327. Azimi N, Tagaya Y, Mariner J, Waldmann TA. 2000. Viral activation of IL-15: characterization of a virus-inducible element in the IL-15 promoter region. *J. Virol.* 74: 7338-48.

328. Novick D, Cohen B, Rubinstein M. 1994. The human IFNα/β receptor: characterization and molecular cloning. *Cell* 77: 391-400.

329. Kim SH, Cohen B, Novick D, Rubinstein M. 1997. Mammalian type I IFN receptors consists of two subunits: IFNAR1 and IFNAR2. *Gene* 196: 279-86

330. Cohen B, Novick D, Barak S, Rubinstein M. 1995. Ligand-induced association of the type I IFN receptor components. *Mol. Cell. Biol.* 15: 4208-14.

331. Velazquez L, Fellous M, Stark GR, Pellegrini S. 1992. A protein tyrosine kinase in the IFN α/β signaling pathway. *Cell* 70: 313-22.

332. Colamonici OR, Uyttendaele H, Domanski P, Yan H, Krolewski JJ. 1994. p135Tyk2, an IFNα-activated tyrosine kinase, is physically associated with an IFNα receptor. *J. Biol. Chem.* 269: 3518-22.

333. Gauzzi MC, Velazquez L, McKendry R, Mogensen KE, Fellous M, Pellegrini S. 1996. IFNα-dependent activation of Tyk2 requires phosphorylation of positive regulatory tyrosines by another kinase. *J. Biol. Chem.* 271: 20494-500.

334. Guschin D, Rogers N, Briscoe J, Witthuhn B, Watling D, Horn F, Pellegrini S, Yasukawa K, Heinrich P, Stark GR, et al. 1995. A major role for the protein tyrosine kinase JAK1 in the JAK/STAT signal transduction pathway in response to interleukin-6. *EMBO J.* 14: 1421-9.

335. Yan H, Krishnan K, Greenlund AC, Gupta S, Lim JT, Schreiber RD, Schindler CW, Krolewski JJ. 1996. Phosphorylated IFNAR1 acts as a docking site for the latent form of the 113 kDa STAT2 protein. *EMBO J.* 15: 1064-74.

336. Li X, Leung S, Kerr IM, Stark GR. 1997. Functional subdomains of STAT2 required for preassociation with the α IFN receptor and for signaling. *Mol. Cell. Biol.* 17: 2048-56.

337. Levy DE, Kessler DS, Pine R, Darnell JE, Jr. 1989. Cytoplasmic activation of ISGF3, the positive regulator of IFNα-stimulated transcription, reconstituted in vitro. *Genes Dev.* 3: 1362-71

338. Levy DE, Lew DJ, Decker T, Kessler DS, Darnell JE, Jr. 1990. Synergistic interaction between IFNα and IFNγ through induced synthesis of one subunit of the transcription factor ISGF3. *EMBO J* 9: 1105-11.

339. Fu XY, Kessler DS, Veals SA, Levy DE, Darnell JE, Jr. 1990. ISGF3, the transcriptional activator induced by IFNα, consists of multiple interacting polypeptide chains. *Proc. Natl. Acad. Sci. U. S. A.* 87: 8555-9.

340. Kessler DS, Veals SA, Fu X-Y, Levy DE. 1990. IFNα regulates nuclear translocation and DNA-binding affinity of ISGF3, a multimeric transcriptional activator. *Genes Dev.* 4: 1753-65.

341. David M, Petricoin E, 3rd, Benjamin C, Pine R, Weber MJ, Larner AC. 1995. Requirement for MAP kinase (ERK2) activity in IFNα- and IFNβ-stimulated gene expression through STAT proteins. *Science* 269: 1721-3.

342. Wen Z, Zhong Z, Darnell JE, Jr. 1995. Maximal activation of transcription by STAT1 and STAT3 requires both tyrosine and serine phosphorylation. *Cell* 82: 241-50.

343. Zhu X, Wen Z, Xu LZ, Darnell JE, Jr. 1997. STAT11 serine phosphorylation occurs independently of tyrosine phosphorylation and requires an activated JAK2 kinase. *Mol. Cell. Biol.* 17: 6618-23.

344. Wen Z, Darnell JE, Jr. 1997. Mapping of STAT3 serine phosphorylation to a single residue (727) and evidence that serine phosphorylation has no influence on DNA binding of STAT1 and STAT3. *Nucleic Acids Res.* 25: 2062-7

345. You M, Yu DH, Feng GS. 1999. Shp-2 tyrosine phosphatase functions as a negative regulator of the IFN-stimulated JAK/STAT pathway. *Mol. Cell. Biol.* 19: 2416-24.

346. Song MM, Shuai K. 1998. SOCS1 and SOCS3 but not SOCS2 proteins inhibit IFN-mediated antiviral and antiproliferative activities. *J. Biol. Chem.* 273: 35056-62.

347. Sakamoto H, Kinjyo I, Yoshimura A. 2000. The JAK inhibitor, Jab/SOCS-1, is an IFN-γ inducible gene and determines the sensitivity to IFNs. *Leuk. Lymphoma* 38: 49-58.

348. Krebs DL, Hilton DJ. 2001. SOCS proteins: negative regulators of cytokine signaling. *Stem Cells* 19: 378-87.

349. Kotaja N, Karvonen U, Janne OA, Palvimo JJ. 2002. PIAS proteins modulate transcription factors by functioning as SUMO-1 ligases. *Mol. Cell. Biol.* 22: 5222-34.

350. Rogers RS, Horvath CM, Matunis MJ. 2003. SUMO modification of STAT1 and its role in PIAS-mediated inhibition of gene activation. *J. Biol. Chem.* 278: 30091-7.

351. Ungureanu D, Vanhatupa S, Kotaja N, Yang J, Aittomaki S, Janne OA, Palvimo JJ, Silvennoinen O. 2003. PIAS proteins promote SUMO-1 conjugation to STAT1. *Blood* 102: 3311-3.

352. Hiscott J, Nguyen H, Lin R. 1995. Molecular mechanisms of IFNβ gene induction. *Sem. Virol.* 6: 161-73.

353. Grandvaux N, tenOever BR, Servant MJ, Hiscott J. 2002. The IFN anti-viral response: from viral invasion to evasion. *Curr. Opin. Infect. Dis.* 15: 259-67.

354. Servant MJ, Grandvaux N, Hiscott J. 2002. Multiple signaling pathways leading to the activation of IRF-3. *Biochem. Pharmacol.* 64: 985-92.

355. Thanos D, Maniatis T. 1995. Virus induction of human IFNβ gene expression requires the assembly of an enhanceosome. *Cell* 83: 1091-100.

356. Kim TK, Maniatis T. 1997. The mechanism of transcriptional synergy of an in vitro assembled IFNβ enhanceosome. *Mol. Cell* 1: 119-29.

357. Agalioti T, Lomvardas S, Parekh B, Yie J, Maniatis T, Thanos D. 2000. Ordered recruitment of chromatin modifying and general transcription factors to the IFNβ promoter. *Cell* 103: 667-78.

358. Merika M, Thanos D. 2001. Enhanceosomes. *Curr. Opin. Genet. Dev.* 11: 205-8.

359. Courey AJ. 2001. Cooperativity in transcriptional control. *Curr. Biol.* 11: R250-2.

360. Goodbourn S, Maniatis T. 1988. Overlapping positive and negative regulatory domains of the human β–IFN gene. *Proc. Natl. Acad. Sci. U. S. A.* 85: 1447-51.

361. Keller AD, Maniatis T. 1991. Identification and characterization of a novel repressor of β- IFN gene expression. *Genes Dev.* 5: 868-79.

362. Maniatis T, Whittenmore L-A, Du W, Fan C-M, Keller AD, Palombella VJ, Thanos D. 1992. Positive and negative control of human IFNβ gene expression. In *Transcriptional Regulation*, ed. KR Yamamoto, SL McKnight, pp. 1193-220. Cold Spring Harbor, N.Y.: Cold Spring Harbor Laboratories.

363. Du W, Thanos D, Maniatis T. 1993. Mechanisms of transcriptional synergism between distinct virus-inducible enhancer elements. *Cell* 74: 887-98.

364. Fan C-M, Maniatis T. 1989. Two different virus-inducible elements are required for human β-IFN gene regulation. *EMBO J.* 8: 101-10.

365. Merika M, Williams AJ, Chen G, Collins T, Thanos D. 1998. Recruitment of CBP/p300 by the IFNβ enhanceosome is required for synergistic activation of transcription. *Mol. Cell* 1: 277-87.

366. Visvanathan KV, Goodbourn S. 1989. dsRNA activates binding of NF-κB to an inducible element in the human β-IFN promoter. *EMBO J.* 8: 1129-38.

367. Lenardo MJ, Fan C-M, Maniatis T, Baltimore D. 1989. The involvement of NF-κB in β-IFN gene regulation reveals its role as widely inducible mediator of signal transduction. *Cell* 57: 287-94.

368. Hiscott J, Alper D, Cohen L, Leblanc J-F, Sportza L, Wong A, Xanthoudakis S. 1989. Induction of human IFN gene expression is associated with a nuclear factor that interacts with the NF-κB site of the HIV enhancer. *J. Virol.* 63: 2557-66.

369. Thanos D, Maniatis T. 1995. Identification of the Rel family members required for virus induction of the human β–IFN gene. *Mol. Cell. Biol.* 15: 152-64.

370. Thanos D, Maniatis T. 1992. The high mobility group protein HMG I(Y) is required for NF-κB dependent virus induction of the human IFNβ gene. *Cell* 71: 777-89.

371. Yie J, Liang S, Merika M, Thanos D. 1997. Intra- and intermolecular cooperative binding of high-mobility-group protein I(Y) to the β-IFN promoter. *Mol. Cell. Biol.* 17: 3649-62.

372. Du W, Maniatis T. 1992. An ATF/CREB binding site is required for virus induction of the human IFNβ gene. *Proc. Natl. Acad. Sci. U. S. A.* 89: 2150-4.

373. Miyamoto M, Fujita T, Kimura Y, Maruyama M, Harada H, Sudo Y, Miyata T, Taniguchi T. 1988. Regulated expression of a gene encoding a nuclear factor, IRF-1, that specifically binds to the IFNβ gene regulatory elements. *Cell* 54: 903-13.

374. Fujita T, Sakakibara J, Sudo Y, Miyamoto M, Kimura Y, Taniguchi T. 1988. Evidence for a nuclear factor(s), IRF-1, mediating induction and silencing properties to human IFNβ gene regulatory elements. *EMBO J.* 7: 3397-405

375. Fujita T, Kimura Y, Miyamoto M, Barsoumian EL, Taniguchi T. 1989. Induction of endogenous IFNα and IFNβ genes by a regulatory transcription factor IRF-1. *Nature* 337: 270-2.

376. Harada H, Fujita T, Miyamoto M, Kimura Y, Maruyama M, Furia A, Miyata T, Taniguchi T. 1989. Structurally similar but functionally distinct factors, IRF-1 and IRF-2, bind to the same regulatory elements of IFN and IFN-inducible genes. *Cell* 58: 729-39.

377. Pine R, Decker T, Kessler DS, Levy DE, Darnell Jr. JE. 1990. Purification and cloning of IFN-stimulated gene factor 2 (ISGF2): ISGF2 (IRF-1) can bind to the promoters of both β-IFN and ISG but is not a primary transcriptional activator of either. *Mol. Cell. Biol.* 10: 2448-57.

378. Lin R, Hiscott J. 1999. A role for CKII phosphorylation in the regulation of IRF-1 transcriptional activity. *Mol. Cell. Biochem.* 191: 169-80.

379. Lin R, Mustafa A, Nguyen H, Gewert D, Hiscott J. 1994. Mutational analysis of IRF-1 and IRF-2. Effects on the induction of IFNβ gene expression. *J. Biol. Chem.* 269: 17542-9.

380. Yamamoto H, Lamphier MS, Fujita T, Taniguchi T, Harada H. 1994. The oncogenic transcription factor IRF-2 possesses a transcriptional repression and a latent activation domain. *Oncogene* 9: 1423-8.

381. Escalante CR, Yie J, Thanos D, Aggarwal AK. 1998. Structure of IRF-1 with bound DNA reveals determinants of IFN regulation. *Nature* 391: 103-6.

382. Watanabe N, Sakakibara J, Hovanessian AG, Taniguchi T, Fujita T. 1991. Activation of IFNβ element by IRF-1 requires a post-translational event in addition to IRF-1 synthesis. *Nucleic Acids Res.* 19: 4421-8.

383. Matsuyama T, Kimura T, Kitagawa M, Watanabe N, Kundig T, Amakawa R, Kishihara K, Wakeham A, Potter J, Furlonger C, Narendran A, Suzuki H, Ohashi P, Paige C, Taniguchi T, Mak T. 1993. Targeted disruption of IRF-1 or IRF-2 results in abnormal type I IFN induction and aberrant lymphocyte development. *Cell* 75: 83-97.

384. Duncan GS, Mittrucker HW, Kagi D, Matsuyama T, Mak TW. 1996. The transcription factor IRF-1 is essential for natural killer cell function *in vivo*. *J. Exp. Med.* 184: 2043-8.

385. Penninger JM, Mak TW. 1998. Thymocyte selection in Vav and IRF-1 gene-defecient mice. *Immunol. Rev.* 165: 149-66.

386. Levy DE. 1995. IFN induction of gene expression through the JAK-STAT pathway. *Sem. Virol.* 6: 181-90.

387. Harada H, Matsumoto M, Sato M, Kashiwazaki Y, Kimura T, Kitagawa M, Yokochi T, Tan RS-P, Takasugi T, Kadokawa Y, Schindler C, Schreiber RD, Noguchi S, Taniguchi T. 1996. Regulation of IFNα/β genes: evidence for a dual function of the transcription factor complex ISGF3 in the production and action of IFNα/β. *Genes Cells* 1: 995-1005.

388. Yoneyama M, Suhara W, Fukuhara Y, Sato M, Ozato K, Fujita T. 1996. Autocrine amplification of type I IFN gene expression mediated by ISGF3. *J. Biochem.* 120: 160-9.

389. Ruffner H, Reis LF, NÑf D, Weissmann C. 1993. Induction of type I IFN genes and IFN-inducible genes in embryonal stem cells devoid of IRF-1. *Proc. Natl. Acad. Sci. U. S. A.* 90: 11503-7.

390. Reis LFL, Ruffner H, Stark G, Aguet M, Weissmann C. 1994. Mice devoid of IRF-1 show normal expression of type I IFN genes. *EMBO J.* 13: 4798-806.

391. Au W-C, Moore PA, Lowther W, Juang Y-T, Pitha PM. 1995. Identification of a member of the IRF family that binds to the IFN-stimulated response element and activates expression of IFN-induced genes. *Proc. Natl. Acad. Sci. U. S. A.* 92: 11657-61.

392. Daly C, Reich NC. 1993. dsRNA activates novel factors that bind to the ISRE. *Mol. Cell. Biol.* 13: 3756-64.

393. Weaver BK, Kumar KP, Reich NC. 1998. IRF-3 and CBP/p300 are subunits of dsRNA-activated transcription factor DRAF1. *Mol. Cell. Biol.* 18: 1359-68.

394. Daly C, Reich NC. 1995. Characterization of specific DNA-binding factors activated by dsRNA as positive regulators of IFNα/β-stimulated genes. *J. Biol. Chem.* 270: 23739-46.

395. Bovolenta C, Lou J, Kanno Y, Park BK, Thornton AM, Coligan JE, Schubert M, Ozato K. 1995. VSV infection induces a nuclear DNA-binding factor specific for the ISRE. *J. Virol.* 69: 4173-81.

396. Juang Y, Lowther W, Kellum M, Au WC, Lin R, Hiscott J, Pitha PM. 1998. Primary activation of IFN α and IFN β gene transcription by IRF-3. *Proc. Natl. Acad. Sci. U. S. A.* 95: 9837-42.

397. Wathelet MG, Lin CH, Parekh BS, Ronco LV, Howley PM, Maniatis T. 1998. Virus infection induces the assembly of coordinately activated transcription factors on the IFNβ enhancer in vivo. *Mol. Cell* 1: 507-18.

398. Lin R, Heylbroeck C, Pitha PM, Hiscott J. 1998. Virus-dependent phosphorylation of the IRF-3 transcription factor regulates nuclear translocation, transactivation potential, and proteasome-mediated degradation. *Mol. Cell. Biol.* 18: 2986-96.

399. Yoneyama M, Suhara W, Fukuhara Y, Fukuda M, Nishida E, Fujita T. 1998. Direct triggering of the type I IFN system by virus infection: activation of a transcription factor complex containing IRF-3 and CBP/p300. *EMBO J.* 17: 1087-95

400. Sato M, Tanaka N, Hata N, Oda E, Taniguchi T. 1998. Involvement of the IRF family transcription factor IRF-3 in virus- induced activation of the IFNβ gene. *FEBS Lett.* 425: 112-6.

401. Lowther WJ, Moore PA, Carter KC, Pitha PM. 1999. Cloning and functional analysis of the human IRF-3 promoter. *DNA Cell. Biol.* 18: 685-92.

402. Lin R, Genin P, Mamane Y, Hiscott J. 2000. Selective DNA binding and association with the CBP coactivator contribute to differential activation of α/β IFN genes by IRF- 3 and -7. *Mol. Cell. Biol.* 20: 6342-53.

403. Lin R, Heylbroeck C, Genin P, Pitha PM, Hiscott J. 1999. Essential role of IRF-3 in direct activation of RANTES chemokine transcription. *Mol. Cell. Biol.* 19: 959-66.

404. Cheng G, Nazar AS, Shin HS, Vanguri P, Shin ML. 1998. IP-10 gene transcription by virus in astrocytes requires cooperation of ISRE with adjacent κB site but not IRF-1 or viral transcription. *J. Interferon Cytokine Res.* 18: 987-97.

405. Kawakami T, Matsumoto M, Sato M, Harada H, Taniguchi T, Kitagawa M. 1995. Possible involvement of the transcription factor ISGF3γ in virus-induced expression of the IFNβ gene. *FEBS Lett.* 358: 225-9.

406. Kimura T, Kadokawa Y, Harada H, Matsumoto M, Sato M, Kashiwazaki Y, Tarutani M, Tan RS-P, Takasugi T, Matsuyama T, Mak TM, Noguchi S, Taniguchi T. 1996. Essential and non-redundant roles of ISGF3γ and IRF-1 in both type I and type II IFN responses, as revealed by gene targeting studies. *Genes Cells* 1: 115-24.

407. Sato M, Hata N, Asagiri M, Nakaya T, Taniguchi T, Tanaka N. 1998. Positive feedback regulation of type I IFN genes by the IFN-inducible transcription factor IRF-7. *FEBS Lett.* 441: 106-10.

408. Lu R, Au WC, Yeow WS, Hageman N, Pitha PM. 2000. Regulation of the promoter activity of IRF-7 gene. Activation by IFN snd silencing by hypermethylation. *J. Biol. Chem.* 275: 31805-12.

409. Au WC, Moore PA, LaFleur DW, Tombal B, Pitha PM. 1998. Characterization of the IRF-7 and its potential role in the transcription activation of IFNα genes. *J. Biol. Chem.* 273: 29210-7.

410. Marie I, Smith E, Prakash A, Levy DE. 2000. Phosphorylation-induced dimerization of IRF-7 unmasks DNA binding and a bipartite transactivation domain. *Mol. Cell. Biol.* 20: 8803-14.

411. Lin R, Mamane Y, Hiscott J. 1999. Structural and functional analysis of IRF-3: localization of the transactivation and autoinhibitory domains. *Mol. Cell. Biol.* 19: 2465-74

412. Servant MJ, ten Oever B, LePage C, Conti L, Gessani S, Julkunen I, Lin R, Hiscott J. 2001. Identification of distinct signaling pathways leading to the phosphorylation of IRF-3. *J. Biol. Chem.* 276: 355-63.

413. Suhara W, Yoneyama M, Iwamura T, Yoshimura S, Tamura K, Namiki H, Aimoto S, Fujita T. 2000. Analyses of virus-induced homomeric and heteromeric protein associations between IRF-3 and coactivator CBP/p300. *J. Biochem.* 128: 301-7.

414. Yoneyama M, Suhara W, Fujita T. 2002. Control of IRF-3 activation by phosphorylation. *J. Interferon Cytokine Res.* 22: 73-6.

415. Servant MJ, Grandvaux N, TenOever BR, Duguay D, Lin R, Hiscott J. 2003. Identification of the minimal phosphoacceptor site required for in vivo activation of IRF-3 in response to virus and dsRNA. *J. Biol. Chem.* 10: 10.

416. Iwamura T, Yoneyama M, Yamaguchi K, Suhara W, Mori W, Shiota K, Okabe Y, Namiki H, Fujita T. 2001. Induction of IRF-3/-7 kinase and NF-κB in response to dsRNA and virus infection: common and unique pathways. *Genes Cells* 6: 375-88.

417. Takahasi K, Suzuki NN, Horiuchi M, Mori M, Suhara W, Okabe Y, Fukuhara Y, Terasawa H, Akira S, Fujita T, Inagaki F. 2003. X-ray crystal structure of IRF-3 and its functional implications. *Nat. Struct. Biol.* 10: 922-7.

418. Heylbroeck C, Balachandran S, Servant MJ, DeLuca C, Barber GN, Lin R, Hiscott J. 2000. The IRF-3 transcription factor mediates Sendai virus-induced apoptosis. *J. Virol.* 74: 3781-92.

419. Weaver BK, Ando O, Kumar KP, Reich NC. 2001. Apoptosis is promoted by the dsRNA-activated factor (DRAF1) during viral infection independent of the action of IFN or p53. *FASEB J.* 15: 501-15.

420. Lin R, Mamane Y, Hiscott J. 2000. Multiple regulatory domains control IRF-7 activity in response to virus infection. *J. Biol. Chem.* 275: 34320-7.

421. Smith EJ, Marie I, Prakash A, Garcia-Sastre A, Levy DE. 2001. IRF-3 and IRF-7 phosphorylation in virus-infected cells does not require PKR or IKK but is blocked by Vaccinia Virus E3L protein. *J. Biol. Chem.* 276: 8951-7.

422. tenOever BR, Servant MJ, Grandvaux N, Lin R, Hiscott J. 2002. Recognition of the Measles viral nucleocapsid as a mechanism of IRF-3 activation. *J. Virol.* 76: 3659-69

423. Navarro L, Mowen K, Rodems S, Weaver B, Reich N, Spector D, David M. 1998. CMV activates IFN immediate-early response gene expression and an IRF-3-containing ISRE-binding complex. *Mol. Cell. Biol.* 18: 3796-802.

424. Yang Y-L, Reis LFL, Pavlovic J, Aguzzi A, Schaefer R, Kumar A, Williams BRG, Aguet M, Weissman C. 1995. Deficient signalling in mice devoid of PKR. *EMBO J.* 14: 6095-106.

425. Abraham N, Stojdl DF, Duncan PI, Methot N, Ishii T, Dube M, Vanderhyden BC, Atkins HL, Gray DA, McBurney MW, Koromilas AE, Brown EG, Sonenberg N, Bell JC. 1999. Characterization of transgenic mice with targeted disruption of the catalytic domain of PKR. *J. Biol. Chem.* 274: 5953-62.

426. Lund J, Sato A, Akira S, Medzhitov R, Iwasaki A. 2003. TLR9-mediated recognition of HSV-2 by plasmacytoid DC. *J. Exp. Med.* 198: 513-20.

427. Navarro L, David M. 1999. p38-dependent activation of IRF-3 by LPS. *J. Biol. Chem.* 274: 35535-8.

428. Sakaguchi S, Negishi H, Asagiri M, Nakajima C, Mizutani T, Takaoka A, Honda K, Taniguchi T. 2003. Essential role of IRF-3 in LPS-induced IFN-β gene expression and endotoxin shock. *Biochem. Biophys. Res. Commun.* 306: 860-6.

429. Doyle S, Vaidya S, O'Connell R, Dadgostar H, Dempsey P, Wu T, Rao G, Sun R, Haberland M, Modlin R, Cheng G. 2002. IRF-3 mediates a TLR3/TLR4-specific anti-viral gene program. *Immunity* 17: 251-63.

430. Karpova AY, Trost M, Murray JM, Cantley LC, Howley PM. 2002. IRF-3 is an *in vivo* target of DNA-PK. *Proc. Natl. Acad. Sci. U. S. A* 26: 26.

431. Jiang Z, Zamanian-Daryoush M, Nie H, Silva AM, Williams BR, Li X. 2003. Poly(I-C)-induced TLR3-mediated activation of NFκB and MAP kinase is through IRAK-independent pathway employing the signaling components TLR3-TRAF6-TAK1-TAB2-PKR. *J. Biol. Chem.* 278: 16713-9.

432. Eisenbeis CF, Singh H, Storb U. 1995. Pip, a novel IRF family member, is a lymphoid-specific, PU.1-dependent transcriptional activator. *Genes Dev.* 9: 1377-87.

433. Brass AL, Kehrli E, Eisenbeis CF, Storb U, Singh H. 1996. Pip, a lymphoid-restricted IRF, contains a regulatory domain that is important for autoinhibition and ternary complex formation with the Ets factor PU.1. *Genes Dev.* 10: 2335-47.

434. Matsuyama T, Grossman H, Mittrucker D, Siderovski DP, Kiefer F, Kawakami T, Richardson CD, Tanaguchi T, Yoshinaga SK, Mak TW. 1995. Moleculare cloning of LSIRF, a lymphoid-specific member of the IRF family that binds the ISRE. *Nucleic Acids Res.* 23: 2127-36.

435. Morris R. 1994. Modes of action of FK506, cyclosporin A, and rapamycin. *Trans. Proc.* 26: 3272-5.

436. Yamagata T, Nishida J, Tanaka T, Sakai R, Mitani K, Yoshida M, Taniguchi T, Yazaki Y, Hirai H. 1996. A novel IRF family transcription factor, ICSAT/Pip/LSIRF, that negatively regulates the activity of IFN-regulated genes. *Mol. Cell. Biol.* 16: 1283-94.

437. Mittrucker H-W, Matsuyama T, Grossman A, Kundig TM, Potter J, Shahinian A, Wakeham A, Patterson B, Ohashi P, Mak TW. 1997. Requirement for the transcription factor LSIRF/IRF4 for mature B- and T-lymphocyte function. *Science* 275: 540-3.

438. Hrdlickova R, Nehyba J, Bose HR, Jr. 2001. IRF-4 contributes to transformation of v-Rel- expressing fibroblasts. *Mol. Cell. Biol.* 21: 6369-86.

439. Saito T, Yamagata T, Takahashi T, Honda H, Hirai H. 1999. ICSAT overexpression is not sufficient to cause adult T-cell leukemia or multiple myeloma. *Biochem. Biophys. Res. Commun.* 260: 329-31.

440. Saxon A, Stevens RH, Golde DW. 1978. T-lymphocyte variant of hairy-cell leukemia. *Ann. Intern. Med.* 88: 323-6.

441. Jeang KT, Derse D, Matocha M, Sharma O. 1997. Expression status of Tax protein in HTLV-I-transformed MT4 cells: recall of MT4 cells distributed by the NIH AIDS Research and Reference Reagent Program. *J. Virol.* 71: 6277-8.

442. Moyer SA, Smallwood-Kentro S, Haddad A, Prevec L. 1991. Assembly and transcription of synthetic VSV nucleocapsids. *J. Virol.* 65: 2170-8.

443. Grossman A, Mittrucker HW, Nicholl J, Suzuki A, Chung S, Antonio L, Suggs S, Sutherland GR, Siderovski DP, Mak TW. 1996. Cloning of human lymphocyte-specific IFN regulatory factor (hLSIRF/hIRF4) and mapping of the gene to 6p23-p25. *Genomics* 37: 229-33.

444. Mamane Y, S. Sharma, L. Petropoulos, R. Lin and J. Hiscott. 2000. Posttranslational regulation of IRF-4 activity by the immunophilin FKBP52. *Immunity* 12: 129-40.

445. Le Page C, Popescu O, Genin P, Lian J, Paquin A, Galipeau J, Hiscott J. 2001. Disruption of NF-κB signaling and chemokine gene activation by retroviral mediated expression of IKKγ/NEMO mutants. *Virology* 286: 422-33.

446. Mueller PR, Wold B. 1989. In vivo footprinting of a muscle specific enhancer by ligation mediated PCR. *Science* 246: 780-6.

447. Garrity PA, Wold B. 1992. Effects of different DNA polymerases in ligation-mediated PCR: enhanced genomic sequencing and *in vivo* footprinting. *Proc. Natl. Acad. Sci. U. S. A.* 89: 1021-5.

448. Boyd KE, Wells J, Gutman J, Bartley SM, Farnham PJ. 1998. c-Myc target gene specificity is determined by a post-DNA binding mechanism. *Proc. Natl. Acad. Sci. U. S. A.* 95: 13887-92.

449. Sharma S, Mamane Y, Grandvaux N, Bartlett J, Petropoulos L, Lin R, Hiscott J. 2000. Activation and regulation of IRF-4 in HTLV-I -infected T-lymphocytes. *AIDS Res. Hum. Retroviruses* 16: 1613-22.

450. Sharma S, Grandvaux N, Mamane Y, Genin P, Azimi N, Waldmann T, Hiscott J. 2002. Regulation of IRF-4 expression in HTLV-I-transformed T-cells. *J. Immunol.* 169: 3120-30.

451. Czar MJ, Owens-Grillo JK, Dittmar KD, Hutchison KA, Zacharek AM, Leach KL, Deibel MR, Jr., Pratt WB. 1994. Characterization of the protein-protein interactions determining the heat shock protein (hsp90.hsp70.hsp56) heterocomplex. *J. Biol. Chem.* 269: 11155-61.

452. Radanyi C, Chambraud B, Baulieu EE. 1994. The ability of the immunophilin FKBP59-HBI to interact with the 90-kDa heat shock protein is encoded by its TPR domain. *Proc. Natl. Acad. Sci. U. S. A.* 91: 11197-201.

453. Perrot-Applanat M, Cibert C, Geraud G, Renoir JM, Baulieu EE. 1995. The 59 kDa FK506-binding protein, a 90 kDa heat shock protein binding immunophilin (FKBP59-HBI), is associated with the nucleus, the cytoskeleton and mitotic apparatus. *J. Cell. Sci.* 108 (Pt 5): 2037-51.

454. Ortiz MA, Light J, Maki RA, Assa-Munti N. 1999. Mutation analysis of the Pip interaction domain reveals critical residues for protein-protein interactions. *Proc. Natl. Acad. Sci. U.S.A.* 96: 2740-5.

455. Kay J. 1996. Structure-function relationships in the FKBP family of the peptidylprolyl cis-trans isomerases. *Biochem. J.* 314: 361-85.

456. Verweij CL, Geerts M, Aarden LA. 1991. Activation of IL-2 gene transcription via the T-cell surface molecule CD28 is mediated through an NF-κB-like response element. *J. Biol. Chem.* 266: 14179-82.

457. Lai JH, Horvath G, Subleski J, Bruder J, Ghosh P, Tan TH. 1995. RelA is a potent transcriptional activator of the CD28RE within the IL-2 promoter. *Mol. Cell. Biol.* 15: 4260-71.

458. Sun SC, Harhaj EW, Xiao G, Good L. 2000. Activation of IKK by the HTLV-I Tax protein: mechanistic insights into the adaptor function of IKKγ. *AIDS Res. Hum. Retroviruses* 16: 1591-6.

459. Xiao G, Harhaj EW, Sun SC. 2000. Domain-specific interaction with the IκB kinase (IKK) regulatory subunit IKKγ is an essential step in Tax-mediated activation of IKK. *J. Biol. Chem.* 275: 34060-7.

460. Ballard DW, Bohnlein E, Lowenthal JW, Wano Y, Franza BR, Greene WC. 1988. HTLV-I Tax induces cellular proteins that activate the κB element in the IL-2 receptor α gene. *Science* 241: 1652-5.

461. Ruben S, Poteat H, Tan T-H, Kawakami K, Roeder R, Haseltine WA, Rosen CA. 1988. Cellular transcription factors and regulation of IL-2 receptor gene expression by HTLV-I *tax* gene product. *Science* 241: 89-92.

462. Civil A, Geerts M, Aarden LA, Verweij CL. 1992. Evidence for a role of CD28RE as a response element for distinct mitogenic T-cell activation signals. *Eur. J. Immunol.* 22: 3041-3.

463. Parra E, McGuire K, Hedlund G, Dohlsten M. 1998. Overexpression of p65 and c-Jun substitutes for B7-1 costimulation by targeting the CD28RE within the IL-2 promoter. *J. Immunol.* 160: 5374-81.

464. McGuire KL, Iacobelli M. 1997. Involvement of Rel, Fos, and Jun proteins in binding activity to the IL-2 promoter CD28RE/AP-1 sequence in human T-cells. *J. Immunol.* 159: 1319-27.

465. Shapiro VS, Truitt KE, Imboden JB, Weiss A. 1997. CD28 mediates transcriptional upregulation of the IL-2 promoter through a composite element containing the CD28RE and NF-IL-2B AP-1 sites. *Mol. Cell. Biol.* 17: 4051-8.

466. Shang C, Attema J, Cakouros D, Cockerill PN, Shannon MF. 1999. NF-AT contributes to the function of the CD28 response region of the granulocyte macrophage-colony stimulating factor promoter. *Int. Immunol.* 11: 1945-56.

467. Lindgren H, Axcrona K, Leanderson T. 2001. Regulation of transcriptional activity of the murine CD40 ligand promoter in response to signals through tcr and the costimulatory molecules CD28 and CD2. *J. Immunol.* 166: 4578-85.

468. Huynh QK, Kishore N, Mathialagan S, Donnelly AM, Tripp CS. 2002. Kinetic mechanisms of IκB-related kinases (IKK) inducible IKK and TBK-1 differ from IKK1/IKK2 heterodimer. *J. Biol. Chem.* 277: 12550-8.

469. Genin P, Algarte M, Roof P, Lin R, Hiscott J. 2000. Regulation of RANTES chemokine gene expression requires cooperativity between NF-κB and IRF transcription factors. *J. Immunol.* 164: 5352-61.

470. Sharma S, tenOever BR, Grandvaux N, Zhou GP, Lin R, Hiscott J. 2003. Triggering the IFN antiviral response through an IKK-related pathway. *Science* 300: 1148-51.

471. Fitzgerald KA, McWhirter SM, Faia KL, Rowe DC, Latz E, Golenbock DT, Coyle AJ, Liao SM, Maniatis T. 2003. IKKε and TBK-1 are essential components of the IRF-3 signaling pathway. *Nat. Immunol.* 4: 491-6.

472. Marks AR. 1996. Cellular functions of immunophilins. *Physiol. Rev.* 76: 631-49.

473. Hunter T. 1998. Prolyl isomerases and nuclear function. *Cell* 92: 141-3.

474. Gonda T. 1998. The c-Myb oncoprotein . *Int. J. Biochem. Cell Biol.* 30: 517-51.

475. Leverson JD, Ness SA. 1998. Point mutations in v-Myb disrupt a cyclophilin-catalyzed negative regulatory mechanism. *Mol. Cell* 1: 203-11.

476. Grumont RJ, Gerondakis S. 2000. Rel induces IRF-4 expression in lymphocytes: modulation of IFN-regulated gene expression by Rel/NF-κB. *J. Exp. Med.* 191: 1281-92.

477. Rengarajan J, Mowen KA, McBride KD, Smith ED, Singh H, Glimcher LH. 2002. IRF-4 interacts with NFATc2 to modulate IL-4 gene expression. *J. Exp. Med.* 195: 1003-12.

478. Jeang KT. 2001. Functional activities of the HTLV-I Tax oncoprotein: cellular signaling through NF-κB. *Cytokine Growth Factor Rev.* 12: 207-17.

479. Azimi N, Brown K, Bamford RN, Tagaya Y, Siebenlist U, Waldmann TA. 1998. HTLV-I Tax protein trans-activates IL-15 gene transcription through an NF-κB site. *Proc. Natl. Acad. Sci. U. S. A.* 95: 2452-7.

480. Imaizumi Y, Kohno T, Yamada Y, Ikeda S, Tanaka Y, Tomonaga M, Matsuyama T. 2001. Possible involvement of IRF-4 in a clinical subtype of ATL. *Jpn. J. Cancer Res.* 92: 1284-92.

481. Iida S, Rao PH, Butler M, Corradini P, Boccadoro M, Klein B, Chaganti RSK, Dalla-Favera R. 1997. Deregulation of MUM1/IRF-4 by chromosomal translocation in multiple myeloma. *Nat. Genet.* 17: 226-30.

482. Tsuboi K, Iida S, Inagaki H, Kato M, Hayami Y, Hanamura I, Miura K, Harada S, Kikuchi M, Komatsu H, Banno S, Wakita A, Nakamura S, Eimoto T, Ueda R. 2000. MUM1/IRF-4 expression as a frequent event in mature lymphoid malignancies. *Leukemia* 14: 449-56.

483. Mamane Y, Grandvaux N, Hernandez E, Sharma S, Innocente SA, Lee JM, Azimi N, Lin R, Hiscott J. 2002. Repression of IRF-4 target genes in HTLV-I infection. *Oncogene* 21: 6751-65.

484. Diebold SS, Montoya M, Unger H, Alexopoulou L, Roy P, Haswell LE, Al-Shamkhani A, Flavell R, Borrow P, Reis e Sousa C. 2003. Viral infection switches non-plasmacytoid DC into high IFN producers. *Nature* 424: 324-8.

485. Guillot L, Medjane S, Le-Barillec K, Balloy V, Danel C, Chignard M, Si-Tahar M. 2004. Response of human pulmonary epithelial cells to LPS involves TLR4-

dependent signaling pathways: evidence for an intracellular compartmentalization of TLR4. *J. Biol. Chem.* 279: 2712-8.

486. Chariot A, Leonardi A, Muller J, Bonif M, Brown K, Siebenlist U. 2002. Association of the adaptor TANK with the IKK regulator NEMO connects IKK complexes with IKKε and TBK-1 kinases. *J. Biol. Chem.* 277: 37029-36.

487. Fujita F, Taniguchi Y, Kato T, Narita Y, Furuya A, Ogawa T, Sakurai H, Joh T, Itoh M, Delhase M, Karin M, Nakanishi M. 2003. Identification of NAP1, a regulatory subunit of IKK that potentiates NF-κB signaling. *Mol. Cell. Biol.* 23: 7780-93.

488. Qin BY, Liu C, Lam SS, Srinath H, Delston R, Correia JJ, Derynck R, Lin K. 2003. Crystal structure of IRF-3 reveals mechanism of autoinhibition and virus-induced phosphoactivation. *Nat. Struct. Biol.* 10: 913-21.

489. McWhirter SM, Fitzgerald KA, Rosains J, Rowe DC, Golenbock DT, Maniatis T. 2004. IRF-3-dependent gene expression is defective in TBK-1-deficient mouse embryonic fibroblasts. *Proc. Natl. Acad. Sci. U. S. A.* 101: 233-8.

490. Talon J, Horvath CM, Polley R, Basler CF, Muster T, Palese P, Garcia-Sastre A. 2000. Activation of IRF-3 is inhibited by the influenza A virus NS1 protein. *J. Virol.* 74: 7989-96.

491. Basler CF, Mikulasova A, Martinez-Sobrido L, Paragas J, Muhlberger E, Bray M, Klenk HD, Palese P, Garcia-Sastre A. 2003. The Ebola virus VP35 protein inhibits activation of IRF-3. *J. Virol.* 77: 7945-56.

492. Foy E, Li K, Wang C, Sumpter R, Jr., Ikeda M, Lemon SM, Gale M, Jr. 2003. Regulation of IRF-3 by the hepatitis C virus serine protease. *Science* 300: 1145-8.

493. Duguay D, Mercier F, Stagg J, Martineau D, Bramson J, Servant M, Lin R, Galipeau J, Hiscott J. 2002. In vivo IRF-3 tumor suppressor activity in B16 melanoma tumors. *Cancer Res.* 62: 5148-52.

494. Bramson JL, Dayball K, Hall JR, Millar JB, Miller M, Wan YH, Lin R, Hiscott J. 2003. Super-activated IRFs can enhance plasmid immunization. *Vaccine* 21: 1363-70.